




TALLAWARRA B POWER STATION CFD PLUME MODELLING AND MEASUREMENT PROGRAM

SUMMARY REPORT

for Energy Australia

24TH OCTOBER 2024

Ref 2407

REVISION HISTORY			
No.	Date	Comment	Signed
0	9 th October 2024	Draft to Energy Australia	
1	21 st October 2024	Minor report updates	
2	24 th October 2024	Correcting typing and formatting errors	

Stacey Agnew Pty. Ltd
Unit 4 35 Limestone Street, Darra, QLD 4076, Australia
P: +61 7 30776770 F: +61 7 30776769
www.staceyagnew.com

EXECUTIVE SUMMARY

Stacey Agnew was engaged to assess the stack plume generated by the Tallawarra B Power Station. The high flow and temperature of the plume has a big impact on the atmospheric flow around the stack, and the high vertical velocities in the exhaust plume can affect aircraft. To limit the plume rise velocities and to meet the Civil Aviation Safety Authority (CASA) requirement, a stack-top diffuser (plume dispersion device or PDD) is mounted on the top of the stack as illustrated in Figure 3.

CASA's Critical Plume Velocity (CPV) of 6.1 m/s is an average vertical velocity within the plume. An average velocity criterion suits simpler assessment methods for stacks with a single upwards outlet. For a Gaussian plume, the peak velocity is twice the average velocity. The Tallawarra B plume, particularly at low heights, is more complicated than can be assessed using the simple plume models, and so computational fluid dynamics (CFD) is used. When assessed using CFD, the peak velocity anywhere in the plume is referenced. The CASA criterion for the Tallawarra B project is to not exceed a maximum vertical plume velocity of 12.2 m/s at 700 ft.

In accordance with CASA's requirements, the peak vertical velocity that is calculated using a CFD model is divided by 2 to produce an average velocity for comparison with CASA's CPV of 6.1 m/s which is based on Gaussian plumes. Stacey Agnew assisted the design process and undertook a detailed 3-dimensional (3D) CFD analysis of the exhaust plume for two wind cases. The wind conditions were provided by Katestone and selected from the TAPM modelling output that resulted in the 99.9th percentile plume average vertical velocity at 700 ft. A third arbitrary wind case (combination of worst conditions from the first two wind cases) to confirm observations and trends was also analysed.

Based on the two relevant analysed wind cases, the CFD modelling confirmed that the proposed PDD design can sufficiently disperse the generated exhaust plume to keep the peak plume rise velocities below 12.2 m/s (corresponds to CPV of 6.1 m/s). The maximum estimated peak plume rise velocity for low wind speeds and ambient temperatures was 11.9 m/s (corresponds to 5.95 m/s according to CASA's criterion definition). The additional wind case (combination of lowest wind speeds and temperatures) confirmed that the plume behaviour and the peak velocities are very sensitive to small changes in the wind speed and ambient temperatures. According to the CFD modelling, if there is almost no wind at low ambient temperatures the peak plume rise velocity can slightly exceed 12.2 m/s. However, wind conditions that lead to such high vertical velocities were not observed in the five years of meteorological data that have been analysed by Katestone. Based on the analysed cases, the highest plume rise velocities are observed below 2000 ft (above mean sea level) in the proximity of the stack centre within a radius of 100 m.

In accordance with the Plume Validation Monitoring Program (PVMP) [21], after completion and commissioning of the Tallawarra B power station, on-site measurements of the exhaust plume were contemplated to confirm the PDD performance and the estimated plume rise velocities. Stacey Agnew was involved to provide support, recommendations and advice on potential measurement methodologies. The measurements were undertaken by the Austrian company TS Avionics GmbH which is a 100% subsidiary of Turbulence Solutions GmbH. The company was chosen due to their world-leading expertise in the measurement of atmospheric turbulence (up- and downdrafts) with a light aircraft and their specific knowledge about aircraft aerodynamics and how turbulence affects them. The measurement campaign was accompanied and supported by Stacey Agnew, Airspeed Aviation, Katestone, Aviation Projects, as well as the Tallawarra B operating and project teams from Energy Australia.

A Cessna 172 hired by Energy Australia and operated by Airspeed Aviation was equipped with tailored and self-contained flow and inertial sensors. The measurements were done in August, seeking cold, calm conditions which were predicted to lead to the highest updraft

velocities. Weather forecasts provided by Katestone and Meteomatics were used to plan the test flight windows, which were constrained also by the ability of the market to accept the power generated by the operating power station. With fortunate weather occurring at the start of the campaign, test flights and plume measurements could be conducted on three consecutive days (5th, 6th and 7th of August 2024). The total flight time was more than 11 hours, including calibration flights, with approximately 430 plume fly-throughs recorded, at different elevations starting from 500 ft up to 2600 ft. During the whole test period, the Tallawarra B power station was running at 100% power to obtain and measure the worst plume conditions. The lowest wind speed in combination with the lowest ambient temperature was on the third test day (7th of August 2024) when the wind direction was changing from a westerly wind with a speed of about 1.5 m/s to an easterly wind with a speed of about 1.9 m/s (with very low wind speed in between). During that period, the highest plume rise velocity of around 12 m/s was measured. This is below the CASA criterion of 12.2 m/s. Similar conditions occurred on the first test day (5th of August 2024, first measurement flights) with highest plume rise velocities just below 12 m/s. At other times and days, the wind speed was higher at very similar ambient temperatures, which resulted in lower measured peak plume rise velocities (peak plume rise velocity was around 10 m/s). That confirms that the CASA criterion will be met for all meteorological conditions that are warmer or windier than the most onerous conditions, which were both observed and modelled.

Even when the peak plume rise velocity was close to the CASA criterion, the air work pilots did not experience aircraft movements or impacts that were unusual compared to aircraft that are exposed to atmospheric turbulence that can be expected during normal flight operations.

However, like atmospheric turbulence, the potential impact on aircraft due to the exhaust plume can be surprising to pilots who fly over the stack while the aircraft is otherwise flying through calm, turbulence-free conditions. Therefore, the pilot in command should be aware of the power plant, and preferably avoid flying over the potential turbulence source, or at least avoid, if possible, crossing above the power plant at elevations below 2000 ft.

To further confirm the modelling results and the appropriateness of the applied modelling methodology, the CFD simulation was re-run with meteorological conditions and stack flow parameters as observed during the test days (7th of August 2024 between 10 and 11 am), with the simulated results then compared with the measurement results.

Figure 1 provides an example of the plume profiles obtained from the CFD (blue lines) compared to the plume profiles obtained from the measurements (red lines). See Section 5.3 for further plume profile comparisons.

Figure 2 summarises the highest recorded plume rise velocity per fly-through, plotted at the relevant elevation, for the individual test days and compares the results to the peak plume rise velocities obtained from the CFD simulations for the different wind cases. The primary x-axis (bottom) depicts the average plume rise velocity in accordance with the CASA criterion (half of peak value) and the secondary x-axis (top) depicts the maximum plume rise velocity. The modelled peak plume rise velocities (and average plume rise velocities) are for one particular time step in the simulation. At one and the same elevation, the modelled peak plume rise velocity (and CASA's average plume rise velocities) can vary over time (see Figure 40). According to the weather data, the wind speed on the 7th of August 2024 in the morning hours (10 to 11 am) was between 0.8 m/s and 1.9 m/s (see Figure 24). For the re-modelling ('observed' wind case), average wind conditions with wind speeds between 1.2 m/s and 1.5 m/s (depending on the height) were applied. This likely has resulted in lower predicted/modelled peak plume rise velocities than observed during the measurements where the wind speed may have been occasionally much lower during that period. The modelled "initial" wind case had similar ambient temperatures and a wind speed

at around 0.6 m/s at elevations below 100 m and therefore compares better with the observed peak plume rise velocities during that survey flight.

The measured plume profiles vary with the flight path through the plume, the exact meteorological conditions and plume shape at the time the aircraft was flying through the plume, and the elevation. Considering that natural variability, together with uncertainties in the modelling, the measurement approach and meteorological conditions, the results from the CFD model correlate well with the measurement results, providing confidence in the applied modelling approach.

Based on the simulation of the relevant most onerous meteorological conditions and the on-site exhaust plume measurements, it can be confirmed that the average plume rise velocities at 700 ft and above are below CASA's Critical Plume Velocity of 6.1 m/s (below peak plume rise velocity of 12.2 m/s).

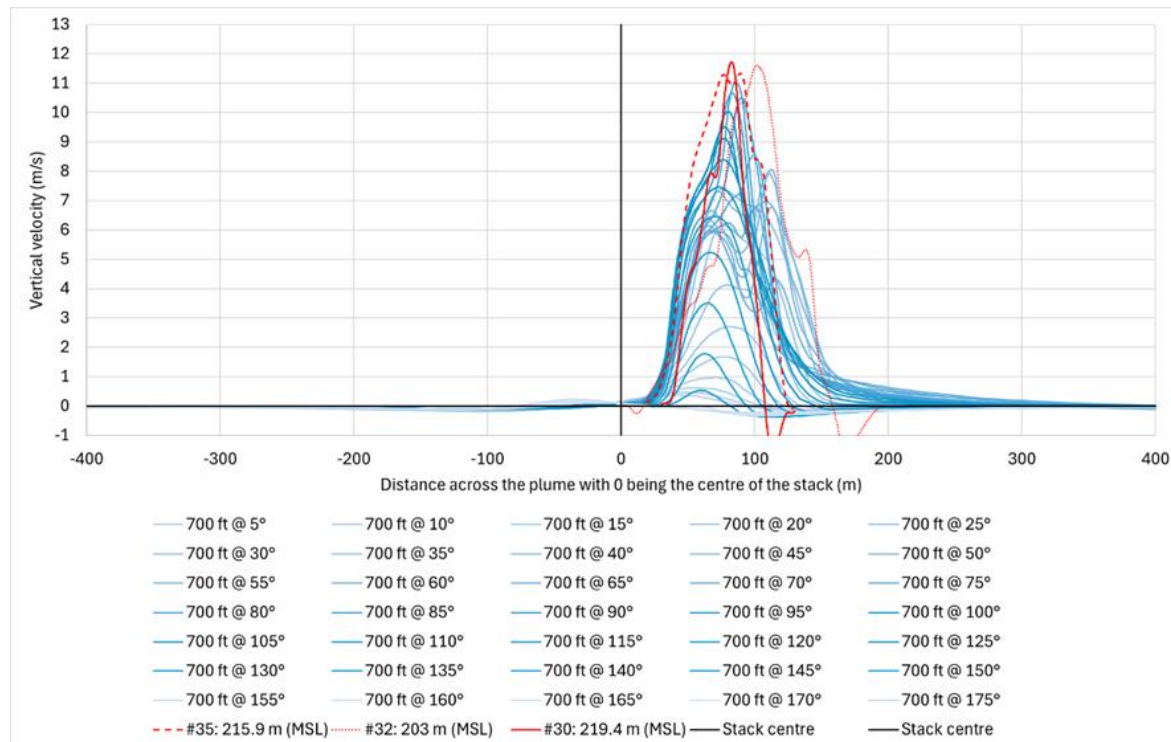


Figure 1. Plume profiles obtained from the CFD simulations based on stack-centred trajectories at 700 ft (AMSL) and a simulation time of 1440 s (blue) compared to the measured plume profiles as sampled at similar elevations on the 7th of August 2024 during the first plume survey flight between 10 am and 11 am (red).

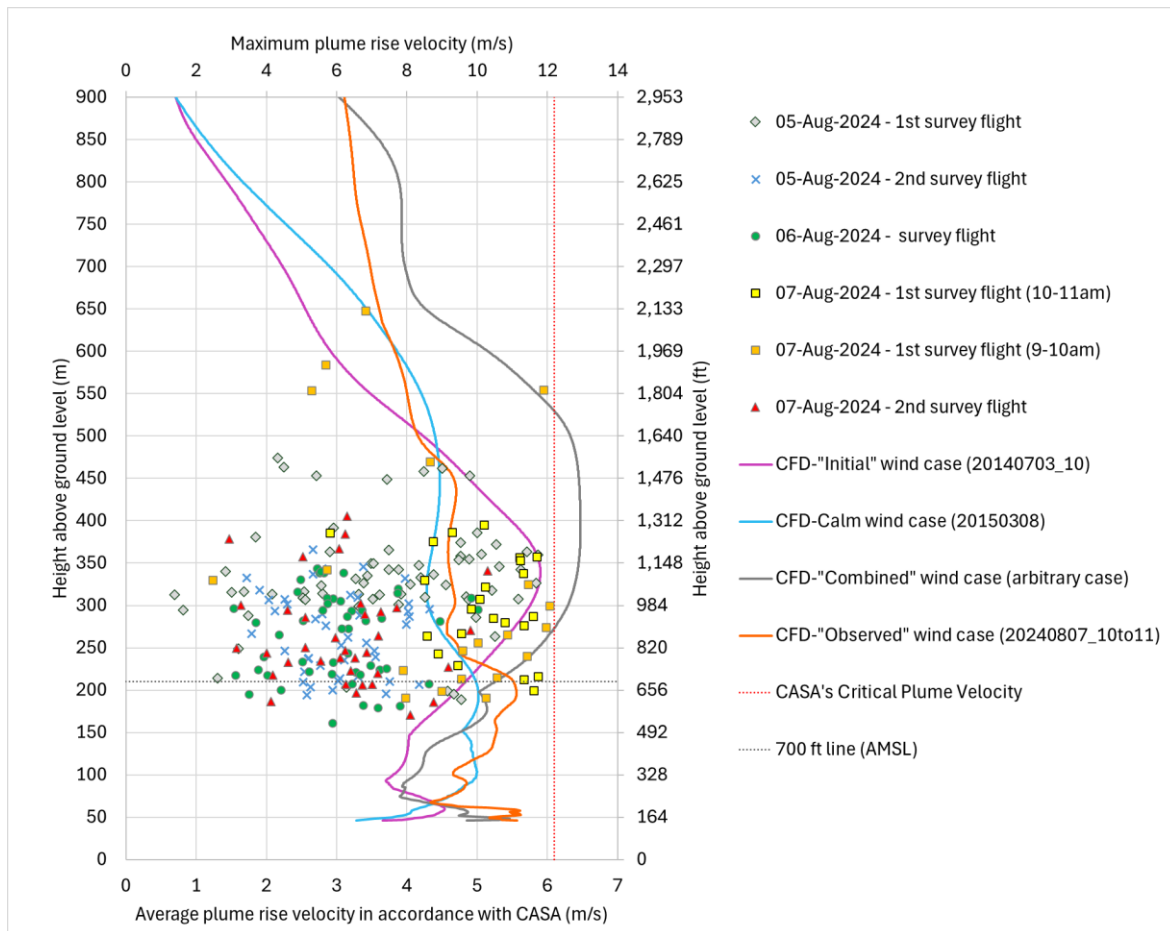


Figure 2. Highest recorded plume rise velocity per fly-through, plotted by elevation, for the individual test periods, compared to the peak plume rise velocities obtained from the CFD simulations for the different wind cases at the evaluated timestep (elevation of peak plume rise velocity and velocity value itself can vary over time). The primary x-axis at the bottom is the average plume rise velocity in accordance with CASA's criterion. The secondary axis at the top of the plot is the peak plume rise velocity, which relates to double the CASA criterion.

Executive summary	3
1 Introduction	8
2 CASA criterion and measures already in place	9
3 Preceding CFD assessment	10
3.1 Simulation software and methodology	10
3.2 Meteorological conditions and terrain	11
3.3 Geometry and computational domain	13
3.4 Input parameters and boundary conditions	15
3.5 Results	16
4 On-site plume measurement	25
4.1 Measuring principle and program	25
4.1.1 Measurement equipment	25
4.1.2 Plume sampling	26
4.1.3 Plume rise velocity estimation from flight data	28
4.2 Preparation and consideration	28
4.2.1 Aircraft safety	28
4.2.2 Meteorological criteria and weather forecast	29
4.3 Timetable and flight statistics during test days	30
4.4 Meteorological conditions during test days and used as input for CFD	33
4.5 Plant operation during test days	35
4.6 Results	37
4.7 Interpretation of results	40
5 CFD re-assessment	41
5.1 Input parameters	41
5.2 Results	42
5.3 Comparison with measurements	46
6 References	53

1 INTRODUCTION

Tallawarra B is a gas fired power project comprising an open-cycle gas turbine (OCGT) plant designed to meet the peaks of electricity demand in the NEM (National Electricity Market). The OCGT plant produces a large flowrate of hot exhaust gas that rises quickly into the atmosphere, generating updraughts with potentially high vertical velocities at high elevations. These updraughts and vertical velocities have potential to adversely affect aircraft flying in the vicinity of the stack.

To reduce temperature, buoyancy, and hence vertical velocity of the plume, a plume dispersion device (PDD) has been mounted on the top of the stack.

Due to the complexity of the buoyant driven flow around the stack, the effectiveness of the PDD has been assessed via Computational Fluid Dynamics (CFD) simulations during the design process.

After completion of the project, tailored aerodynamic measurements of the plume have been undertaken to confirm the appropriateness of the CFD modelling and that the Civil Aviation Safety Authority (CASA) criterion on the vertical plume rise velocity is met.

To compare the observations from the flight measurements and the CFD modelling approach, the exhaust plume has been modelled again based on the meteorological conditions observed on-site during the flight measurements. The model results are then compared to the measured plume rise velocities for very similar meteorological conditions.

This document summarises the methodology and results of the previous CFD study undertaken during the design process (Section 3) and the on-site aerodynamic plume measurements (Section 4). The re-modelling of the exhaust plume based on the meteorological conditions during the measurement campaign, and a comparison with the measured values, is discussed in Section 5.

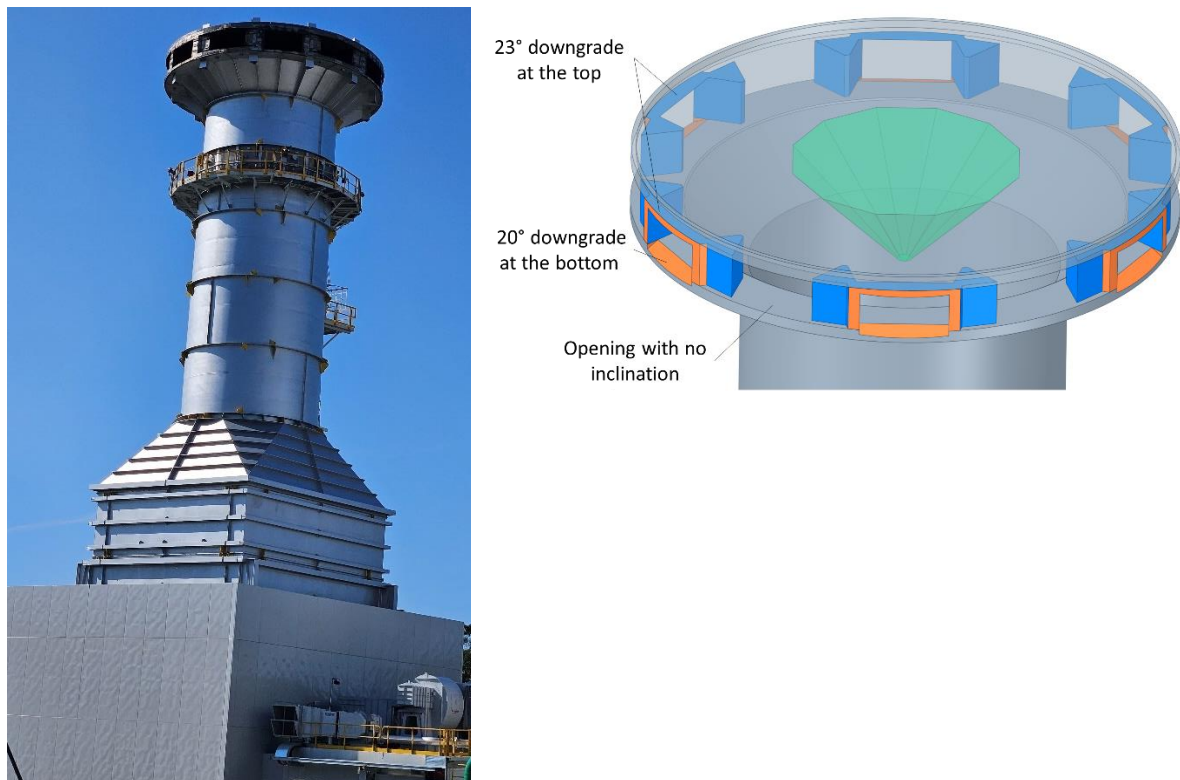


Figure 3. Photo of the Tallawarra B stack (left) and sketch of the plume dispersion device on top of the stack, as designed by the supplier (right) [12].

2 CASA CRITERION AND MEASURES ALREADY IN PLACE

Exhaust plumes can create substantial vertical updrafts and so the potential impact of plume rises on aircraft needs to be assessed. The Advisory Circular (AC 139.E-02 v1.0) issued by CASA (Civil Aviation Safety Authority) [16] proposes to use CFD modelling or scaled, physical modelling to assess the exhaust plume of stacks with engineering modifications such as the use of a PDD. For the current project, CFD modelling was seen to be appropriate for assessing the exhaust plume rise of the Tallawarra B power plant, in combination with post-commissioning on-site measurements to confirm the efficacy of the modelling.

In accordance with Advisory Circular (AC 139.E-02 v1.0) [16] and CASA's notification on the Tallawarra B project [10], the average plume velocity should not exceed 6.1 m/s at 700 ft.

If the vertical velocity profile has a Gaussian distribution, the average plume rise velocity ('top hat' profile velocity) would be half of the maximum plume rise velocity (peak plume rise velocity). However, the velocity profile of a plume released by a PDD does not have a Gaussian distribution. As the real velocity profile differs from a Gaussian distribution, the equivalent top hat velocity will no longer necessarily be half of the maximum velocity. The averaging area is also uncertain, with the plume edges being indistinct. CASA stated that they will accept half of the maximum CFD-derived plume rise velocity as the average plume velocity at 700 ft, for comparison with CASA's Critical Plume Velocity of 6.1 m/s. That is, the criterion for the current project is to not exceed a peak plume rise velocity of 12.2 m/s at 700 ft.

Even if that criterion is seen to be sufficient for CASA, it is noted that such velocity criterion is unlikely to be sufficient to fully capture the potential impacts on aircraft (e.g. G-load). Beyond specific aircraft parameters (e.g. weight, wingspan, speed etc.) the G-load not only depends on the peak plume rise velocity, but also depends on how fast the peak is reached (very wide plume with moderate velocity increase/decrease vs. very narrow plume with an abrupt velocity increase/decrease).

Pilots need to be aware of the presence of the power plant and exercise caution when the Tallawarra B stack is in operation. It is noted that a multi-layered risk mitigation program has been implemented by Energy Australia as follows:

- Alerting through Aviation Information Packages (AIP): Added plume symbol to aeronautical charts; issued NOTAM (Notice to Airmen) and ERSA (En Route Supplement Australia) note including FAC (Facilities) note included in Local Traffic Regulators to the effect that aircraft should avoid overflying the power station when it is operating.
- Tallawarra B has flashing lights on exhaust stack when operating (lights medium intensity, white in daylight hours and red at night) – per CASA requirements
- Completed a pilot awareness program

3 PRECEDING CFD ASSESSMENT

This section summarises the CFD modelling and assessment that has been carried out during the design process prior construction. A more detailed documentation of the plume modelling can be found in [9] and [11].

3.1 Simulation software and methodology

Tallawarra B Power Station plume modelling was carried out using the CFD-software ANSYS Fluent (Release 2020 R1) [1], [2], [3]. Fluent is a commercial generic CFD software for modelling fluid flow, heat transfer and chemical reactions in complex geometries. Table 1 lists the CFD model parameters used.

Table 1. CFD model parameters.

Parameter	Description
CFD-method and solver	Pressure based, steady-state Reynolds-averaged Navier-Stokes (RANS) solver with a spatial discretisation method of 2 nd order. A second order discretisation method was used in order to avoid numerical diffusion. As the flow field gave indication of a transient behaviour, a unsteady Reynolds-average Navier-Stokes (URANS) solver was used to analyse the transient plume behaviour in a final stage.
Turbulence model	Realizable k- ϵ model with scalable wall function [2], [4]. The Realizable k- ϵ was developed to more accurately predict the spreading rate of planar and round jets (involving all jet regions) and provides adequate performance for flows involving rotation, boundary layers under strong adverse pressure gradients, separation and recirculation [1], [2]. This turbulence model was used because of the anticipated flow behaviour (jet flow at stack). A scalable wall function was used for the ground effects.
Thermal conditions	Ground surface was considered as flat, with a constant ground temperature according to the meteorological data provided [5]. The buoyancy effects of the hot smoke at the stack outlet are considered by using the incompressible ideal gas law and solving the energy equation rather than using the Boussinesq approach. The former approach determines the air density via the ideal gas law at a defined operating pressure, whereas the latter considers the buoyancy forces in the momentum equation where the density is determined via the thermal expansion coefficient β and a constant operating temperature T_0 . The Boussinesq approximation eliminates the density from the buoyancy term and is only valid as long as changes in actual density are small $\beta(T-T_0) \ll 1$ [1].

3.2 Meteorological conditions and terrain

The meteorological input data for the validation case were provided by Katestone [5] and [6]. The following data were extracted from the “20140703_10” and 20150308 - Calm data set provided:

- Wind speed
- Wind direction
- Potential temperature (The temperature difference between a rising parcel of air and the adjacent ambient air)

Figure 4 illustrates the profiles of the applied atmospheric boundary layer (ABL). The plume rise was analysed for the meteorological conditions “20140703_10” as illustrated in Figure 4. These conditions were selected from the TAPM modelling output that resulted in the 99.9th percentile plume average vertical velocity at 700 ft. Based on the initial study and CFD results, a further wind case with rather calm wind conditions has been analysed, to assess the sensitivity of the plume behaviour and the maximum plume rise velocity to the wind. A calm wind was defined by Katestone as being less than 0.5 m/s.

Figure 5 shows the segment of occurring wind direction relative to the domain orientation for both wind cases. Depending on the height, the wind direction for the ‘initial’ wind case (20140703_10) changes from NNE (7°) to SSW (212°) and the wind speed from 0.5 to 6 m/s (2000 m above ground level). The wind profile for the calm wind case (20150308 – Calm) changes direction from NNE (17°) to W (272°) and the wind speed changes from 0.1 to 3.8 m/s as the elevation changes from 0 to 2000 m (0 to 6562 ft) above ground level. At around 210 m (about 700 ft), the wind speed is less than 0.5 m/s. In both wind cases, the potential temperature increases with height, which relates to a stable atmosphere. The domain orientation (as shown in Figure 5) was chosen to suit each wind profile so that the majority of the wind directions are captured with the inlet boundary conditions and so the domain orientation is different for the two wind profiles.

Compared to the initial wind profile, the average ambient temperature (from ground level to 2000 m or 6562 ft) for the calm wind profile is 7.2°C higher. A change of 7.2°C in the ambient temperature seems very minor. However, it seems that calm wind case has very different results to the ‘initial’ wind case, so there was a need to understand the temperature and wind effects separately. To analyse the sensitivity of the plume rise velocity to the wind speed and the ambient temperature individually, a third wind case has also been assessed. This ‘rather artificial’ wind case combines the wind direction and speed of the calm wind case (20150308 – Calm) with the “cooler” temperature profile of the ‘initial’ wind case (20140703_10). The resulting three wind cases analysed are summarised in Table 2 below.

Table 2. Wind cases used for the CFD-study.

Wind case	Wind profile	Temperature profile	Average ambient temperature
'Initial' wind case	20140703_10		16.4°C
Calm wind case	20150308 – Calm		23.6°C
'Combined' wind case	20150308 – Calm	20140703_10	16.4°C

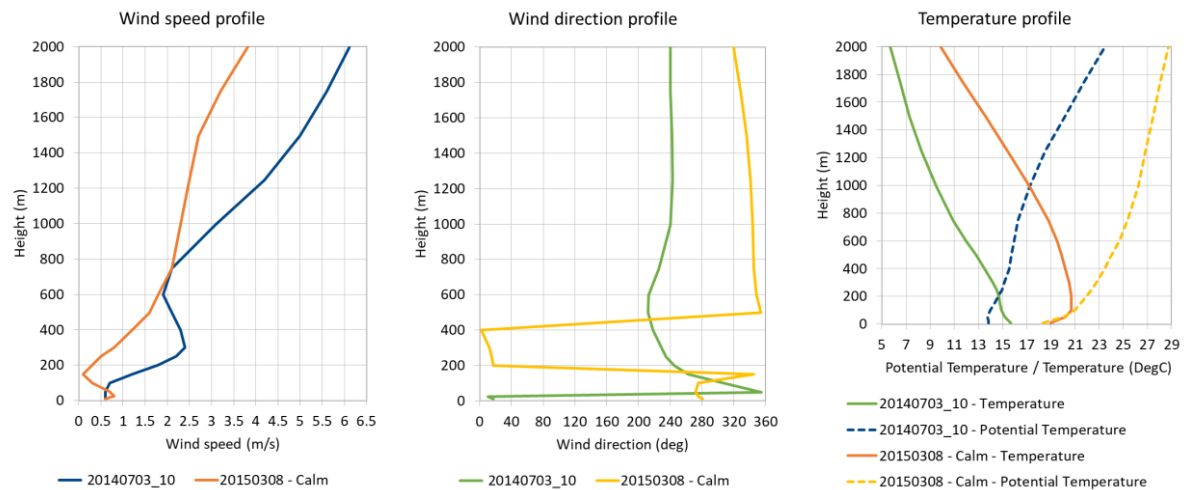
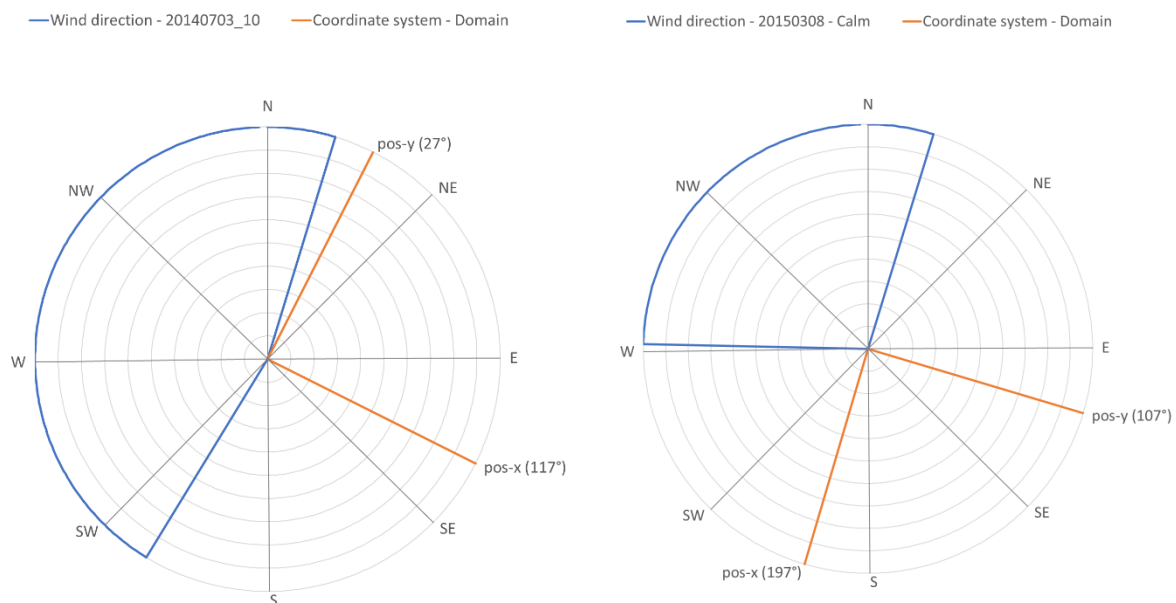
**Figure 4. Profiles of wind speed (left), wind direction (middle) and temperature (right) used for the assessment [5], [6].****Figure 5. Segment of occurring wind direction (blue) and coordinate system of the computational domain (orange) for the 'initial' (left) and the calm (right) wind profile.**

Figure 6 shows the terrain within an area of 34 × 34 km around the assessed site with a resolution of 1 km. As can be seen in Figure 6, the terrain around the power station within several kilometres is relatively flat (red circle). Because the domain for the CFD plume analysis is within the order of the terrain resolution, a flat terrain was used for the investigation. It was assumed that the terrain and surface influences were included in the velocity profile provided.

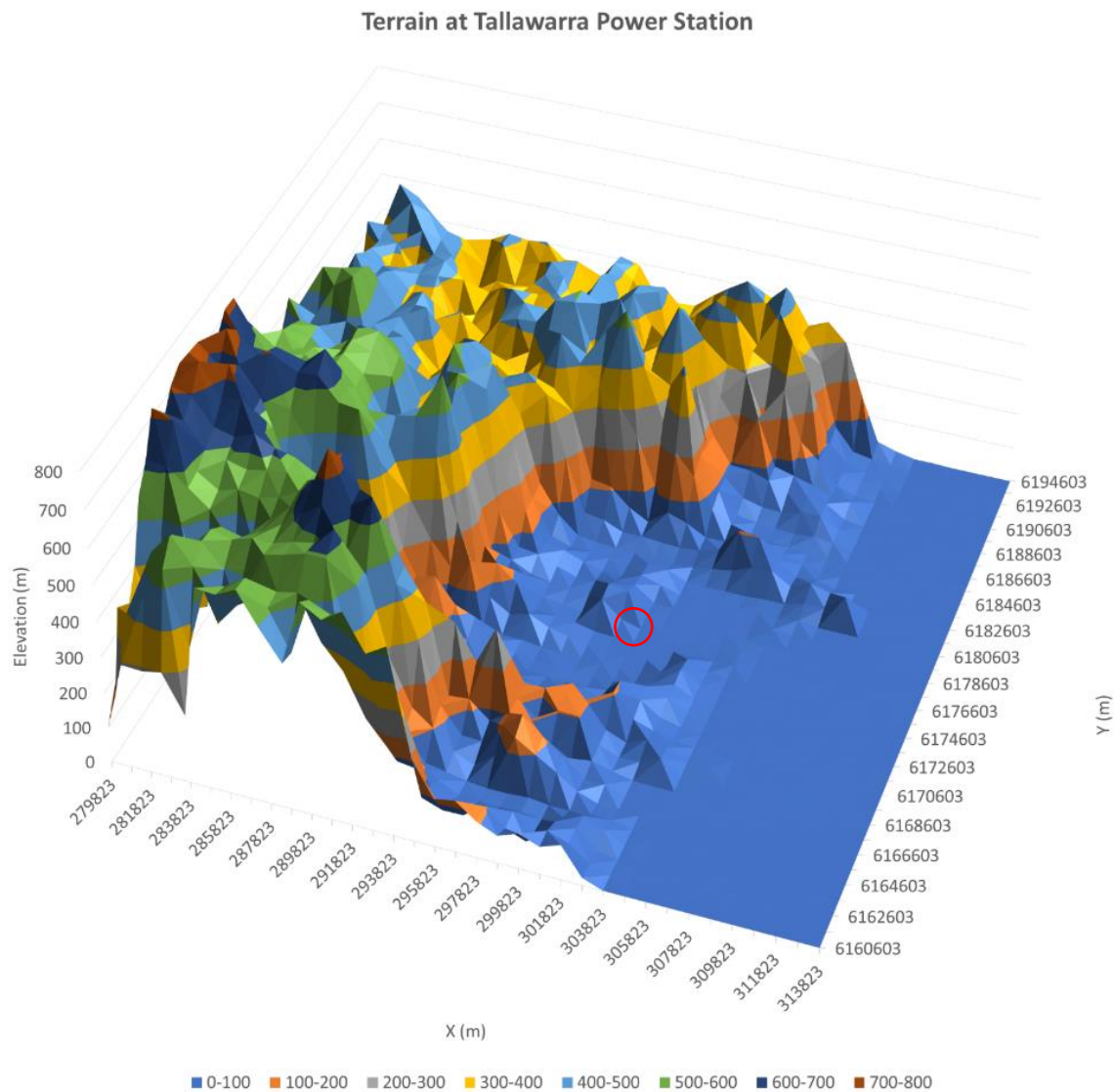


Figure 6. Terrain within an area of 34 km x 34 km around the site (resolution: 1 km).

3.3 Geometry and computational domain

Figure 7 depicts the computational domain and mesh for the plume modelling. An overall domain size of 3700 x 3700 m with a height of 2000 m was adopted so that the boundary conditions would have no adverse influence on the simulated plume flow around the stack. Domain orientation for the two velocity profiles is illustrated in Figure 5. The stack was positioned in the middle of the domain (in x-direction) and 3000 m upwind of the outlet boundary condition (in y-direction). The station building was not modelled. The point of origin is at the stack centre at ground level. The adapted design of the PDD has in total 12 openings all at the same level evenly distributed around the circumference. To increase the separation between the individual jets and increase the overall entrainment, the outlet of every second opening has a downgrade inclination with a 23° deflector at the upper surface and a 20° chamfer at the bottom surface. Table 3 lists the geometric stack and PDD parameters according to [12] to [15]¹. Figure 3 shows a sketch of the assessed PDD design.

Table 3. Geometric parameters of the PDD solution according to [12] to [15].

Parameter	Value
Stack X coordinate (m)	298,895
Stack Y coordinate (m)	6,177,812
PDD exit height above ground (m)	45
PDD outlet dimensions (m)	1.93 x 0.98 1.85 ¹ x 0.96 (inclined)
PDD total outlet area (m ²)	22.1
PDD outlet angle from vertical (deg)	90 113 (every 2 nd opening)
PDD stack split number	12
PDD exit distance from stack CL (m)	5.7

¹ The PDD diameter in the provided Parasolid 3D CAD file [14] was about 20 mm less than the PDD diameter (11.456 m) noted in the “as built” drawings [13]. The PDD diameter of the provided 3D CAD geometry used for the CFD study has been adjusted to reflect the “as built” diameter. That resulted into a slightly reduced opening area for the inclined openings.

The geometry was meshed with polyhedral surface elements in combination with hexahedral-core elements (see Figure 7). Polyhedral elements are only employed to connect the prism with the hexahedral elements in the direct proximity of the walls and boundaries. As shown in Figure 7, the remaining domain is discretised with hexahedral elements exclusively. To resolve the boundary layer at walls, prism elements were used. The maximum element sizes employed were as follows:

- outer domain surface (top, sides and ground): 10 m
- stack surface: between 0.8 and 0.4 m, and;
- global mesh size within the domain: 25 m.

A body of influence with a total height of 200 m was used to create a fine mesh around the stack plume for enhanced resolution. Element sizes were defined based on distance away from the stack as follows:

- 0.1 m within the internal diffuser region and immediately outside;
- 0.6 m within the first 40 m, and;
- 1.2 m within the following 120 m.

The resulting initial mesh had approximately 15 million elements.

Based on this initial mesh, several mesh refinement steps within the plume region were undertaken so that the plume area was sufficiently resolved. The refinement steps and mesh resolution used were obtained from the mesh refinement study already undertaken during the validation case. The final maximum element size within the plume region was about 3.2 m. These parameters resulted in a mesh size with approximately 35 million elements.

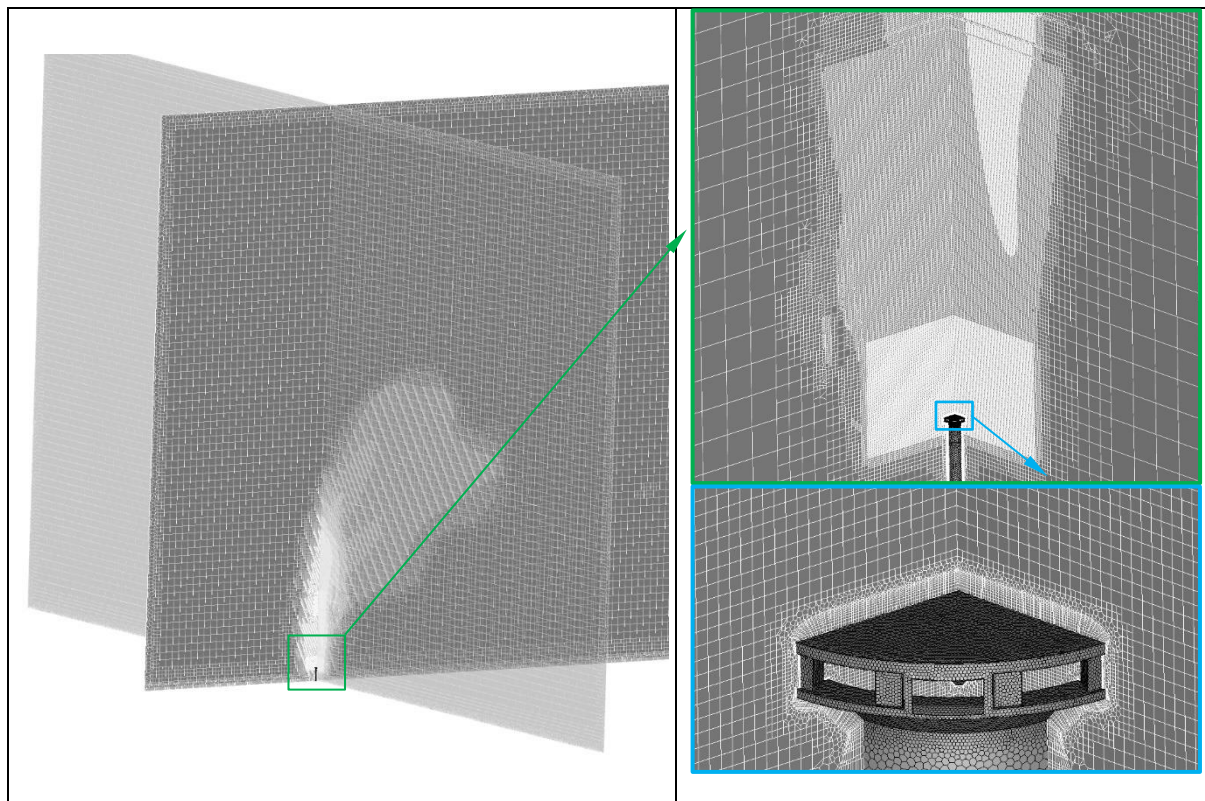


Figure 7. Computational mesh after several mesh refinement steps.

3.4 Input parameters and boundary conditions

The flow field around the stack is defined by the wind speed and temperature profile according to Figure 4. As the profiles of the ABL start at a height of 10 m, all values were extrapolated to the ground level. The wind direction and potential temperature were kept constant from 10 m to the ground, whereas the velocity was extrapolated by assuming 0 m/s and a roughness height of 0 m at ground level. The surface roughness has only a slight influence on the velocity profile below a relative elevation of 10 m. The stack flow parameters according to [15] are given in Table 4. Table 5 lists all applied boundary conditions for the plume modelling.

Table 4. Stack flow parameters [15].

Parameter	Value
Average exit velocity at each nozzle outlet ²	89.15 m/s*
Total mass flow rate	760.9 kg/s
Exit temperature	639.3 °C

² Hand calculation based on average opening/outlet area, total mass flow rate, exit temperature / density and an atmospheric pressure of 101.325 kPa.

Table 5. Boundary conditions for the validation plume modelling.

Location	Boundary condition
Two sides of the domain (negative x and y)	Velocity inlet with ABL (including wind direction and temperature) according to Figure 4 [5].
Two sides of the domain (positive x and y)	Pressure outlet with temperature profile according to Figure 4
Top of the domain	Wall with full slip condition and constant temperature of 23.4°C to for wind case '20140703_10' and 28.8°C for wind case '20150308 – Calm' to maintain the velocity and temperature on the top of the domain.
Ground	Wall with fixed wall temperature of 13.9°C for wind case '20140703_10' and 18.4°C for wind case '20150308 – Calm' (surface roughness height $z_0 = 0.0\text{ m}$)
Stack wall	Adiabatic wall
Stack outlet	Mass flow inlet (according to Table 4, right column) applied down in the cylindrical stack as the internal nozzle and stack geometry is resolved (see Figure 7).

3.5 Results

The plume generated by the PDD led to quite high fluctuations of the monitored plume velocities, indicating a transient behaviour. To appropriately assess the plume rise velocity, the flow field was finally analysed with a transient solver over a period of up to 30 minutes. Figure 8 to Figure 10 illustrate the time-dependent peak velocity fluctuations at three different heights for the wind cases analysed. The monitored values are the maximum occurring vertical velocity values within a horizontal plane cut through the whole domain. Based on the transient simulation, the detailed plume behaviour (see Figure 11 to Figure 14) was assessed at the times when the maximum peak rise velocity occurred at the three monitored elevations for the individual wind cases.

For the 'initial' wind case this was at 1000 ft above mean sea level (AMSL) at 370 s, for the calm wind case it was at 650 ft (AMSL) at 560 s, and for the 'combined' wind case it was at 1000 ft (AMSL) at 1060 s. For the three wind cases, the average value, as well as the maximum and minimum occurring peak rise velocities observed during the simulation period of up to 30 minutes for the different elevations, are listed in Table 6.

Note that the plume rise velocity values at the different elevations were monitored at 1 s intervals, but result files were saved every 10 s. Therefore, a result file close to the observed peak value was chosen for the detailed analysis.

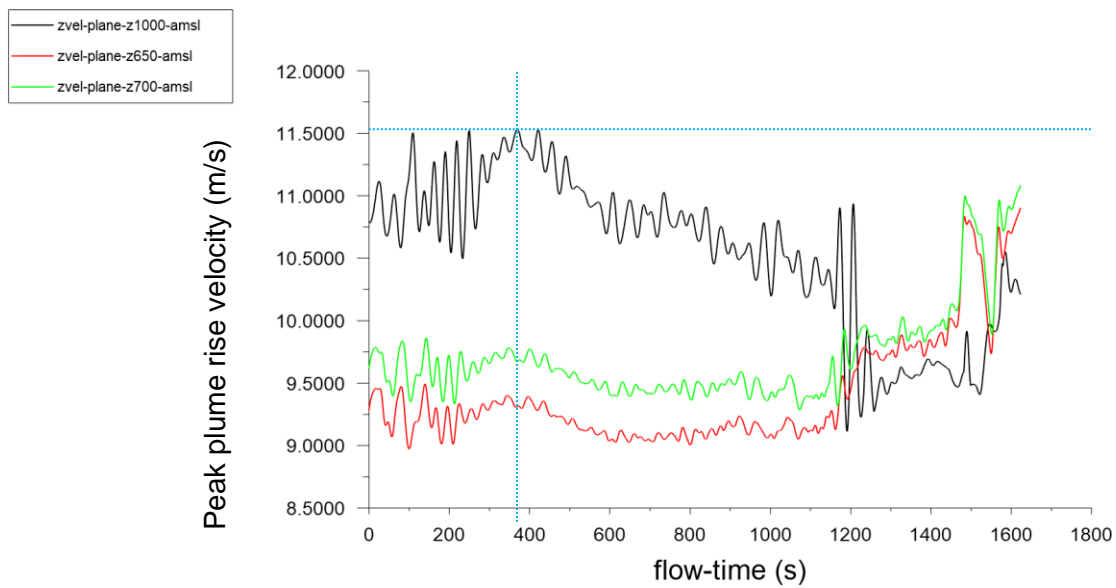


Figure 8. Monitored peak velocities at different heights depending on the simulation time – ‘Initial’ wind case. The blue dotted vertical line illustrates the simulation time chosen for the detailed analysis.



Figure 9. Monitored peak velocities at different heights depending on the simulation time – Calm wind case. The dashed orange vertical line illustrates the simulation time chosen for the detailed analysis.

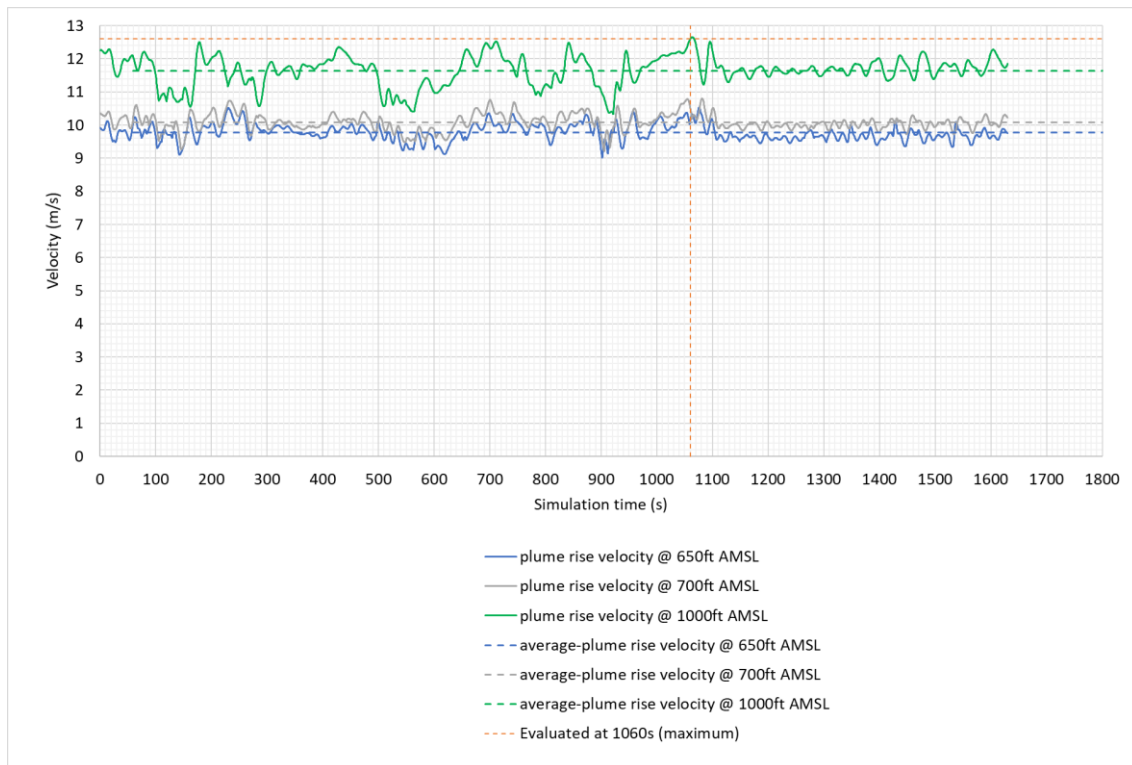


Figure 10. Monitored peak velocities at different heights depending on the simulation time – ‘Combined’ wind case. The dashed orange vertical line illustrates the simulation time chosen for the detailed analysis.

Table 6. Average values and outliers of the peak plume rise velocity at different heights observed during the simulation period of about 30 minutes. Numbers in parentheses are deviations from the average.

Elevation	Average peak plume rise velocity (m/s)	Maximum peak plume rise velocity (m/s)	Minimum peak plume rise velocity (m/s)
‘Initial’ wind case (20140703_10)			
650 ft AMSL	9.3	11.0 (+1.7)	9.0 (-0.3)
700 ft AMSL	9.6	11.2 (+1.6)	9.3 (-0.3)
1000 ft AMSL	10.8	11.6 (+0.8)	9.1 (-1.7)
Calm wind case (20150308 – Calm)			
650 ft AMSL	8.9	10.1 (+1.2)	7.2 (-1.7)
700 ft AMSL	8.8	10.0 (+1.2)	7.1 (-1.7)
1000 ft AMSL	8.3	9.6 (+1.3)	6.9 (-1.5)
‘Combined’ wind case (Wind: 20150308 – Calm, Temperature: 20140703_10)			
650 ft AMSL	9.8	10.5 (+0.7)	9.0 (-0.8)
700 ft AMSL	10.1	10.8 (+0.7)	9.2 (-0.9)
1000 ft AMSL	11.6	12.7 (+1.1)	10.3 (-1.3)

Based on the chosen time step, Figure 11 shows the plume envelope of 6 m/s velocity for the three different wind cases. The lower wind speed and ambient temperature leads to a slimmer and more vertical stretched single jet where the core temperature is slightly higher and more maintained. This results in a higher buoyancy force and therefore higher plume rise velocities compared to the other wind cases with higher wind speeds or higher ambient

temperatures. As demonstrated in Figure 8 to Figure 10, the plume behaviour and plume rise velocities show a transient behaviour. Depending on the time and local flow situation, jets detach and attach again, so that the plume rise velocity increases and decreases depending on the time and height. For the combined wind case, this leads to peak plume rise velocities that can exceed 12.2 m/s at 1000 ft and above for short periods. At the analysed simulation time (1060 s) the highest observed peak plume rise velocity is 12.9 m/s at 1270 ft. This is illustrated by Figure 12 that shows the maximum vertical and absolute plume velocity against height as well as the atmospheric wind speed profile according to Figure 4.

Figure 13 provides information about the horizontal displacement of the peak plume rise velocity relative to the stack centre for the three wind cases. In general, the horizontal displacement of the plume is mainly caused by the applied wind conditions (relative to the buoyancy force) and will vary for different wind speeds, directions and ambient temperatures. Based on the analysed cases the highest plume rise velocities are observed in the proximity of the stack centre within a radius of 100 m (see Figure 12 vs Figure 13).

Figure 14 and Figure 15 illustrate the plume extent at 700 ft and 1000 ft respectively for all three wind cases based on value-clipped contour plots for vertical velocity. Only vertical velocities > 1 m/s are shown in the plots and so the shown plume extent needs to be interpreted in that context/accordingly. Depending on the elevation, there can be several pointy peaks or a more stretched/wider single peak of the vertical velocity.

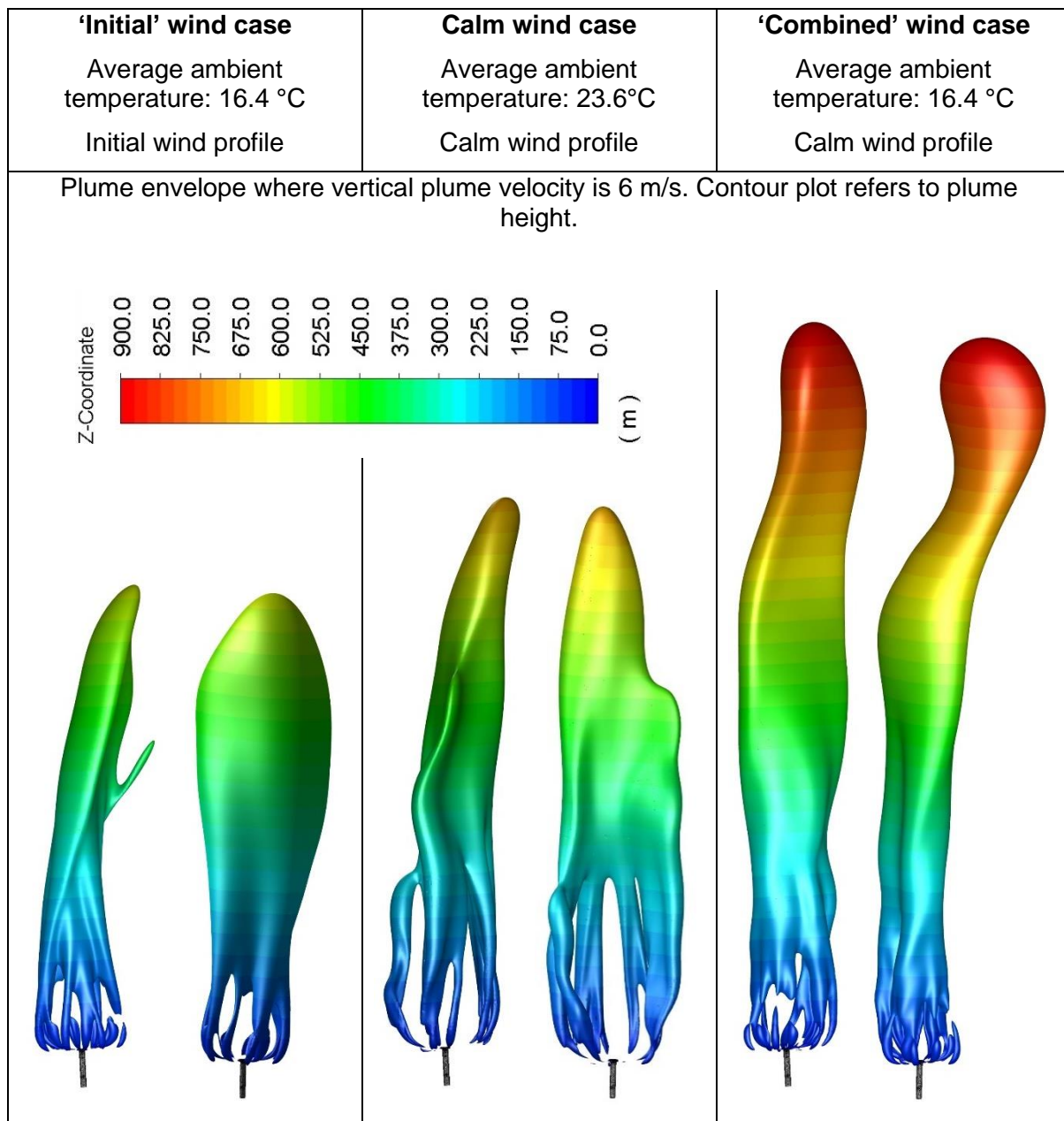


Figure 11. Plume envelope where the plume rise velocity is 6 m/s for assessed PDD design and the different wind scenarios. Colouring of the envelope depicts the plume height.

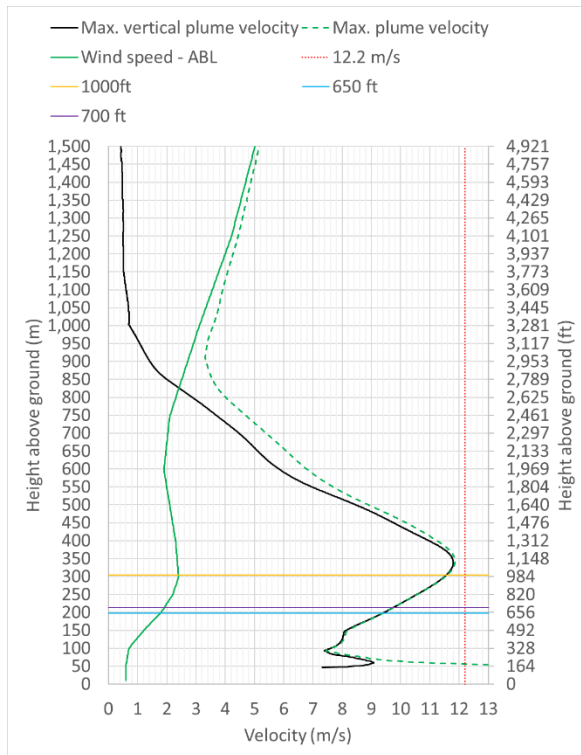
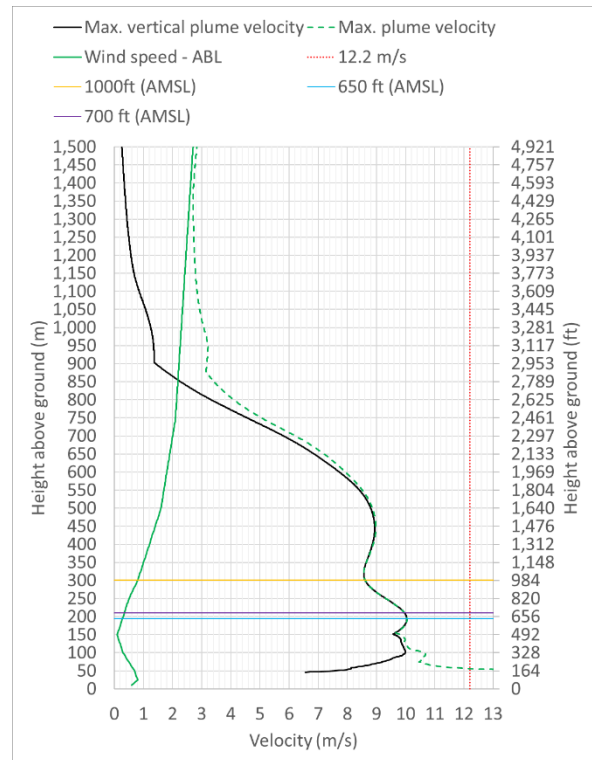
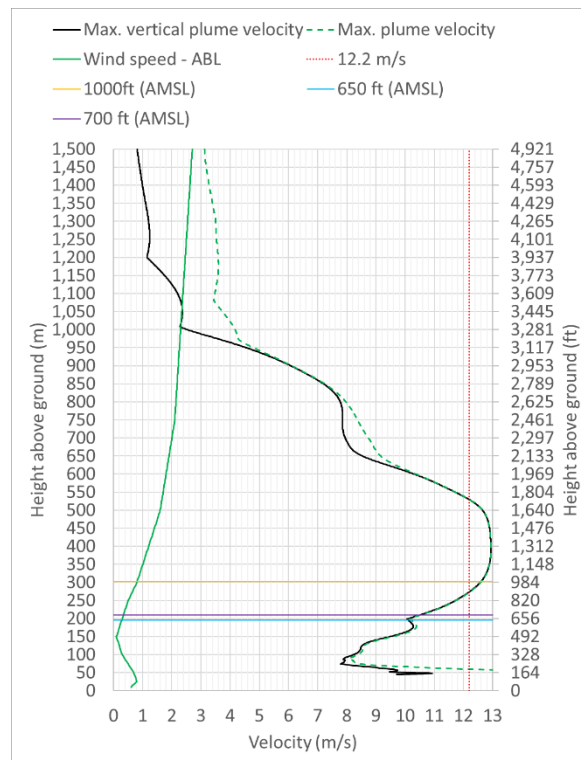
‘Initial’ wind case**Calm wind case****‘Combined’ wind case**

Figure 12. Wind speed and maximum vertical and absolute plume velocity against height for the three analysed wind cases.

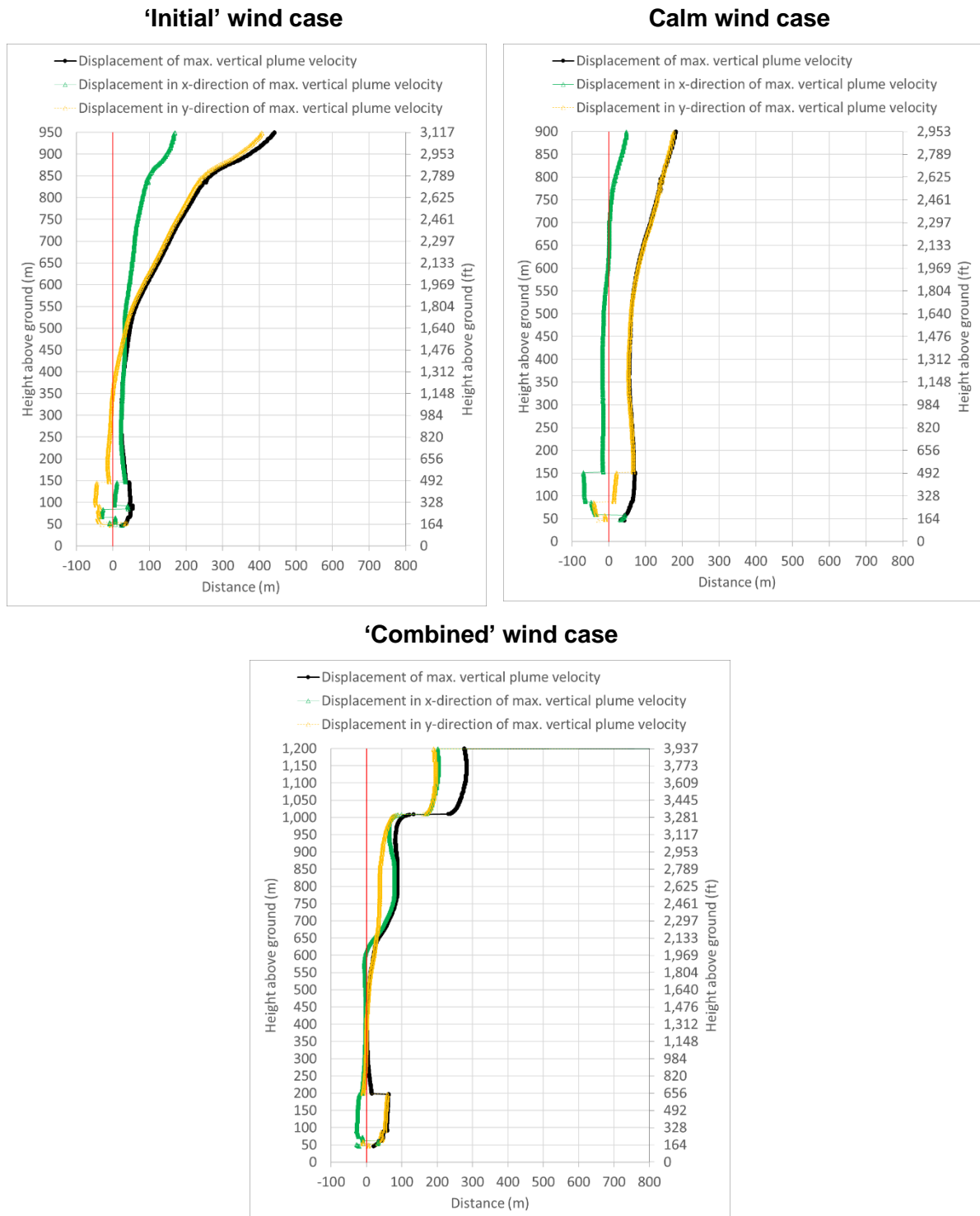


Figure 13. Displacement of maximum vertical velocity component against height for the three analysed wind cases.

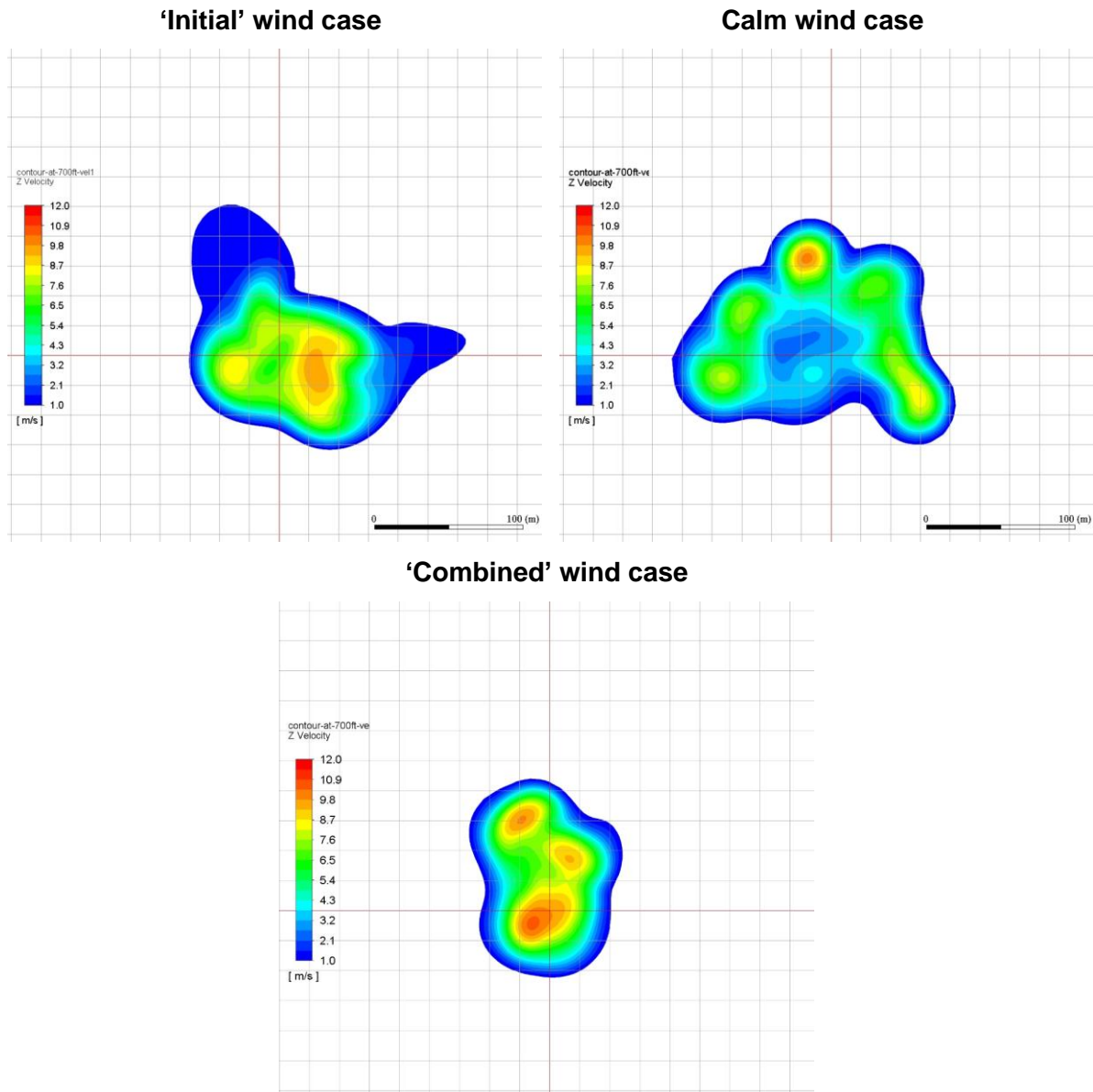


Figure 14. Plume extent shown as a contour plots of vertical velocity in a horizontal plane at 213 m (700 ft) elevation for the three analysed wind cases. The plume area is clipped to vertical plume velocity > 1 m/s. Grid spacing is 20 m with stack centre at the origin (red lines).

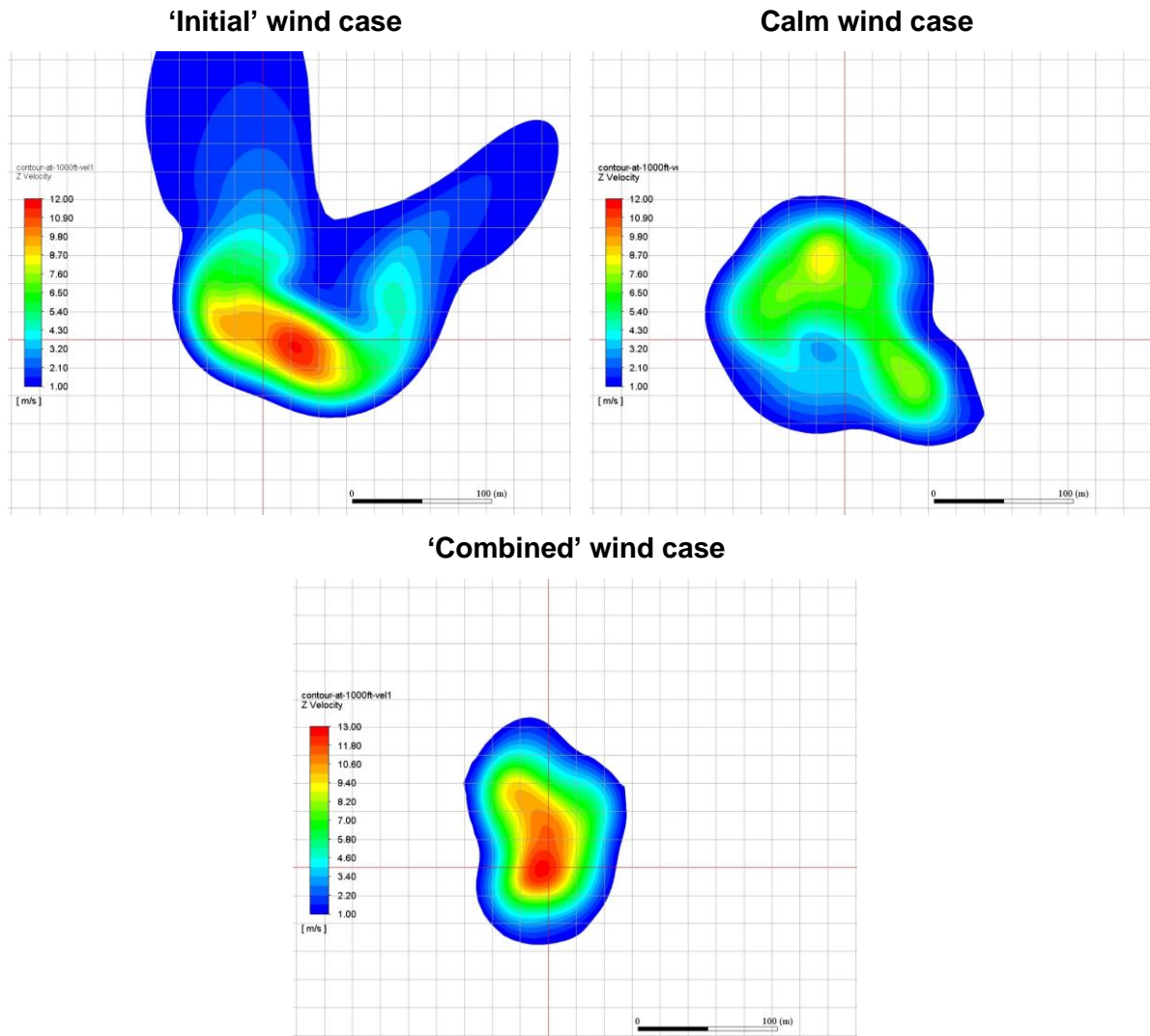


Figure 15. Plume extent shown as a contour plots of vertical velocity in a horizontal plane at 305 m (1000 ft) elevation for the three analysed wind cases. The plume area is clipped to vertical plume velocity > 1 m/s. Grid spacing is 20 m with stack centre at the origin (red lines).

4 ON-SITE PLUME MEASUREMENT

The on-site plume measurements were performed by the Austrian company TS Avionics GmbH which is a 100% subsidiary of Turbulence Solutions GmbH. Turbulence Solutions is developing an innovative aircraft stability product and, in doing so, has world-leading expertise in the measurement of atmospheric turbulence, and the effect that turbulence has on aircraft. The specialised expertise in this area made that company perfectly suited for measuring and analysing the turbulence and vertical wind speeds created by the exhaust plume of the Tallawarra B power station.

This section documents the on-site plume measurements undertaken, presents measurement results in relation to the CASA criterion, and discusses potential impacts on aircraft.

4.1 Measuring principle and program

4.1.1 Measurement equipment

A Cessna 172 hired by Energy Australia and operated by Airspeed Aviation was equipped with a self-contained measurement probe mounted on the strut (see Figure 16) and inertial sensors IMU¹ and AHRS²) mounted in the cockpit at the centre of gravity. The flow sensor probe measures the flow field based on differential pitot pressures in three different directions, while the flight dynamics impact is measured by the inertial sensors in the cockpit as well as by acceleration and gyroscope sensors in the probe mounted at the strut. Barometric pressure and GPS signals are also logged by sensors in the cockpit. By measuring the motion of the aircraft in combination with the flow field and the sensor motion, it is possible to extract the flow impact on the measurement probe due to the aircraft motion, and account for that to obtain the flow field and turbulence in the atmosphere, or in this case of the exhaust plume. The probe samples data at 500 Hz and the cockpit logger at 200 Hz. The result is a high-rate sampling of the flow the aircraft is flying through (500 Hz, one measurement every 2 ms which is equivalent to 0.1 m sampling at a flight speed of 50 m/s). Further information on the measuring principle and the flow sensor can be found in [17], [18] and [19].

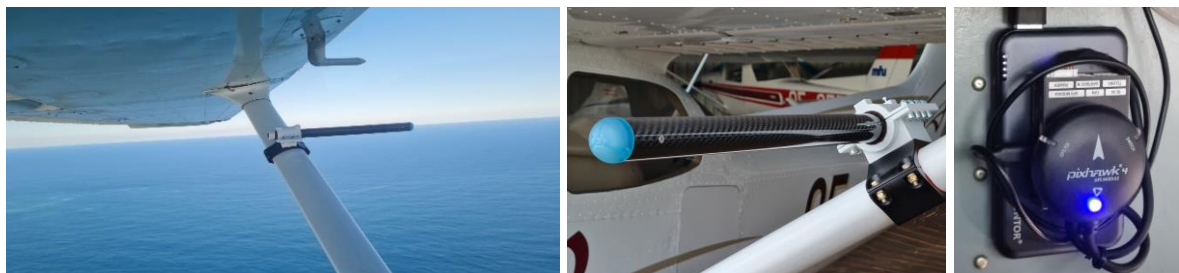


Figure 16. Self-contained flow sensor probe mounted on the strut (left and middle picture) and inertial sensors mounted in the cockpit (right picture)

¹ Inertial Measurement Unit

² Attitude and Heading Reference System

4.1.2 Plume sampling

The exact position and extent of the exhaust plume depend on the meteorological conditions (temperature, wind speed and direction). Therefore, a large number of fly-throughs are required to collect sufficient plume sampling data to be able to assess the plume characteristics with sufficient confidence.

A figure-eight manoeuvre was seen to be the most efficient pattern to optimise number of fly-throughs of the Tallawarra B exhaust plume, in the available time within weather windows with appropriate conditions. Beginning from the initial fly-through the anticipated figure-eight (see left plot in Figure 17) is defined by 1) a 10 s straight segment, 2) a 10 s high-bank turn, 3) a 10 s straight segment preparing the second fly-through, 4) a 10 s straight segment, 5) a 10 s turn to return to the sampling target, 6) a 10 sec straight segment preparing the next fly-through. This would result in 2 fly-throughs every 60 s, and for multiple sequential manoeuvres, in 120 fly-throughs per hour. The discussed pattern is for an airspeed of 35 m/s, i.e. 10 sec corresponds to 350 m, as indicated by the 6 legs. That requires a turn rate of $21^\circ/\text{sec}$, which leads to 1.6 g turns for 35 m/s and is well within the normal operational envelope of the aircraft. The 10 s turn rate was optimised during the test flights to reduce the g-load during the turns.

The exact position and angle of the pattern was varied to sample a variety of tracks through the plume. These variations were achieved by actively offsetting the pattern for sequential fly-throughs (GPS feedback), but also occur naturally during actual flight tests due to typical flight control variations, as well as the change of the actual plume shape and location. Multiple sequential manoeuvres after six individual 30 minutes flights will result in an overall sampling pattern as depicted in the right plot of Figure 17.

Such sampling was conducted from 500 ft to 2600 ft above ground level (AGL) to capture the variation of the plume rise velocity at different elevations and make sure that the elevation with the highest peak velocity was collected.

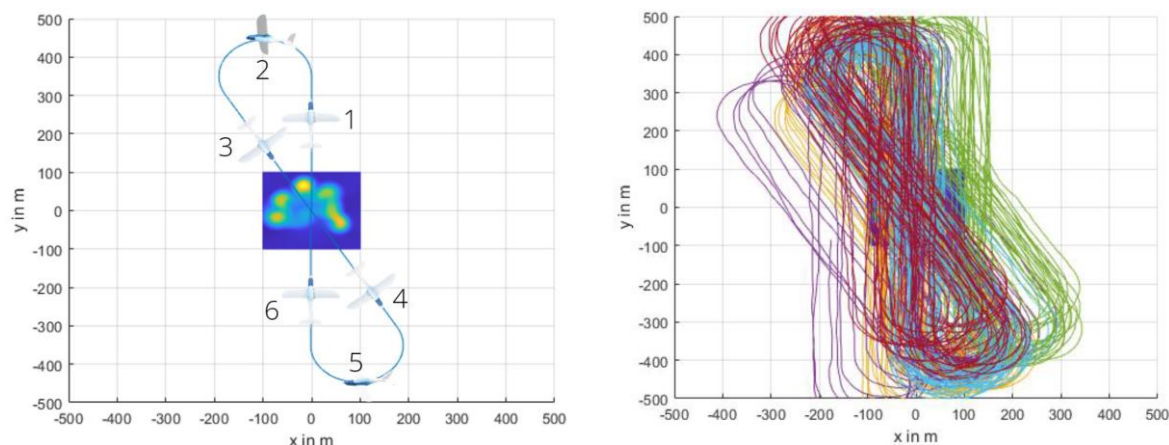


Figure 17. Planned definition of figure-eight manoeuvre (left) and expected sampling based on multiple figure eights after six individual 30 minute flights (right).

Using the velocity profile of the exhaust plume from the simulation with calm wind conditions at 650 ft above mean sea level (AMSL) as an example (contour plot in middle of the charts in Figure 17) the proposed measurement program would capture the most critical plume features multiple times. Figure 18 below illustrates the time signal of the estimated plume rise velocity for one example simulated 30 minute flight and shows the periodic fly-throughs, where some are directly hitting the most critical features, and some are sampling less intense updraft areas of the plume. The close-up view in Figure 18 shows that the specific pattern of the sampled plume section can be accurately resolved spatially (a sample interval of 2 ms at an airspeed of 50 m/s leads to one measurement every 0.1 m). One entire plume

profile is recorded in about 5 s (e.g. 1710 s to 1715 s), e.g. 2500 datapoints for a centred fly-through.

To collect sufficient and appropriate data from the exhaust plume, the overall aim was to measure the plume behaviour at meteorological conditions close to the conditions that has been assessed in the CFD analysis as the worst case (calm wind and low ambient temperature as shown in Figure 4) on two to three individual days while the Tallawarra B power station was operating at full power. Such conditions were expected to occur during the winter season and so measurements were planned to be conducted in August 2024.

Based on that, it was planned to have the flight and measurement team on-site for three weeks, starting in early August 2024. This allowed the team to be ready for measurements whenever suitable meteorological conditions were met within the three weeks. Luckily, the first three consecutive days (5th to 7th of August 2024) had the target meteorological conditions, and so the plume measurements could be done efficiently with the test team leaving site earlier than planned.

By performing fly-throughs at various altitudes on different days sufficient flight data was obtained to be able to assess the plume characteristics and its impact on aircraft with confidence.

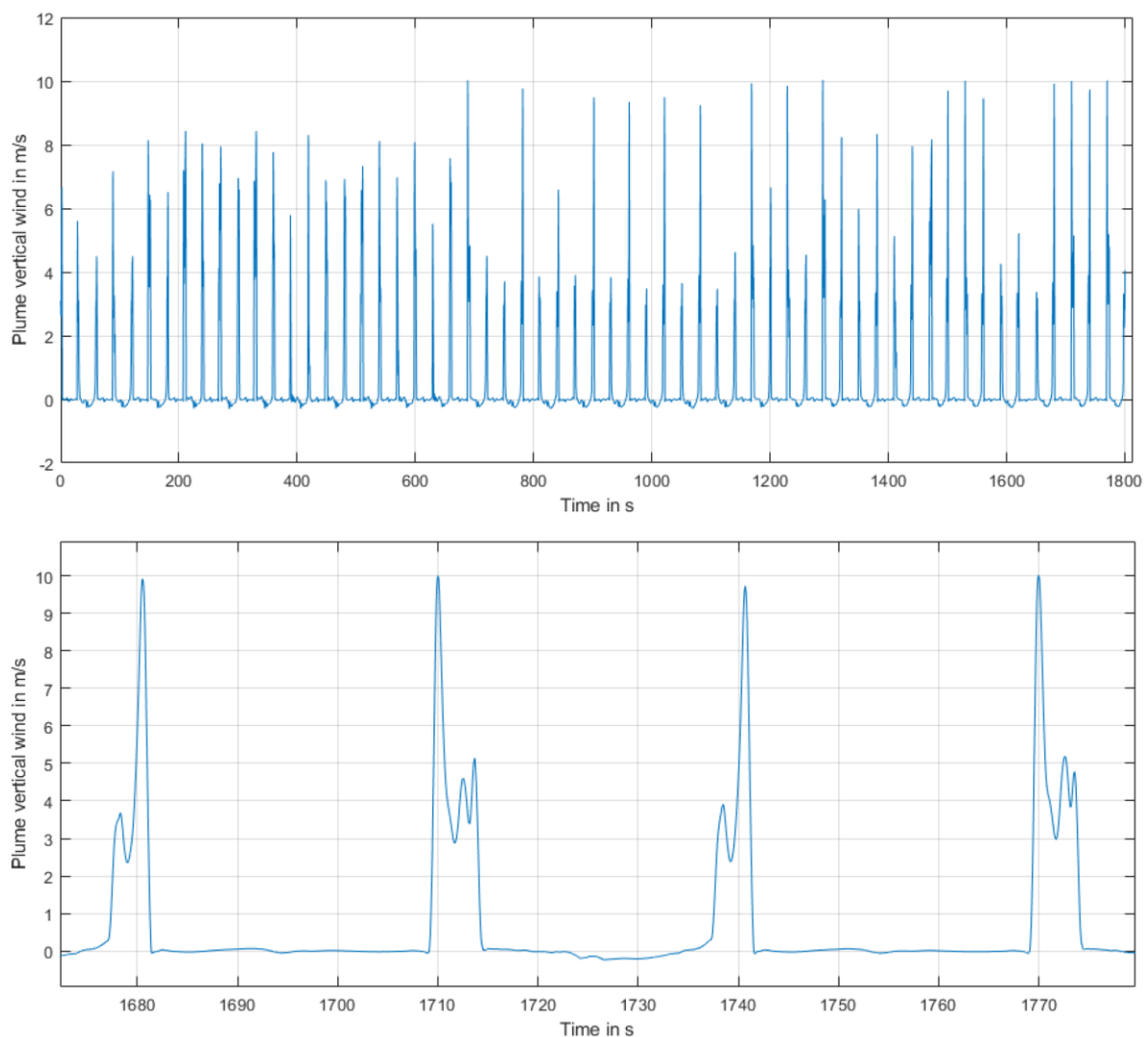


Figure 18. Time signal of the estimated plume rise velocity (CFD results of calm wind condition at 650 ft AMSL, see Section 3) for one example simulated 30 minute flight (top) with a close-up view of the time signal (bottom).

4.1.3 Plume rise velocity estimation from flight data

The measured flow signal can be simulated as it is to be expected for the given plume flow field and flight dynamics. If the green line in Figure 19 is the actual plume rise velocity required to be measured, the blue line would be the velocity signal measured by the flow sensor mounted on the strut. The blue line corresponds to the local relative flow as seen by the sensor (red) with added sensor noise. To get to the estimated flow (purple), the compensation signal (yellow) based on flight dynamics and aerodynamics needs to be added. The estimated plume profile (purple) corresponds to a very high degree to the actual plume profile (green) with a deviation of less than 3% RMS.

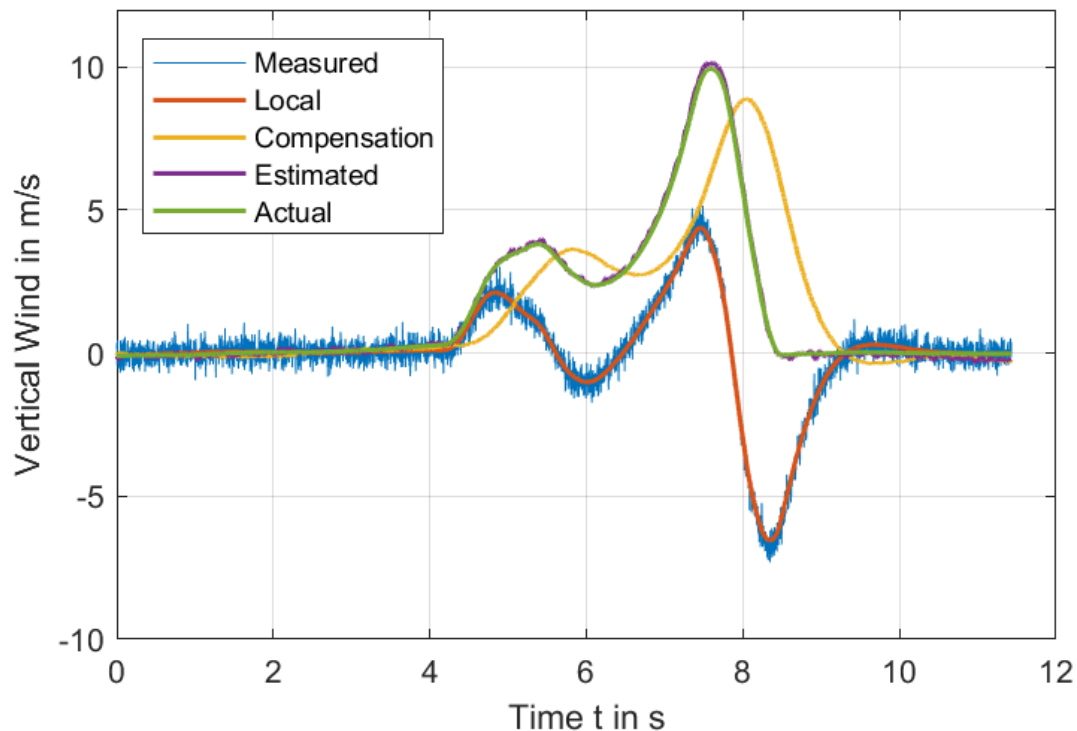


Figure 19. Illustration of plume rise velocity estimation obtained from flight data. Illustration is based on a simulation.

4.2 Preparation and consideration

4.2.1 Aircraft safety

Three air work pilots with experience in flight instruction and aerobatics were provided by the local company Airspeed Aviation. To limit the risk to the measurement team and the pilots, the expected aircraft response was assessed based on flight dynamics simulations using the flow field obtained from the CFD simulations. Figure 20 below shows the worst flight paths through the plume obtained from CFD simulations for worst-case g-load impact (blue path, maximum longitudinal slope) and for worst-case roll impact (red path, maximum lateral slope). With the aircraft dynamics of a Cessna 172 at a speed of 50 m/s, the flight dynamics simulations confirmed that the expected g-load impact and expected roll response were within the range of normal and safe aircraft operation. This analysis informed the risk assessment conducted before work was undertaken.

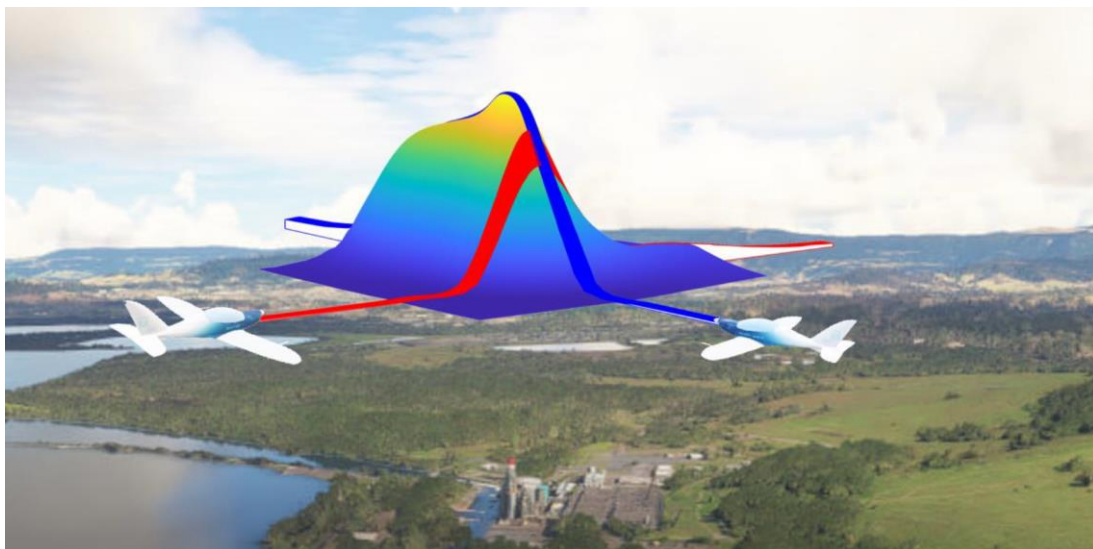


Figure 20. Most onerous flight paths for g-load impact (blue) and roll response (red) through the plume as an example. The aircraft in the picture is for illustration purpose only and does not represent a high wing Cessna 172 that was used for the analysis and measurements.

To provide local operators sufficient situational awareness of the plant measurements and operation over the Tallawarra B power plant as well as reduce traffic interactions with measurement flights, a Temporary Danger Area (TDA) was arranged for the expected time frame during the measurement campaign [20]. The arrangement of the Temporary Danger Area over the project area (500 m radius centred over the Tallawarra B power station and vertical extent up to 2000 ft above mean sea level) was organised and submitted via the Aviation State Engagement Forum (AvSEF) by Aviation Projects. In addition, to alert pilots of operational changes to the airfield, a NOTAM (Notice to Airmen) was prepared by Aviation Projects and issued on each day prior to test flights commencing.

4.2.2 Meteorological criteria and weather forecast

The objective was to sample the exhaust plume characteristics at meteorological conditions that are aligned and consistent with the modelled worst-case scenarios. Therefore, target criteria for the meteorological conditions with GO / NO-GO criteria were implemented for conducting measurements (see Table 7). In addition, the meteorological conditions according to the visual flight rules (VFR) as listed in Table 8 needed to be met.

Table 7. Target meteorological conditions for exhaust plume measurements.

Meteorological condition	Target
Wind direction	No constraints
Atmospheric stability	Neutral or stable (assessed based on potential temperature profile)
Wind speed at 10 m (AGL)	<1 m/s (<1.94 kt)
Wind speed below 500 m (AGL)	<3 m/s (<5.8 kt)
Temperature below 500 m (AGL)	<20°C

Table 8. Minimum visual/weather conditions to satisfy visual flight rules.

Flight condition	Target
Visual meteorological conditions (VMC) minima	Clear of cloud with 5 km visibility below 3,000 ft (AGL) plus further required minima according to VFR (visual flight rules), no fog
Time of day	Day VFR only, no flight before daylight, or after daylight

For preparing the measurements and the Tallawarra B power station operation, an hourly average weather forecast for the local project area out to 7 days was provided by Meteomatics (via Katestone). The forecast was updated every 6 hrs (4 times a day) based on data from European model³. The detailed and local weather forecast was used to inform the measurement team and Energy Australia if the meteorological conditions as listed in Table 7 were likely to be met, and if measurements and power plant operation could likely be commenced within the next day. As the team was on-site waiting for the best conditions, decisions could be made very effectively and quickly according to the updated weather forecast and requirements on the plant operation.

4.3 Timetable and flight statistics during test days

Based on the preparations and the weather forecast, instrument calibration flights and exhaust plume surveys were commenced on three different days as listed in Table 9 below. That gave a total time of 2 hours and 45 minutes for calibration flights and 8 hours and 35 minutes for exhaust plume survey flights, with approximately 430 individual fly-throughs at different elevations. Figure 21 provides an overview of the approximate number of fly-throughs at the different elevations. Fly-throughs are binned together around rounded elevation values. Elevation 650 ft represents fly-throughs at around 650 ft and below. Not all the fly-throughs were analysed in detail, as some of them were missing the plume peak or had very low vertical velocities with little resulting impact on the aircraft. The results from the inertia sensor were used to pick the plume passes with the higher impacts for detailed analysis. All detailed plume shapes are presented in the test report provided by Turbulence Solutions [22]

Table 9. Summary of conducted test flights.

Date	Flight purpose	Flight time	Flight duration
5-Aug-2024 (Mon)	1 st calibration flights	10:00 am to 11:00 am	1 h
	1 st set of plume surveys	12:00 pm to 2:40 pm	2 h 40 min
	2 nd set of plume surveys	3:15 pm to 4:10 pm	55 min
	2 nd calibration flights	4:10 pm to 4:25 pm	15 min
6-Aug-2024 (Tue)	1 st calibration flights	9:00 am to 10:00 am	1 h
	Plume surveys	3:30 pm to 4:55 pm	1 h 25 min
	2 nd calibration flights	4:55 pm to 5:10 pm	15 min
7-Aug-2024 (Wed)	1 st set of plume surveys	9:10 am to 11:15 am	2 h 5 min
	2 nd set of plume surveys	12:30 pm to 2:00 pm	1
	Calibration flights	2:00 pm to 2:15 pm	15 min
Total time plume survey flights			8 h 35 min
Total time calibration flights			2 h 45 min

³ Enhanced downscaled model data based on the European Center for Medium-Range Weather Forecasts' (ECMWF) Integrated forecasting System (IFS), which is the world's leading atmospheric global circulation model that describes the dynamical evolution of the atmosphere worldwide and is used for medium-range forecasts. The downscaling improves the coarse grid native representation down to a resolution of 90 m. This is achieved by applying high-resolution land usage data, soil, terrain data, astronomical computations & other sources.

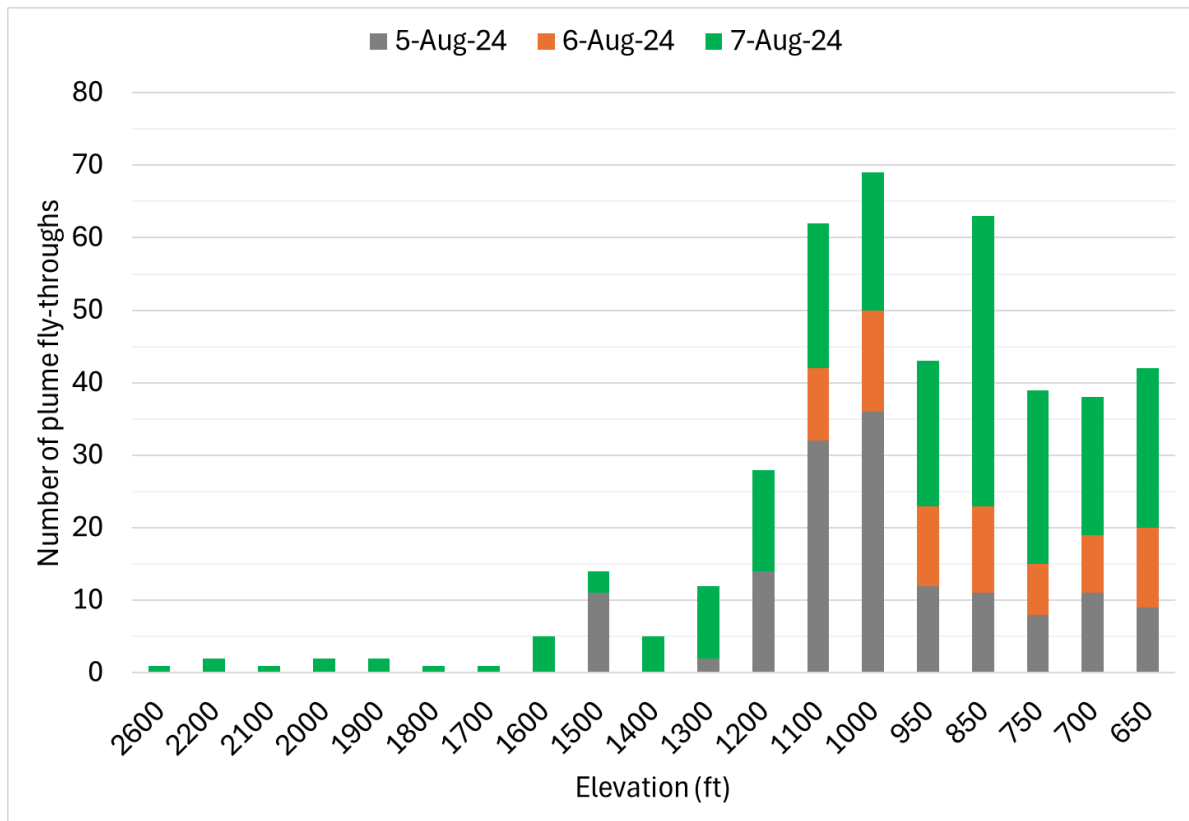


Figure 21. Number of plume fly-throughs depending on the elevation and the test day.



Figure 22. Photos taken during the plume surveys on 5th of August 2024 (left) and 7th of August 2024 (right)

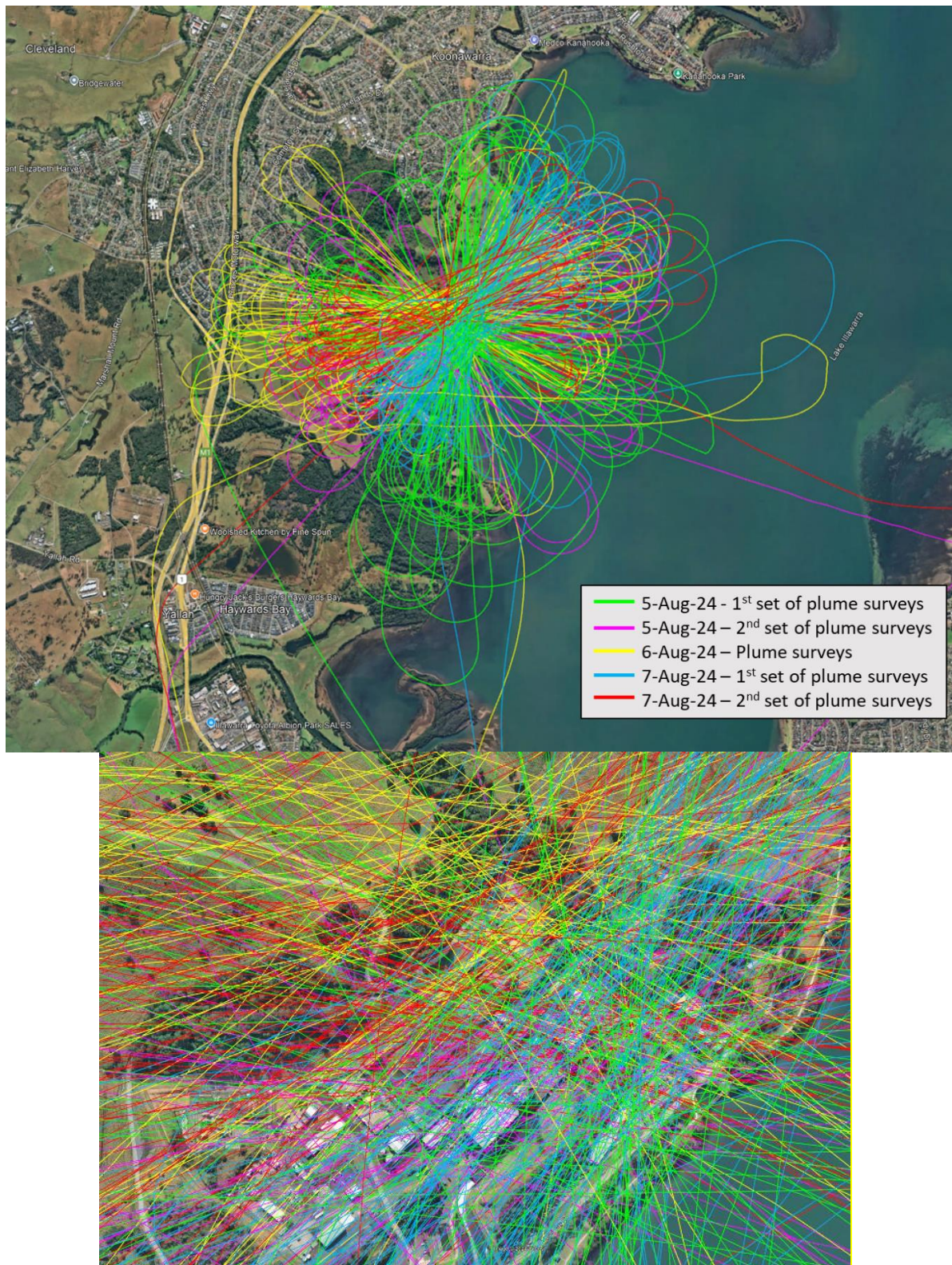


Figure 23. Figure-eight manouvers and tracks through the exhaust plume based on recorded GPS data for the individual test days and plume surveys. Close-up view over the power station is depicted at the bottom.

4.4 Meteorological conditions during test days and used as input for CFD

The detailed meteorological conditions during the test days at the local project area were provided from Meteomatics downscaled ECMWF³ model with some parameters calibrated using data from nearby weather stations (within a radius of approximately 50 km). The data calibrated are temperature, dew point and relative humidity at 2 m above ground level as well as wind speed and wind gusts at 10 m above ground level. The weather data provided above these levels was not calibrated. Recorded data from all nearby weather stations were used for the calibration to adjust the model output more closely to the observations. A dynamic downscaling technique is used to refine the output of the ECMWF³ model, enhancing the data through post-processing with NASA's global terrain and elevation model. With a spatial resolution of 90 metres, NASA's model encompasses detailed information about the Earth's surface, including elevation data, land cover, and terrain features.

The meteorological data were required to give more detailed information about the prevailing meteorological conditions during the measurements. In addition, the detailed profiles were used as input for additional CFD assessments to compare CFD modelling results with measurements, as well as allowing comparison of the conditions with the conditions used for previous CFD modelling. The meteorological modelling results are based on hourly averaged values, which means that there is one set of data for each individual hour. Detailed information between these hours is not available. For example, the wind direction transition on the morning of the 7th August, in which the wind passed briefly through complete calm, cannot be captured by such hourly data.

Figure 24 and Figure 25 summarise the wind speed, temperature, potential temperature and wind direction for the hours during the test days. The profiles used for the preceding CFD assessment (see also Section 3.2 and Figure 4) are included for comparison. Compared to what was previously modelled, the wind speed below 100 m was slightly higher (1.1 m/s vs. 0.6 m/s) but the temperature above 100 m (for the profiles with low wind speeds, 10 am on the 7th of August 2024) was lower. To compare the measurement results with the CFD results for similar meteorological conditions, the CFD model has been rerun with a higher wind speed but lower temperature. The profile used for the additional CFD case is the average of the values of the profiles 7-Aug-2024 at 10 am and 7-Aug-2024 at 11 am, as also shown in the plots below (20240807_10to11 in Figure 24 and Figure 25). The additional CFD modelling is documented in Section 5.

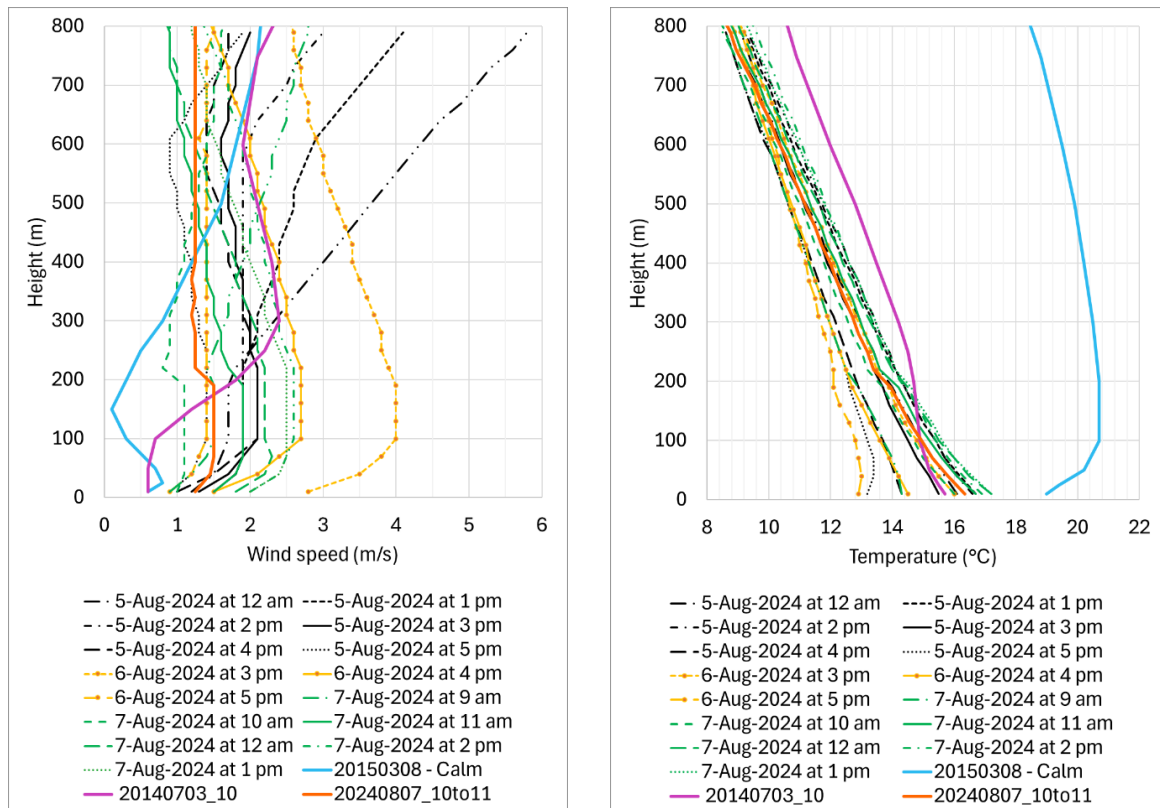


Figure 24. Wind speed (left) and temperature (right) depending on the elevation (AGL) during the test days. Profiles used as input for the CFD assessment are also included for comparison.

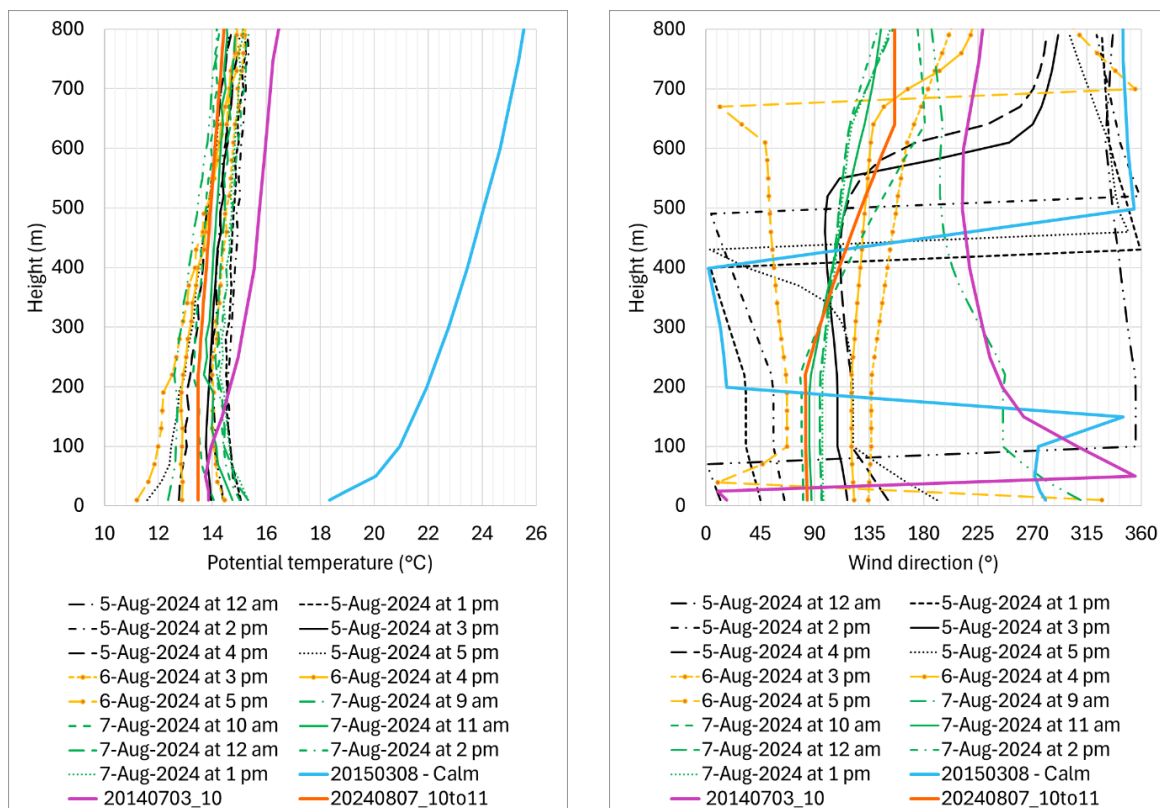


Figure 25. Potential temperature (left) and wind direction (right) depending on the elevation (AGL) during the test days. Profiles used as input for the CFD assessment are also included for comparison.

4.5 Plant operation during test days

To confirm the power plant operation during the measurements, the stack flow parameters for the Tallawarra A and B plants were recorded and provided by the control room. The stack flow parameters during the test flights are plotted in Figure 26 to Figure 28 for the individual test days. The time stamps indicating the individual measurement periods are also included in the plots. The stack flow parameters used for the preceding CFD assessment are marked in the plots for comparison.

On the first day (5th August 2024) the Tallawarra A power plant was off during the whole test period and the Tallawarra B was first set to 50% power (for the first hour) and then ramped up to 100% power. The 50% power operation was established to do the first plume surveys and explore the aircraft impact at reduced power.

On the second day (6th of August 2024), the Tallawarra A power plant had to be operated at 50% load during the test period in the afternoon due to grid demand. Tallawarra B was operated at 100%. Tallawarra A exhaust stack is located south-west of the Tallawarra B exhaust stack. During the plume surveys in the afternoon (from 3:30pm to 4:55 pm) the wind was predominately coming from south-east (see Figure 25) and therefore no interaction between the two exhaust plumes was expected. Further, the mass flow rate and especially the exhaust temperature of the Tallawarra A exhaust are much lower, so that the impact of the Tallawarra A exhaust plume and its extent is considerably smaller than the Tallawarra B exhaust plume.

On the third day (7th of August 2024), only the Tallawarra B power station was running, at 100% power, over the whole measurement period.

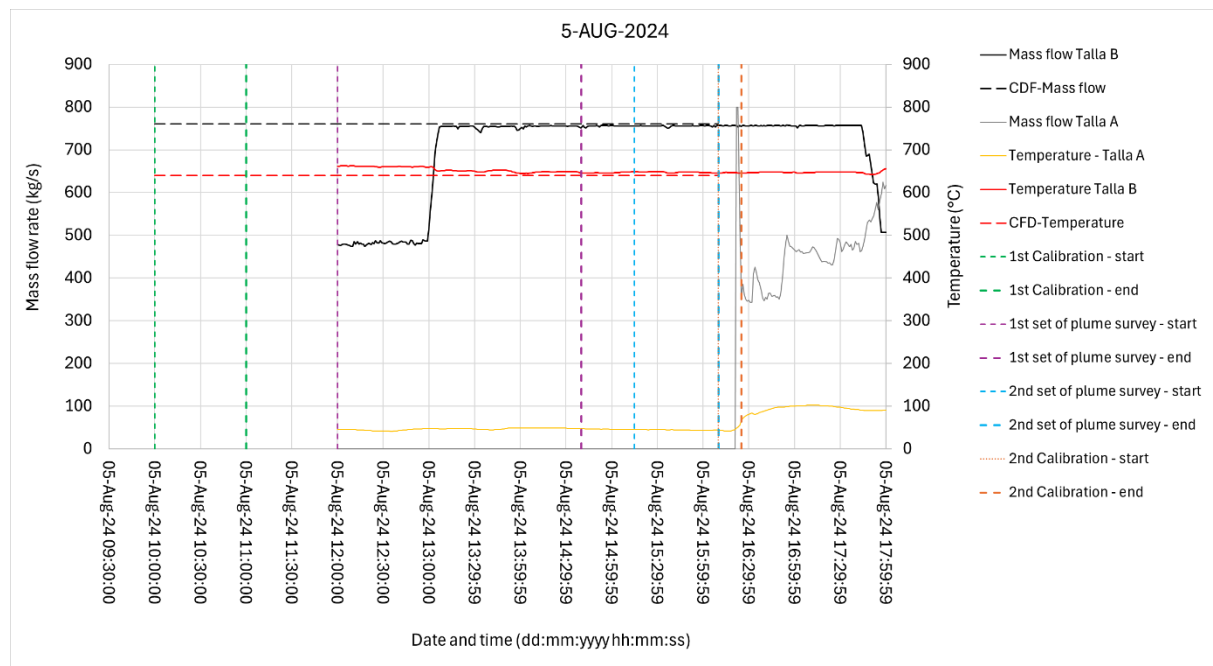


Figure 26. Mass flow rate and exit temperature at Tallawarra A and B exhaust stack during the first test day (5th August 2024). Time stamps of the test periods and parameters used for the preceding CFD assessment (see Section 3) are also included.

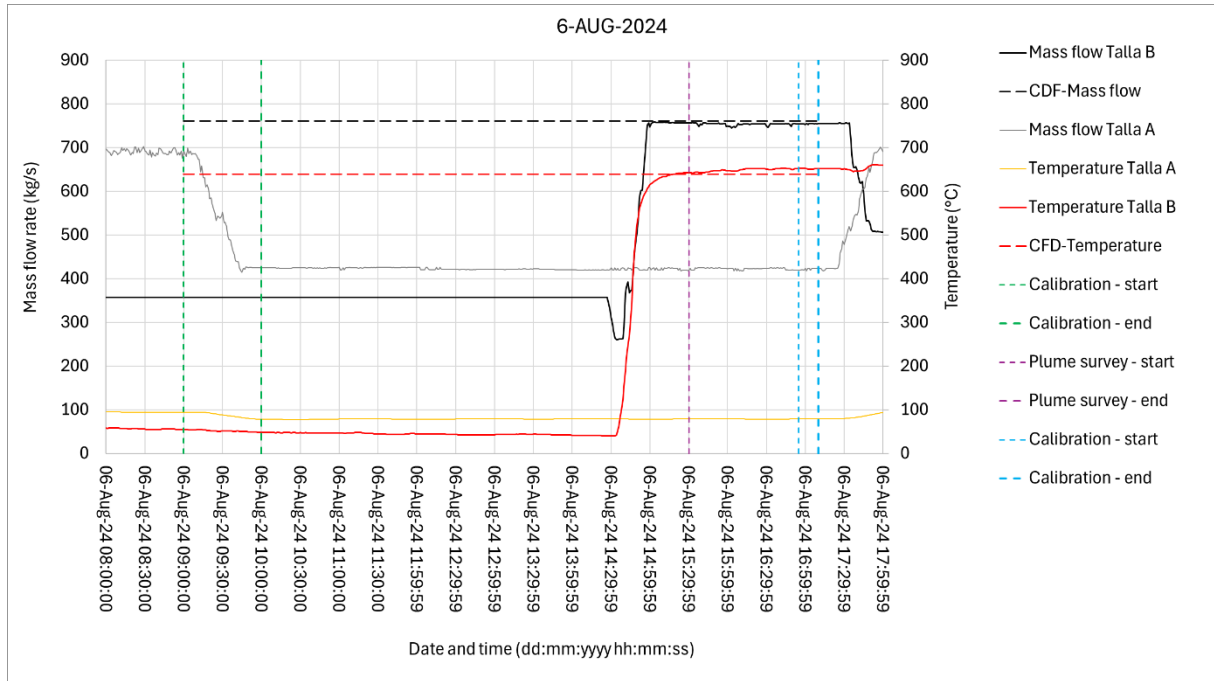


Figure 27. Mass flow rate and exit temperature at Tallawarra A and B exhaust stack during the second test day (6th August 2024). Time stamps of the test periods and parameters used for the preceding CFD assessment (see Section 3) are also included.

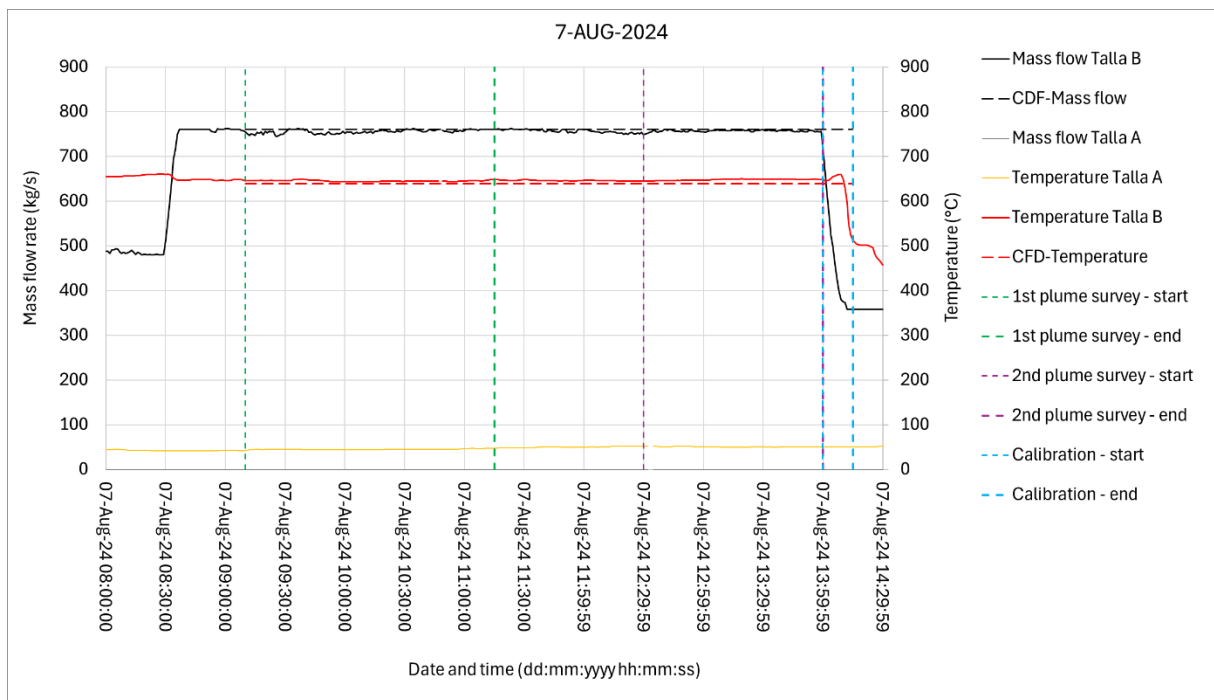


Figure 28. Mass flow rate and exit temperature at Tallawarra A and B exhaust stack during the third test day (7th August 2024). Time stamps of the test periods and parameters used for the preceding CFD assessment (see Section 3) are also included.

4.6 Results

The high sampling frequency (500 Hz, sampling the flow at 2 ms intervals) ensured that the peak velocity along a high speed (around 50 m/s) flight path through the plume did not get missed. However, that made the measurement also more sensitive to local micro-fluctuations and sensor noise. Such turbulent fluctuations at a small spatial scale (about 0.1 m) might be real but have no impact on the aircraft as they get damped and aerodynamically cancelled over the wing area. Based on that, filtering and spatial smoothing was applied on the measured signals to reduce sensor noise and the irrelevant small scale turbulent fluctuations.

As explained in Section 4.1.3, the measured velocities were corrected for flight dynamic and aerodynamic considerations to obtain a clean vertical velocity profile of the exhaust plume. That is, the effect of the relative aircraft motion on altering the measured values was allowed for.

Figure 29 shows the highest recorded plume rise velocity per fly-through for the most impactful plume passes (out of the approximately 430 fly-throughs) over the three test days. The primary x-axis (bottom) is the average plume rise velocity in accordance with the CASA criterion, which is half of the maximum plume rise velocity shown on the secondary x-axis at the top of the plot.

The highest peak plume rise velocities occurred during the morning survey (1st survey flight) on the 7th of August 2024 with the highest measured peak value just above 12 m/s (12.06 m/s). During that time, the wind changed direction from a westerly wind with a speed of about 1.5 m/s to an easterly wind with a speed of about 1.9 m/s. That means that the wind speed during that period was potentially very low and probably almost zero for a very short period. Depending on the elevation, the point when the wind changed direction could have happened at a different time potentially causing maximum peak values at different times at each elevation.

With almost the same ambient temperature in the afternoon on the same day (7-Aug-2024 2nd survey flight) the wind speed was higher and between 2.2 to 2.6 m/s. The higher wind speed causes more mixing and entrainment (cooling of the hot exhaust plume), so that the peak plume rise velocities were considerably lower.

During the plume survey on the 6th of August (afternoon), the wind speed was generally higher but calmed down from 2.7 m/s to 1.4 m/s. The three to four points with the highest peak plume rise velocity in that period were measured towards the end, when the wind had calmed down.

Even if the wind speed in the afternoon during the first and second plume surveys on the 5th of August were similar according to the meteorological model, it seems that there were short periods of low wind speeds during the first plume survey that led to maximum plume rise velocities close to 12 m/s. The measured plume rise velocities during the second plume survey are generally lower (<8 m/s) and the prevailing weather conditions during that period appear to be more aligned with the meteorological model data.

Figure 30 to Figure 32 depict the measured plume shape and peak plume rise velocities for each set of plume surveys. Only the profiles with the two highest peaks per measurement set are shown as examples. All detailed plume shapes are presented in the test report provided by Turbulence Solutions [22]. The shape and extent of the plume depend on the elevation, the meteorological conditions at the time of the fly-through and on the aircraft path itself. As indicated in Figure 14, the plume can have multiple peaks at the same elevation, so depending on the path through the plume, the measured velocity profile can show those multiple peaks.

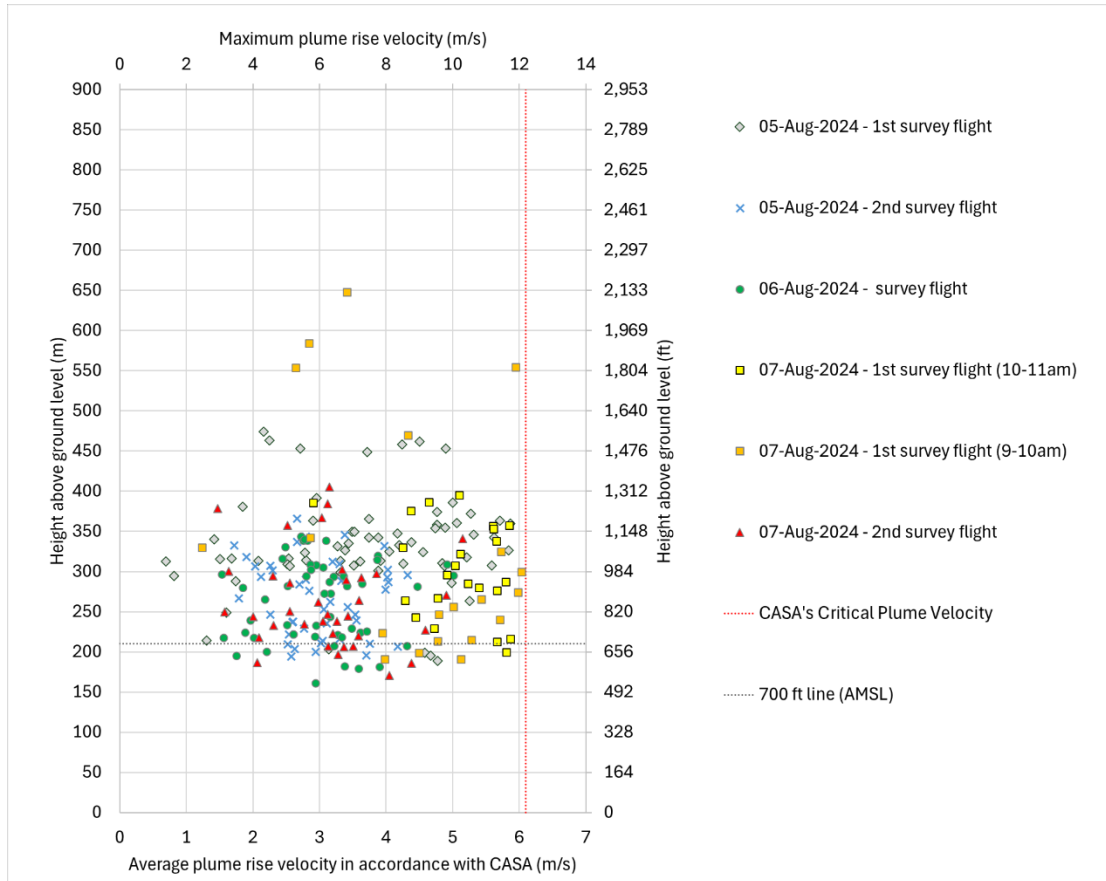


Figure 29. Highest recorded plume rise velocity per fly-through and elevation for the individual test periods. The primary x-axis at the bottom is the average plume rise velocity in accordance with CASA's criterion. The secondary axis at the top of the plot is the peak plume rise velocity, which relates to double the CASA criterion.

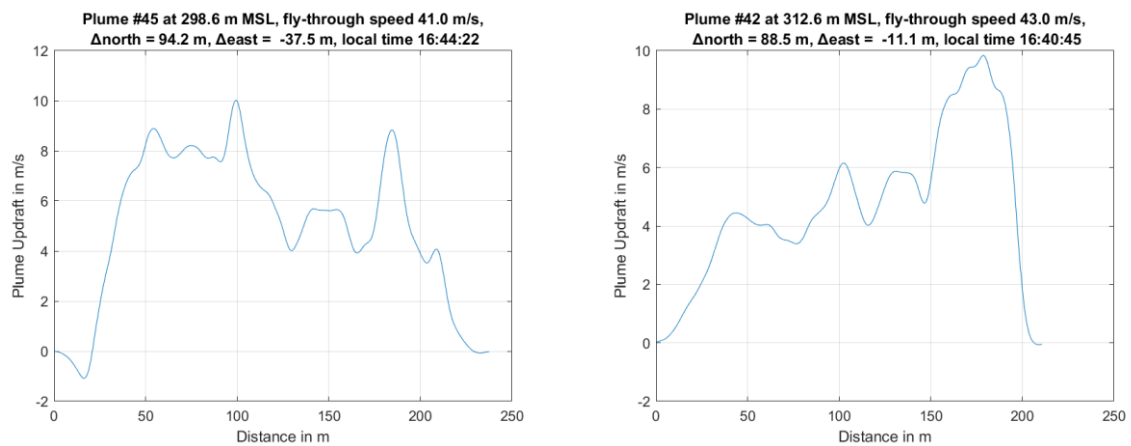


Figure 30. Velocity profiles for the two highest peak velocities recorded during the plume survey on the 6th of August 2024 [22].

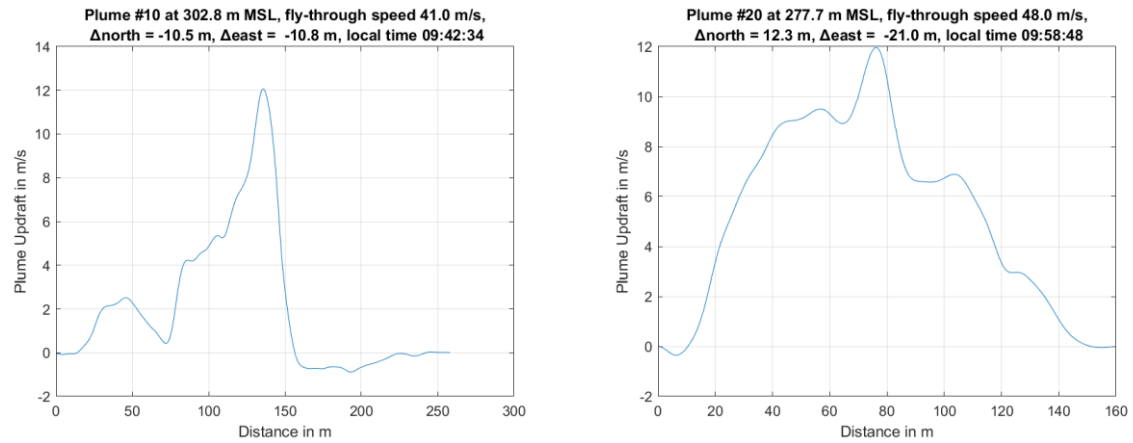


Figure 31. Velocity profiles for the two highest peak velocities recorded during the first plume survey on the 7th of August 2024 [22].

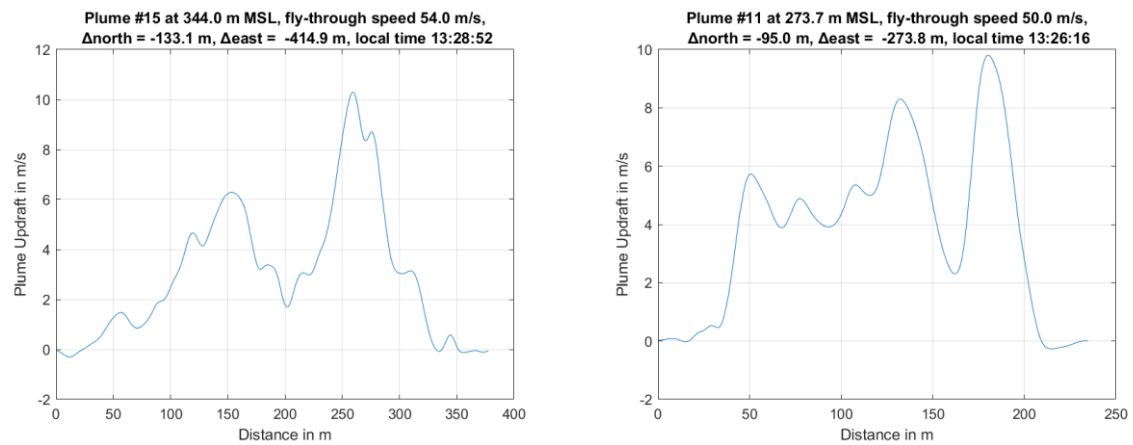


Figure 32. Velocity profiles for the two highest peak velocities recorded during the second plume survey on the 7th of August 2024.

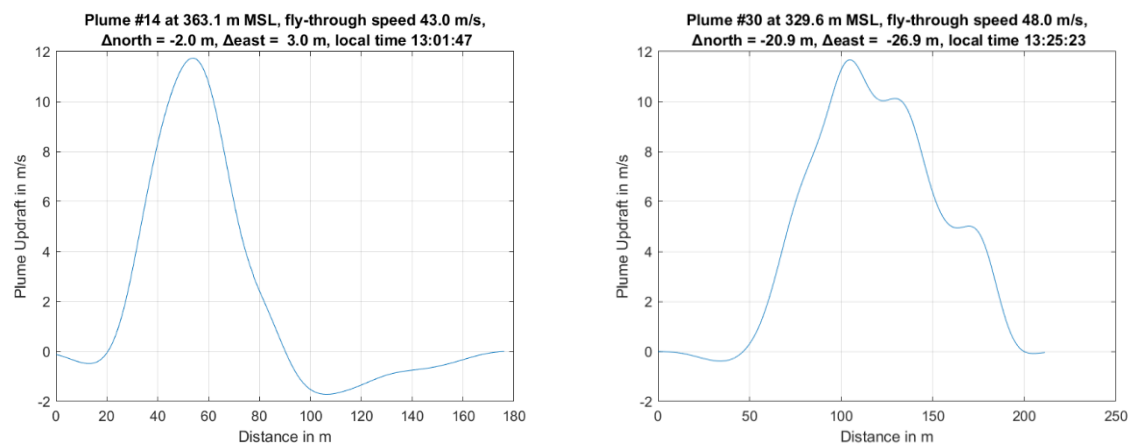


Figure 33. Velocity profiles for the two highest peak velocities recorded during the first plume survey on the 5th of August 2024 [22].

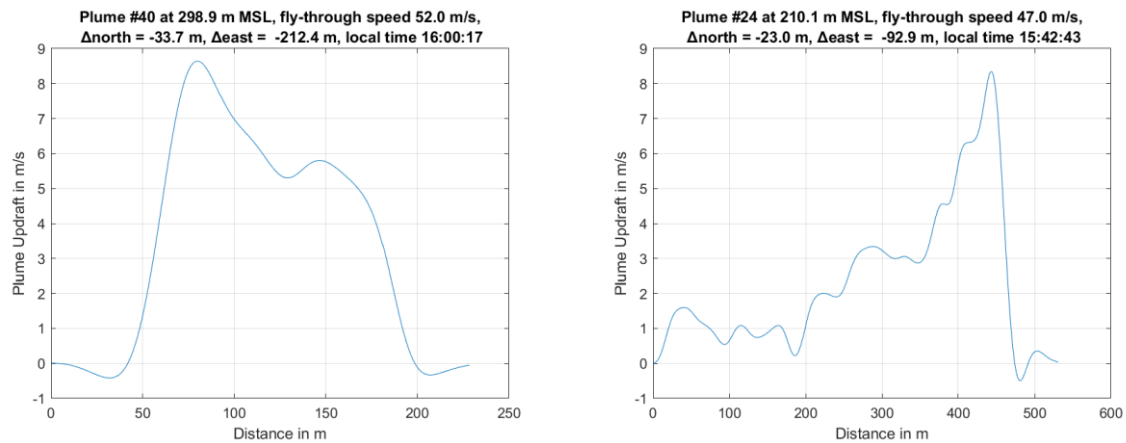


Figure 34. Velocity profiles for the two highest peak velocities recorded during the second plume survey on the 5th of August 2024 [22].

4.7 Interpretation of results

According to the measurements (over 400 plume fly-throughs on 3 individual days) during worst meteorological conditions (low ambient temperature and low wind speed), the maximum peak plume rise velocity at 700 ft and above is at around 12 m/s and below the CASA criterion of 12.2 m/s⁴.

Even if the measurements confirmed that the CASA criterion has been met for the most onerous known meteorological conditions, it is possible that in some unforeseen weather conditions the vertical peak velocity might exceed 12 m/s for short periods.

The simulations, as well as the measurements at different wind conditions (at similar ambient temperatures), showed that the peak plume rise velocity is sensitive to the wind speed. At a wind speed > 2 m/s, the maximum peak plume rise velocity has already dropped below 10 m/s.

However, based on the pilot's experience after multiple plume-passes and based on flight dynamic analysis, the impact on aircraft does not necessarily correlate directly with the magnitude of the vertical velocity value. There were several plume passes that recorded high peak velocities but showed less impact in terms of aircraft movement compared to other passes where the peak velocity was lower. The essential parameters for a given aircraft (aerodynamics, wing span, weight etc.) regarding the impact are the speed of the aircraft, the shape of the plume (narrow, wide, multiple peaks) and how 'steep' the velocity increase is. A narrow plume with a pointy peak velocity of say 8 m/s can result into a much higher impact compared to a very wide plume with a shallower rise to a peak velocity of say 12 m/s. The speed of the aircraft has different effects. For a given velocity profile and aircraft, the higher the speed of the aircraft, the higher the g-load if the aircraft is flying over the peak, but the lower the speed of the aircraft the higher is the roll response if the peak is only under one wing (see Figure 20). These effects are not considered when looking at a single peak velocity value.

Even if the peak plume rise velocity was close to the CASA criterion, the pilots did not experienced aircraft movements or impacts that were unusual compared to aircraft that are exposed to the level of atmospheric turbulence that can be expected during normal flight

⁴ In accordance with CASA's requirements, the peak vertical velocity that is calculated using a CFD model is divided by 2 to produce an average velocity for comparison with CASA's Critical Plume Velocity of 6.1 m/s.

operations. When hitting the plume at lower elevations, there could be multiple smaller impacts as the plume from the PDD is more spread out into 'plumelets', and therefore can have multiple peaks. At higher elevation, the plume is more combined, and it is more likely that there is only a single impact when flying through the exhaust plume. Depending on the wind conditions, at elevations close to 2000 ft, the plume extent is much wider, and the plume rise velocities are more uniform (less pointy), so that the pilots noted a 'rambling' motion of the aircraft when flying through the plume. According to the air work pilots, at low to calm wind speeds, the strongest impact can be expected between 800 ft and 1200 ft. With higher wind speeds the plume core gets more displaced from the stack centre, and the overall impact reduces. If the aircraft hits the plume but is not centred over the plume core, there is a tendency to get rolled out (like normal thermal updrafts).

However, similar to atmospheric turbulence, the potential impact on aircraft due to the exhaust plume can be surprising to pilots who fly over the stack while the aircraft is flying through otherwise calm, turbulence-free conditions. Therefore, the pilot in command should be aware of the Tallawarra B power station and avoid flying over the potential turbulence source, or at least cross the power plant at elevations higher than 2000 ft, if possible.

5 CFD RE-ASSESSMENT

As already noted in Section 4.4, the meteorological conditions during the test days were slightly different to the conditions that were used for the preceding CFD assessments. The wind speed at lower elevations (below 200 m) was a bit higher than simulated, but the ambient temperatures were a bit lower. Further, during the measurements, the test team observed that, even at lower elevations, the exhaust plume was a bit more displaced from the stack centre (100 to 150 m) compared to the preceding CFD modelling results. To confirm the consistency between the model and observations, the CFD model was rerun with updated stack flow parameters and meteorological conditions, closely matching those applicable to the test flights.

5.1 Input parameters

The modelling methodology was kept the same as previously documented [9], [11] (see also Section 3). For the CFD re-assessment, the profile with the lowest wind speed in combination with the lowest temperature was taken as new input. Therefore, the values of the two profiles 7-Aug-2024 at 10 am and 7-Aug-2024 at 11 am were averaged to obtain representative conditions over that measurement period. The profiles used for the re-assessment are shown in Figure 24 and Figure 25 (20240807_10to11). To increase the stability of the numerical simulation, the temperature below 100 m (AGL) were slightly reduced and kept constant. Due to the lower temperature and lower wind speed at higher elevations (400 m above ground level) the exhaust plume reached higher elevations. To avoid adverse influences of the domain's boundary conditions, the computational domain was extended in height by 1000 m. To allow for greater lateral drift with that extra height, the inlet boundaries were also moved further away from the stack centre. The updated domain has an overall size of 4400 x 4400 m, with a height of 3000 m. The stack was positioned in the middle of the domain (in x-direction) and 3000 m upwind of the outlet boundary condition (in y-direction). Mesh parameters were adopted as listed in Section 3.3.

Figure 35 shows the segment of occurring wind direction relative to the domain orientation for the new wind case (20240807_10to11 in Figure 25). Depending on the height, the wind direction changes from E (84°) to SSE (158°) and the wind speed from 1.2 to 2.6 m/s (2000 m above ground level). The wind direction did not change drastically above 650 m and therefore was kept constant up to the top domain boundary. This reduces the range of the wind direction in the domain and enhanced the robustness of the simulation. The domain orientation (as shown in Figure 35) was chosen to suit the wind profile so that the

majority of the wind directions are captured with the inlet boundary conditions. For that reason, the domain orientation is different to the orientation in the preceding CFD assessment with different wind profiles.

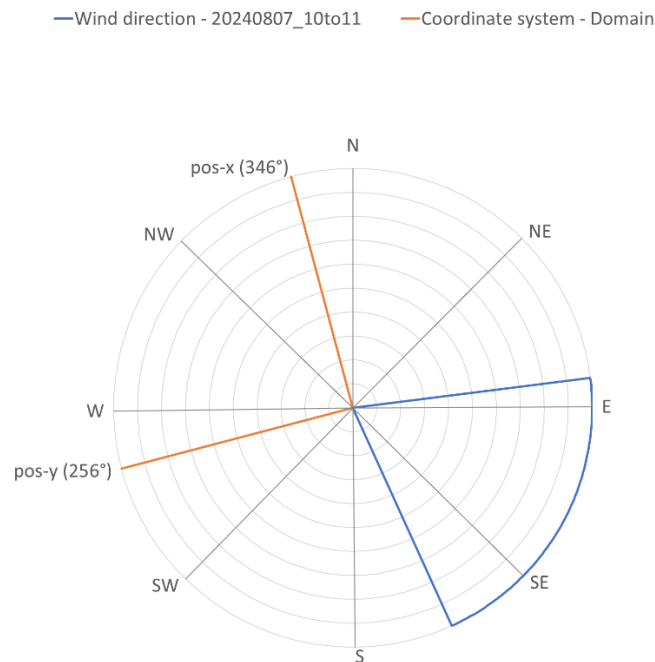


Figure 35. Segment of occurring wind direction (blue) and coordinate system of the computational domain (orange) for the ‘observed’ wind profile.

The stack flow parameters were based on the recorded data from the control room (see Figure 28) on the 7th August 2024 and have been averaged over the relevant measurement period from 10 am to 11 am. Table 10 lists the adopted averaged values.

Table 10. Stack flow parameters from the 7th of August 2024 averaged over the period from 10 am to 11 am.

Parameter	Value
Average exit velocity at each nozzle outlet*	89.09 m/s*
Total mass flow rate	756.35 kg/s
Exit temperature	644.2°C

* Hand calculation based on average opening/outlet area, total mass flow rate, exit temperature / density and an atmospheric pressure of 101.325 kPa.

5.2 Results

As observed during the previous assessment (see Section 3.5), the plume generated by the PDD led to high fluctuations of the monitored plume velocities, indicating a transient behaviour. To appropriately assess the plume rise velocity, the flow field was finally analysed with a transient solver over a period of 25 minutes. Figure 36 illustrates the time-dependent peak velocity at three different heights, for the wind cases analysed. The monitored values are the maximum occurring vertical velocity values within a horizontal plane cut through the whole domain. Based on the transient simulation, the detailed plume behaviour (see Figure 37 to Figure 39) was assessed at the times when the maximum peak rise velocity occurred at the three monitored elevations for the new ‘observed’ wind case. This was at 650 ft above mean sea level at 1440 s. The average values, as well as the

maximum and minimum occurring peak rise velocities observed during the simulation period for the different elevations, are summarised in Table 11.

Note that the plume rise velocity values at the different elevations were monitored at 1 s intervals, but result files were saved every 10 s. Therefore, a result file close to the observed peak value was chosen for the detailed analysis.

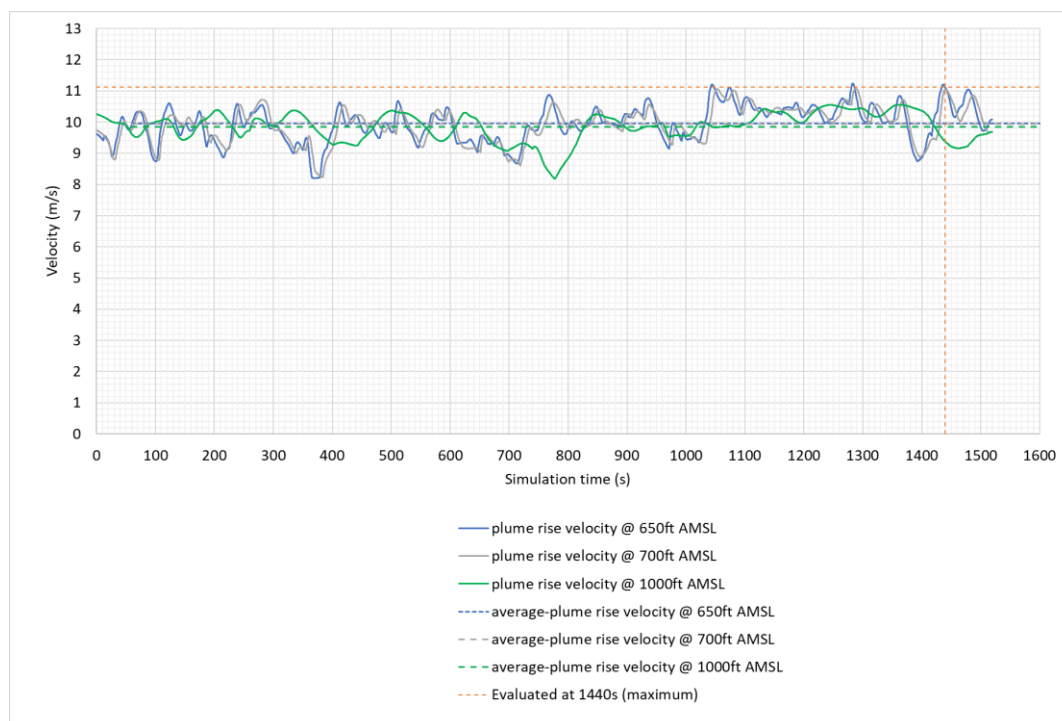


Figure 36. Monitored peak velocities at different heights depending on the simulation time – ‘observed’ wind case. The dashed orange line illustrates the simulation output chosen for the detailed analysis.

Table 11. Average values and outliers of the peak plume rise velocity at different heights observed during the simulation period of about 25 minutes. Numbers in parentheses are deviations from the average.

Elevation	Average peak plume rise velocity (m/s)	Maximum peak plume rise velocity (m/s)	Minimum peak plume rise velocity (m/s)
‘Observed’ wind case (20240807_10to11)			
650 ft AMSL	10.0	11.2 (+1.2)	8.2 (-1.8)
700 ft AMSL	9.9	11.1 (+1.2)	8.2 (-1.7)
1000 ft AMSL	9.8	10.6 (+0.8)	8.2 (-1.6)

Based on the chosen time step, Figure 37 (left) shows the plume envelope of 6 m/s velocity. As observed during the measurements, with higher wind speeds at lower elevations, the exhaust plume is more displaced from the stack centre (see also Figure 38). However, the peak plume rise velocities are similar to those from previous simulations (see Table 6). Compared to the previously assessed wind cases, the wind speed is higher at lower elevation and lower at elevations above 400 m, as the wind speed stays almost the same over a wide range of elevation. The lower wind speed at higher elevations leads to a slower decay of the peak plume rise velocity with the increase in elevation. This is illustrated by Figure 37 (right plot) that shows the maximum vertical and absolute plume velocity against

height as well as the applied atmospheric wind speed profile (20240807_10to11) according to Figure 24.

Figure 38 provides information about the horizontal displacement of the peak plume rise velocity relative to the stack centre for the new wind cases. The horizontal displacement of the plume core is very sensitive to the wind speed and direction and is just a result of the applied wind conditions. The change of the displacement in x-direction at a height of around 650 m is related to a change in wind direction, blowing in positive x-direction at elevations above and close to 650 m (see Figure 35 and Figure 25). The change in wind direction leads to a different 'branch' of the plume taking over as the one with the highest velocity, so the curve 'jumps' sideways to the location of the core/peak in that other branch.

Figure 39 illustrates the plume extent at 700 ft and 1000 ft based on value-clipped contour plots for vertical velocity.

Only vertical velocities > 1 m/s are shown in the plots and the indicated plume extent needs to be interpreted accordingly. Depending on the elevation, there can be several pointy peaks or a more stretched/wider single peak of the vertical velocity.

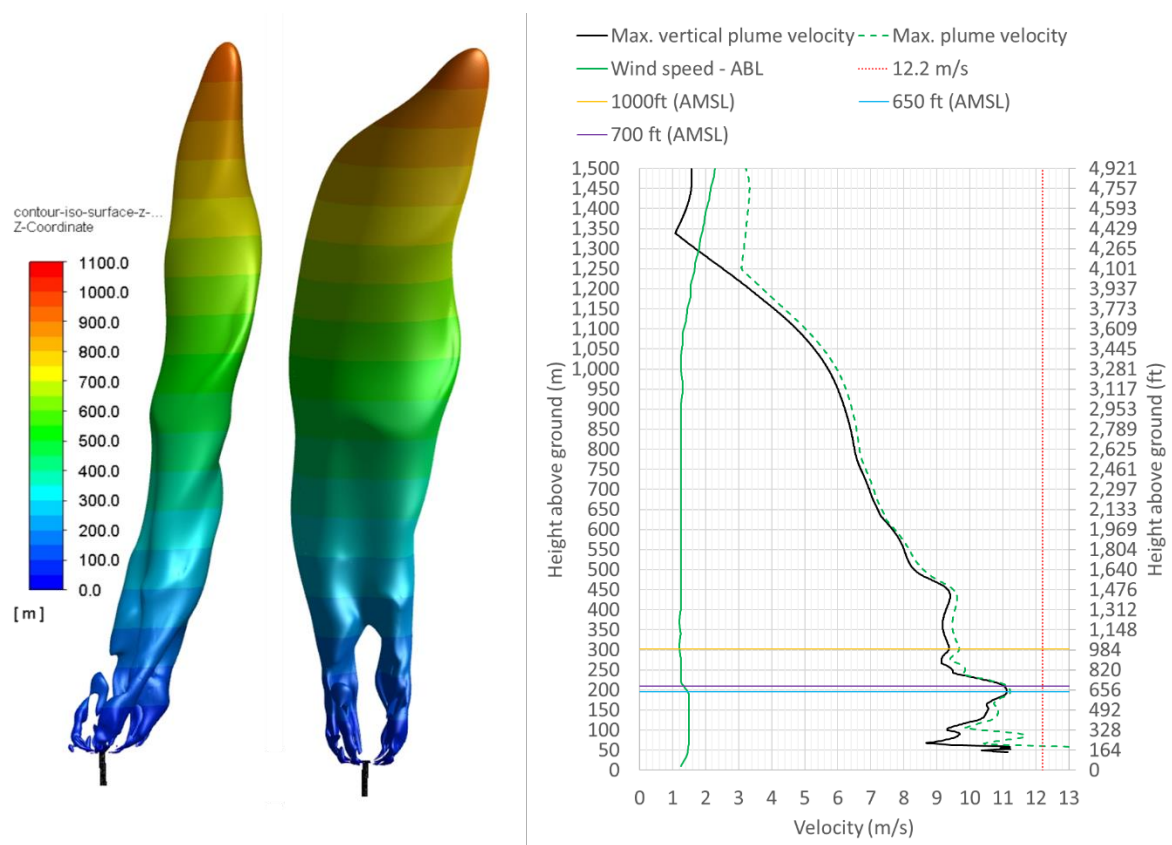


Figure 37. Plume envelope where the plume rise velocity is 6 m/s (left) and wind speed and maximum vertical and absolute plume velocity against height (right) for the 'observed' wind case. Colouring of the envelope depicts the plume height.

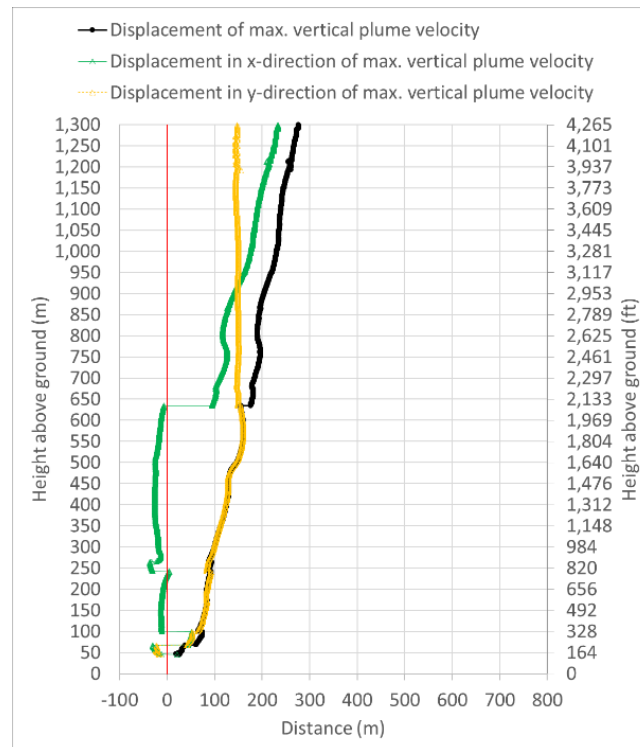


Figure 38. Displacement of maximum vertical velocity component against height for the 'observed' wind case.

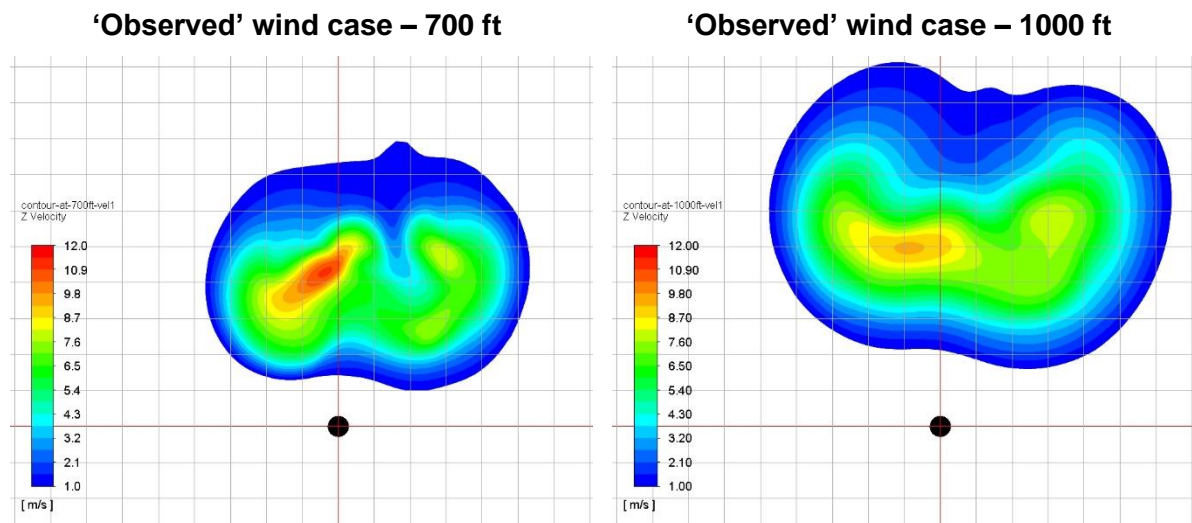


Figure 39. Plume extent shown as contour plots of vertical velocity in a horizontal plane at 213 m (700 ft) and at 305 m (1000 ft) elevation for the 'observed' wind cases. The plume area is clipped to vertical plume velocity > 1 m/s. Grid spacing is 20 m, with stack centre at the origin (red lines).

Depending on the time and local flow situation, jets detach and attach again, so that the peak plume rise velocity increases and decreases depending on the time and height. Figure 40 shows the peak rise velocity depending on the elevation for the entire simulation period in 10 s intervals. The red line depicts the simulation time (1440 s) when the maximum peak plume rise velocity occurred (identical to the black line in right plot of Figure 37). Using the 650 ft elevation (around 200 m) as example, the maximum vertical velocity varies over time from 8 m/s up to 11.2 m/s at constant meteorological conditions. These variations can further increase if the meteorological conditions also change over time.

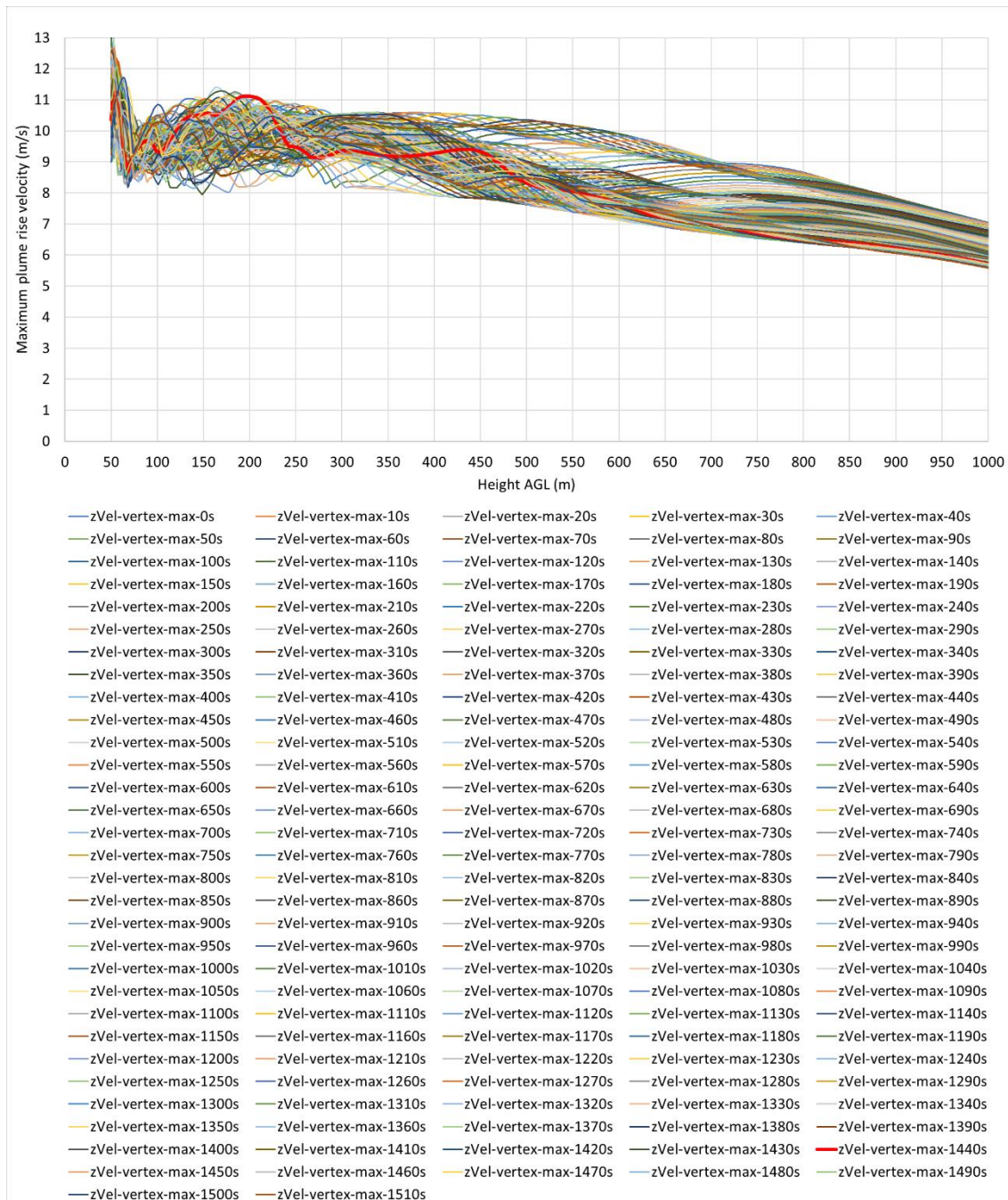


Figure 40. Maximum vertical plume velocity against height for the entire simulation period in 10 s intervals. The red line depicts the time step when the highest peak value above 650 ft occurred.

5.3 Comparison with measurements

As already noted, and indicated in Figure 40, even at constant wind conditions the plume shape and vertical velocities change over time. However, the wind conditions are usually not constant for a longer period, but change over time. That leads to a much bigger variation in the plume shape and exhaust plume velocities in reality compared to the simulation with the constant meteorological conditions. This circumstance makes it hard to compare the shape and peak of velocity profiles of individual plume passes with the simulation results. Further, the meteorological data are supported by weather stations but are based on weather modelling to obtain the local prevailing weather conditions during the measurement

period. The modelled weather data are based on hourly averaged values and therefore detailed information about the meteorological conditions between any two hours is not available. During the relevant plume survey flight (7th of August 2024 1st survey flight between 10 am and 11 am), the wind conditions will have been changing and so the results from the measurement may not compare perfectly with the simulation results where the wind conditions were constant, even if both measurements and simulations were 'perfect'.

To evaluate the plume profile at different elevations and time steps in an effective and uniform way, virtual flight trajectories were placed through the centre of the stack and were rotated in 5° intervals as illustrated in Figure 41. The plume shapes evaluated on those trajectories are compared to the measured plume profiles at different elevations and time steps. Only the relevant plume sampling data from the 1st plume survey flight collected between 10 am and 11 am on the 7th August 2024 is used for the comparison. Beyond the other influences, the particular shape of the plume profile depends on the orientation of the trajectory. A trajectory from the left to the right would give one or two peaks whereas a trajectory through the centre of the stack would only give one peak or maximum two small peaks.

Figure 41 compares the plume shapes obtained from the CFD simulation at stack-centred trajectories (blue lines) with the plume shapes obtained from the measurements (red lines) at different elevations and simulation times. Measured plume profiles with an elevation close to the evaluated elevations have been bundled together in one plot.

In general, the maximum plume rise velocities obtained during the relevant test flights are about 1 m/s higher than from the CFD results with the 'observed' wind condition. During the plume survey on the 7th of August between 10 am and 11 am, the wind speed changed from 0.8 to 1.9 m/s below 400 m whereas the wind speed applied in the CFD model was about 1.5 m/s below 400 m. This difference in the low-level wind speed could be a potential reason for the slight underestimation of the maximum peak plume rise velocity by the CFD. It is also likely that the local wind speeds were changing over short periods and dropping below the hourly averaged wind speed from time to time also causing higher vertical plume velocities in some plume fly-throughs.

Figure 43 compares the highest recorded plume rise velocity per fly-through and elevation for the individual test periods with the peak plume rise velocities obtained from the CFD simulations for the different wind cases at the evaluated timestep. The primary x-axis (bottom) is the average plume rise velocity in accordance with the CASA criterion, which is half of the maximum plume rise velocity shown on the secondary x-axis at the top of the plot. As already mentioned in Section 4.6, during the first plume survey flight on the 7th of August (yellow squares) the wind direction changed from a westerly wind with a speed of about 1.5 m/s to an easterly wind with a speed of about 1.9 m/s. Before the wind direction changes, the wind speed approached values close to zero which is more aligned with the 'initial' and 'combined' wind conditions previously simulated.

Considering uncertainties in the applied modelling and measurement methodologies, as well as in the exact meteorological conditions during a plume pass, the simulation results correlate well with the measurement results and gives confidence that the applied CFD modelling methodology can be used for estimating/assessing exhaust plume rise velocities with sufficient accuracy.

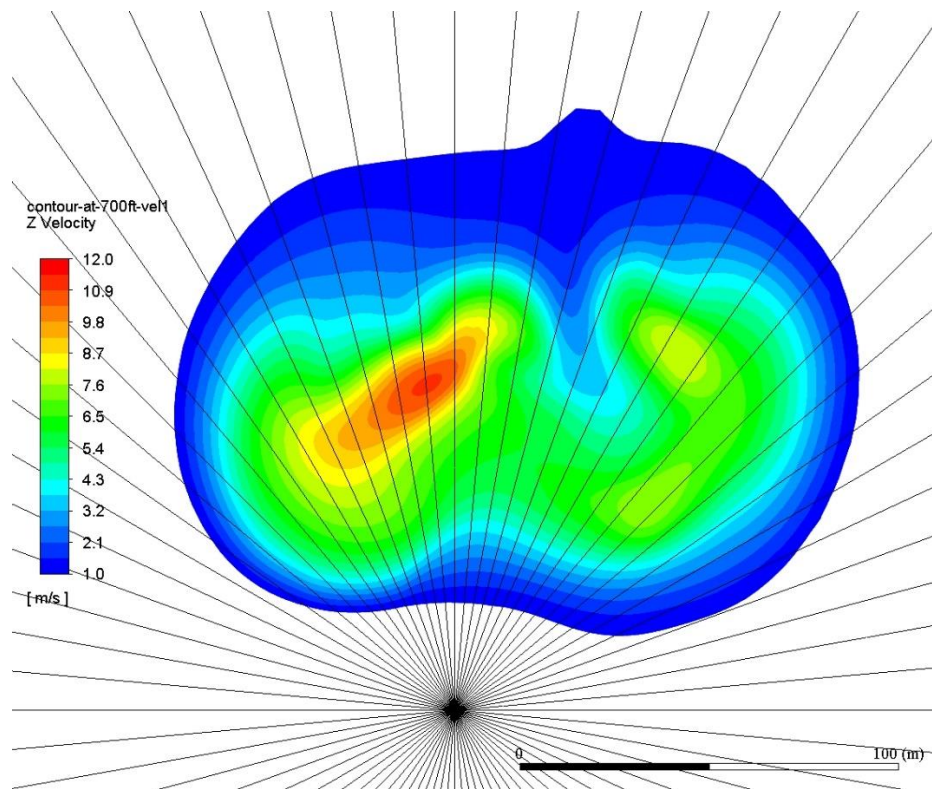
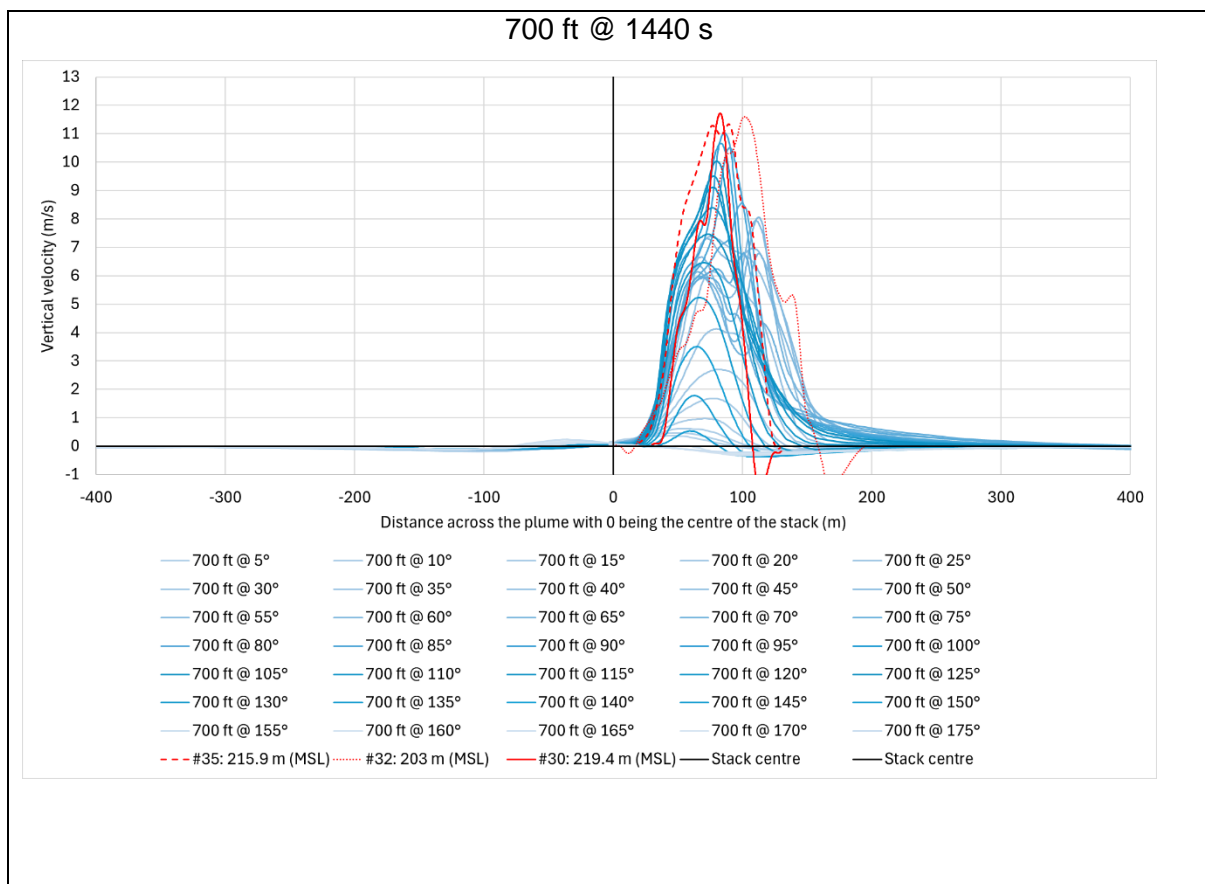
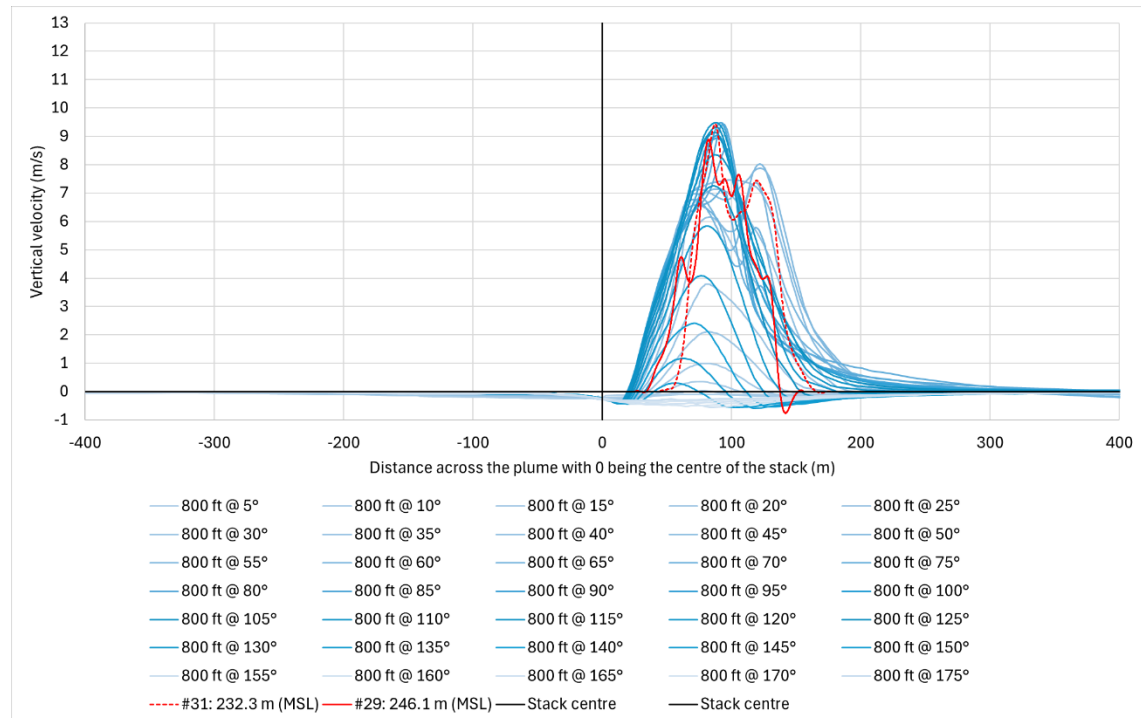


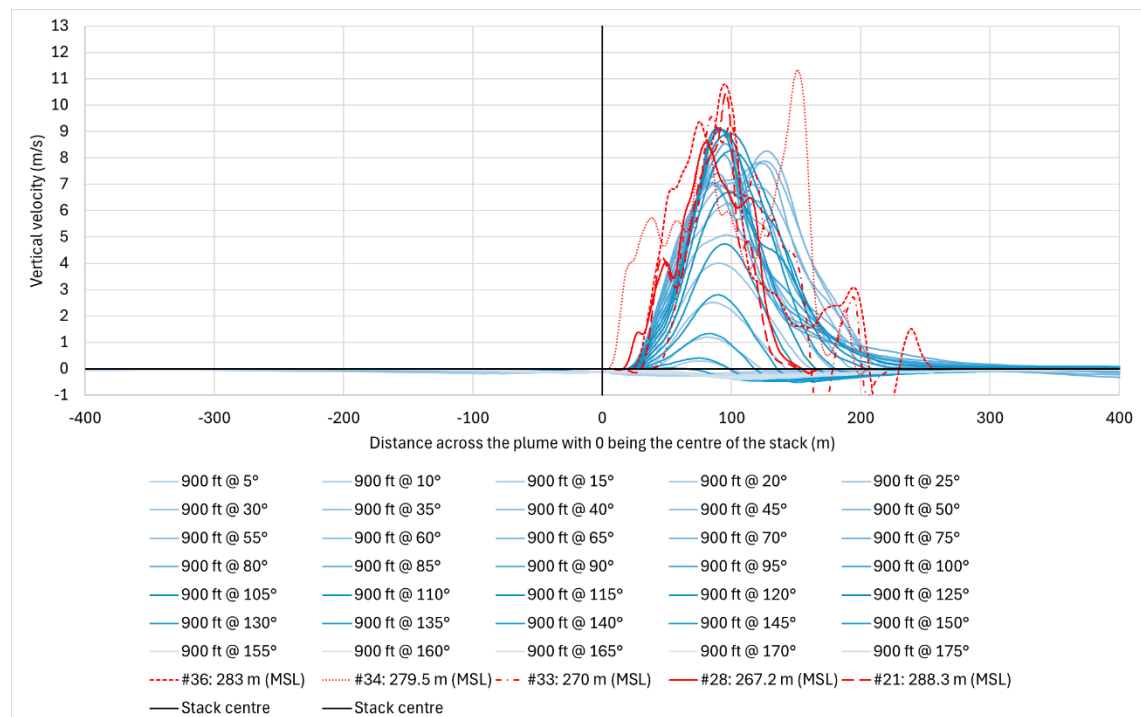
Figure 41. Trajectories through the plume in 5° intervals with the stack centre being the origin. Plume extent at 700 ft and a simulation time of 1440 s (same as shown in Figure 39) is used as an example.



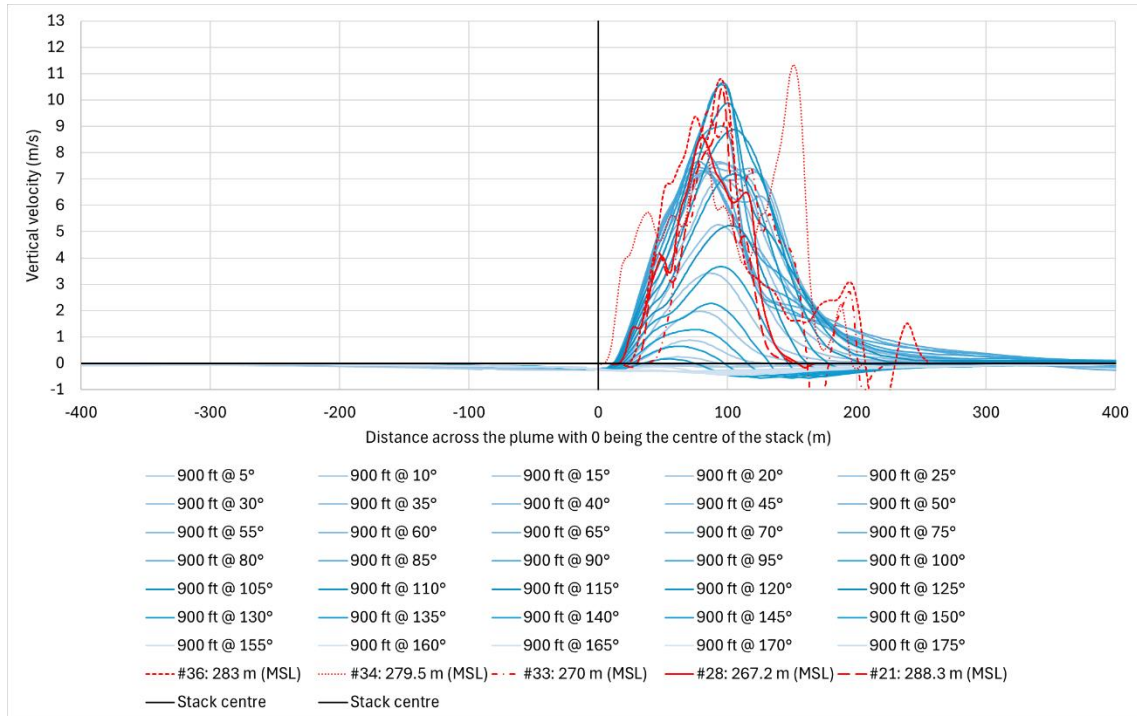
800 ft @ 1440 s



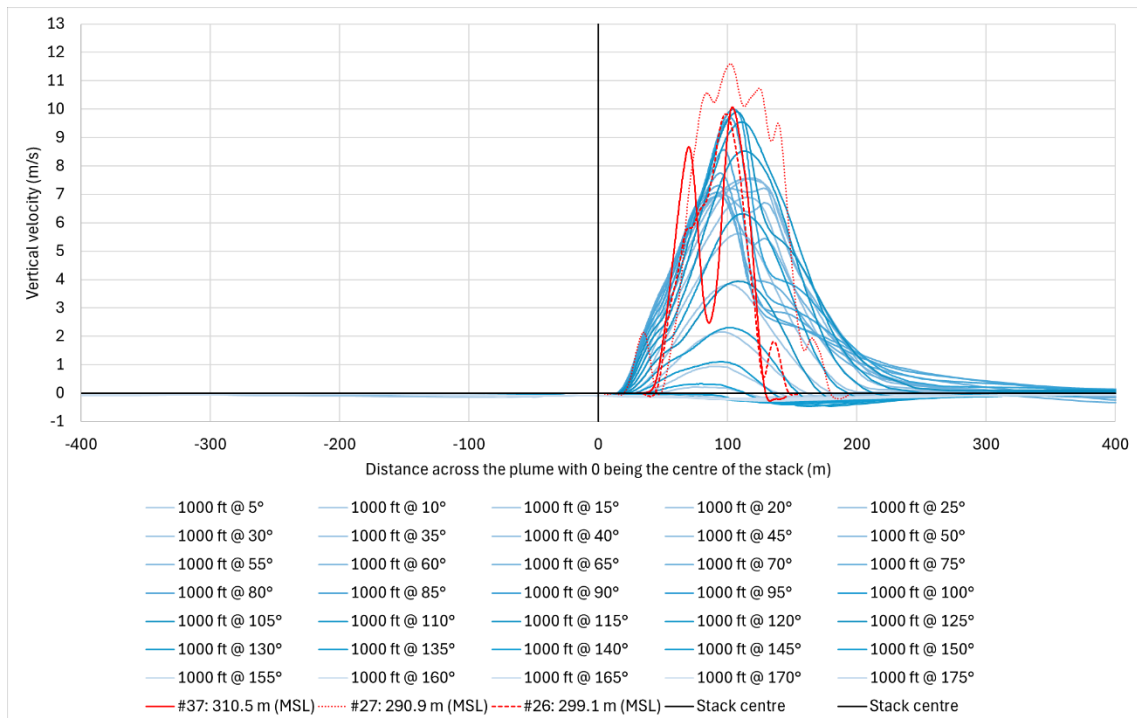
900 ft @ 1440 s



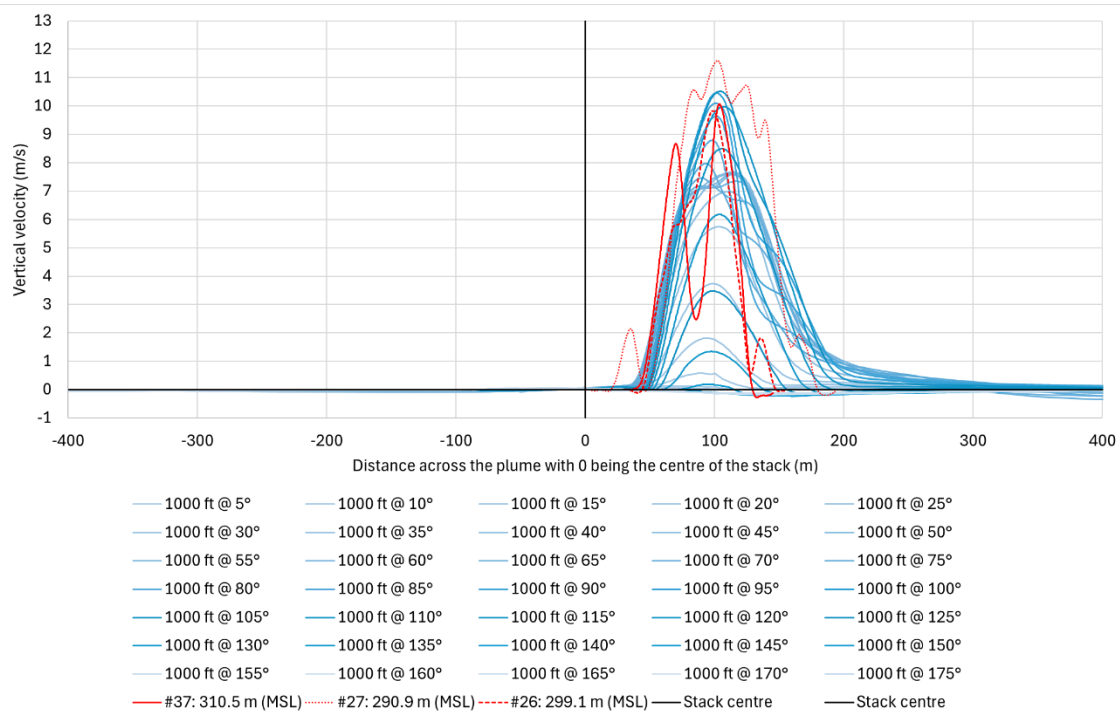
900 ft @ 1110 s



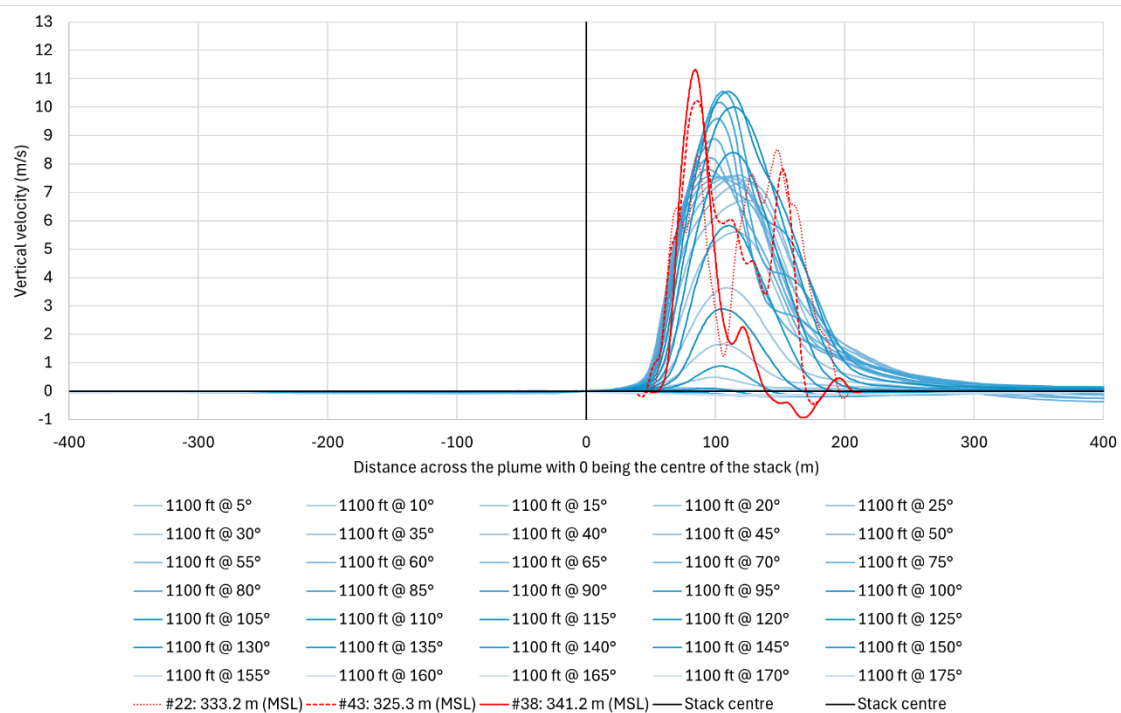
1000 ft @ 1110 s



1000 ft @ 1370 s



1100 ft @ 1370 s



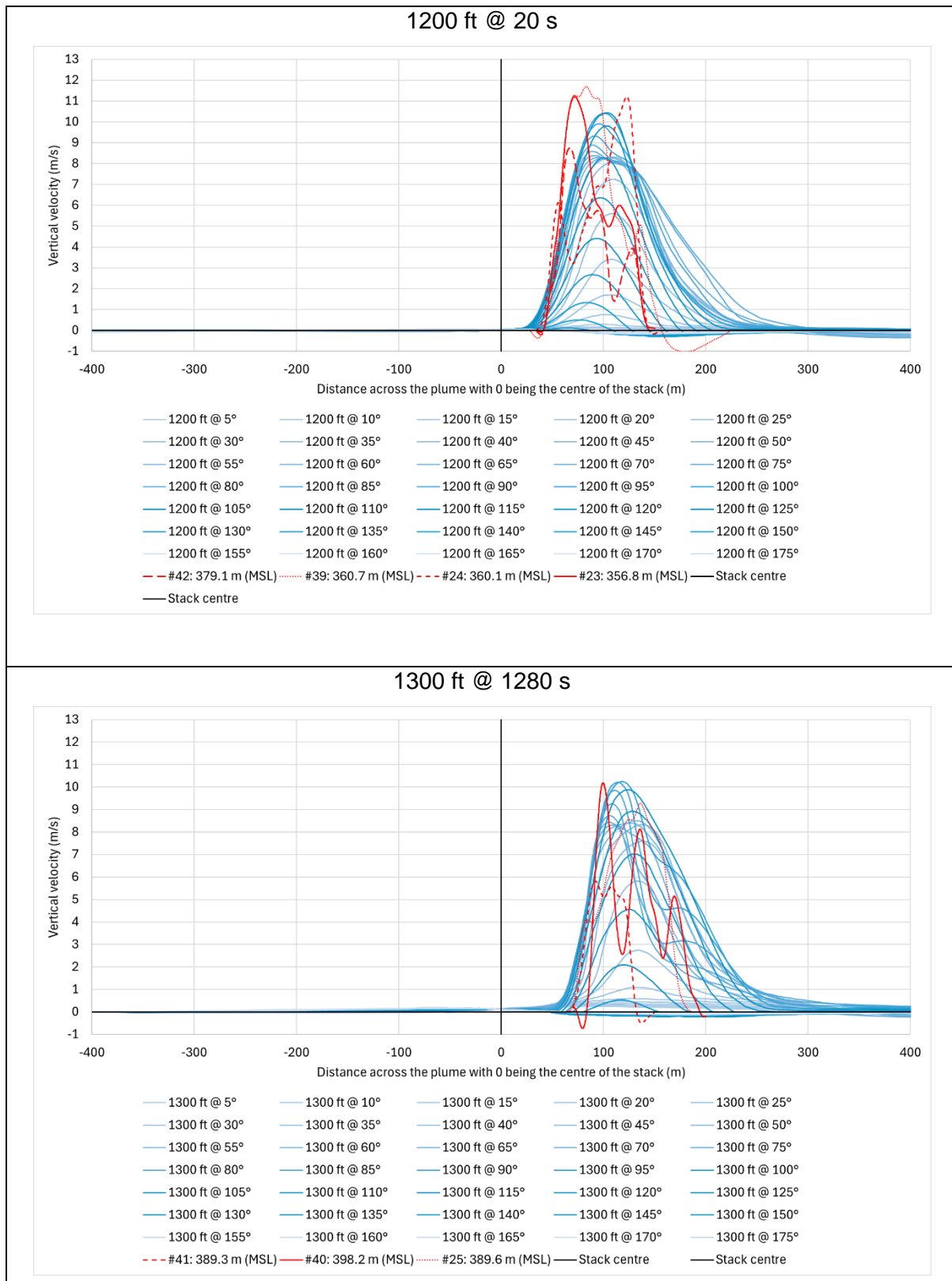


Figure 42. Plume profiles obtained from the CFD simulations based on stack-centred trajectories (blue) compared to the measured plume profiles as sampled on the 7th of August 2024 during the first plume survey flight between 10 am and 11 am (red). Plots are presented for different elevations and simulation times.

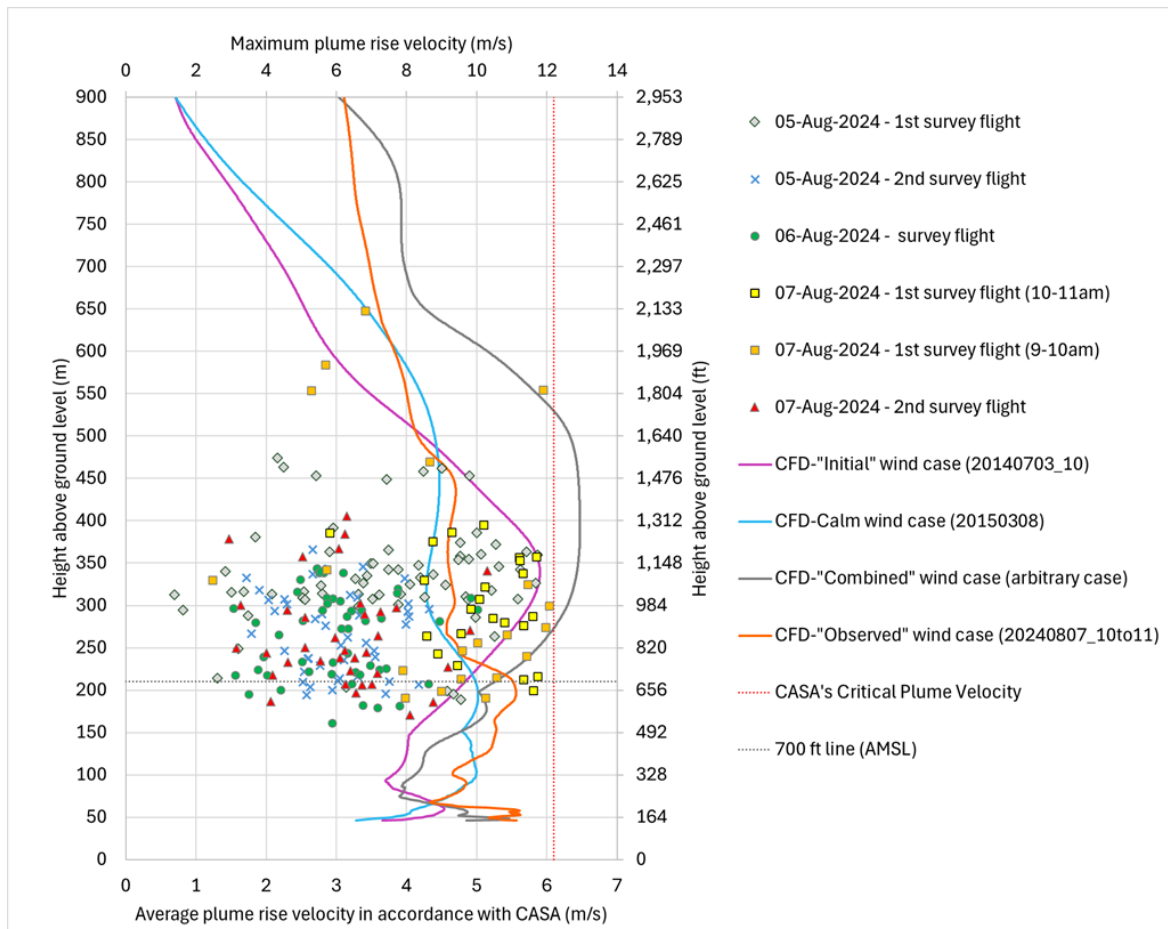


Figure 43. Highest recorded plume rise velocity per fly-through and elevation for the individual test periods, compared to the peak plume rise velocities obtained from the CFD simulations for the different wind cases at the evaluated timestep (elevation of peak plume rise velocity and velocity value itself can vary over time). The primary x-axis at the bottom is the average plume rise velocity in accordance with CASA's criterion. The secondary axis at the top of the plot is the peak plume rise velocity, which relates to double the CASA criterion.

6 REFERENCES

- [1] Ansys, Inc.: ANSYS Fluent User's Guide, Release 2020 R1, USA, January 2020
- [2] Ansys, Inc.: ANSYS Fluent Theory Guide, Release 2020 R1, USA, January 2020
- [3] Ansys, Inc.: ANSYS Fluid Dynamics Verification Manual, Release 2020 R1, USA, January 2020
- [4] T.-H. Shih, W.W. Liou, A. Shabbir, Z. Yang, and J. Zhu. "A New - Eddy-Viscosity Model for High Reynolds Number Turbulent Flows - Model Development and Validation". Computers Fluids. 24(3). 227–238. 1995.
- [5] Meteorological data (case: 20140703_10) provided to Stacey Agnew on 31 January 2020 per email.
- [6] Meteorological data (case: 20150308) provided to Stacey Agnew on 28 April 2021 per email.
- [7] GE Exhaust Stack Modification for CASA Compliance 02April2020.pdf provided to Stacey Agnew on 15 April 2020 per email.
- [8] Terrain data provided to Stacey Agnew on 5 February 2020 per email.
- [9] Stacey Agnew: Tallawarra B Power Station CFD Plume Modelling – Validation Case, Short Summary Report from 11th February 2020 - Draft.

- [10] Australian Government – Civil Aviation Safety Authority – Air Navigation, Airspace and Aerodromes, Letter regarding Tallawarra B Gas-Fire Power Station Project, File Ref: F17/8039-27 from 29/03/2021.
- [11] Stacey Agnew: Tallawarra B Power Station CFD Plume Modelling – GE-Modified PDD Design, Summary Report from 13th August 2021 version 6.
- [12] General Electric: Tallawarra B Power Station Plume Dispersion Device – CFD Report, Rev C2, TALLAB-GECL-61810-MEC020-0002 from 22nd April 2022.
- [13] General Electric: Tallawarra B Power Station Arrangement Exhaust System GA DIS100, Rev C, Document ID 116V3531 from 4th May 2022.
- [14] General Electric: 3D CAD Parasolid PDD geometry file (PDD_MOD3B_20DegBot_23DegTop_Final_01Feb23.x_t) provided per email by Tony Anthony on 9th February 2023.
- [15] General Electric: 1431277 – 9F.05 FL18 Tallawarra B – Plume Dispersion Device (PDD) Modification 3B – CFD Report, Revision R0 from 8th February 2023 (9F05_Tallawarra_Modification-3B_PDD_CFD_Report_EA_08Feb2022-R0.pdf) provided per email by Simon Welchman on 16th February 2023.
- [16] Australian Government – Civil Aviation Safety Authority – Advisory Circular AC 139.E-02v1.0, Plume rise assessments, March 2023, File ref: D22/198264, <https://www.casa.gov.au/plume-rise-assessments>.
- [17] A. Galfy, R. Gaggl, R. Mühlbacher, D. Frank, J. Schlarp, and G. Schitter, Turbulence load prediction for manned and unmanned aircraft by means of anticipating differential pressure measurements, CEAS Aeronautical Journal, vol. 12, 2021, <https://link.springer.com/article/10.1007/s13272-021-00512-y>.
- [18] A. Galfy, J. Schlarp, D. Frank, R. Mühlbacher, and G. Schitter, Turbulence prediction for aircraft by means of high-dynamic differential pressure measurements, in Proceedings of the Aerospace Europe Conference AEC2020, 2020, https://publik.tuwien.ac.at/files/publik_292322.pdf.
- [19] A. Galfy, F. Car, and G. Schitter, Calibration and flight test of a 3D printed 5-hole probe for high-dynamic wind measurements for UAV, in Proceedings of the International Workshop on Research, Education and Development on Unmanned Aerial Systems, 2019, https://publik.tuwien.ac.at/files/publik_282543.pdf.
- [20] Temporary Danger Area in the Shellharbour Area: https://www.avsef.gov.au/consultations/temporary-danger-area-shellharbour-area?utm_source=Swift%20Digital&utm_medium=Email&utm_campaign=AvSafety%20Seminars
- [21] Energy Australia, Plume Validation Monitoring Program – Tallawarra B Power Station, Final, Revision D from 8 July 2024.
- [22] Turbulence Solutions, Tallawarra B Plume Measurement Flights – Plume Updraft Velocity by In-Flight Flow Measurements 2024-08-05 until 2024-08-07 from 21-10-2024.



Tallawarra B Plume Measurement Flights

Plume Updraft Velocity by In-Flight Flow Measurements 2024-08-05 until 2024-08-07

2024-10-21, DI András Gálffy

Table of Contents

1	Executive Summary.....	2
2	Plume Analysis.....	2
3	Simulated Test Flights and Evaluation	4
4	Actual Test Flights: 2024-08-05, 2024-08-06, 2024-08-07.....	8
5	Measured Plumes: 2024-08-05 First Flight.....	11
6	Measured Plumes: 2024-08-05 Second Flight.....	45
7	Measured Plumes: 2024-08-06 Flight.....	68
8	Measured Plumes: 2024-08-07 First Flight.....	94
9	Measured Plumes: 2024-08-07 Second Flight.....	116

1 Executive Summary

The objective of the test flight campaign was to measure the flow characteristics of the exhaust plume at Tallawarra B power station, by sampling the plume with airborne sensors. The test flights were conducted on three consecutive days with well-suited weather conditions on August 5, 6 and 7.

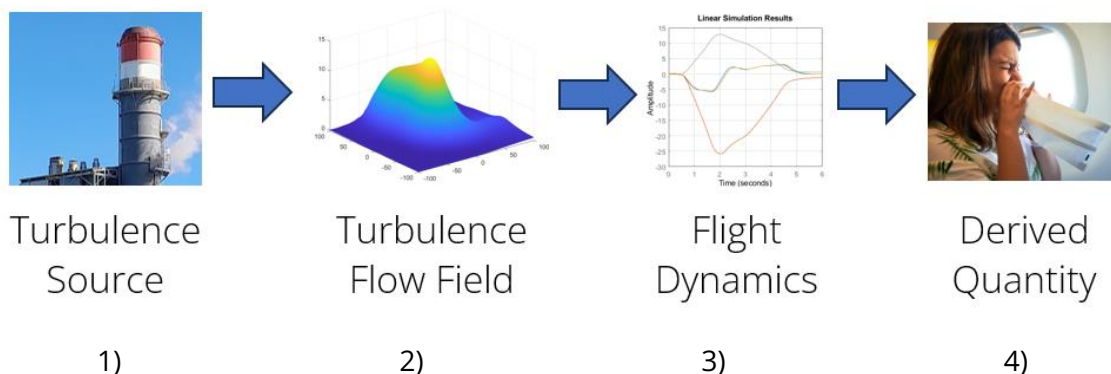
The plume fly-throughs were conducted as planned, with no incidents or any safety-relevant situation. The airspace around the power station was declared as a temporary danger area by NOTAM, which was kindly respected by the pilots operating at Shellharbour airport. During aerial work in progress, periodic radio calls were performed, to make sure all pilots were aware of the flight sampling operation close to Tallawarra B power station.

In total, 240 plume fly-throughs were analyzed and included in this report. Fly-throughs which recorded trivial updraft were not included. The highest maximum plume velocity could be observed during the very calm wind conditions on August 7, with some peaks at around 12 m/s, however, all were below the CASA criterion of 12.2 m/s (in accordance with CASA, half of that peak value is the average Critical Plume Velocity of 6.1 m/s).

2 Plume Analysis

Context Introduction

A typical impact cascade of inflight turbulence consists of a 1) turbulence source (ground roughness/terrain, surface heating, artificial turbulence source), which leads to a 2) turbulence flow field (spatial and time dependent flow field), which changes aerodynamic forces impacting the 3) flight dynamics (vertical acceleration, pitch and roll motion), which itself impacts 4) derived quantities (safety, comfort, trust, fear of flying, loss of control, etc.):



In case of the Tallawarra power station the turbulence source is the exhaust gases released by the stack with given velocity and temperature, leading to a plume as source of updrafts and turbulence. The expected plume characteristics had been predicted by CFD simulation. The scope of flight campaign was to verify the result by inflight measurements. The flight tests allowed measurement of the flight dynamics 3) by inertial sensors and the turbulence field 2) by flow sensors.

Test Flight Specifications

Obtain high-rate data:

- Accelerations at probe location
- Accelerations at center of gravity
- Turn rates at probe location
- Turn rates at CG
- Pressures at probe location
- 360 deg video of cockpit

Calibrate sensors:

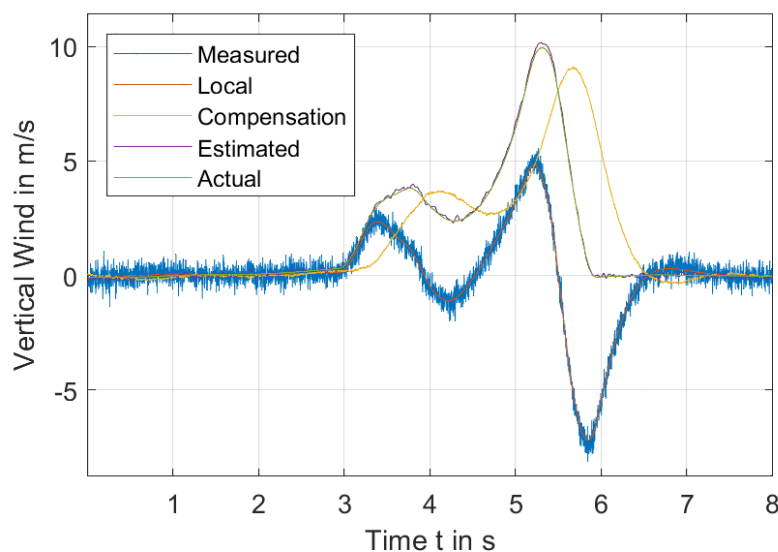
- ID flight manoeuvre (rectangle pitch input, no turbulence)
- Flight in turbulence (zero pitch input, probe sensor to acceleration)
- Panel method simulation

Perform fly-throughs:

- Fixed controls during fly-through (minimum or ideally no pilot pitch & roll input)
- Various airspeeds
- Straight and level flight before entering plume

Plume Estimation from Flight Data

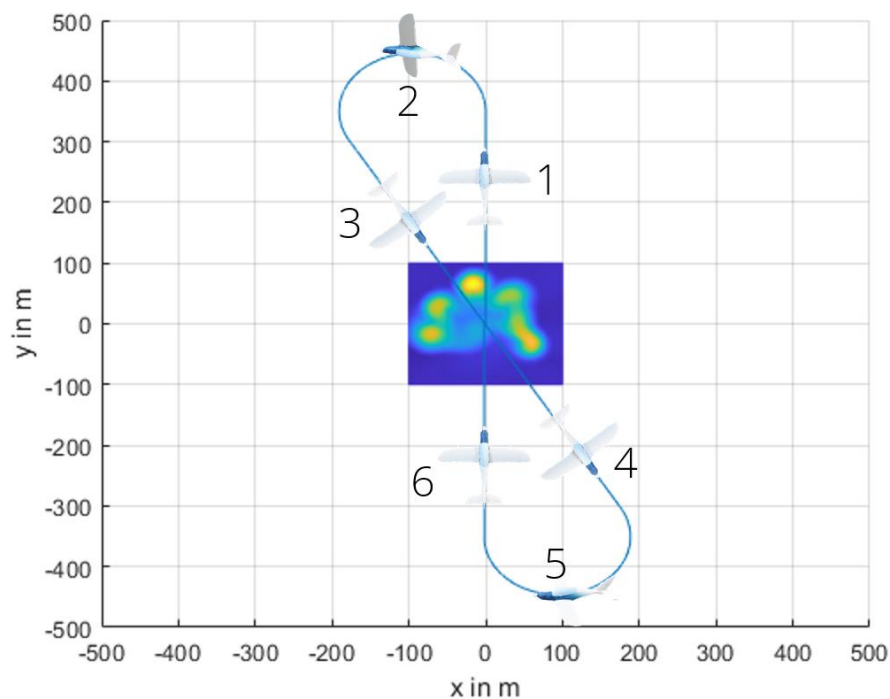
Before the flight tests, the measured flow signal was simulated as it was to be expected for the CFD-predicted plume flow field and predicted flight dynamics. The blue line in the figure below shows the actual measured flow at the turbulence flow sensor (turbulence probe), which corresponds to the local flow (red line) with added sensor noise. To get to the estimated flow (purple line), the compensation flow (yellow line) based on flight dynamics and aerodynamics needs to be added. The estimated flow then corresponds to a very high degree to the actual flow of the plume flow field (green line).



3 Simulated Test Flights and Evaluation

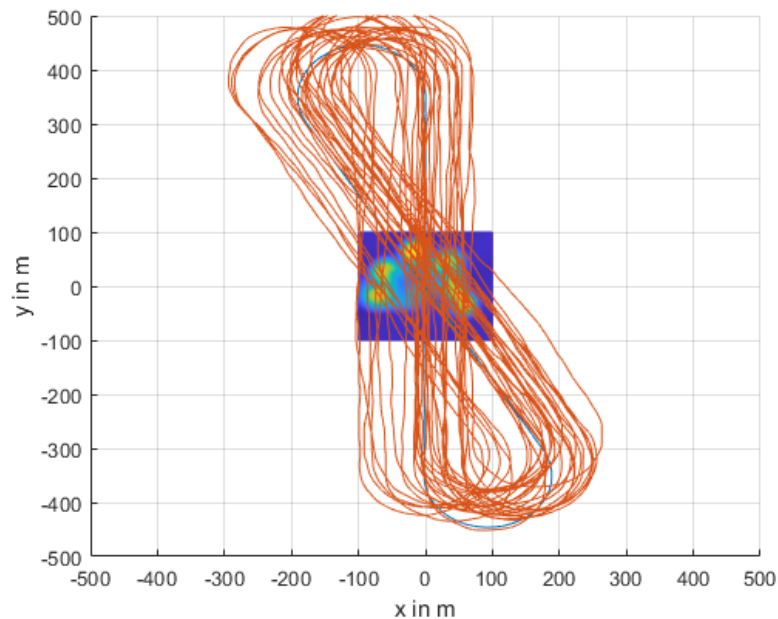
While prior knowledge w.r.t. approximate plume dimensions and expected velocities comes from CFD simulations of the plume, the exact shape and position of the plume (time and spatial variations) during any test flight is a priori unknown. Even for hypothetical constant wind conditions, the plume itself shows dynamic behavior, like the “dancing” flame of a candle. Additionally, actual environmental conditions show at least slight alteration of wind speeds and direction, further repositioning and reshaping the plume. Therefore, a large number of fly-throughs was to be performed in order to collect sufficient plume sampling data to be able to assess the plume characteristics with confidence.

An efficient pattern to optimize the number of fly-throughs of the Tallawarra B exhaust plume w.r.t. the available time, within appropriate weather windows, is the following figure-eight maneuver:

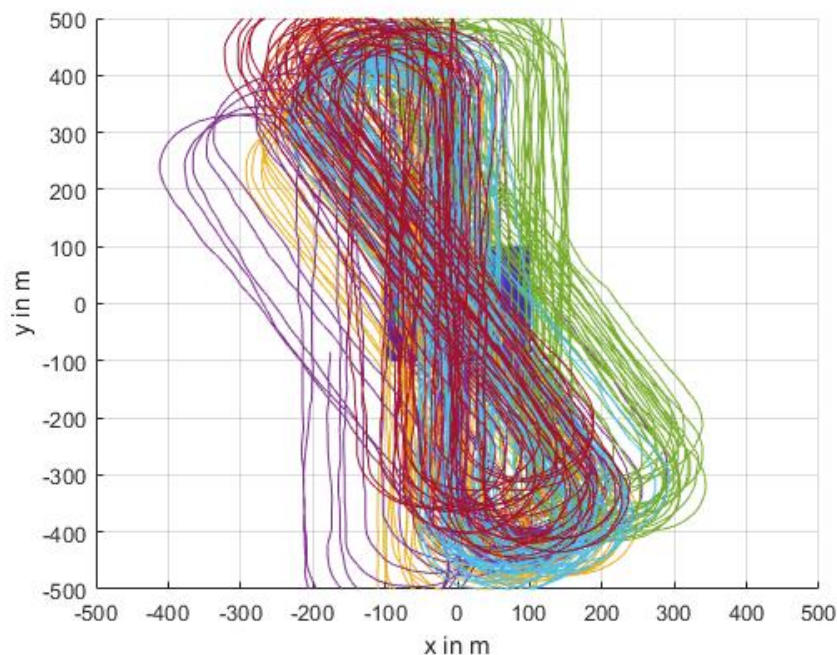


Beginning from the initial fly-through 1) approx. 10 sec straight segment, 2) approx. 10 sec high-bank turn, 3) approx. 10 sec straight segment preparing the second fly-through, 4) approx. 10 sec straight segment, 5) approx. 10 sec turn to return to the sampling target, 6) approx. 10 sec straight segment preparing the third fly-through. This results in up to 2 fly-throughs every 60 sec. For multiple sequential manoeuvres, up to 120 fly-throughs per hour can be achieved. The basic principle is unchanged for various airspeeds, only the pattern gets smaller or bigger according to the change of airspeed. The above depicted pattern is for an airspeed of 35 m/s, i.e. 10 sec correspond to 350 m, as can be seen for the 6 legs. For this, a turn rate of $21^{\circ}/\text{sec}$ is required, which leads to 1.6 g turns for 35 m/s, which is well within the normal operational envelope of the aircraft.

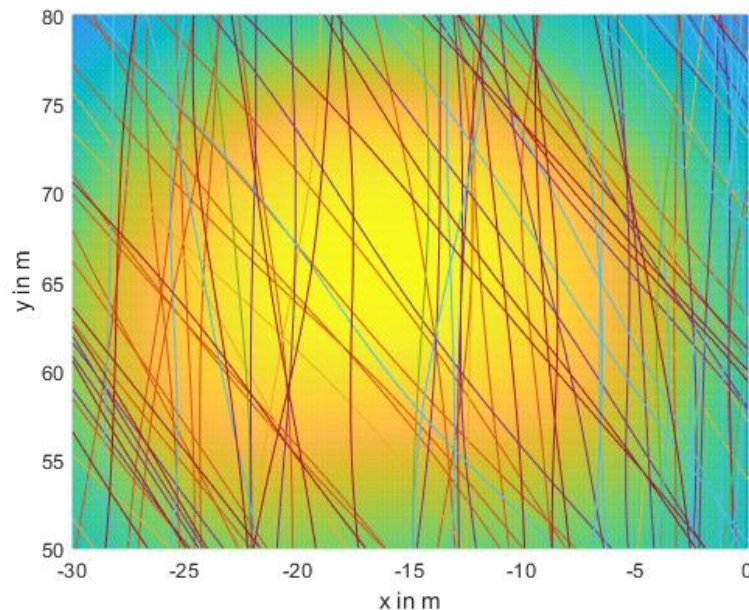
The exact position and angle of the pattern was planned to be varied, to sample a variety of flow points of the plume. These variations can be achieved by actively offsetting the pattern for sequential fly-throughs (ground reference or GPS feedback), but also occurs naturally during actual flight tests due to typical flight control variations, as well as change in the actual plume shape and location as discussed (plume dynamics, changing wind conditions). Multiple sequential manoeuvres result in an overall sampling pattern similar to that depicted in red below (compared to ideal pattern in blue):



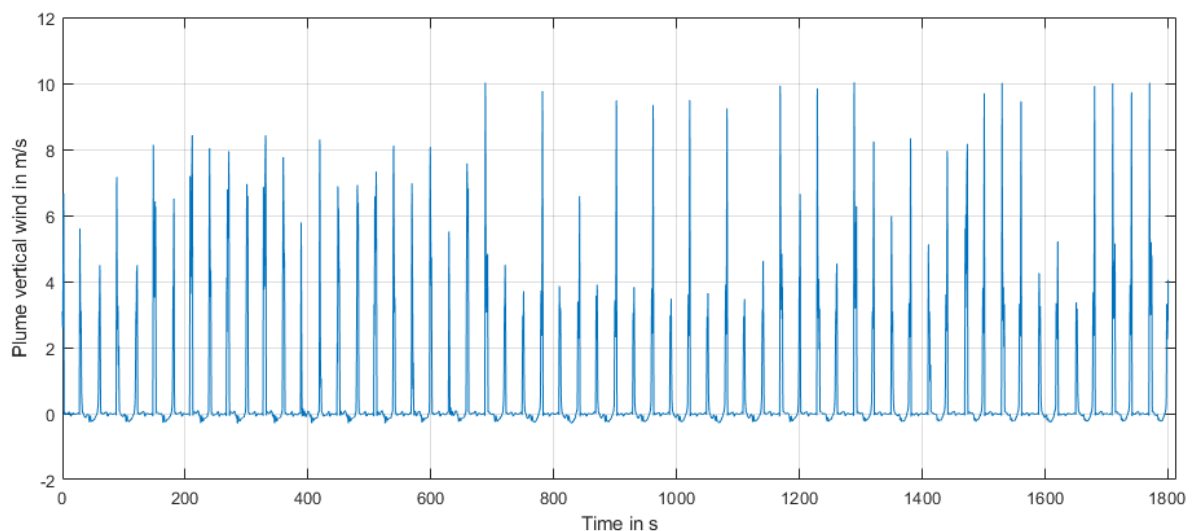
This corresponds to 30 figure-eight manoeuvres, i.e. 30 min of flight testing, resulting in ideally 60 fly-throughs (2 fly-throughs for each figure-eight manoeuvre).



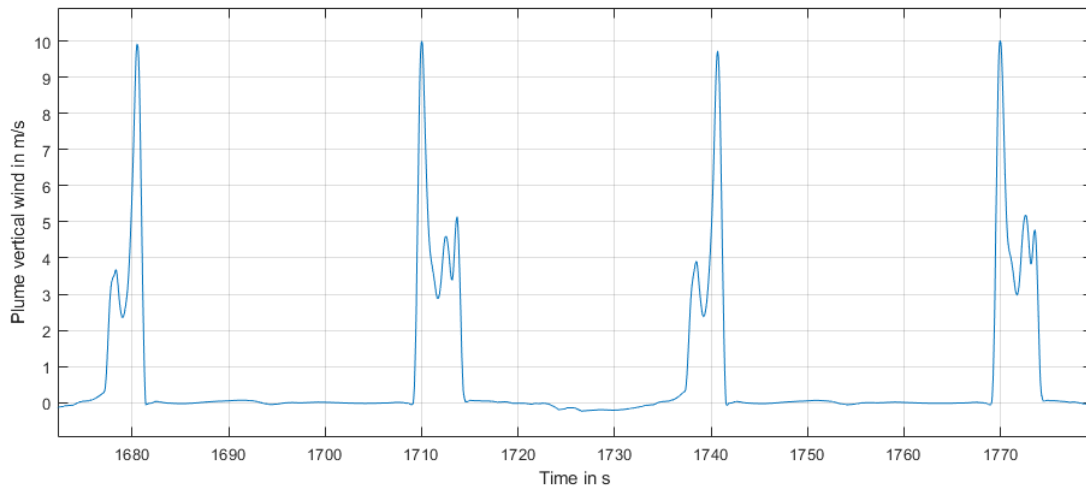
Six individual 30 min test flights result in a dense sampling of the plume field, with up to 360 fly-through attempts and the analysis of 200-300 measured plume profiles expected. Assuming a constant plume shape, the most critical plume features (individual columns of high-flow rising air) are sampled multiple times for every individual flight. These can then be compared to the CFD simulation for similar weather conditions. Additionally, by flying in the critical weather conditions (calm and cold air) the compliance with the maximum updraft criterion can also be validated directly.



The time signal of the estimated plume vertical velocity for one example simulated 30 min flight shows the periodic fly-throughs, where some are directly hitting the most critical flow features, while some are sampling less intense updraft areas of the plume. Note that for varying plume shape and position (plume dynamics and varying wind conditions) it is to be expected that some attempted fly-throughs will miss the plume, without measuring significant plume rise velocities.



Zooming into a sequence of fly-throughs shows that also the specific pattern of the sampled plume section can be accurately resolved spatially (sample time of 2 ms at an airspeed of 50 m/s leads to one sample every 0.1 m). One entire plume section is recorded in about 5 seconds (e.g. 1709 s until 1715 s), i.e. 2500 samples for a centred fly-through.



By performing fly-throughs at various altitudes and in various weather conditions (primarily focusing on the worst case scenarios obtained by simulation), sufficient flight data can be obtained to be able to assess the plume characteristics and its impact with sufficient confidence.

4 Actual Test Flights: 2024-08-05, 2024-08-06, 2024-08-07

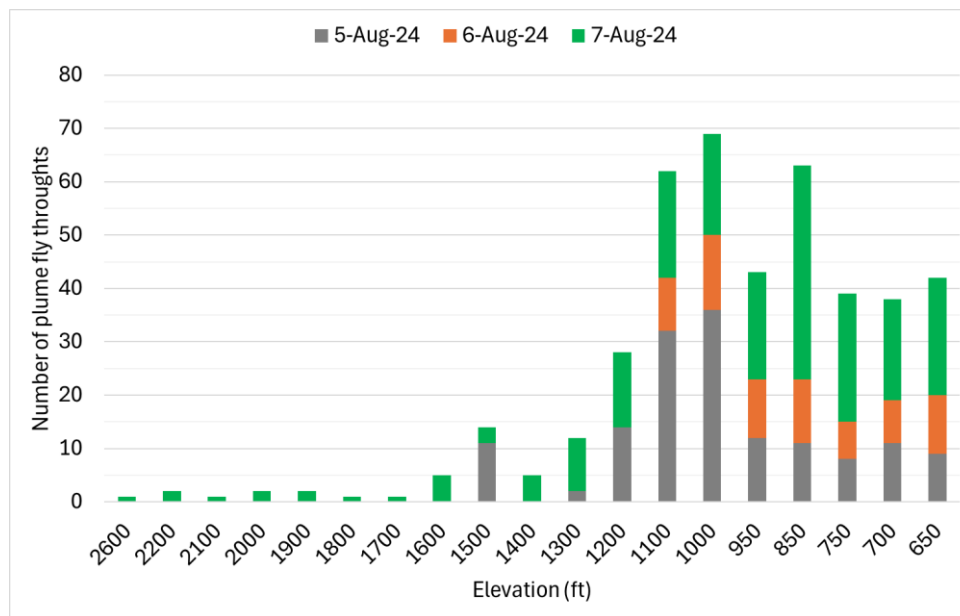
The actual flight tests were performed on 5th, 6th, and 7th of August 2024 with a Cessna 172 operated from Shellharbour Airport. The airflow sensor was installed on the left wing strut:



Additionally an Inertial Measurement Unit (IMU) was installed on the co-pilot side of the cockpit:



The fly-throughs were mainly focused on altitudes from 800 ft to 1200 ft, where the highest plume velocities were expected from CFD simulations (and also noted during the flight tests). Additionally, on August 7 during very calm wind conditions (westerly wind shifting to easterly wind with almost perfect calm wind in between) with expected stable plumes up to higher altitudes, flights up to 2600 ft were performed. In total, 240 plume profiles were analyzed and are included in this report. The highest plume velocity peaks could be observed during the very calm wind conditions on August 7 with some peaks close to 12 m/s. However, all were below the CASA criterion of 12.2 m/s (in accordance with CASA, half of that peak value is the average Critical Plume Velocity of 6.1 m/s).

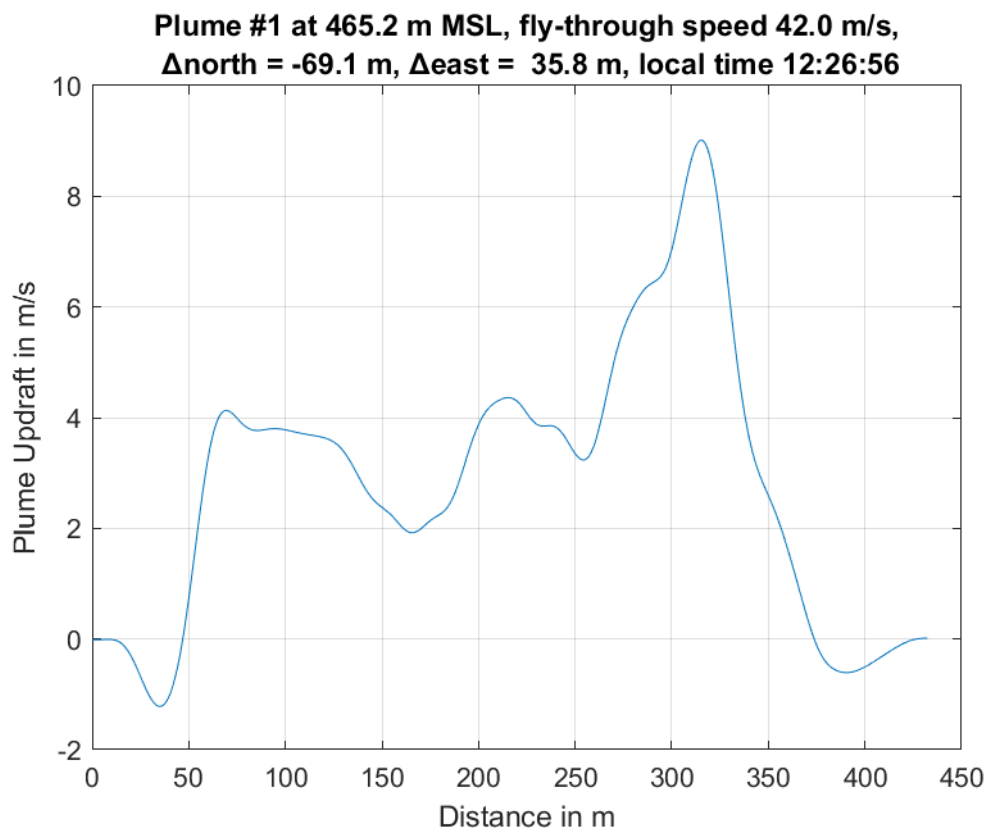
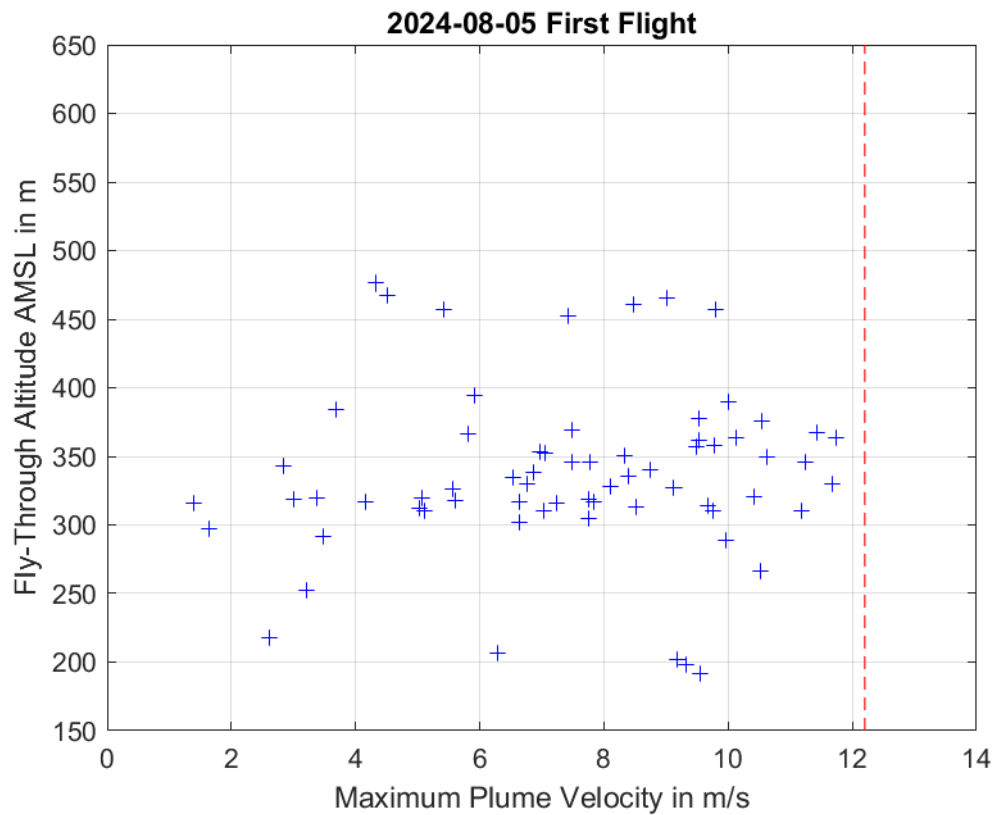


Date	Item	Flight Time	Flight Duration
Monday 5/08/2024	Calibration flight	10:00am-11:00am & 04:10pm-04:25pm	1 hour and 15 minutes
Monday 5/08/2024	Measurement flight	12:00pm-02:40pm & 03:15pm-04:10pm	3 hours and 35 minutes
Tuesday 6/08/2024	Calibration flight	09:00am-10:00am & 04:55pm-05:10pm	1 hour and 15 minutes
Tuesday 6/08/2024	Measurement flight	03:30pm-04:55pm	1 hour and 25 minutes
Wednesday 7/08/2024	Calibration flight	02:00pm-02:15pm	15 minutes
Wednesday 7/08/2024	Measurement flight	09:10am-11:15am & 12:30pm-02:00pm	3 hours and 35 minutes

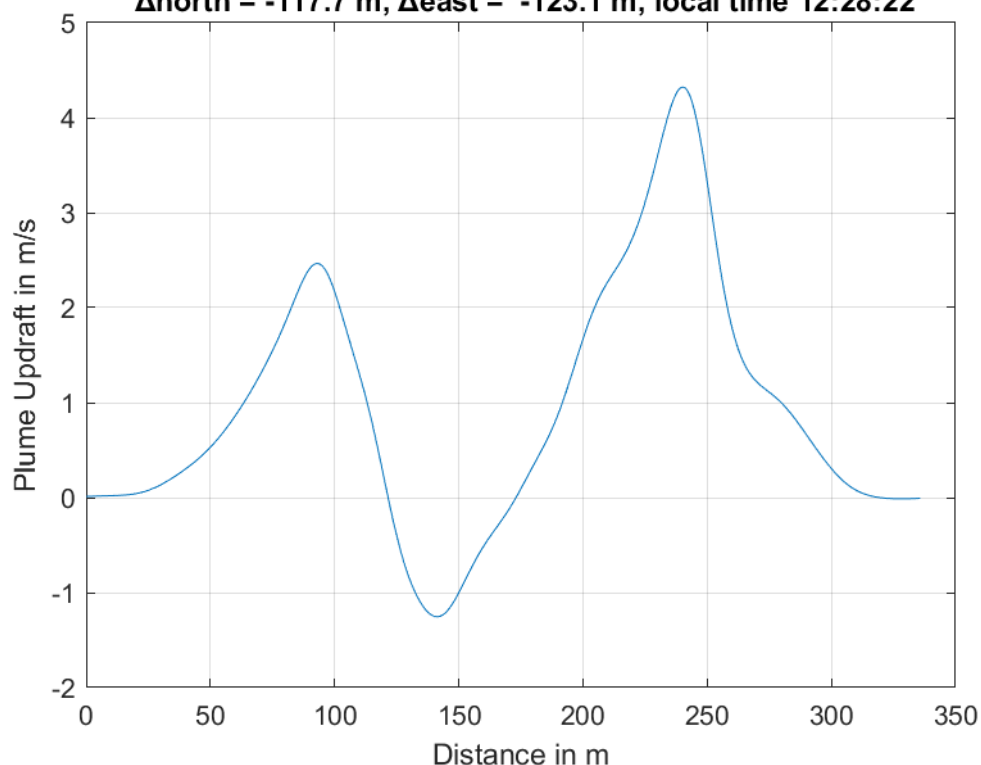




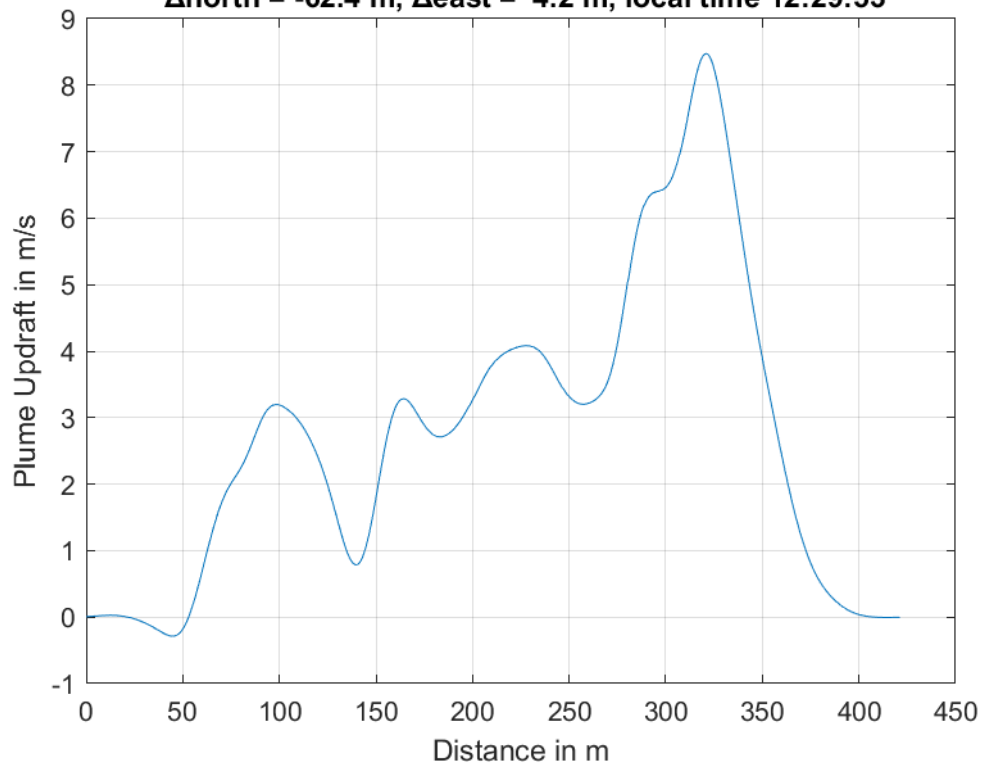
5 Measured Plumes: 2024-08-05 First Flight



**Plume #2 at 477.1 m MSL, fly-through speed 42.0 m/s,
 $\Delta_{\text{north}} = -117.7$ m, $\Delta_{\text{east}} = -123.1$ m, local time 12:28:22**

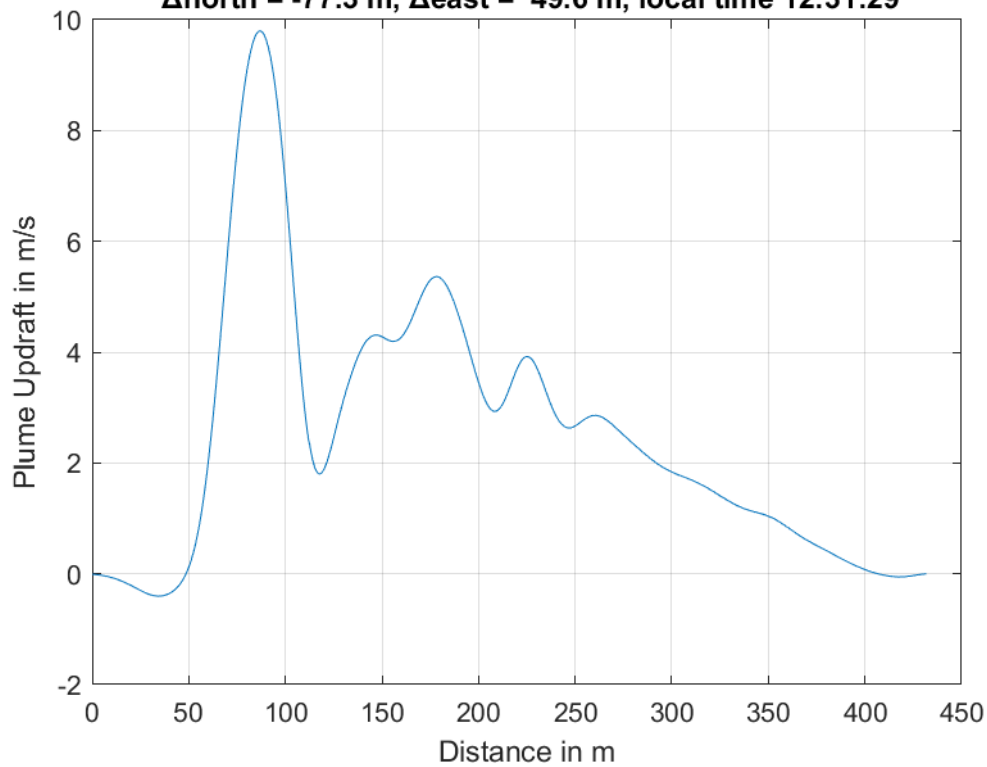


**Plume #3 at 461.2 m MSL, fly-through speed 43.0 m/s,
 $\Delta_{\text{north}} = -62.4$ m, $\Delta_{\text{east}} = 4.2$ m, local time 12:29:53**

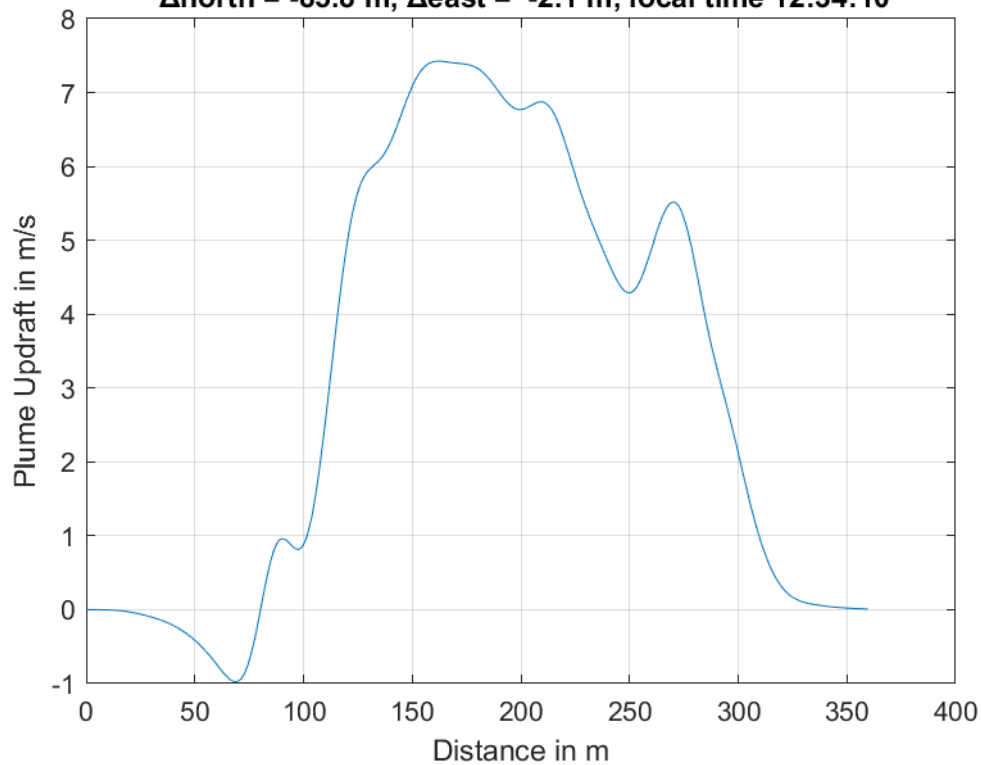




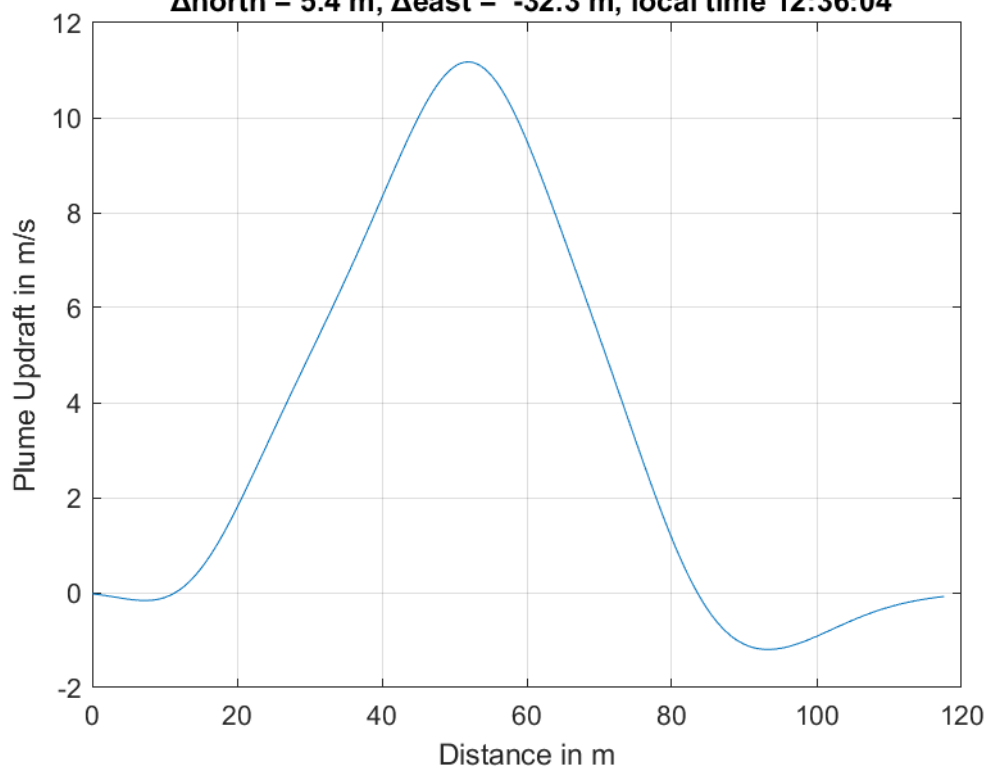
**Plume #4 at 456.8 m MSL, fly-through speed 45.0 m/s,
 $\Delta_{\text{north}} = -77.3$ m, $\Delta_{\text{east}} = 49.6$ m, local time 12:31:29**



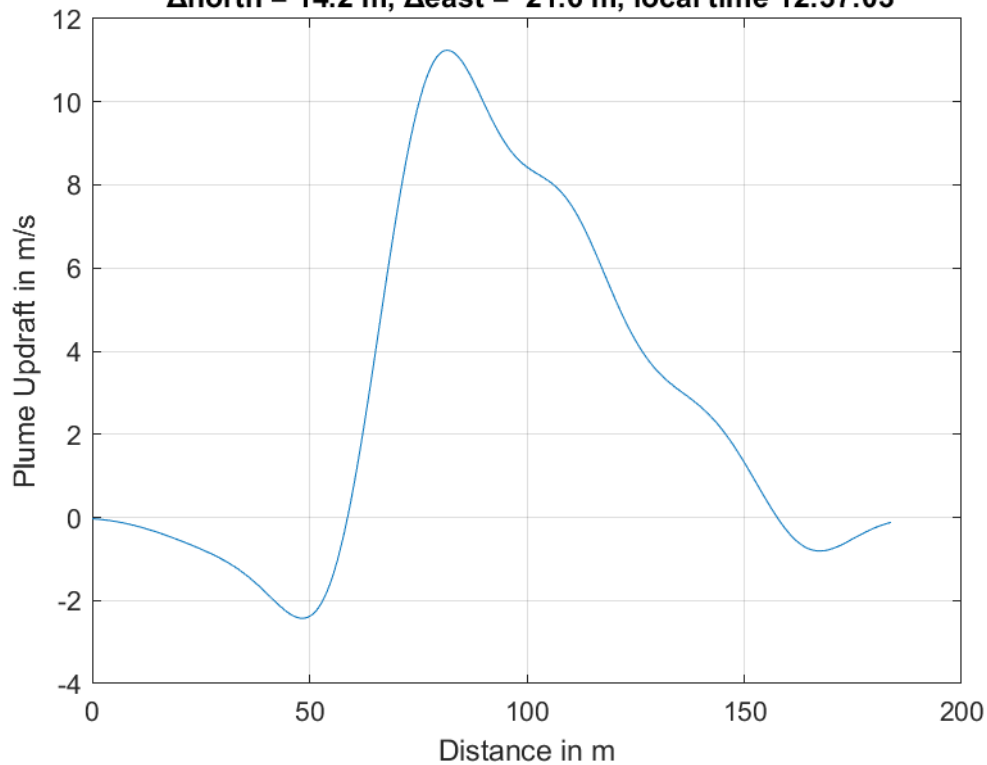
**Plume #5 at 452.2 m MSL, fly-through speed 45.0 m/s,
 $\Delta_{\text{north}} = -85.8$ m, $\Delta_{\text{east}} = -2.1$ m, local time 12:34:10**



**Plume #6 at 310.6 m MSL, fly-through speed 42.0 m/s,
 $\Delta_{\text{north}} = 5.4$ m, $\Delta_{\text{east}} = -32.3$ m, local time 12:36:04**

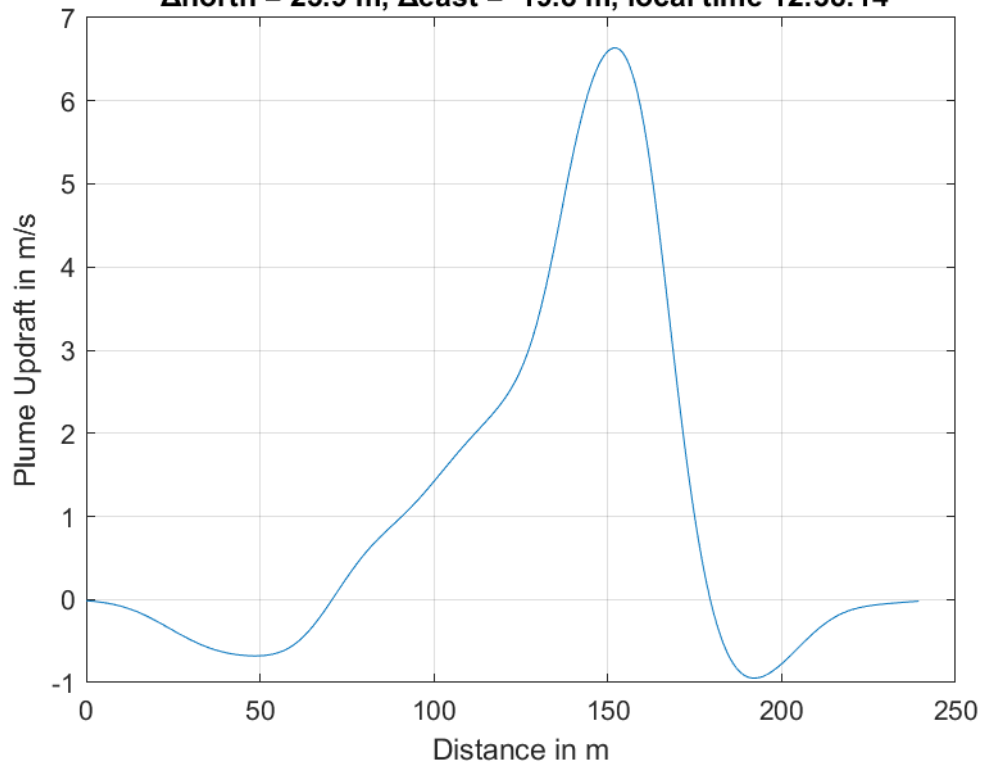


**Plume #7 at 345.9 m MSL, fly-through speed 46.0 m/s,
 $\Delta_{\text{north}} = 14.2$ m, $\Delta_{\text{east}} = 21.6$ m, local time 12:37:03**

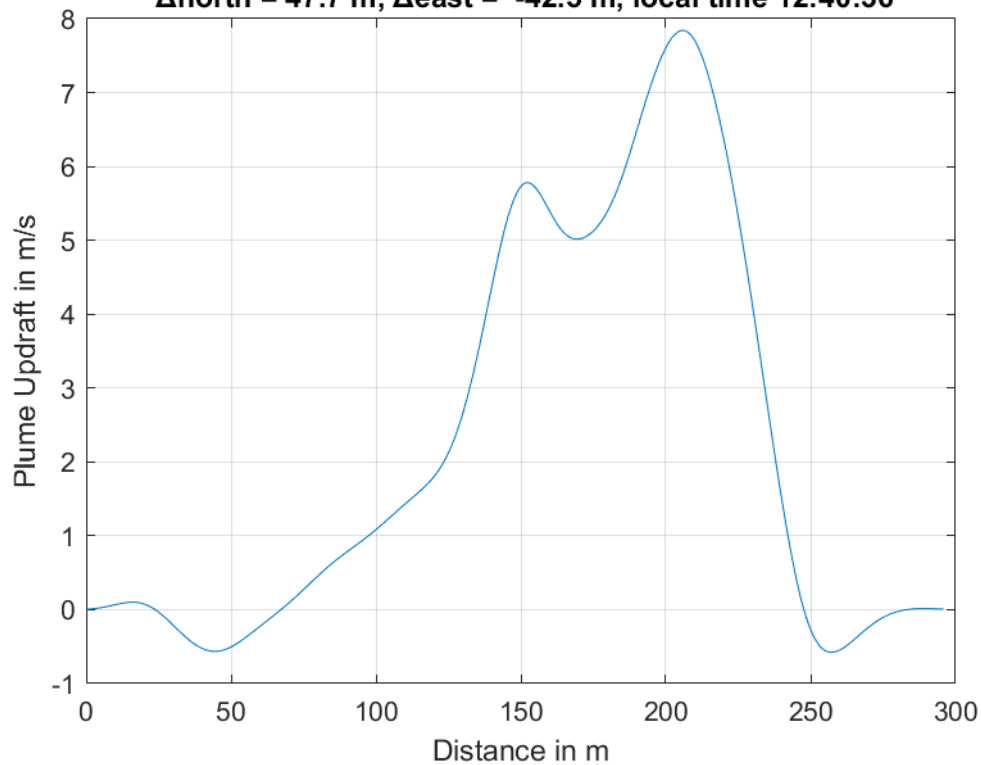




**Plume #8 at 316.6 m MSL, fly-through speed 47.0 m/s,
 $\Delta_{\text{north}} = 23.9$ m, $\Delta_{\text{east}} = 19.8$ m, local time 12:38:14**

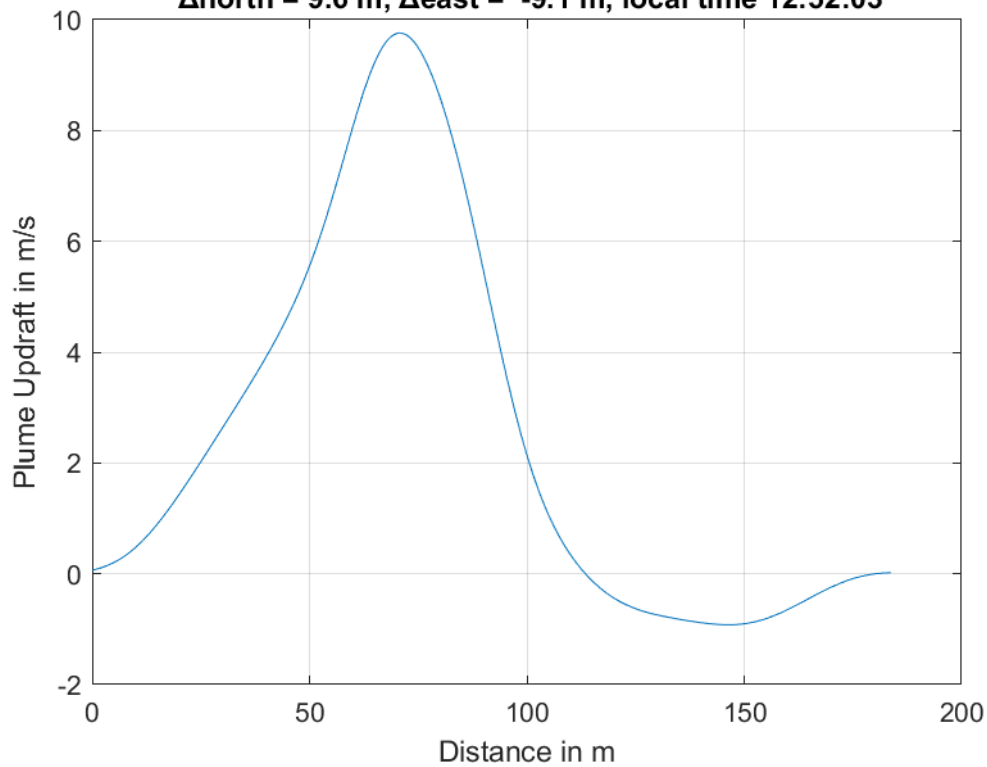


**Plume #9 at 316.4 m MSL, fly-through speed 47.0 m/s,
 $\Delta_{\text{north}} = 47.7$ m, $\Delta_{\text{east}} = -42.5$ m, local time 12:40:36**

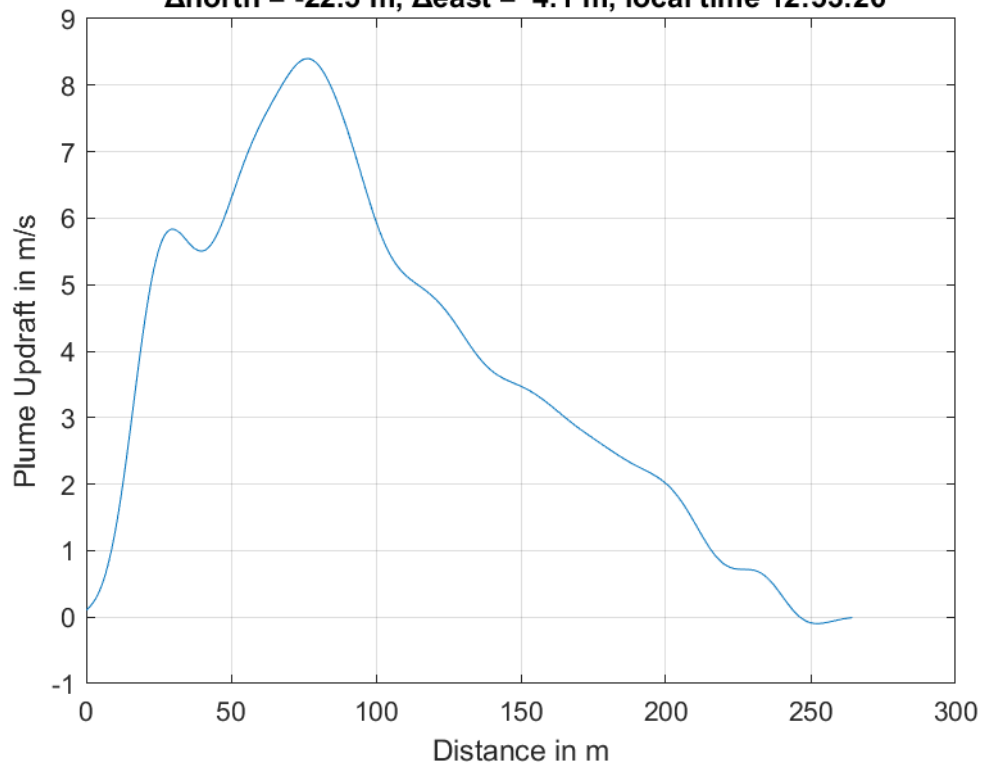




**Plume #10 at 309.9 m MSL, fly-through speed 46.0 m/s,
 $\Delta_{\text{north}} = 9.6$ m, $\Delta_{\text{east}} = -9.1$ m, local time 12:52:03**

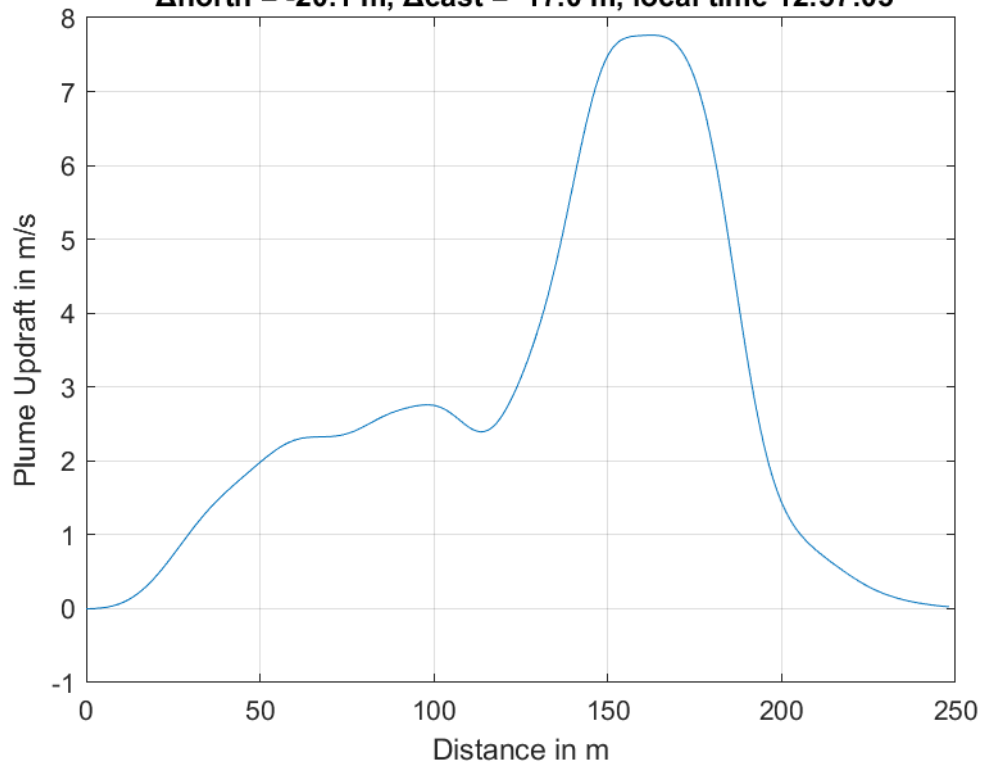


**Plume #11 at 335.9 m MSL, fly-through speed 42.0 m/s,
 $\Delta_{\text{north}} = -22.5$ m, $\Delta_{\text{east}} = 4.1$ m, local time 12:53:26**

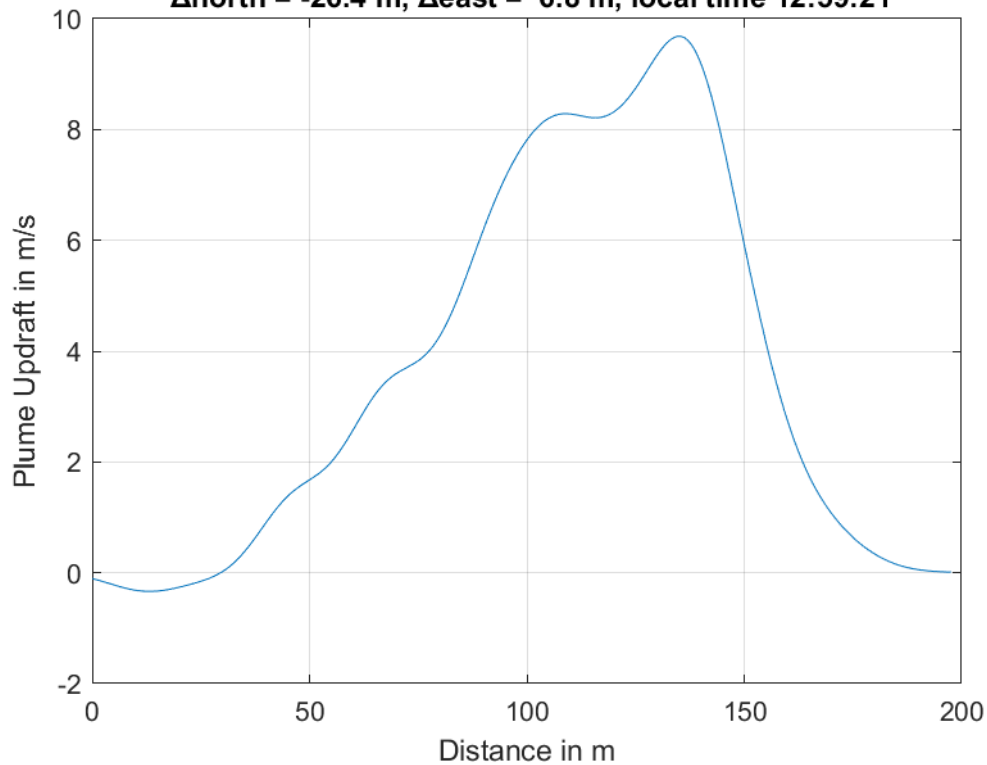




**Plume #12 at 318.5 m MSL, fly-through speed 46.0 m/s,
 $\Delta_{\text{north}} = -20.1$ m, $\Delta_{\text{east}} = 17.0$ m, local time 12:57:05**

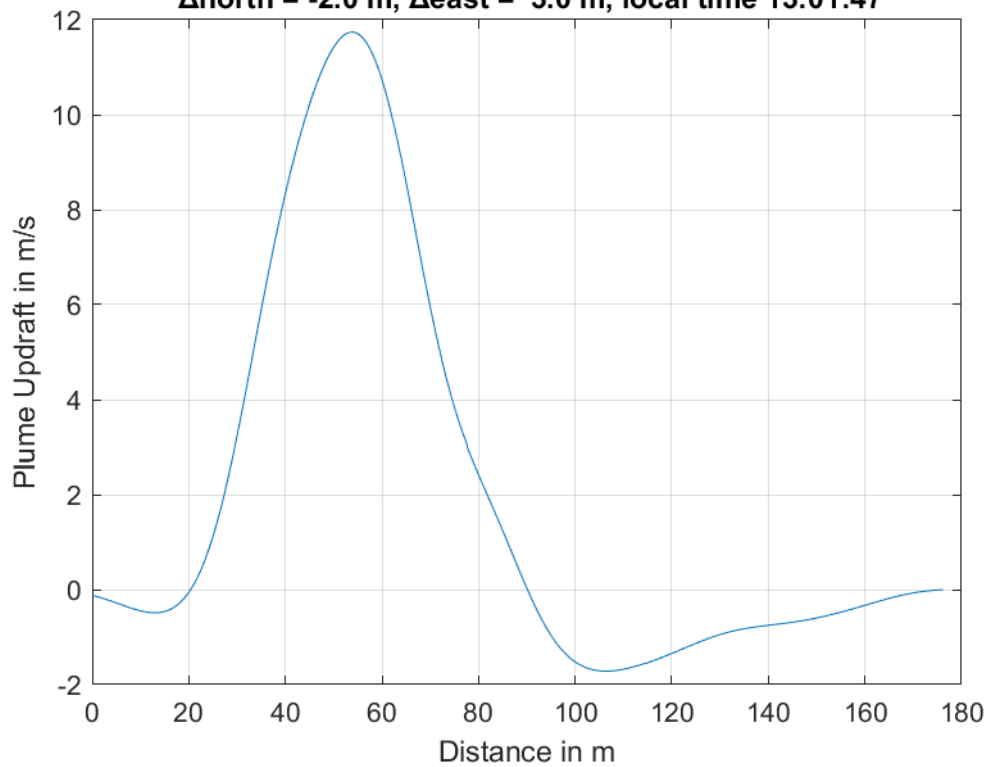


**Plume #13 at 313.7 m MSL, fly-through speed 43.0 m/s,
 $\Delta_{\text{north}} = -26.4$ m, $\Delta_{\text{east}} = 6.8$ m, local time 12:59:21**

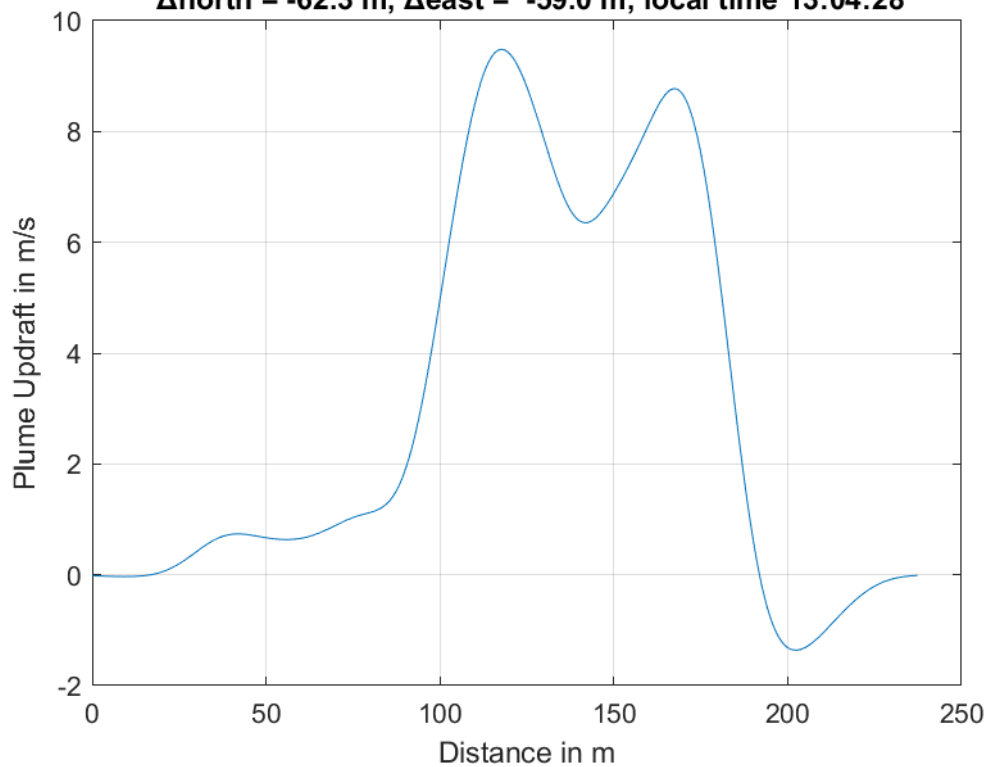




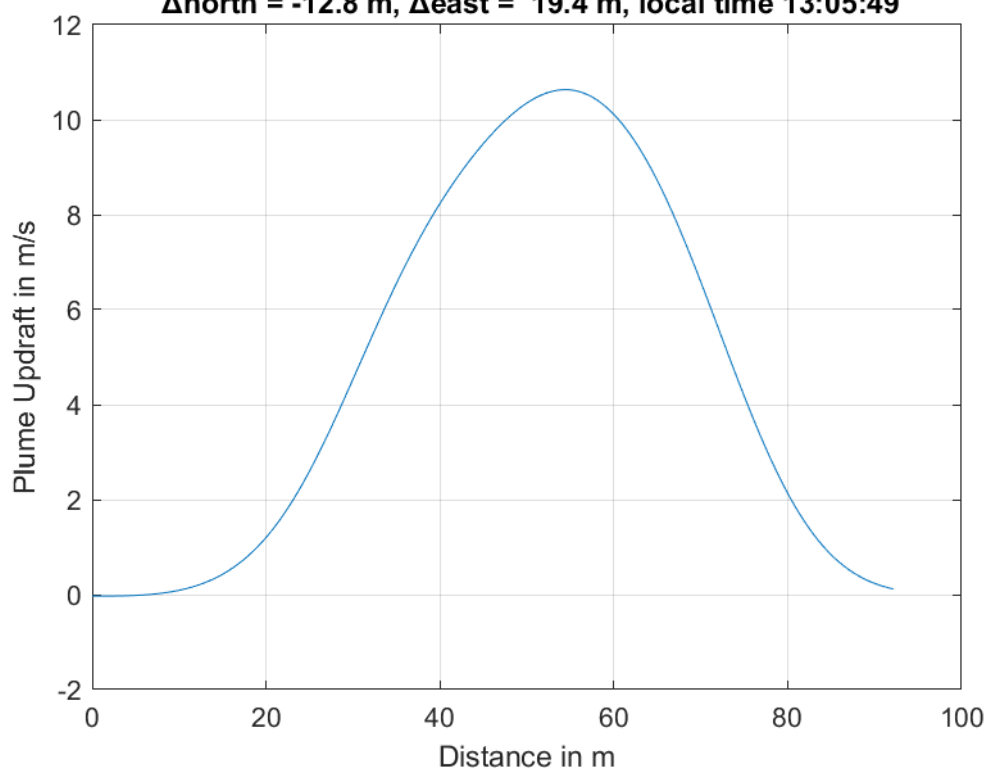
**Plume #14 at 363.1 m MSL, fly-through speed 43.0 m/s,
 $\Delta_{\text{north}} = -2.0$ m, $\Delta_{\text{east}} = 3.0$ m, local time 13:01:47**



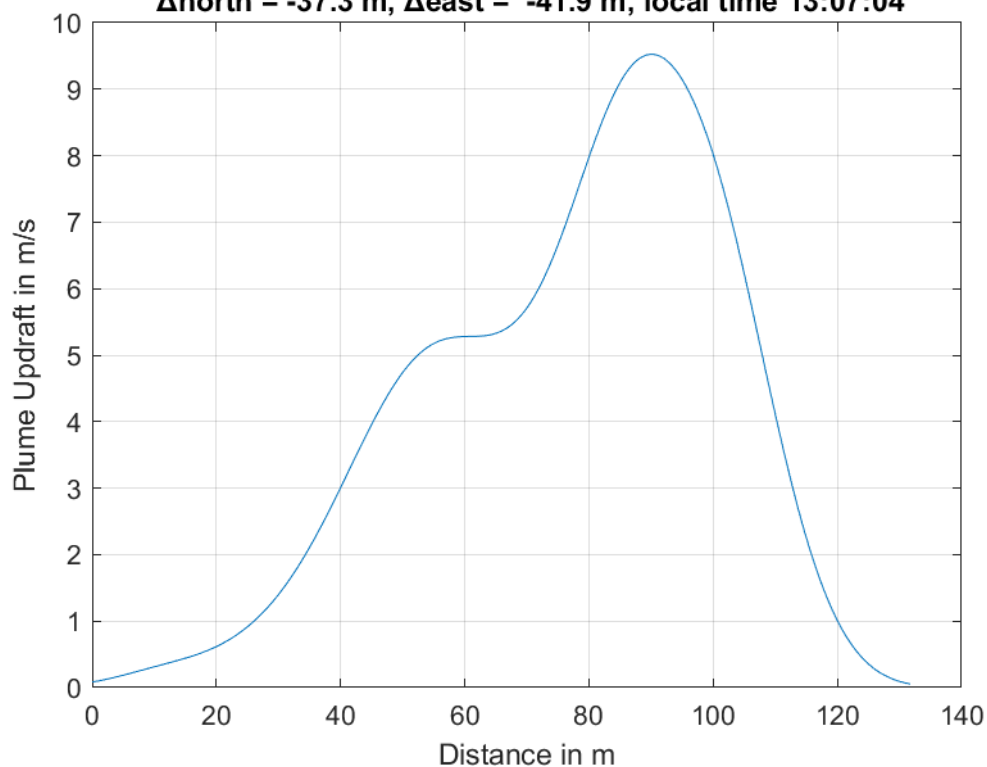
**Plume #15 at 357.3 m MSL, fly-through speed 44.0 m/s,
 $\Delta_{\text{north}} = -62.3$ m, $\Delta_{\text{east}} = -59.0$ m, local time 13:04:28**



**Plume #16 at 349.1 m MSL, fly-through speed 44.0 m/s,
 $\Delta_{\text{north}} = -12.8$ m, $\Delta_{\text{east}} = 19.4$ m, local time 13:05:49**

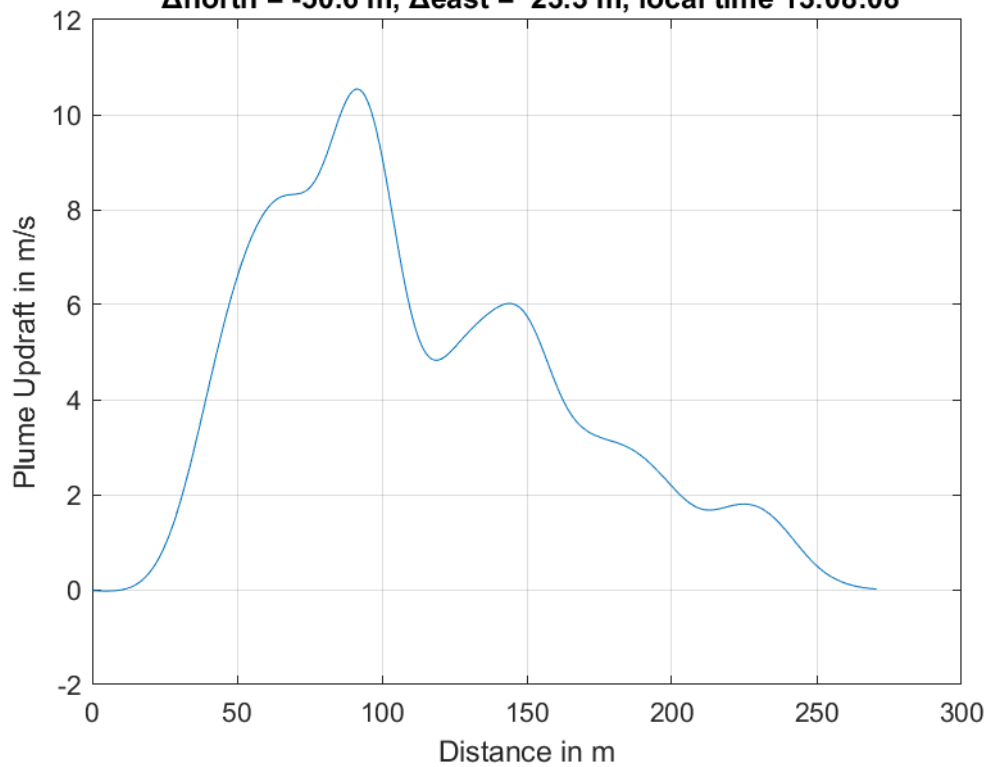


**Plume #17 at 361.7 m MSL, fly-through speed 44.0 m/s,
 $\Delta_{\text{north}} = -37.3$ m, $\Delta_{\text{east}} = -41.9$ m, local time 13:07:04**

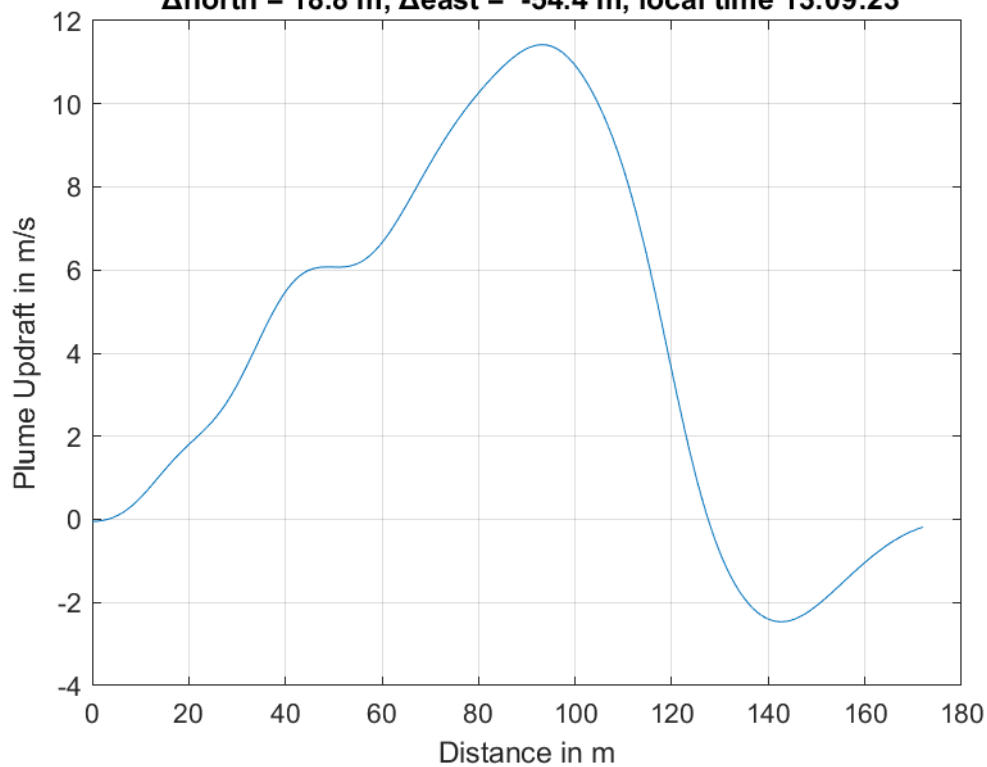




**Plume #18 at 375.4 m MSL, fly-through speed 43.0 m/s,
 $\Delta_{\text{north}} = -50.6$ m, $\Delta_{\text{east}} = 23.3$ m, local time 13:08:08**

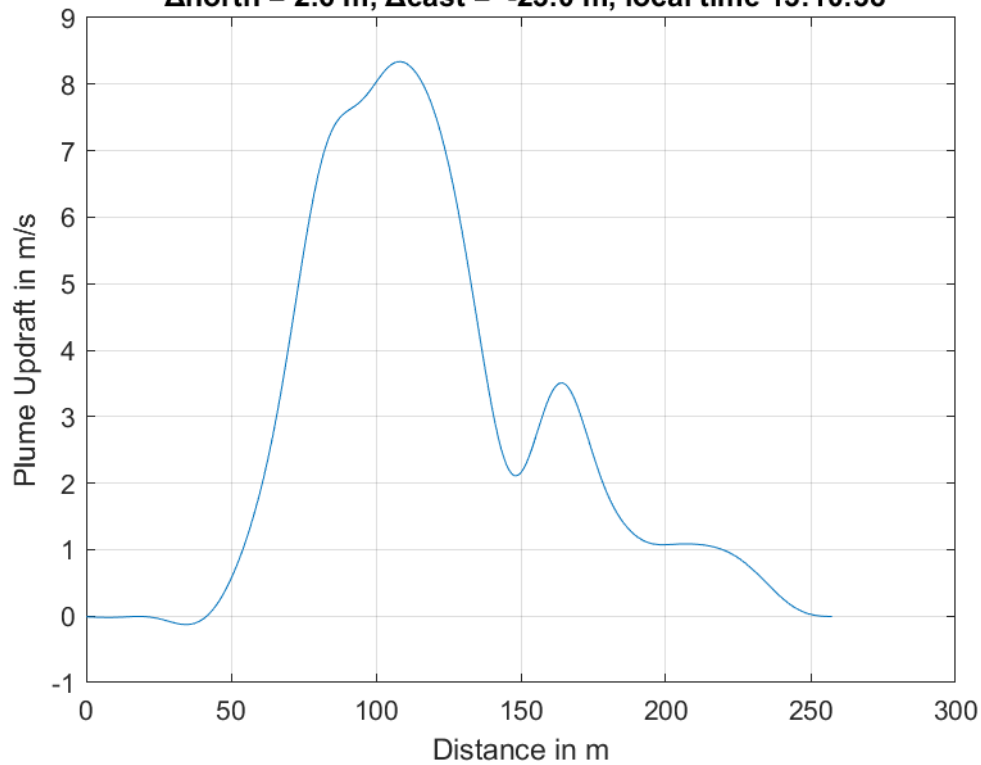


**Plume #19 at 366.8 m MSL, fly-through speed 42.0 m/s,
 $\Delta_{\text{north}} = 18.8$ m, $\Delta_{\text{east}} = -54.4$ m, local time 13:09:23**

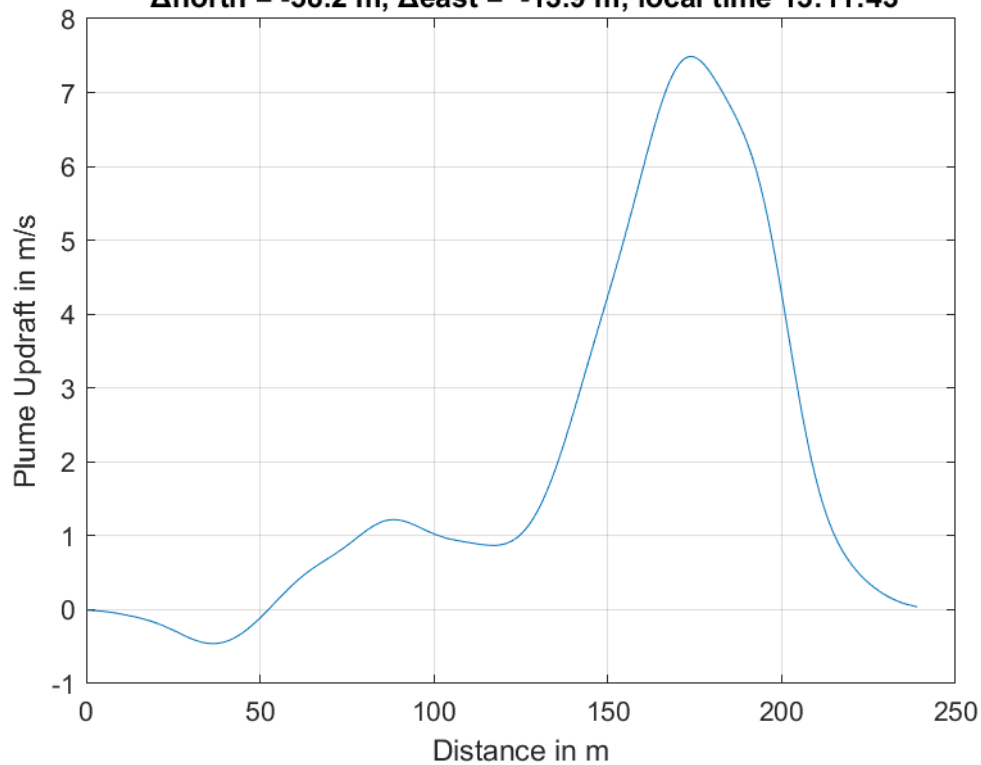




**Plume #20 at 350.7 m MSL, fly-through speed 46.0 m/s,
 $\Delta_{\text{north}} = 2.6$ m, $\Delta_{\text{east}} = -23.0$ m, local time 13:10:38**

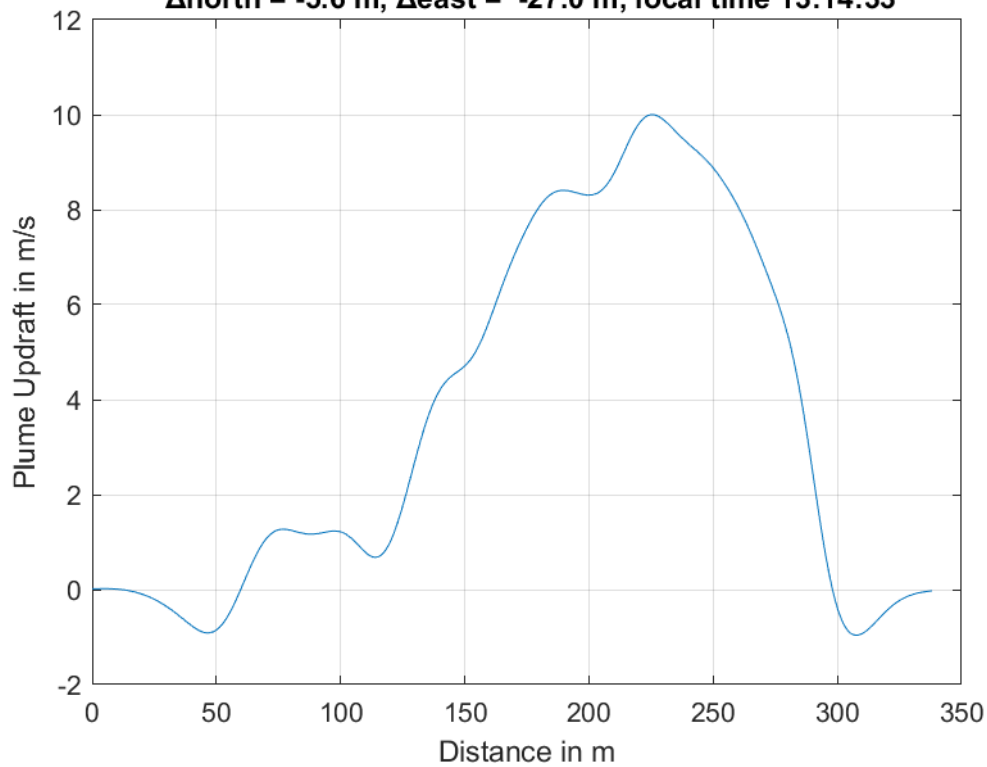


**Plume #21 at 345.5 m MSL, fly-through speed 46.0 m/s,
 $\Delta_{\text{north}} = -58.2$ m, $\Delta_{\text{east}} = -13.9$ m, local time 13:11:43**

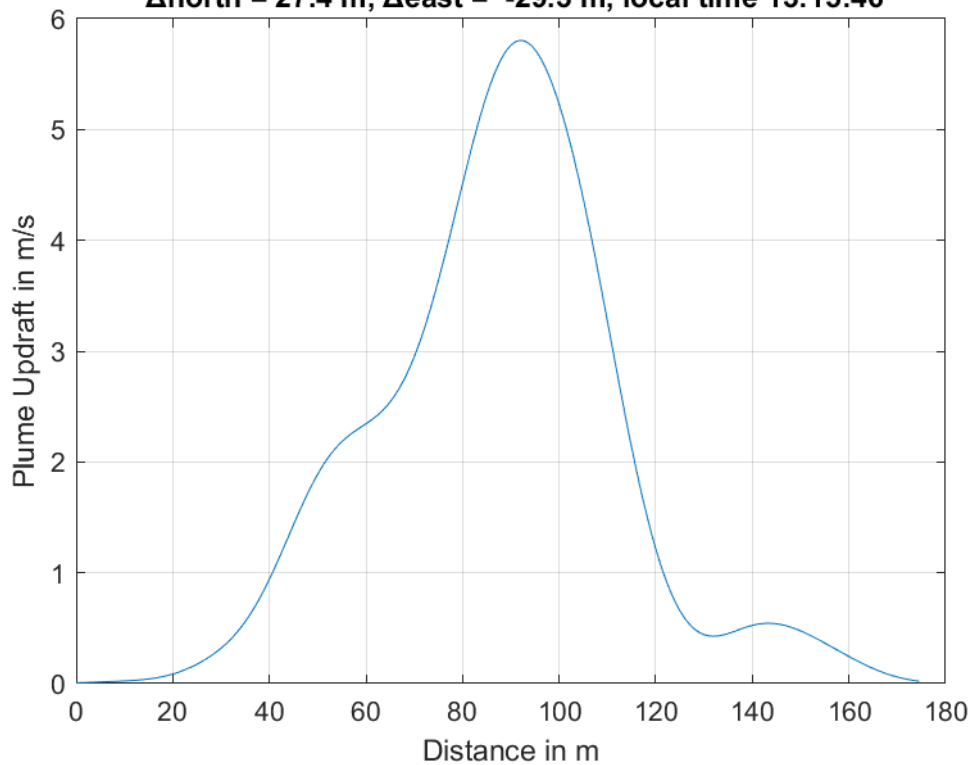




**Plume #22 at 389.4 m MSL, fly-through speed 47.0 m/s,
 $\Delta_{\text{north}} = -5.6$ m, $\Delta_{\text{east}} = -27.0$ m, local time 13:14:33**

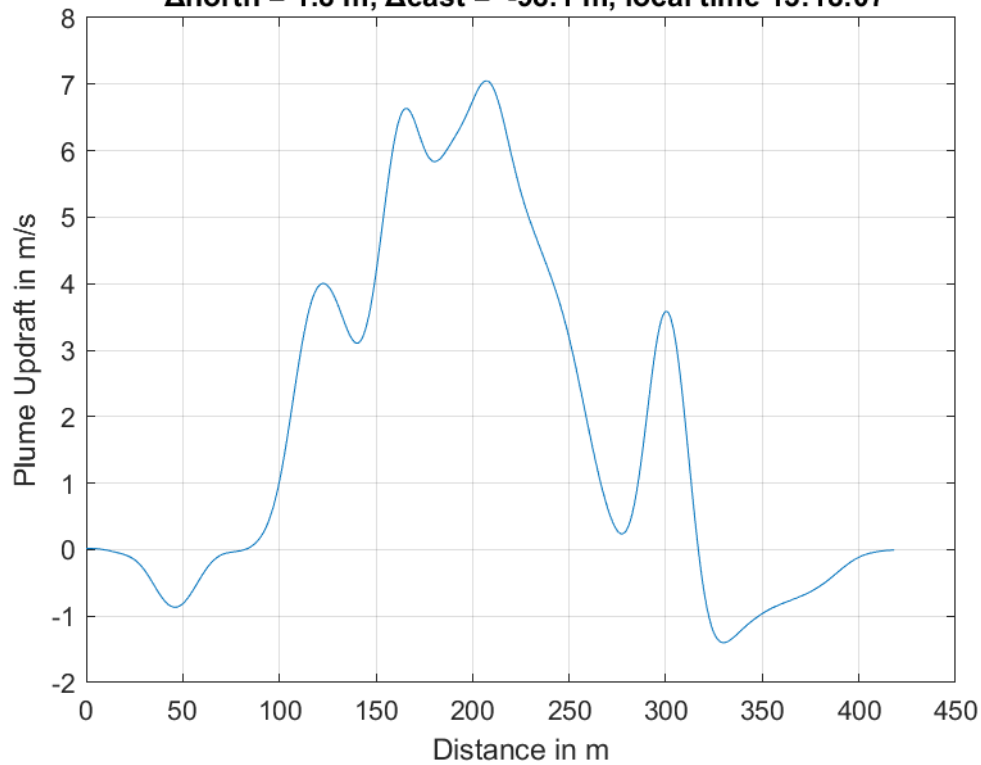


**Plume #23 at 366.5 m MSL, fly-through speed 46.0 m/s,
 $\Delta_{\text{north}} = 27.4$ m, $\Delta_{\text{east}} = -29.3$ m, local time 13:15:46**

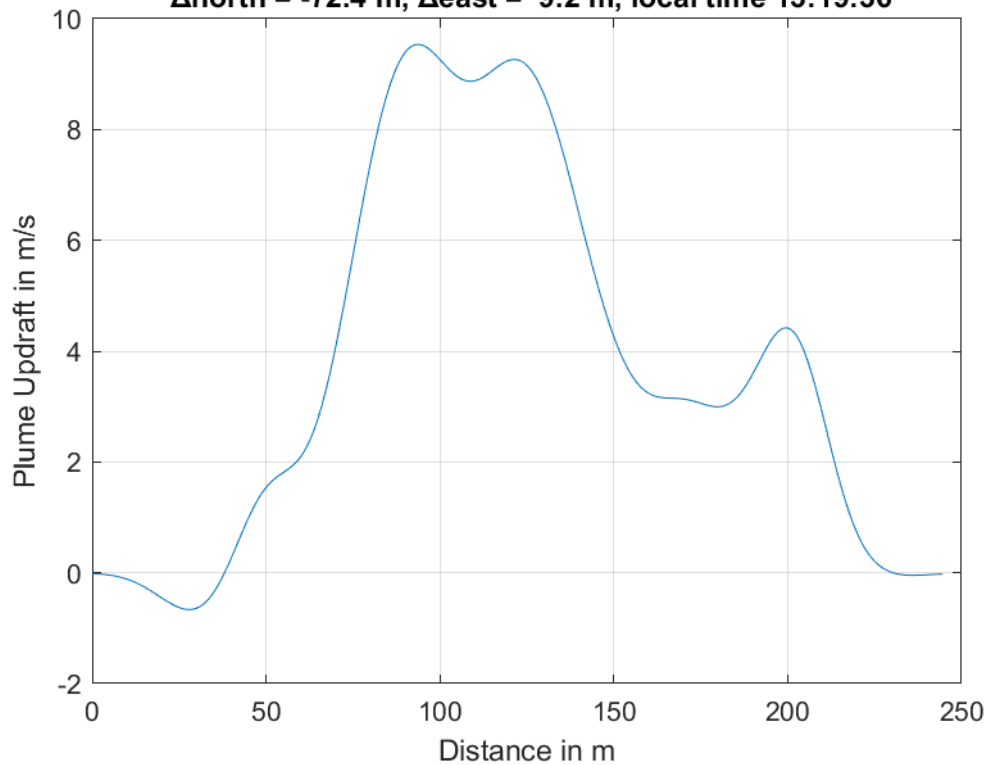




**Plume #24 at 352.6 m MSL, fly-through speed 45.0 m/s,
 $\Delta_{\text{north}} = 1.8$ m, $\Delta_{\text{east}} = -98.1$ m, local time 13:18:07**

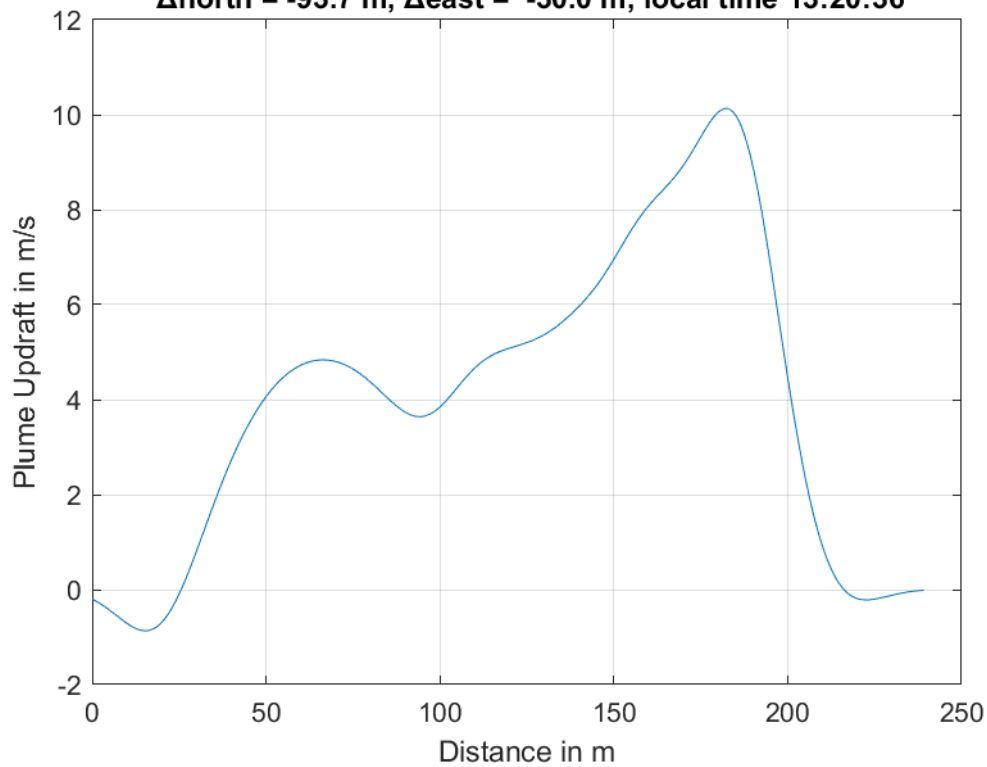


**Plume #25 at 377.3 m MSL, fly-through speed 48.0 m/s,
 $\Delta_{\text{north}} = -72.4$ m, $\Delta_{\text{east}} = 9.2$ m, local time 13:19:36**

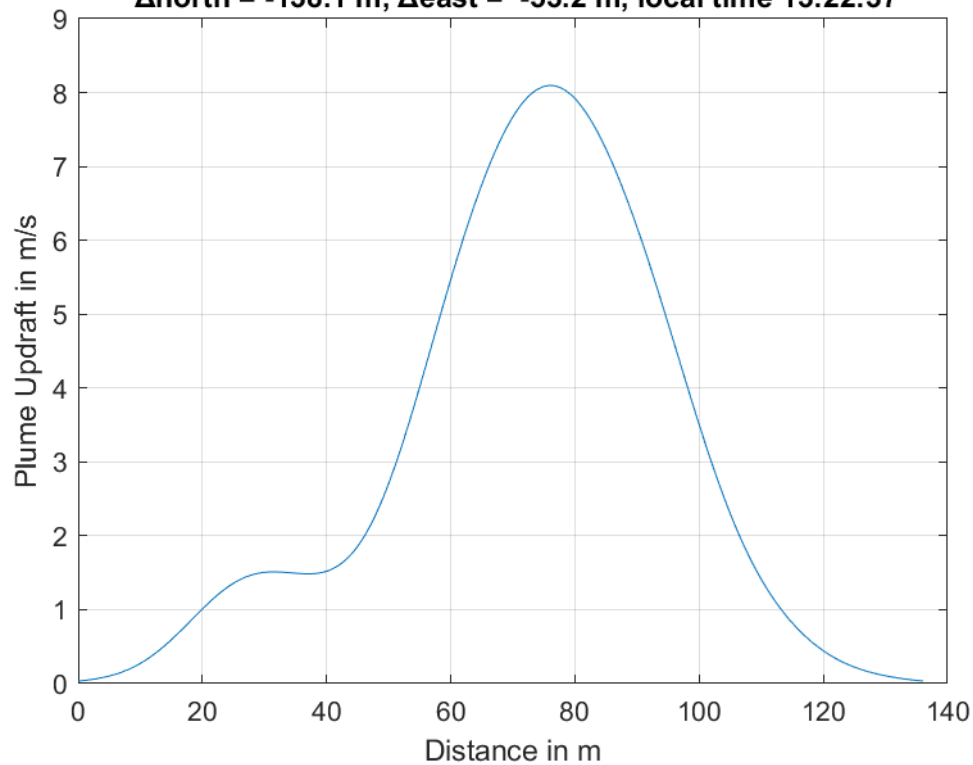




**Plume #26 at 364.0 m MSL, fly-through speed 46.0 m/s,
 $\Delta_{\text{north}} = -93.7$ m, $\Delta_{\text{east}} = -30.0$ m, local time 13:20:36**

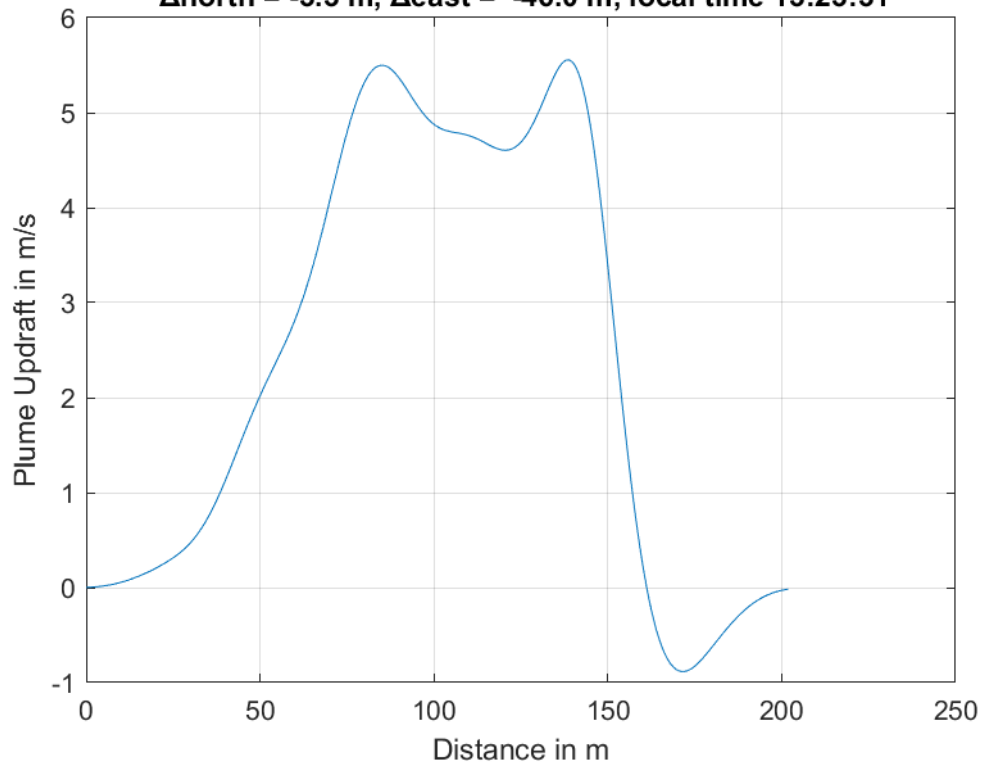


**Plume #27 at 328.0 m MSL, fly-through speed 47.0 m/s,
 $\Delta_{\text{north}} = -138.1$ m, $\Delta_{\text{east}} = -53.2$ m, local time 13:22:37**

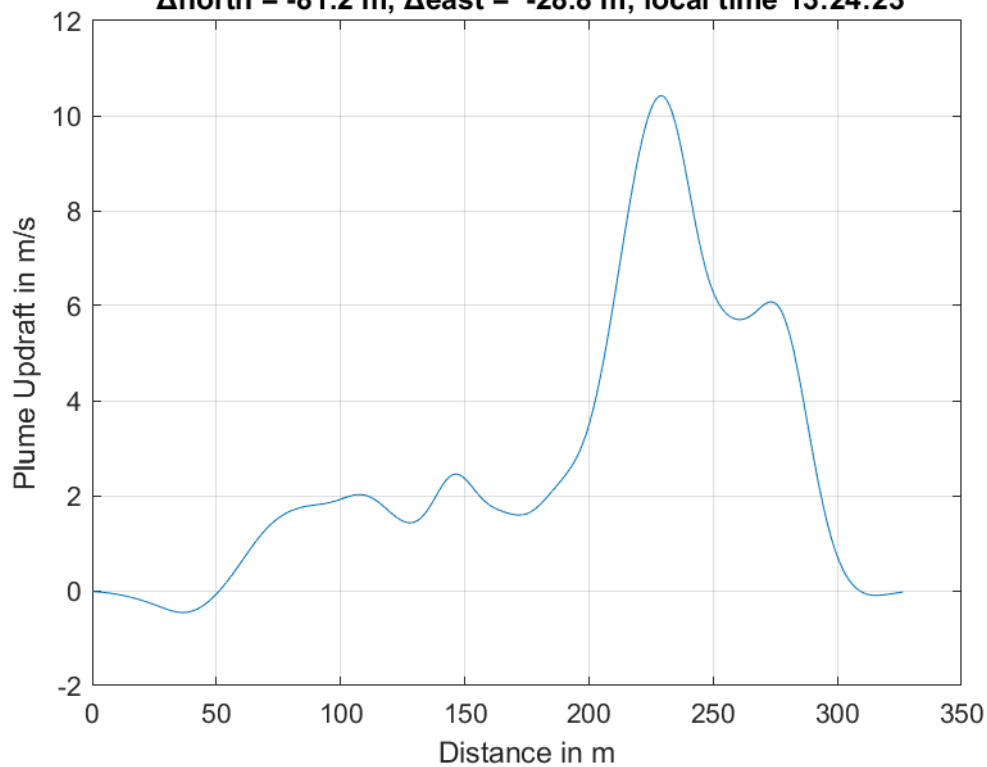




**Plume #28 at 326.4 m MSL, fly-through speed 47.0 m/s,
 $\Delta_{\text{north}} = -3.3$ m, $\Delta_{\text{east}} = -46.0$ m, local time 13:23:31**

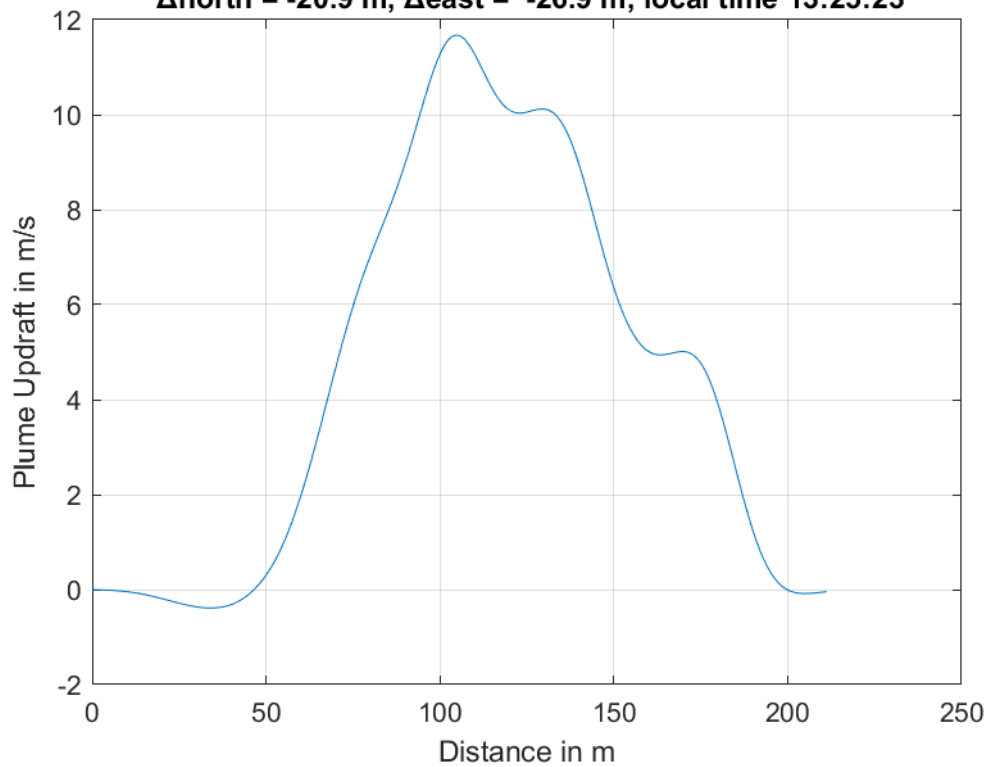


**Plume #29 at 320.7 m MSL, fly-through speed 46.0 m/s,
 $\Delta_{\text{north}} = -81.2$ m, $\Delta_{\text{east}} = -28.8$ m, local time 13:24:23**

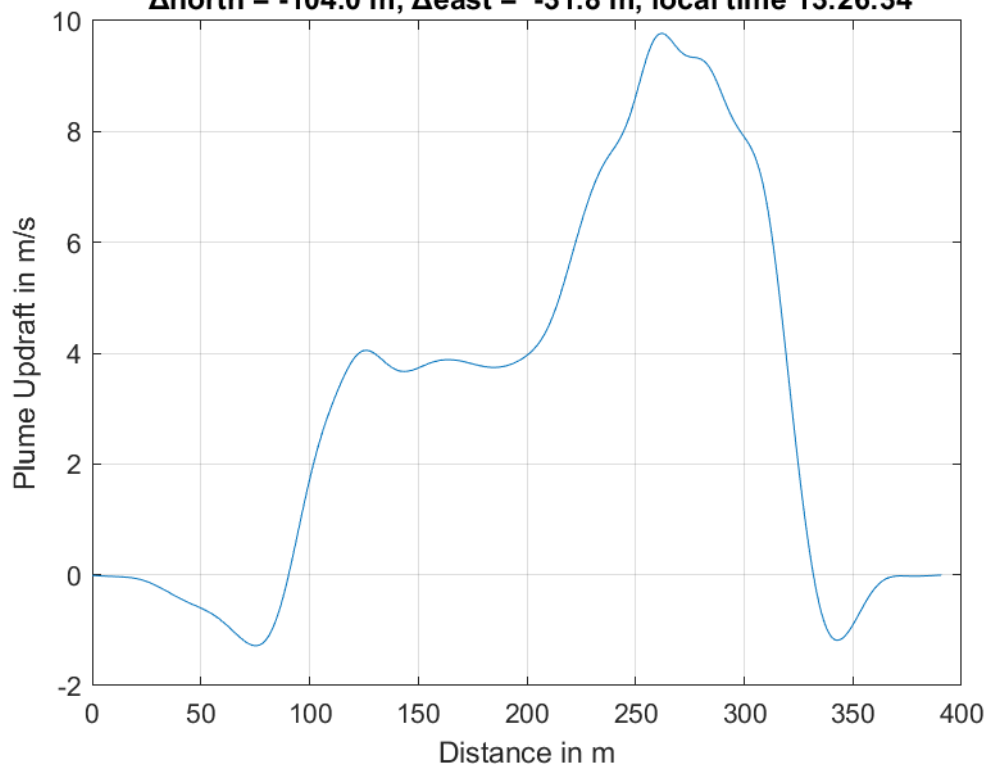




**Plume #30 at 329.6 m MSL, fly-through speed 48.0 m/s,
 $\Delta_{\text{north}} = -20.9$ m, $\Delta_{\text{east}} = -26.9$ m, local time 13:25:23**

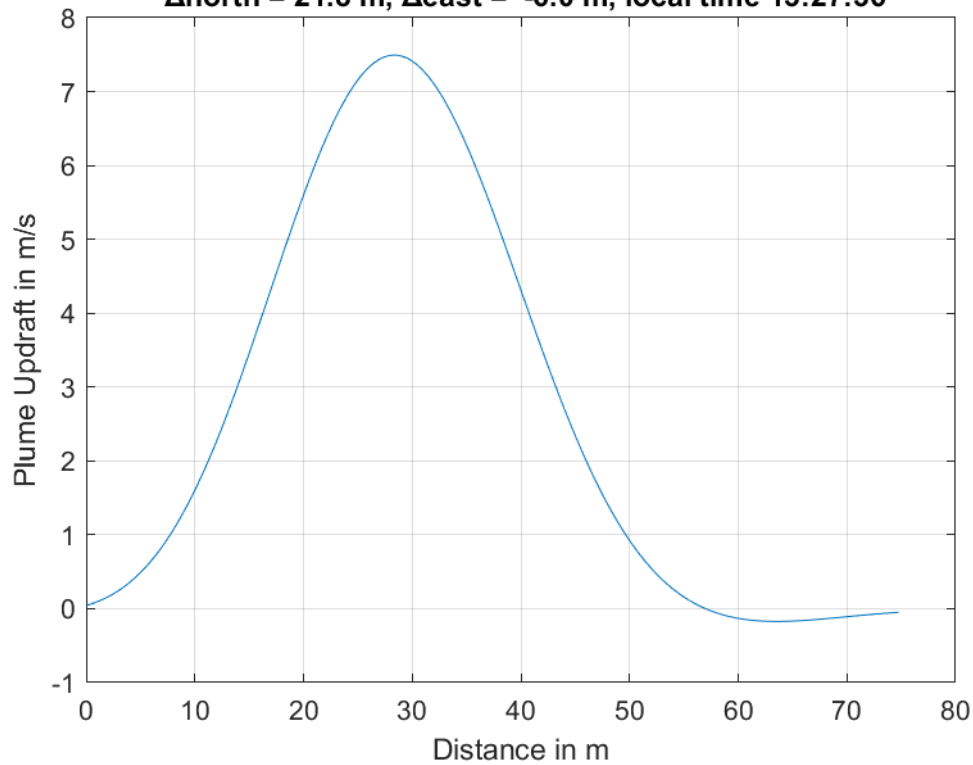


**Plume #31 at 357.6 m MSL, fly-through speed 46.0 m/s,
 $\Delta_{\text{north}} = -104.0$ m, $\Delta_{\text{east}} = -31.8$ m, local time 13:26:34**

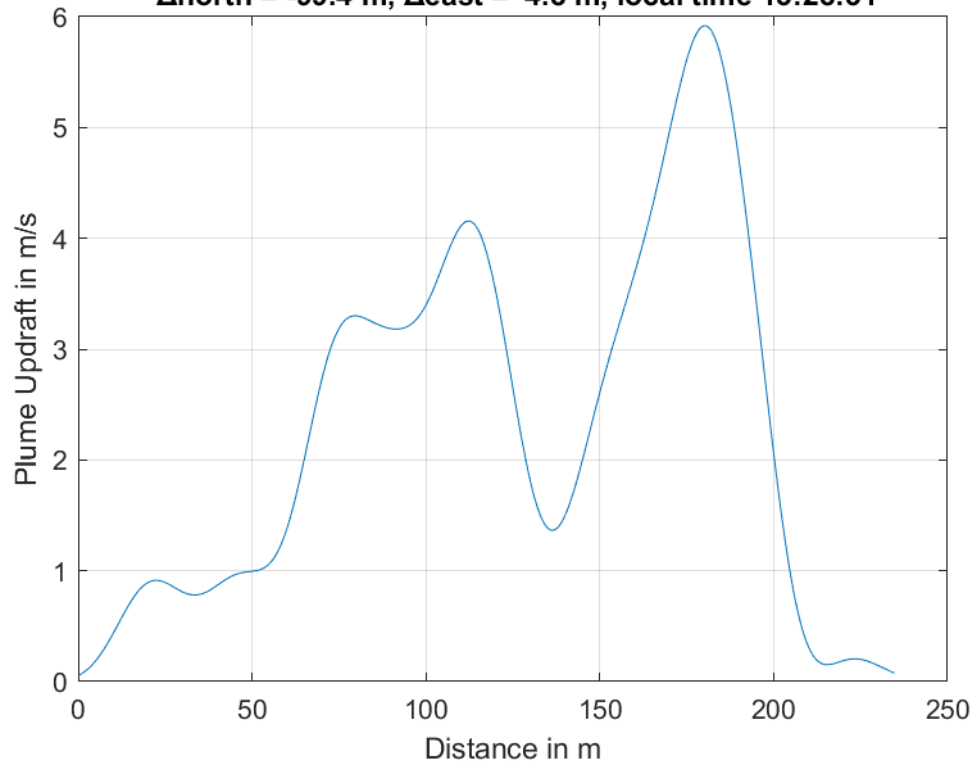




**Plume #32 at 368.7 m MSL, fly-through speed 50.0 m/s,
 $\Delta_{\text{north}} = 21.8$ m, $\Delta_{\text{east}} = -6.0$ m, local time 13:27:36**

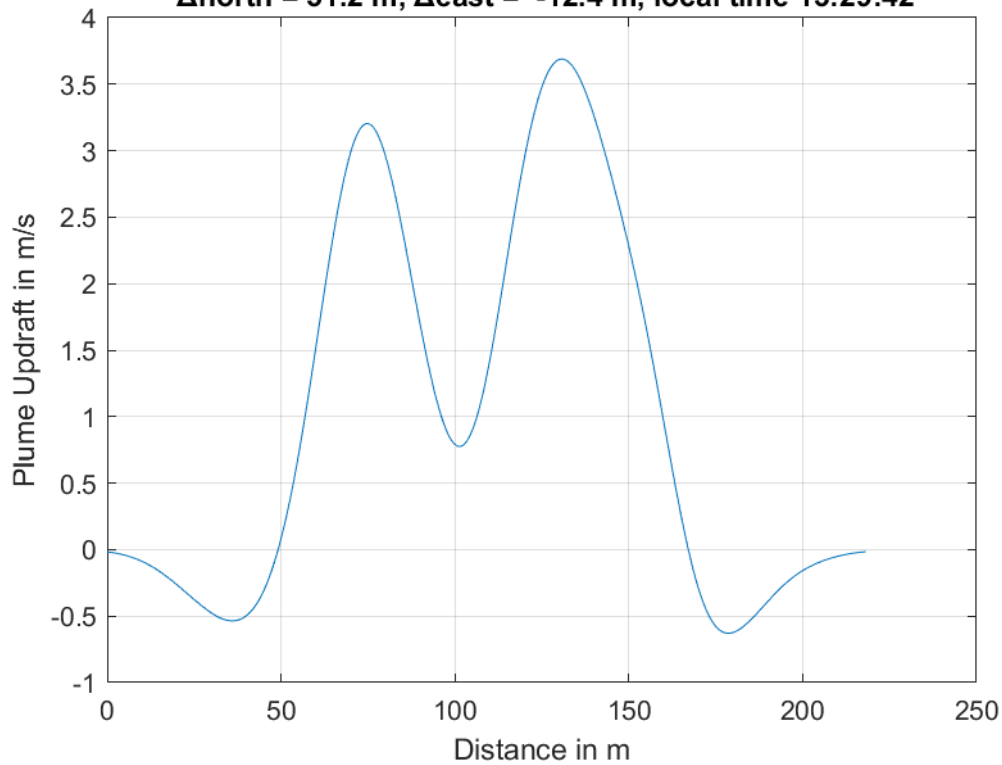


**Plume #33 at 394.9 m MSL, fly-through speed 47.0 m/s,
 $\Delta_{\text{north}} = -99.4$ m, $\Delta_{\text{east}} = 4.8$ m, local time 13:28:31**

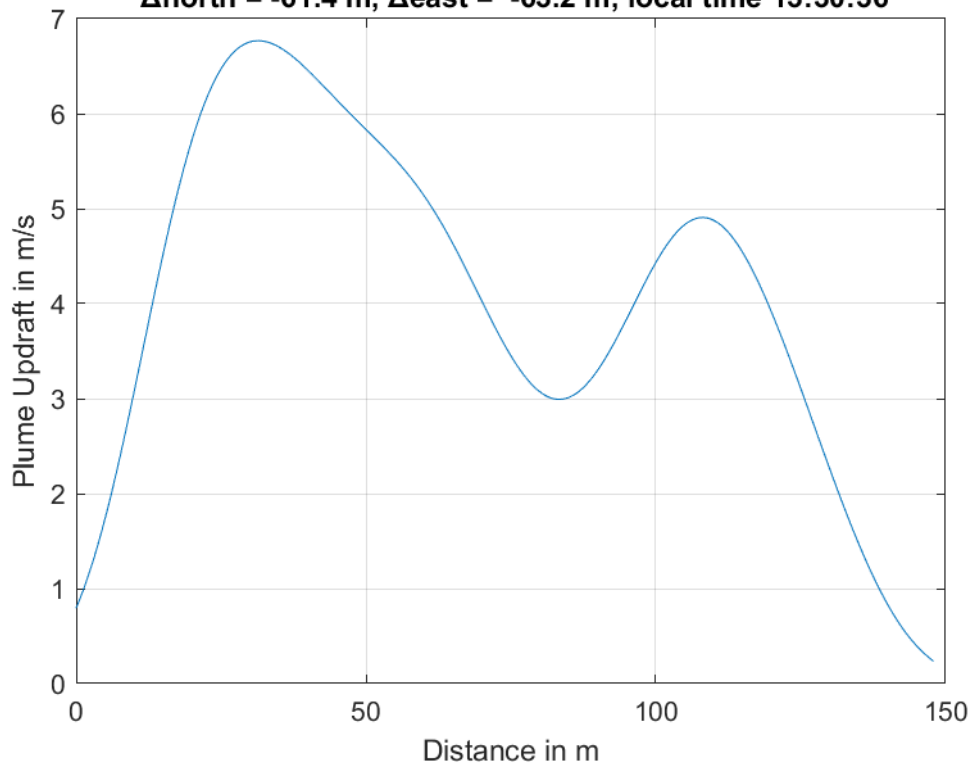




**Plume #34 at 383.8 m MSL, fly-through speed 56.0 m/s,
 $\Delta_{\text{north}} = 51.2$ m, $\Delta_{\text{east}} = -12.4$ m, local time 13:29:42**

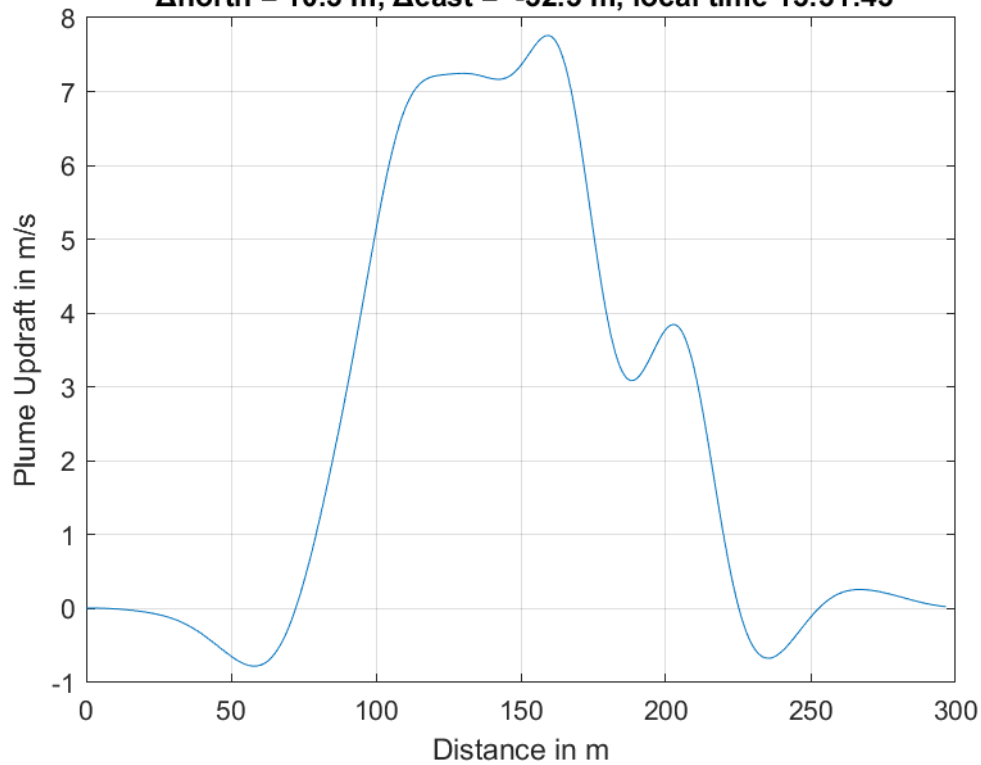


**Plume #35 at 330.0 m MSL, fly-through speed 57.0 m/s,
 $\Delta_{\text{north}} = -61.4$ m, $\Delta_{\text{east}} = -63.2$ m, local time 13:30:36**

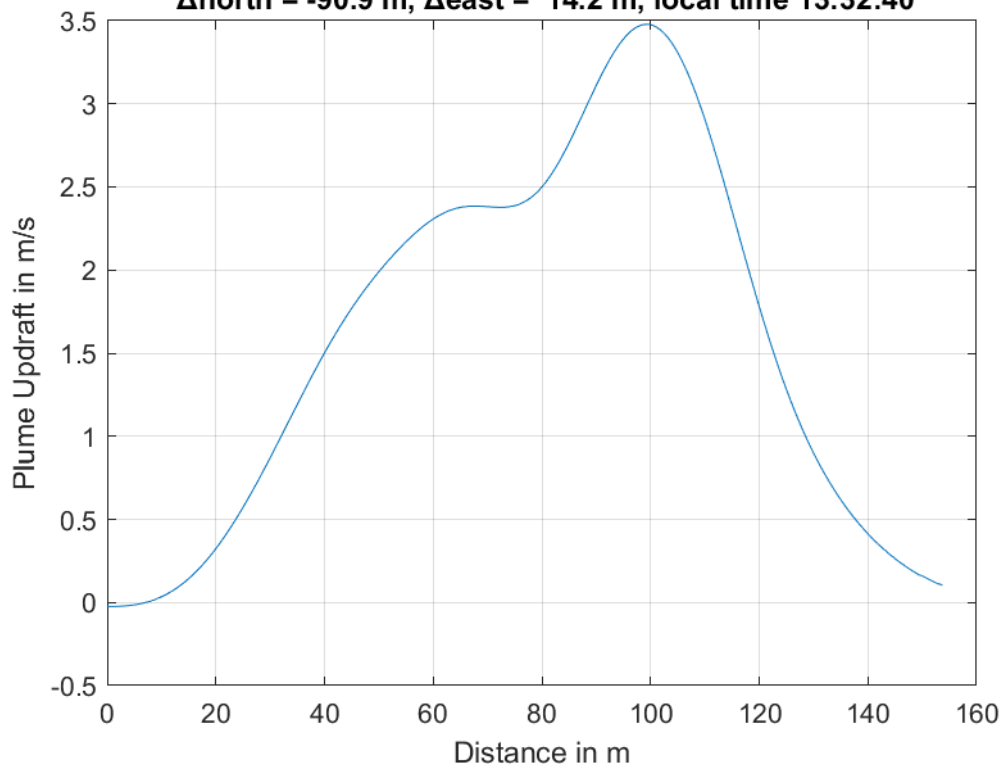




**Plume #36 at 304.6 m MSL, fly-through speed 55.0 m/s,
 $\Delta_{\text{north}} = 10.3$ m, $\Delta_{\text{east}} = -32.3$ m, local time 13:31:43**

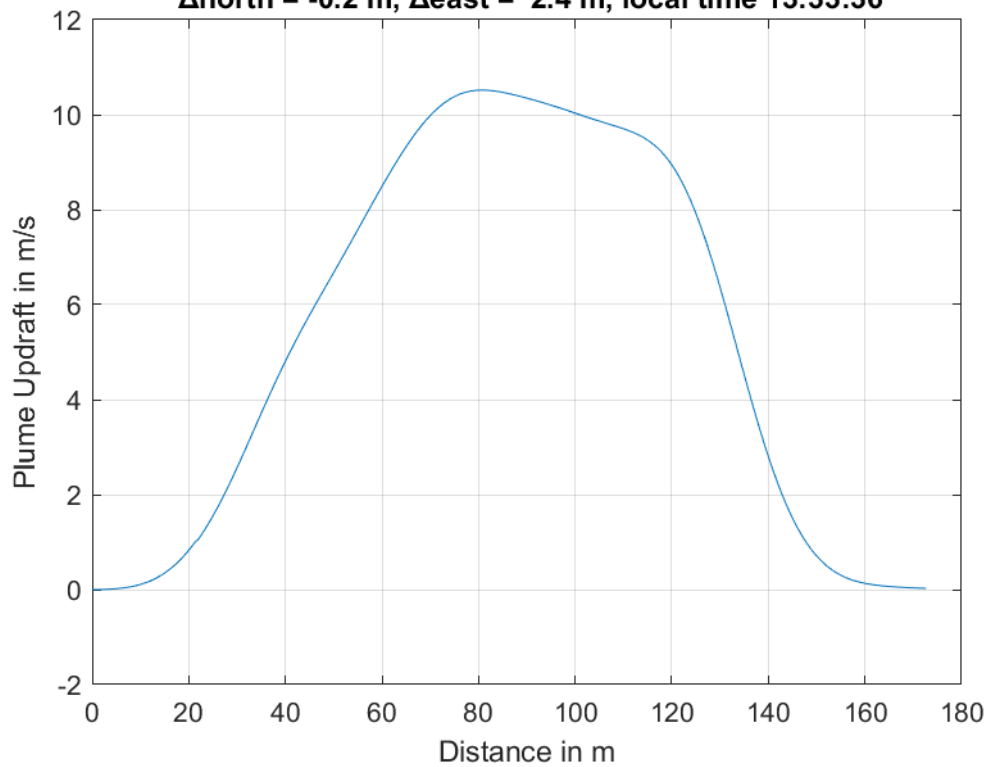


**Plume #37 at 291.4 m MSL, fly-through speed 57.0 m/s,
 $\Delta_{\text{north}} = -90.9$ m, $\Delta_{\text{east}} = 14.2$ m, local time 13:32:40**

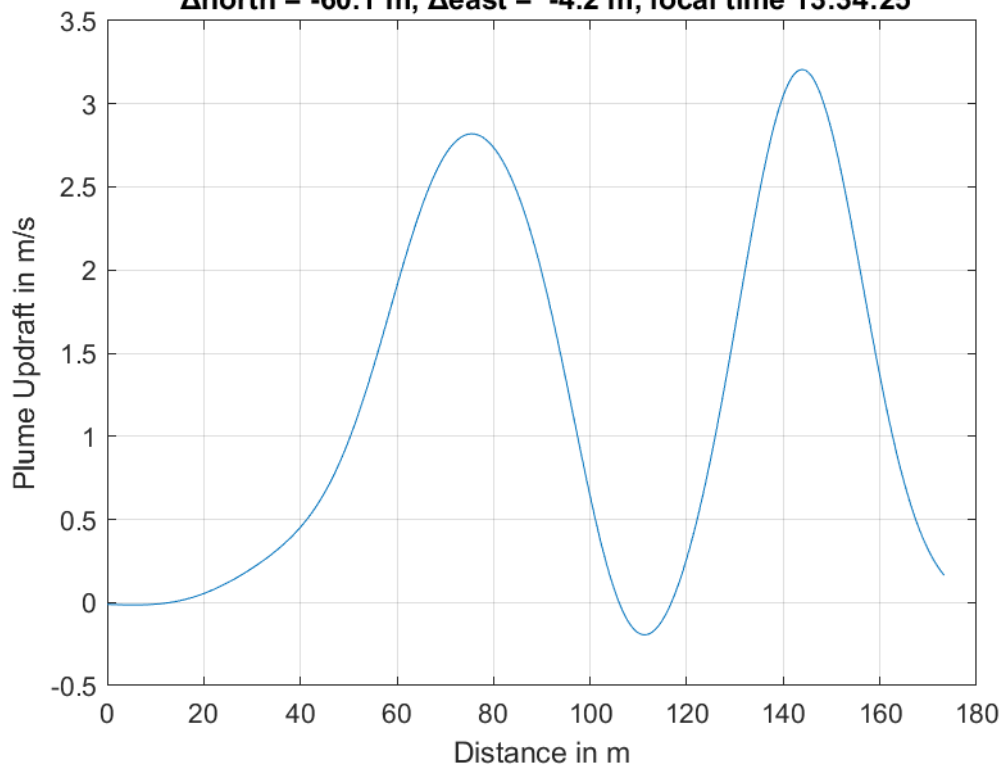




**Plume #38 at 266.4 m MSL, fly-through speed 54.0 m/s,
 $\Delta_{\text{north}} = -0.2$ m, $\Delta_{\text{east}} = 2.4$ m, local time 13:33:36**

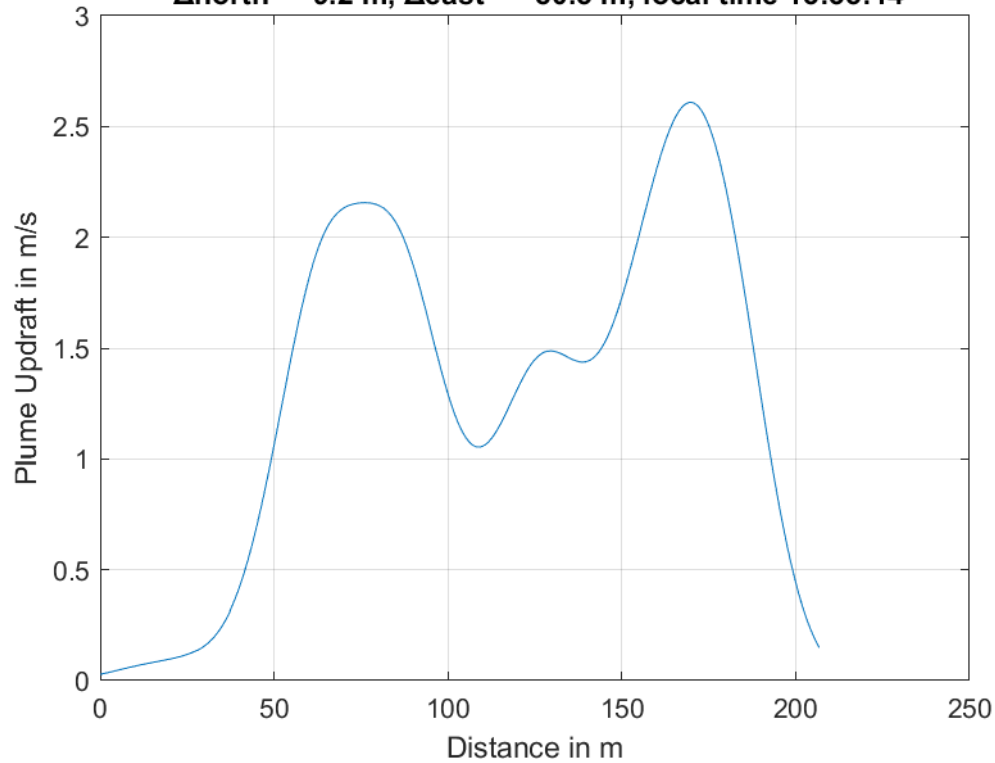


**Plume #39 at 252.4 m MSL, fly-through speed 56.0 m/s,
 $\Delta_{\text{north}} = -60.1$ m, $\Delta_{\text{east}} = -4.2$ m, local time 13:34:25**

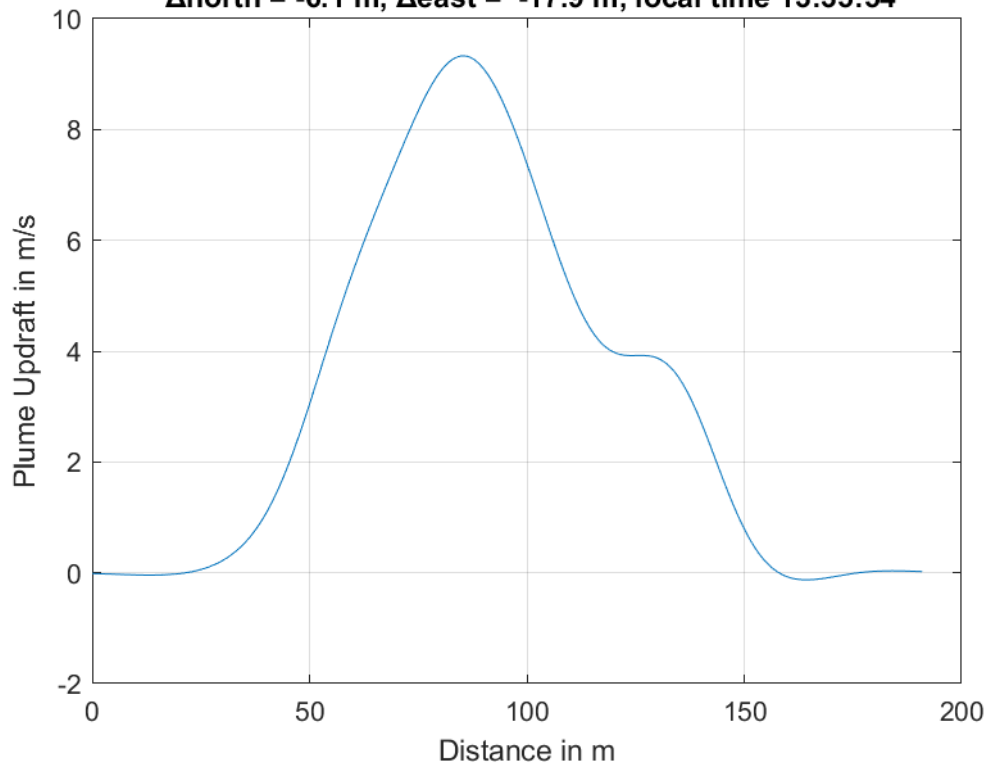




**Plume #40 at 217.5 m MSL, fly-through speed 56.0 m/s,
 $\Delta_{\text{north}} = -9.2$ m, $\Delta_{\text{east}} = -80.5$ m, local time 13:35:14**

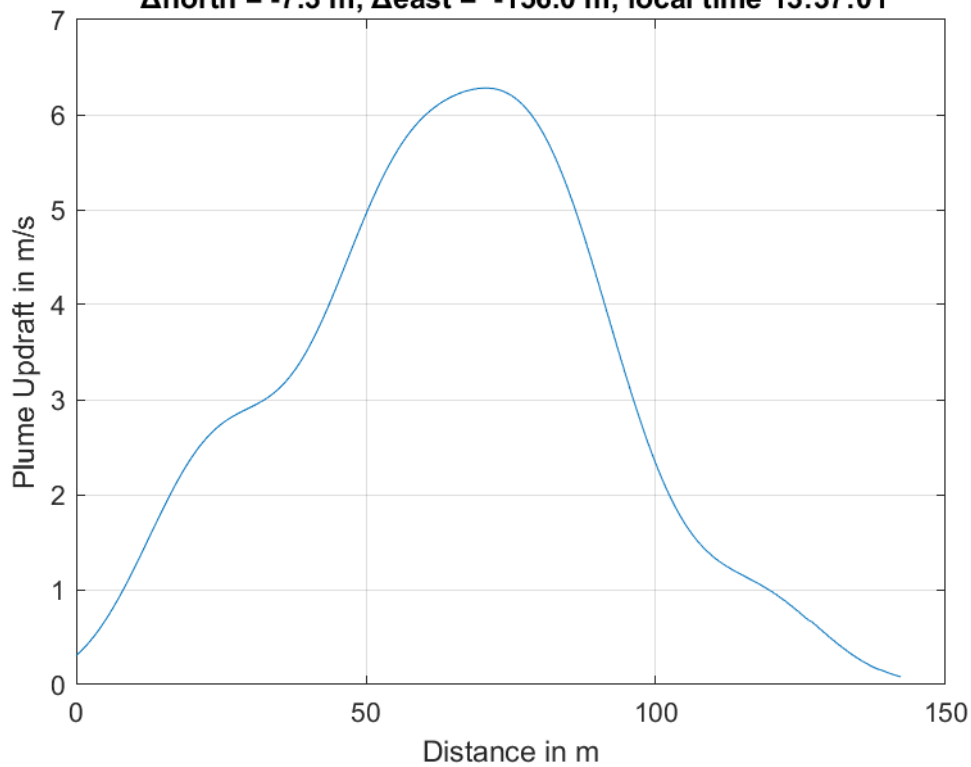


**Plume #41 at 198.3 m MSL, fly-through speed 58.0 m/s,
 $\Delta_{\text{north}} = -6.1$ m, $\Delta_{\text{east}} = -17.9$ m, local time 13:35:54**

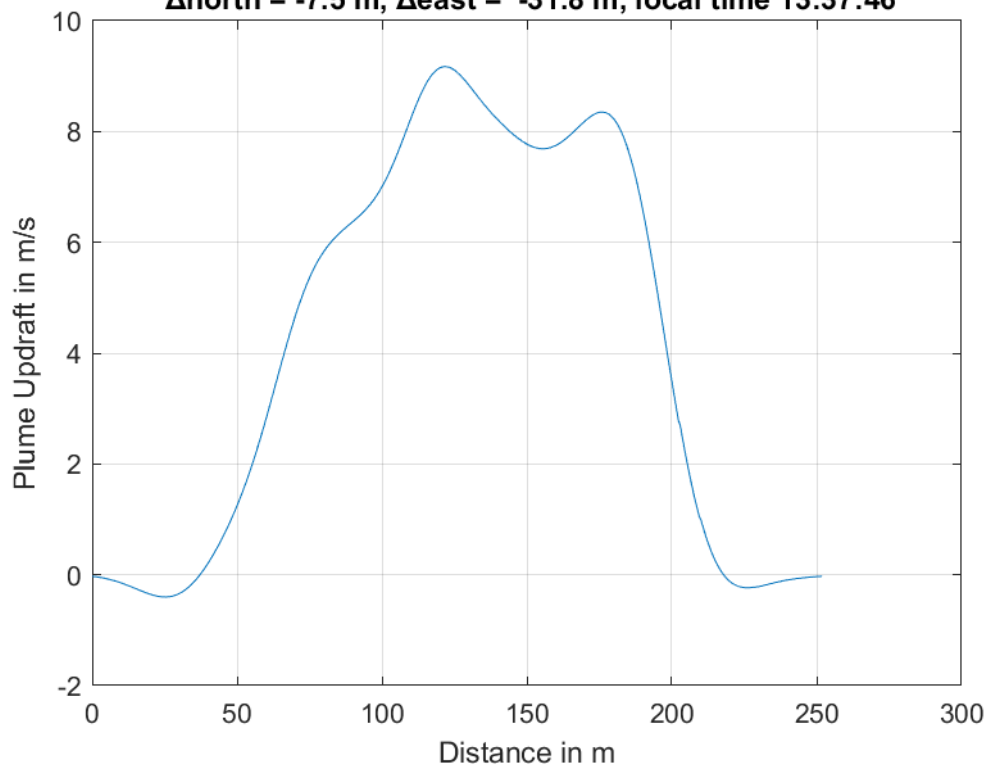




**Plume #42 at 206.9 m MSL, fly-through speed 57.0 m/s,
 $\Delta_{\text{north}} = -7.3$ m, $\Delta_{\text{east}} = -156.0$ m, local time 13:37:01**

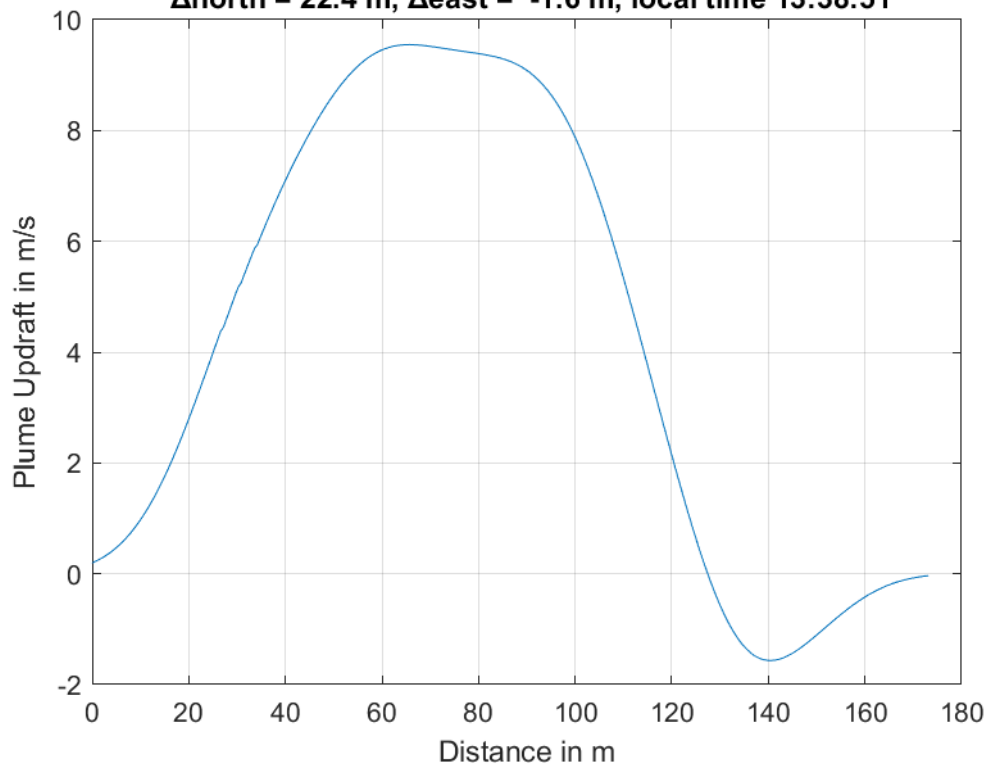


**Plume #43 at 202.2 m MSL, fly-through speed 60.0 m/s,
 $\Delta_{\text{north}} = -7.5$ m, $\Delta_{\text{east}} = -31.8$ m, local time 13:37:46**

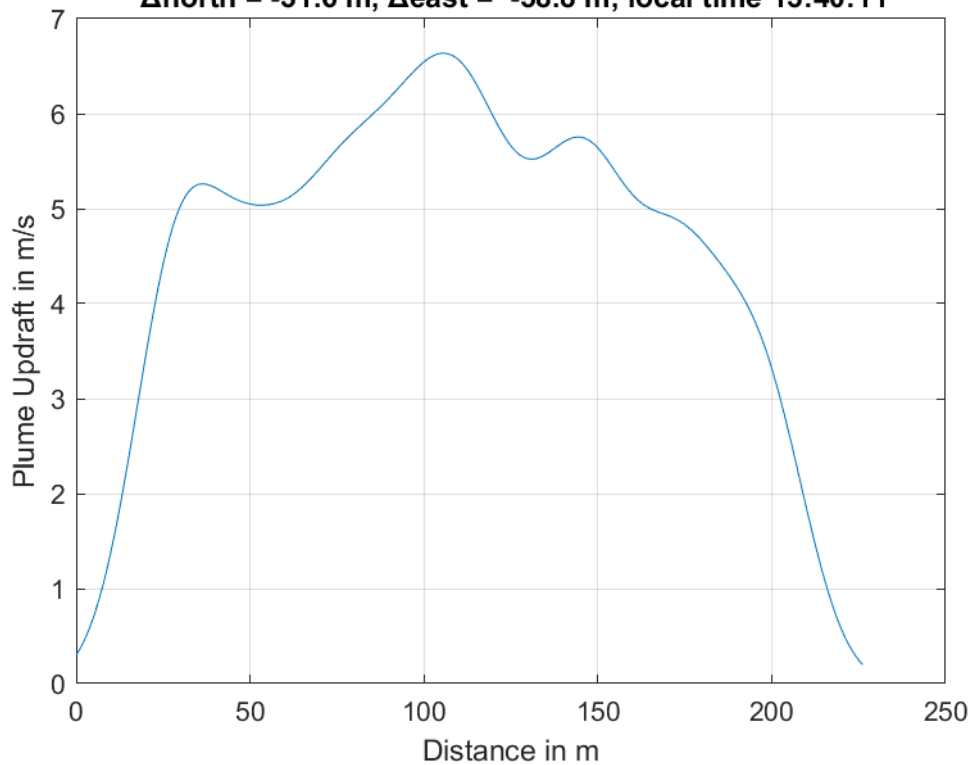




**Plume #44 at 192.0 m MSL, fly-through speed 56.0 m/s,
 $\Delta_{\text{north}} = 22.4$ m, $\Delta_{\text{east}} = -1.6$ m, local time 13:38:51**

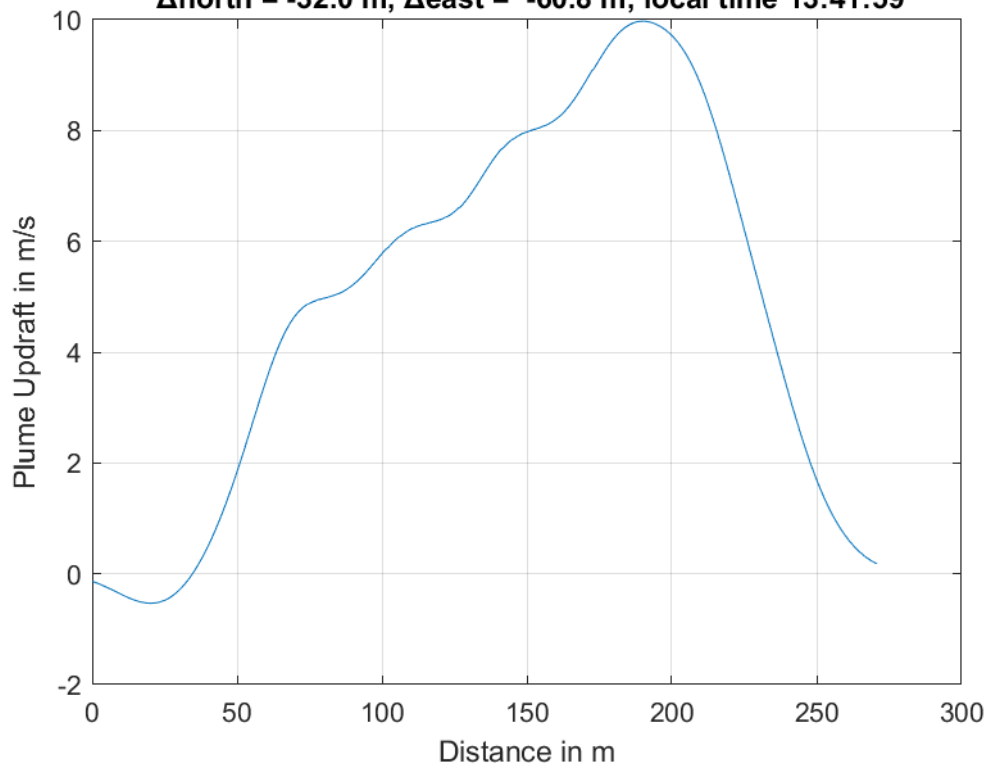


**Plume #45 at 301.9 m MSL, fly-through speed 58.0 m/s,
 $\Delta_{\text{north}} = -31.6$ m, $\Delta_{\text{east}} = -58.8$ m, local time 13:40:11**

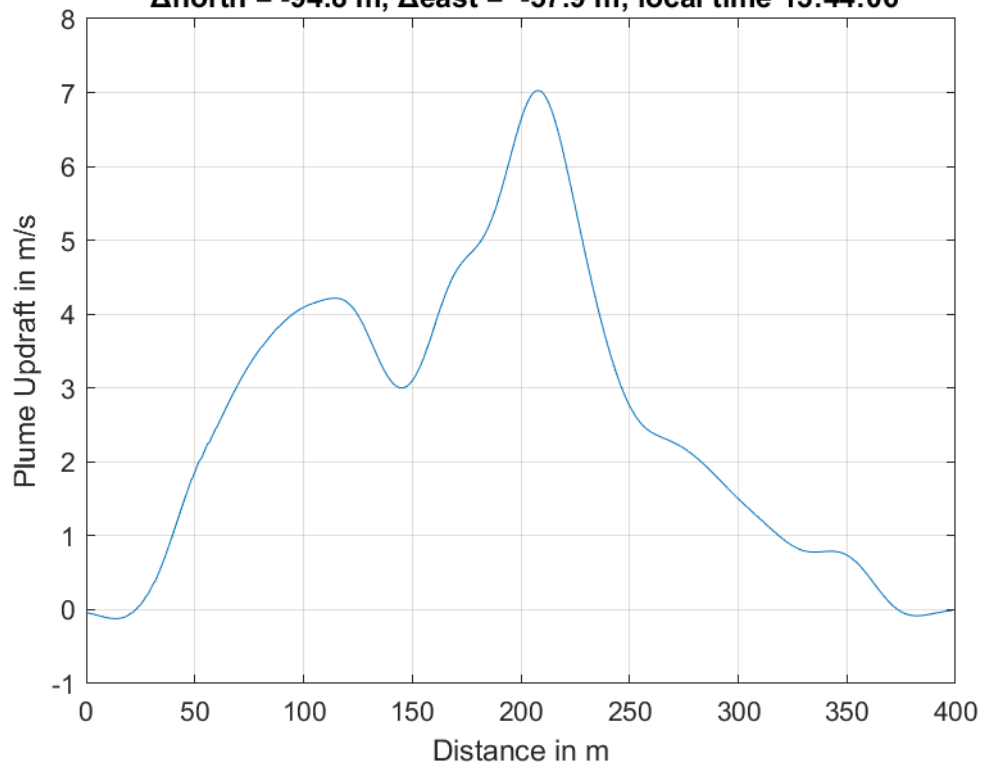




**Plume #46 at 289.0 m MSL, fly-through speed 63.0 m/s,
 $\Delta_{\text{north}} = -32.0$ m, $\Delta_{\text{east}} = -60.8$ m, local time 13:41:59**

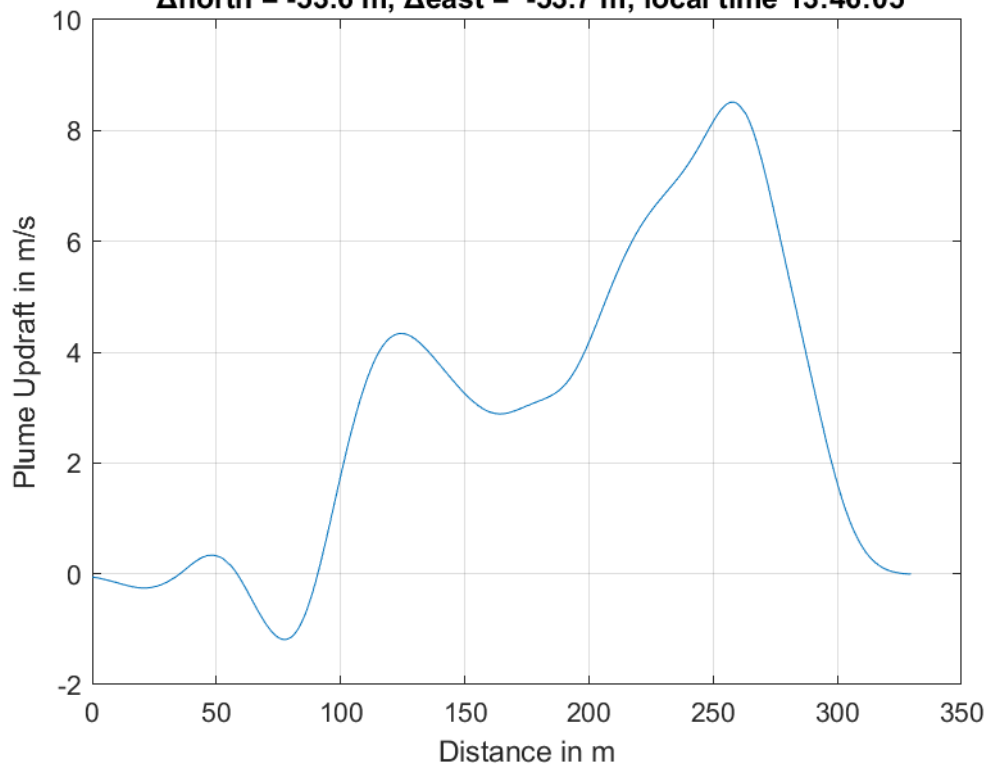


**Plume #47 at 310.6 m MSL, fly-through speed 57.0 m/s,
 $\Delta_{\text{north}} = -94.8$ m, $\Delta_{\text{east}} = -57.9$ m, local time 13:44:06**

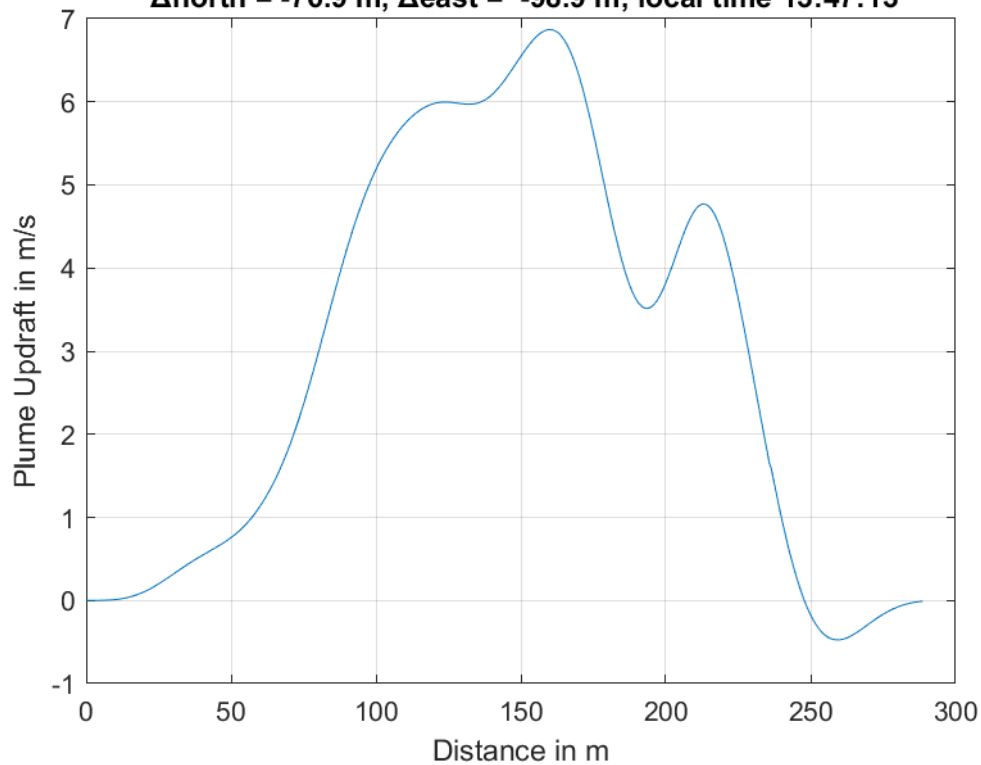




**Plume #48 at 313.2 m MSL, fly-through speed 60.0 m/s,
 $\Delta_{\text{north}} = -53.6$ m, $\Delta_{\text{east}} = -53.7$ m, local time 13:46:05**

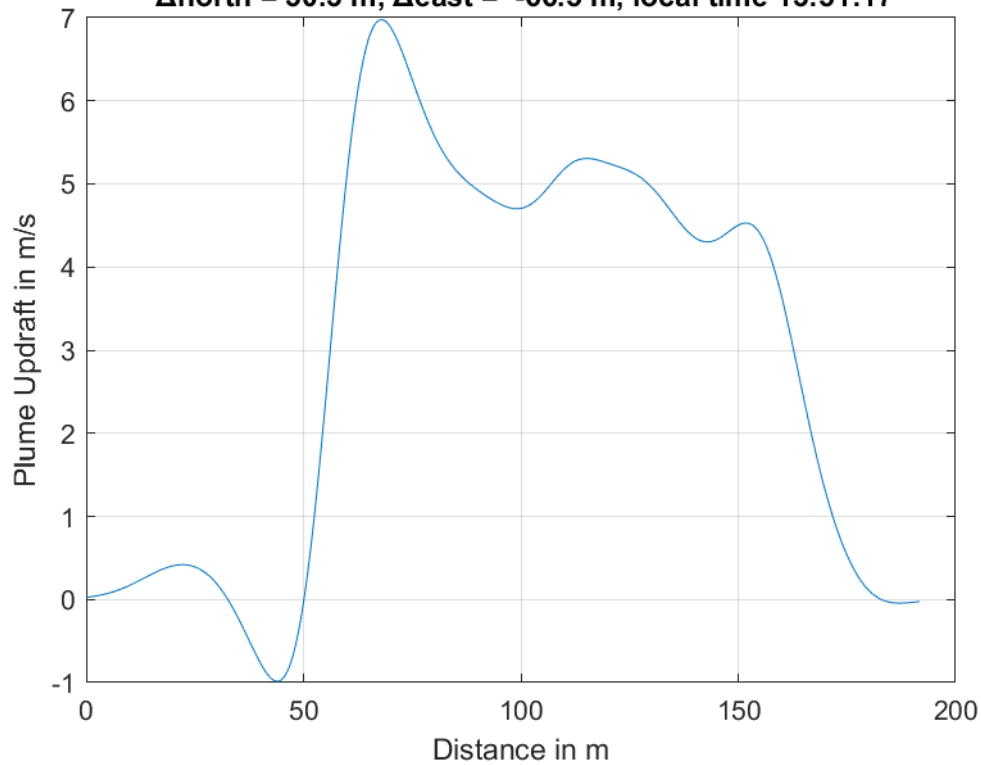


**Plume #49 at 338.1 m MSL, fly-through speed 59.0 m/s,
 $\Delta_{\text{north}} = -76.9$ m, $\Delta_{\text{east}} = -98.9$ m, local time 13:47:13**

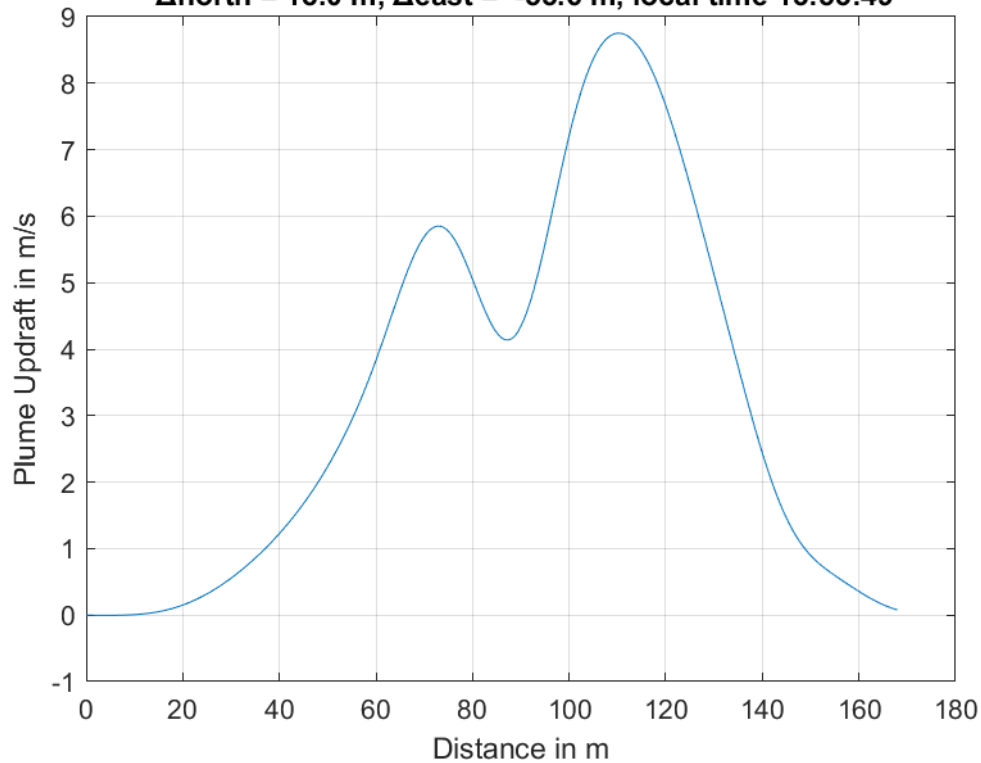




**Plume #50 at 353.1 m MSL, fly-through speed 40.0 m/s,
 $\Delta_{\text{north}} = 30.3$ m, $\Delta_{\text{east}} = -66.5$ m, local time 13:51:17**

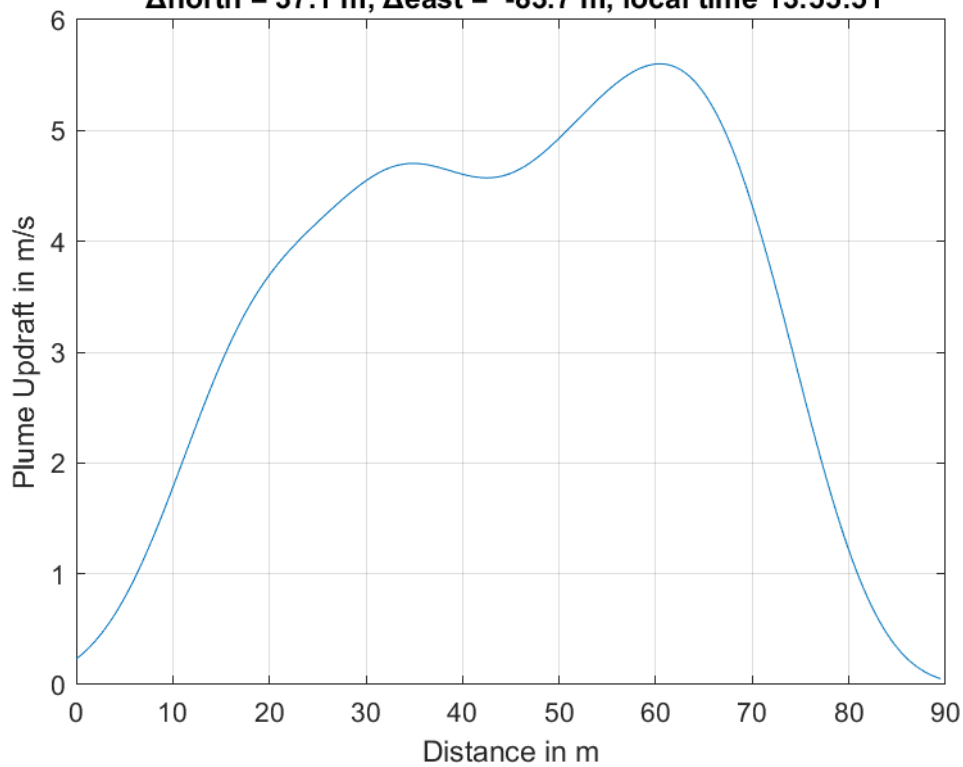


**Plume #51 at 339.8 m MSL, fly-through speed 41.0 m/s,
 $\Delta_{\text{north}} = 18.0$ m, $\Delta_{\text{east}} = -55.6$ m, local time 13:53:49**

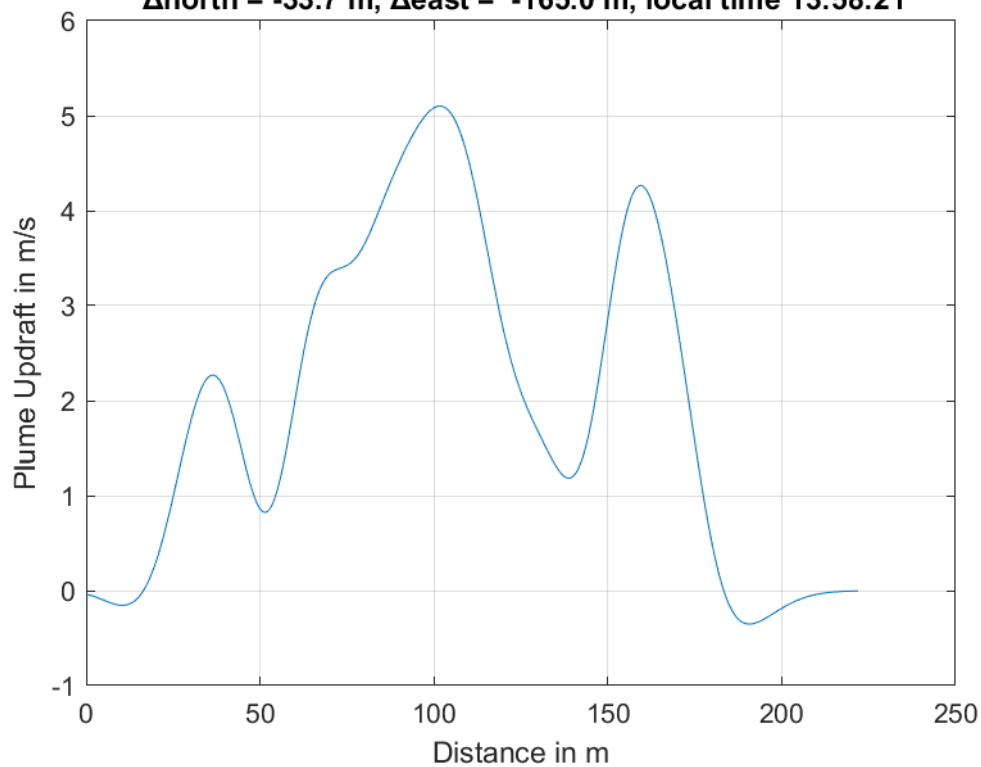




**Plume #52 at 317.4 m MSL, fly-through speed 39.0 m/s,
 $\Delta_{\text{north}} = 37.1$ m, $\Delta_{\text{east}} = -83.7$ m, local time 13:55:51**

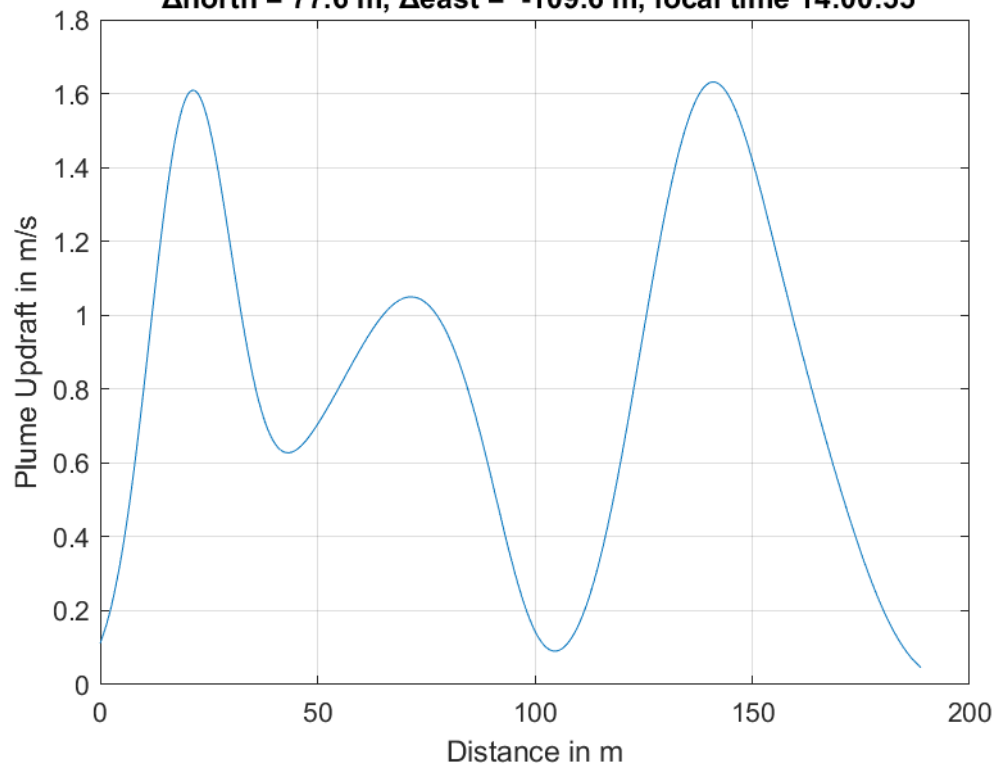


**Plume #53 at 309.9 m MSL, fly-through speed 37.0 m/s,
 $\Delta_{\text{north}} = -33.7$ m, $\Delta_{\text{east}} = -165.0$ m, local time 13:58:21**

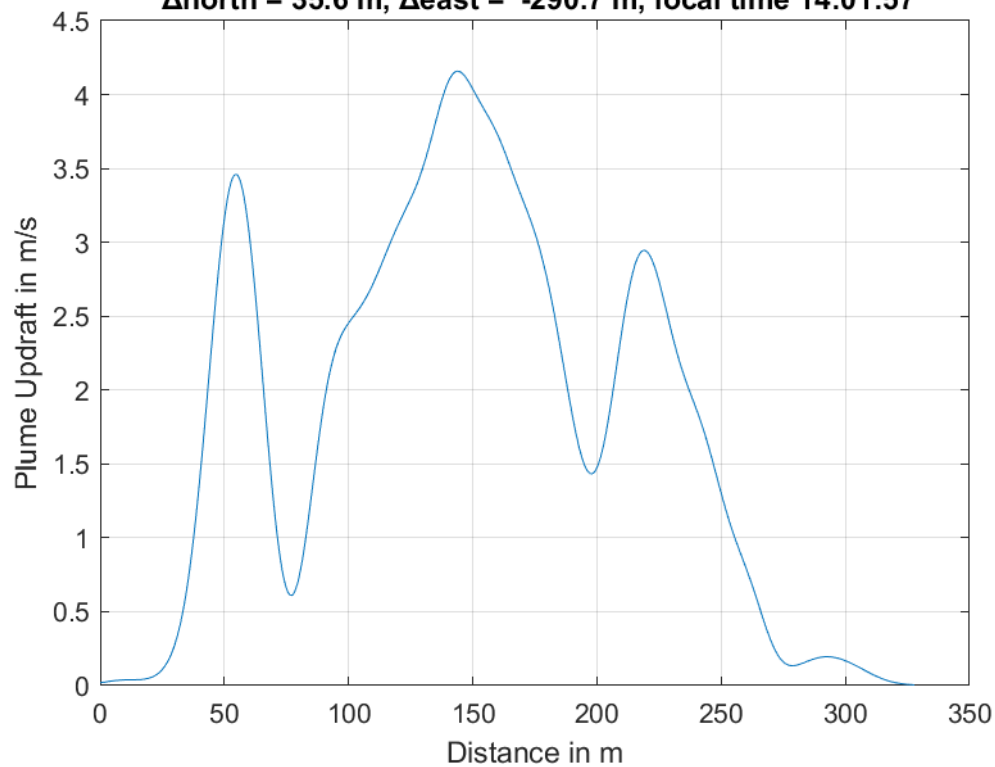




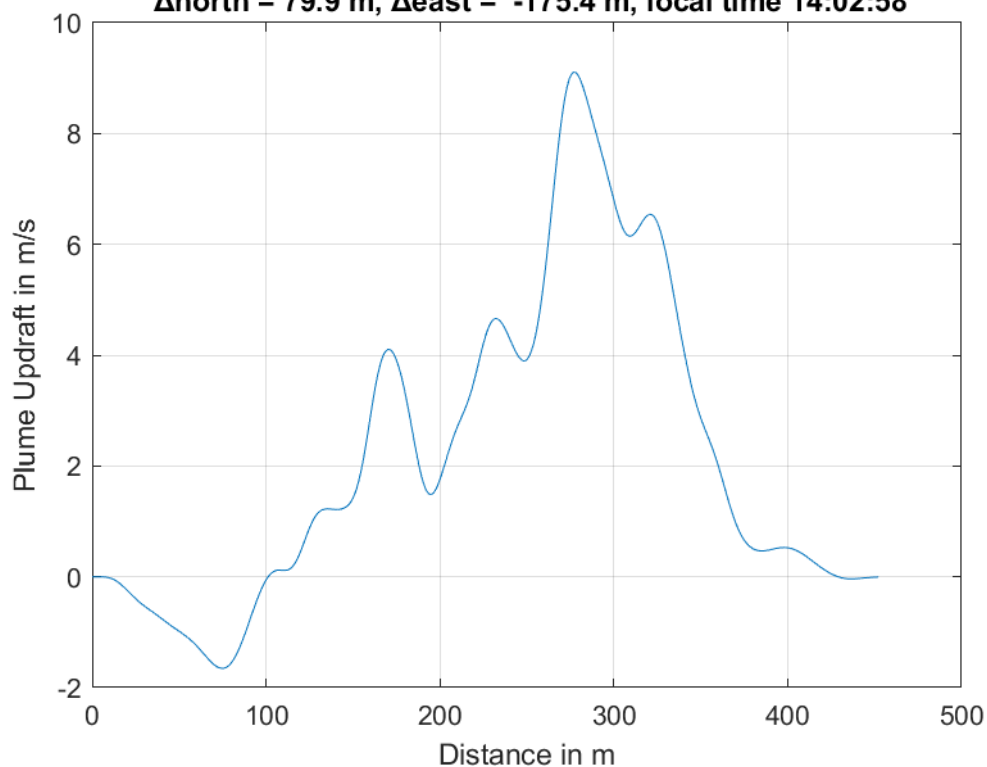
**Plume #54 at 297.5 m MSL, fly-through speed 42.0 m/s,
 $\Delta_{\text{north}} = 77.6$ m, $\Delta_{\text{east}} = -109.6$ m, local time 14:00:55**



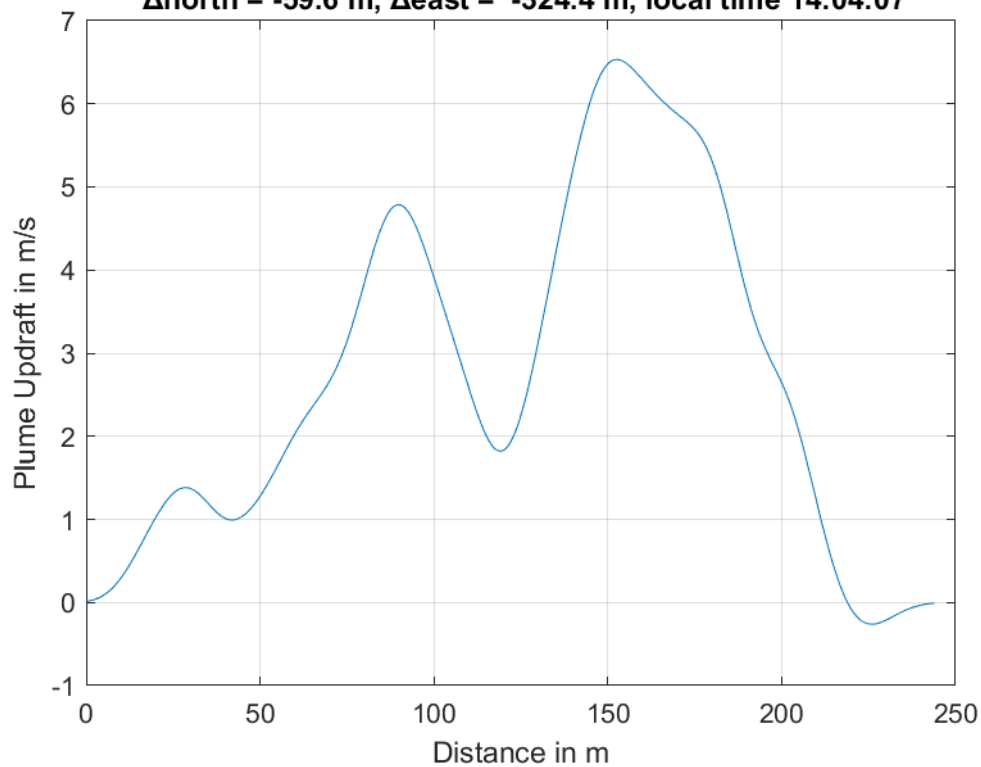
**Plume #55 at 316.4 m MSL, fly-through speed 41.0 m/s,
 $\Delta_{\text{north}} = 35.6$ m, $\Delta_{\text{east}} = -290.7$ m, local time 14:01:57**



**Plume #56 at 327.3 m MSL, fly-through speed 39.0 m/s,
 $\Delta_{\text{north}} = 79.9$ m, $\Delta_{\text{east}} = -175.4$ m, local time 14:02:58**

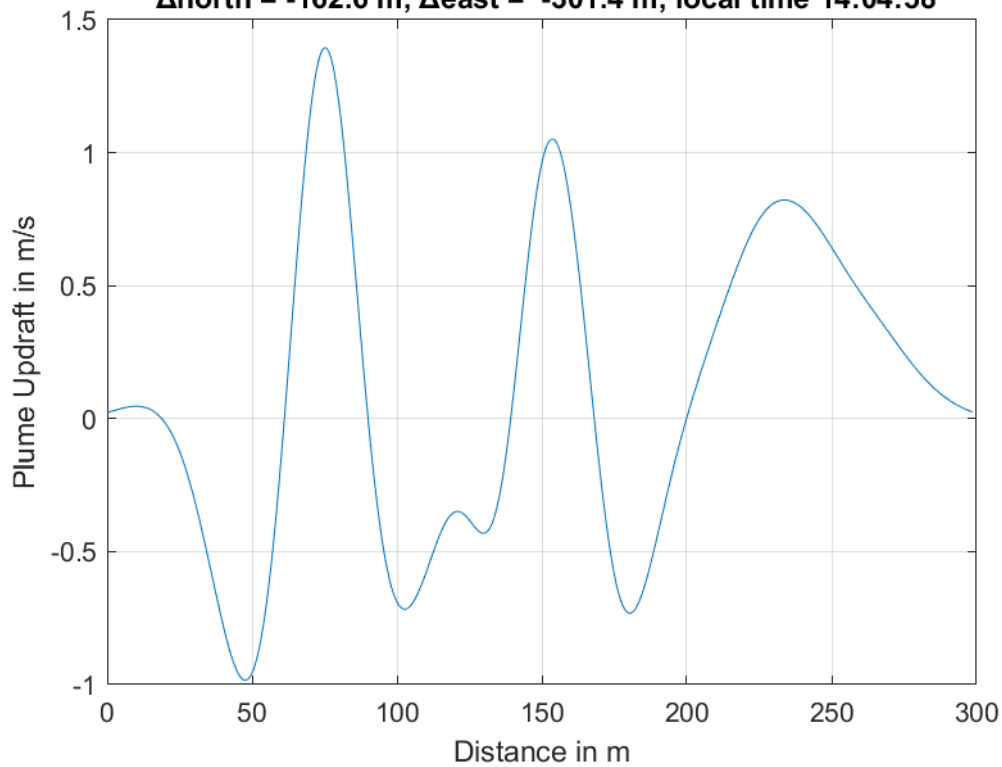


**Plume #57 at 334.5 m MSL, fly-through speed 40.0 m/s,
 $\Delta_{\text{north}} = -59.6$ m, $\Delta_{\text{east}} = -324.4$ m, local time 14:04:07**

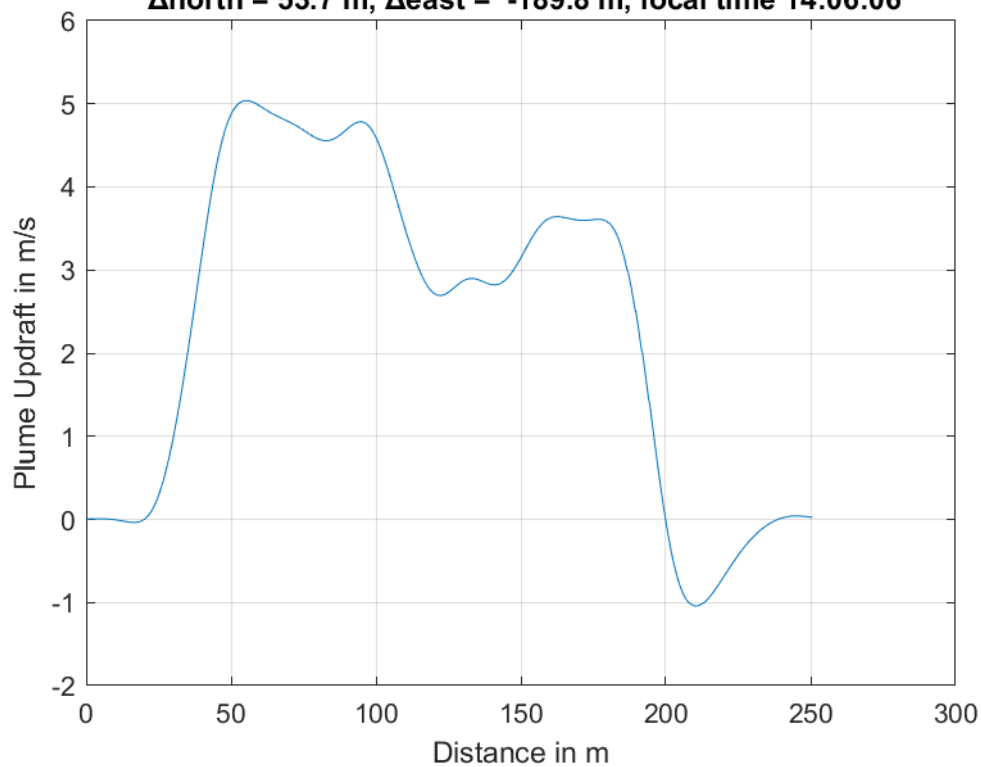




**Plume #58 at 316.1 m MSL, fly-through speed 46.0 m/s,
 $\Delta_{\text{north}} = -162.6$ m, $\Delta_{\text{east}} = -301.4$ m, local time 14:04:58**

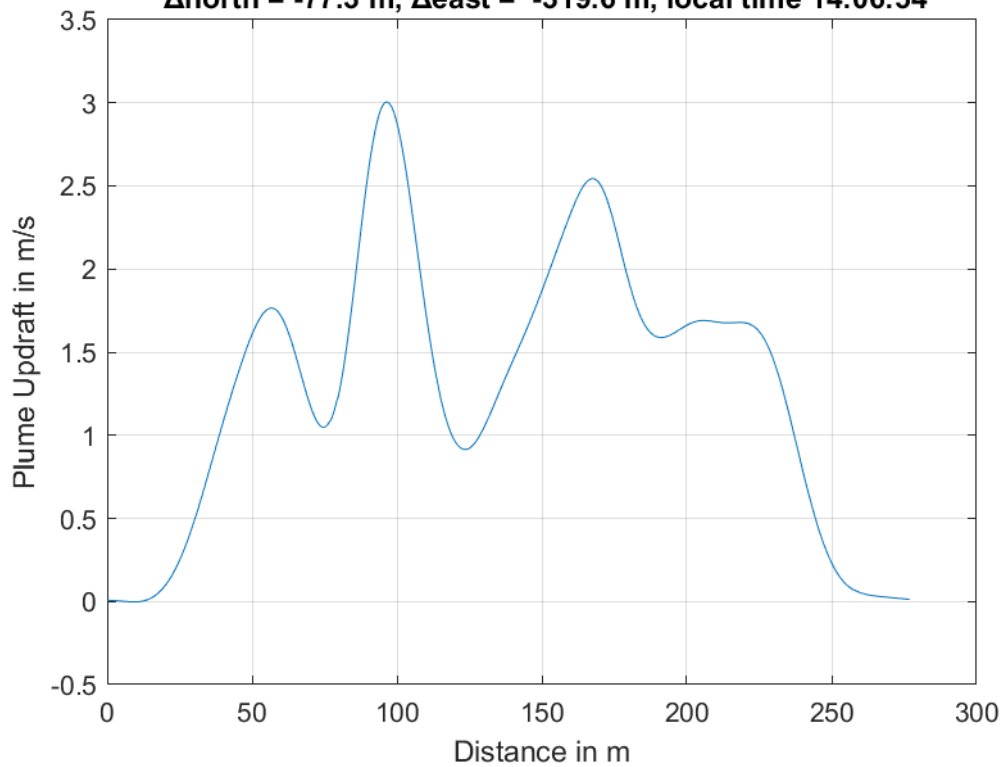


**Plume #59 at 312.1 m MSL, fly-through speed 38.0 m/s,
 $\Delta_{\text{north}} = 53.7$ m, $\Delta_{\text{east}} = -189.8$ m, local time 14:06:06**

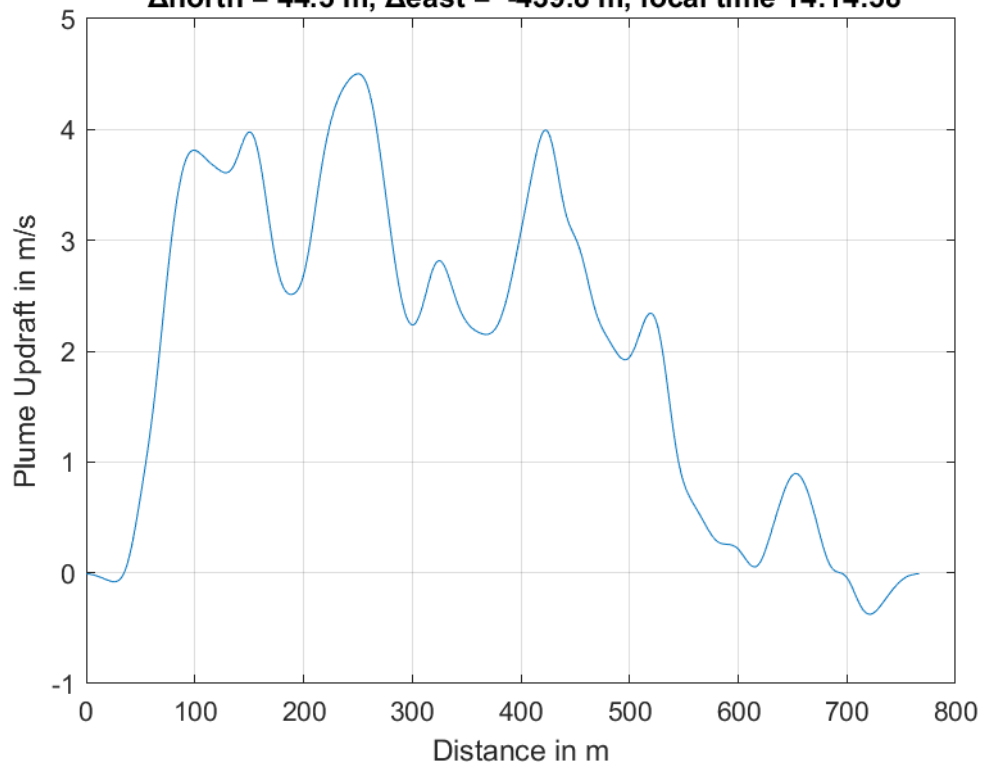




**Plume #60 at 318.5 m MSL, fly-through speed 44.0 m/s,
 $\Delta_{\text{north}} = -77.3$ m, $\Delta_{\text{east}} = -319.6$ m, local time 14:06:54**

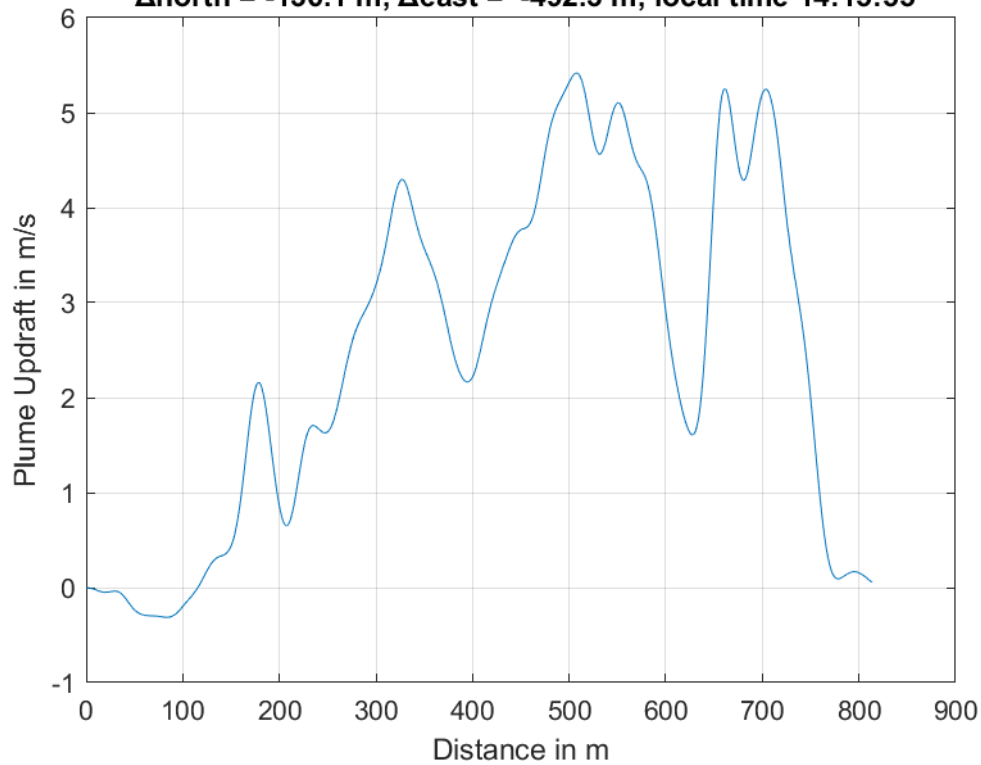


**Plume #61 at 466.9 m MSL, fly-through speed 54.0 m/s,
 $\Delta_{\text{north}} = 44.5$ m, $\Delta_{\text{east}} = -439.8$ m, local time 14:14:58**

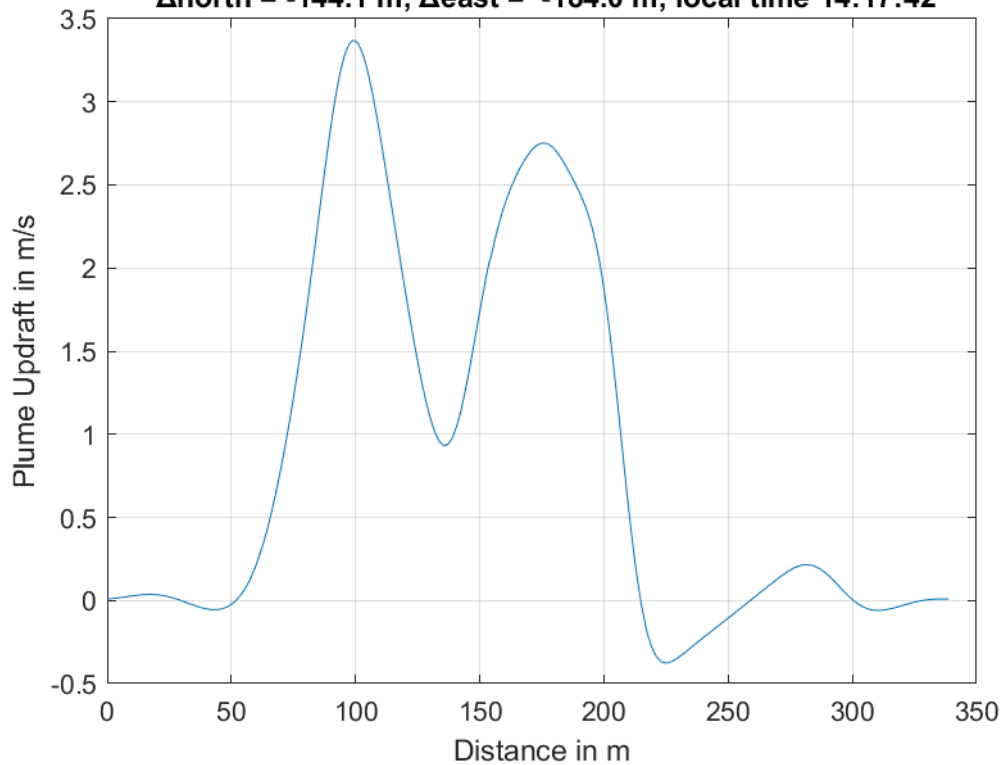




**Plume #62 at 456.7 m MSL, fly-through speed 55.0 m/s,
 $\Delta_{\text{north}} = -136.1$ m, $\Delta_{\text{east}} = -492.3$ m, local time 14:15:55**

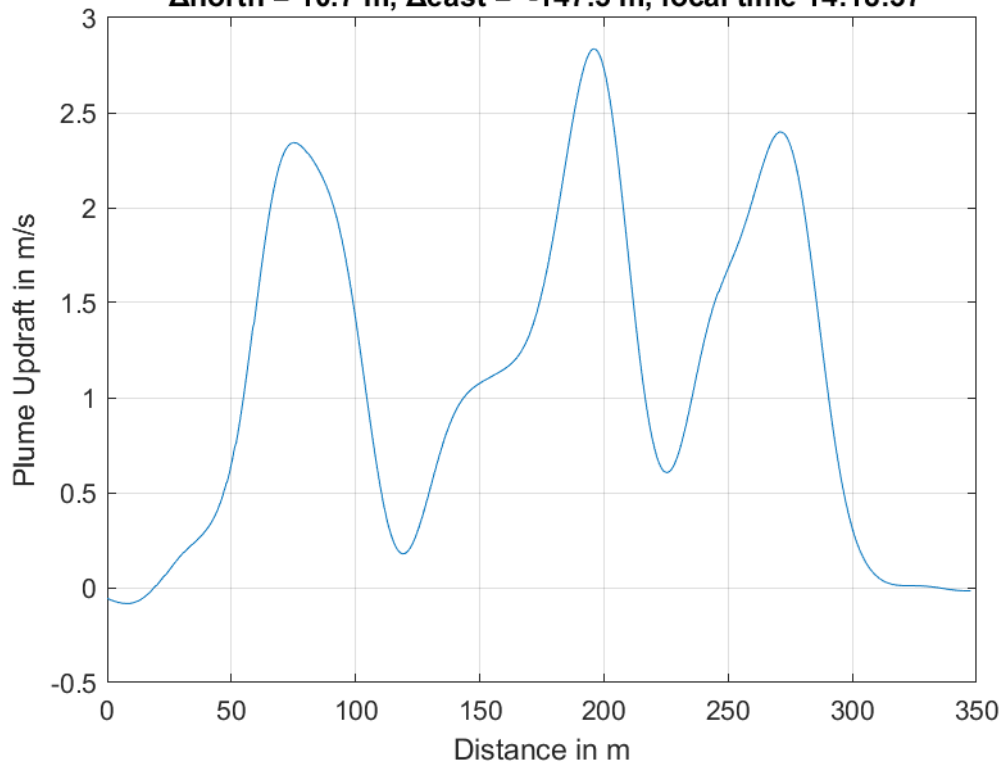


**Plume #63 at 319.4 m MSL, fly-through speed 53.0 m/s,
 $\Delta_{\text{north}} = -144.1$ m, $\Delta_{\text{east}} = -184.0$ m, local time 14:17:42**

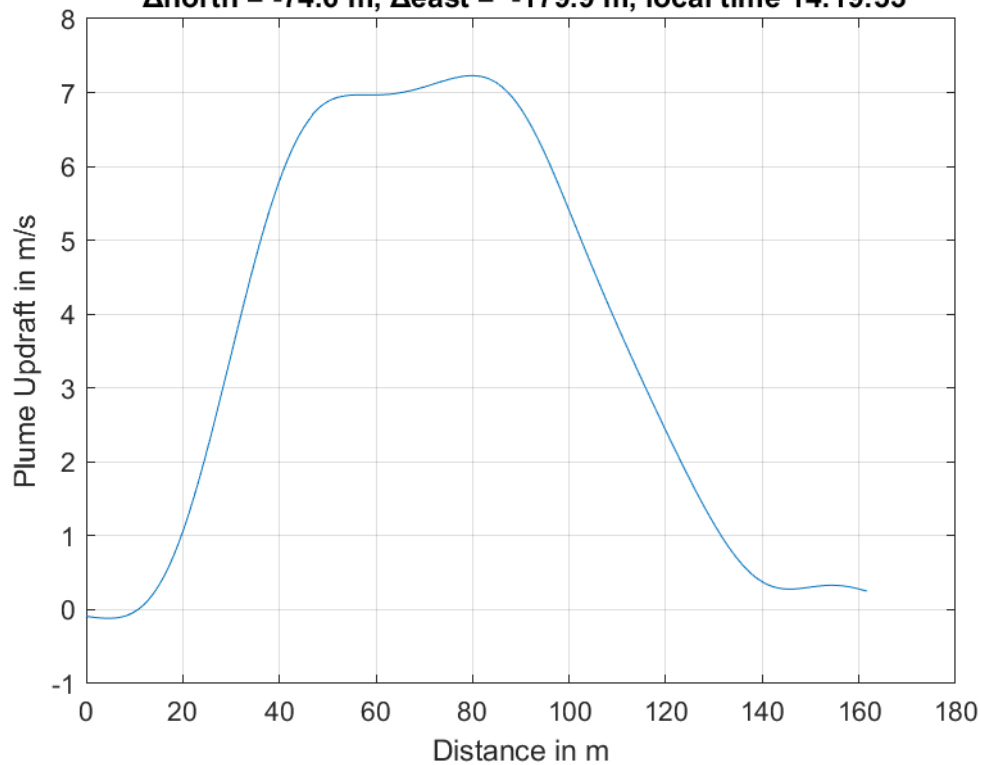




**Plume #64 at 343.4 m MSL, fly-through speed 58.0 m/s,
 $\Delta_{\text{north}} = 10.7$ m, $\Delta_{\text{east}} = -147.5$ m, local time 14:18:37**

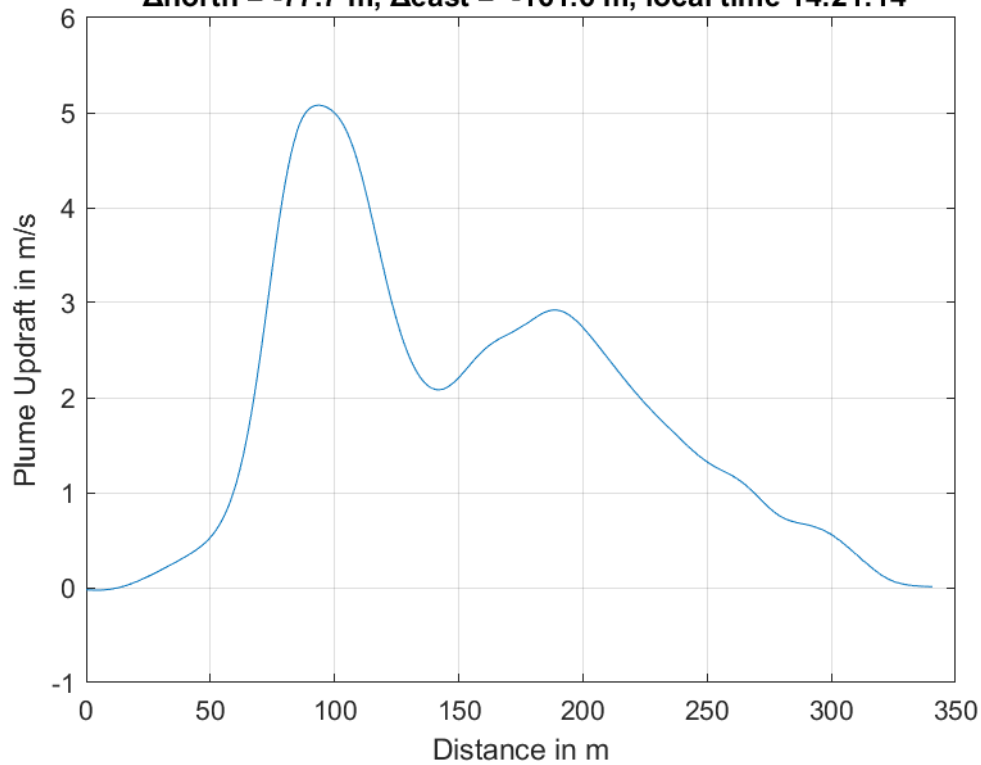


**Plume #65 at 315.8 m MSL, fly-through speed 54.0 m/s,
 $\Delta_{\text{north}} = -74.6$ m, $\Delta_{\text{east}} = -179.9$ m, local time 14:19:53**

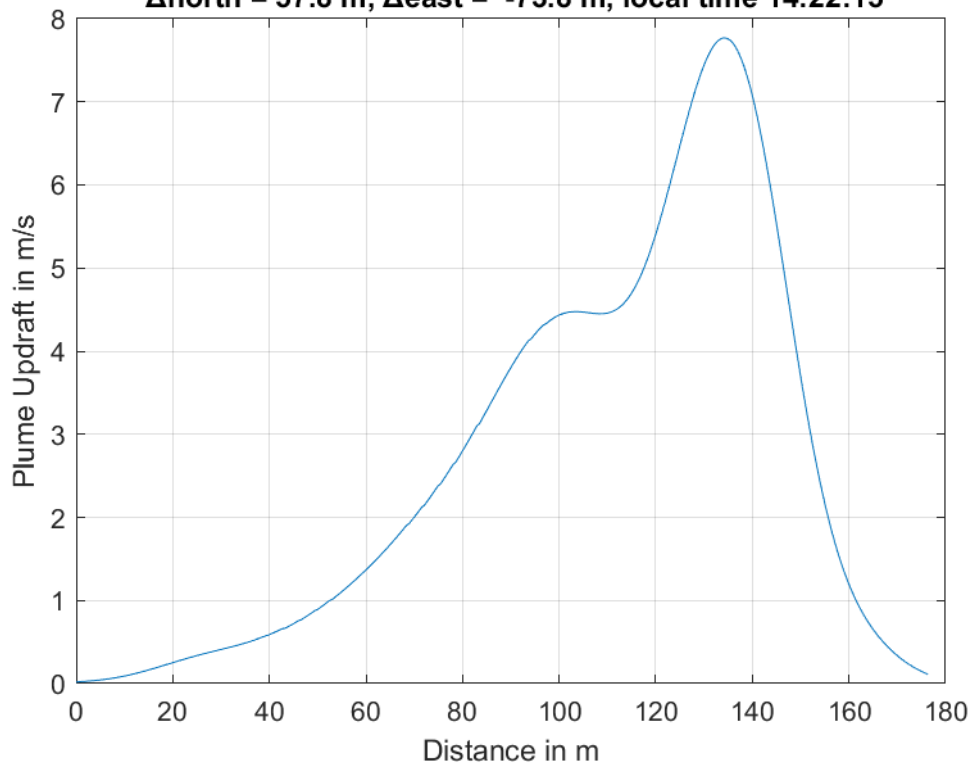




**Plume #66 at 319.3 m MSL, fly-through speed 55.0 m/s,
 $\Delta_{\text{north}} = -77.7$ m, $\Delta_{\text{east}} = -161.6$ m, local time 14:21:14**

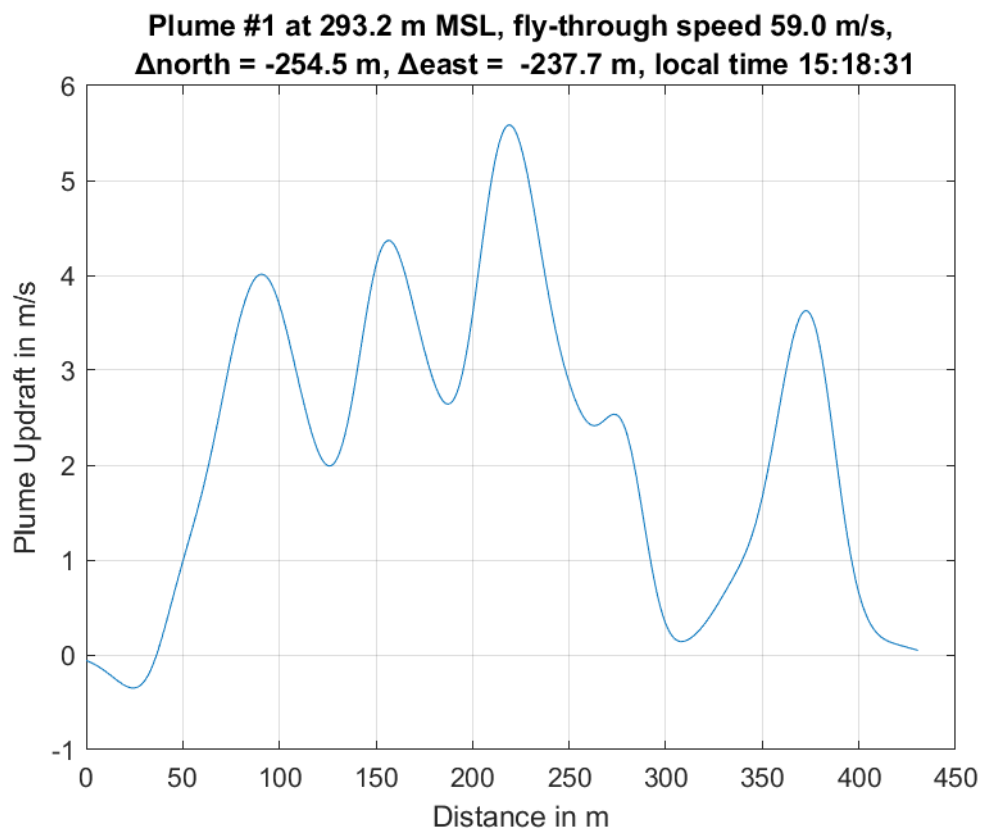
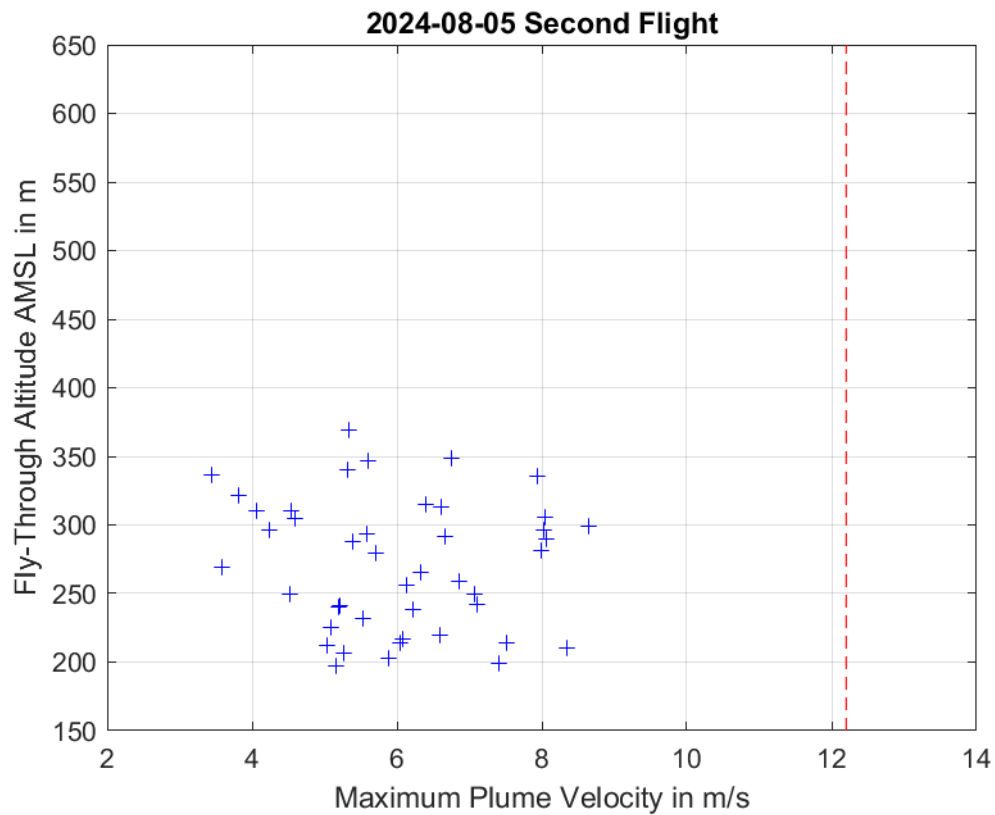


**Plume #67 at 345.6 m MSL, fly-through speed 52.0 m/s,
 $\Delta_{\text{north}} = 57.8$ m, $\Delta_{\text{east}} = -73.8$ m, local time 14:22:15**



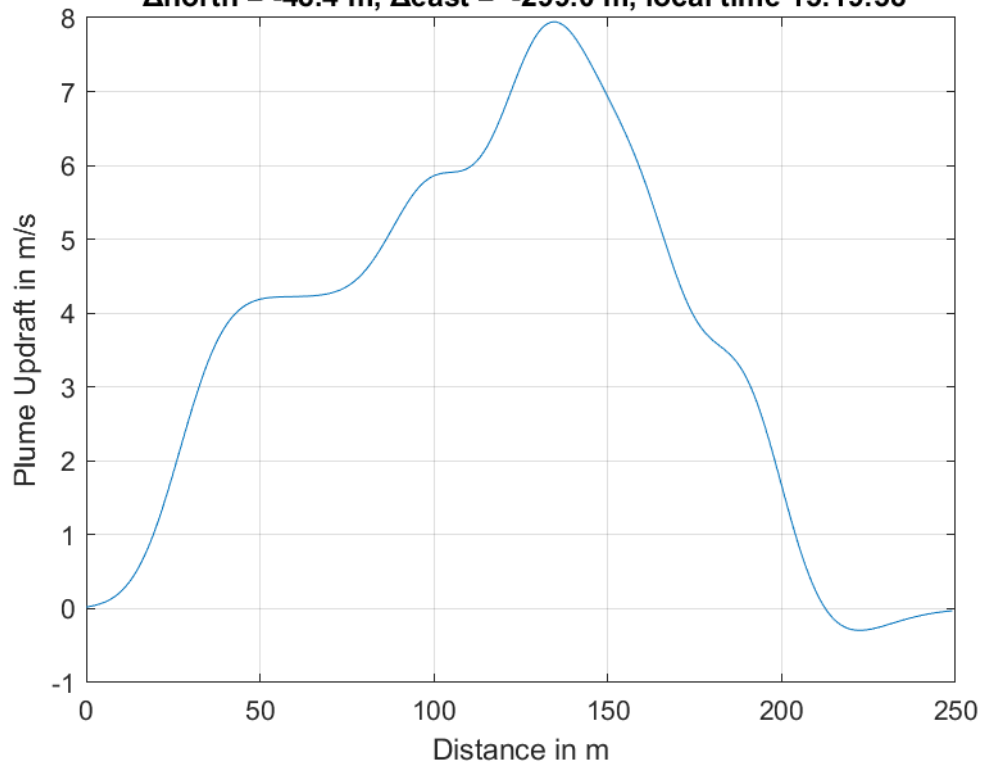


6 Measured Plumes: 2024-08-05 Second Flight

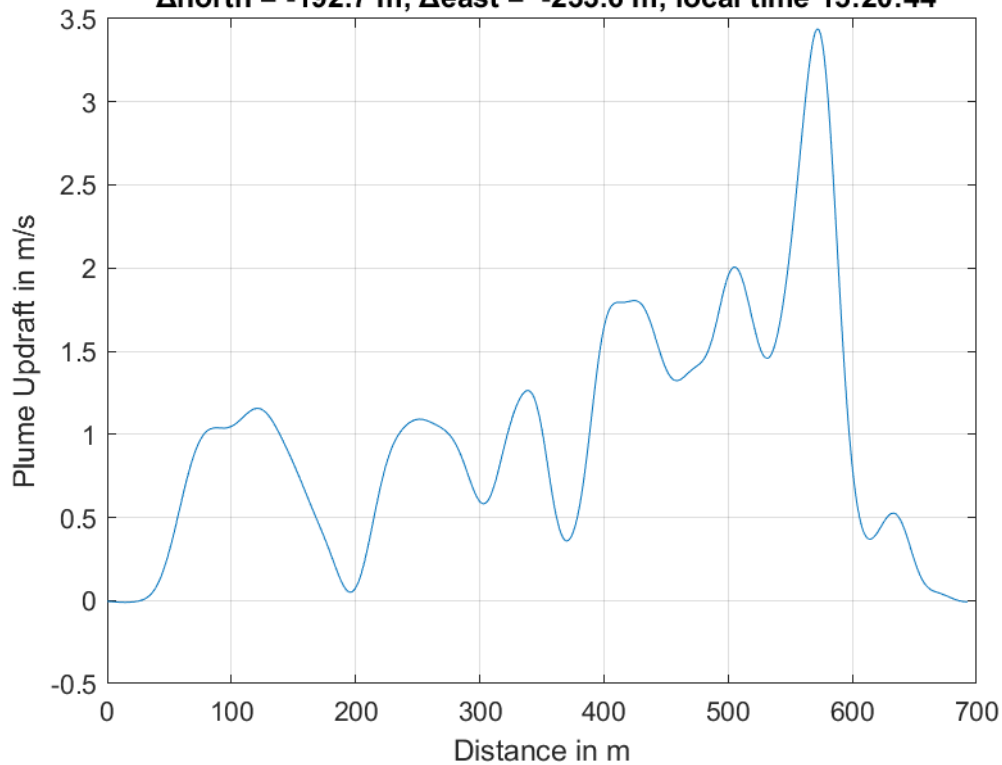




**Plume #2 at 335.4 m MSL, fly-through speed 58.0 m/s,
 $\Delta_{\text{north}} = -48.4$ m, $\Delta_{\text{east}} = -299.0$ m, local time 15:19:58**

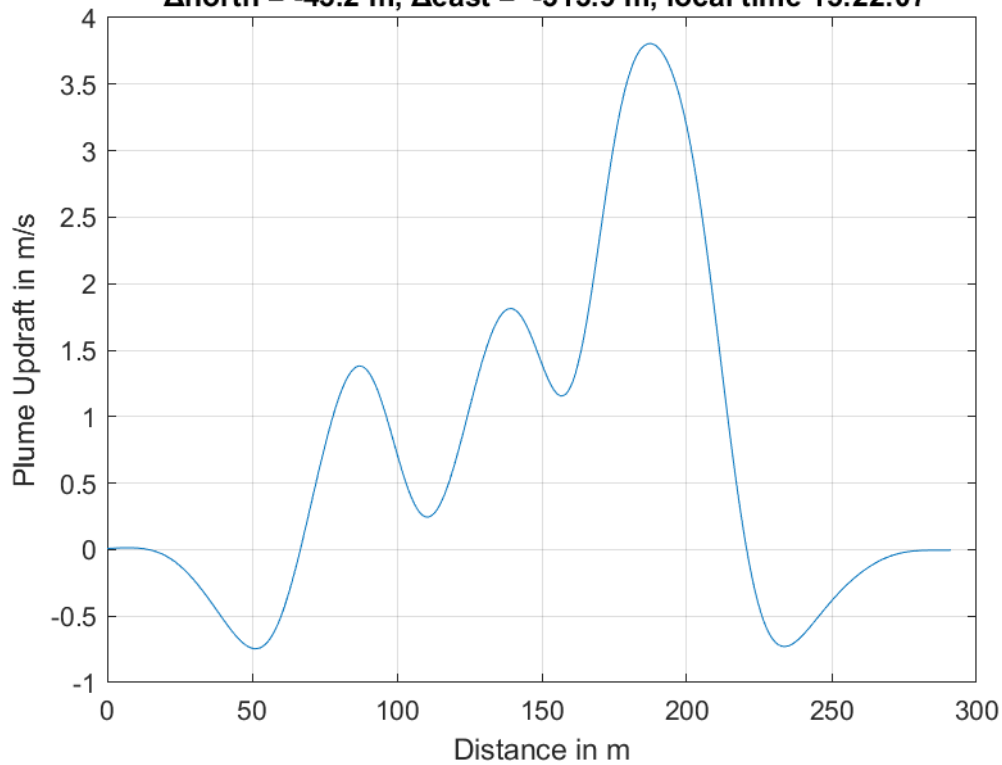


**Plume #3 at 336.0 m MSL, fly-through speed 63.0 m/s,
 $\Delta_{\text{north}} = -192.7$ m, $\Delta_{\text{east}} = -233.6$ m, local time 15:20:44**

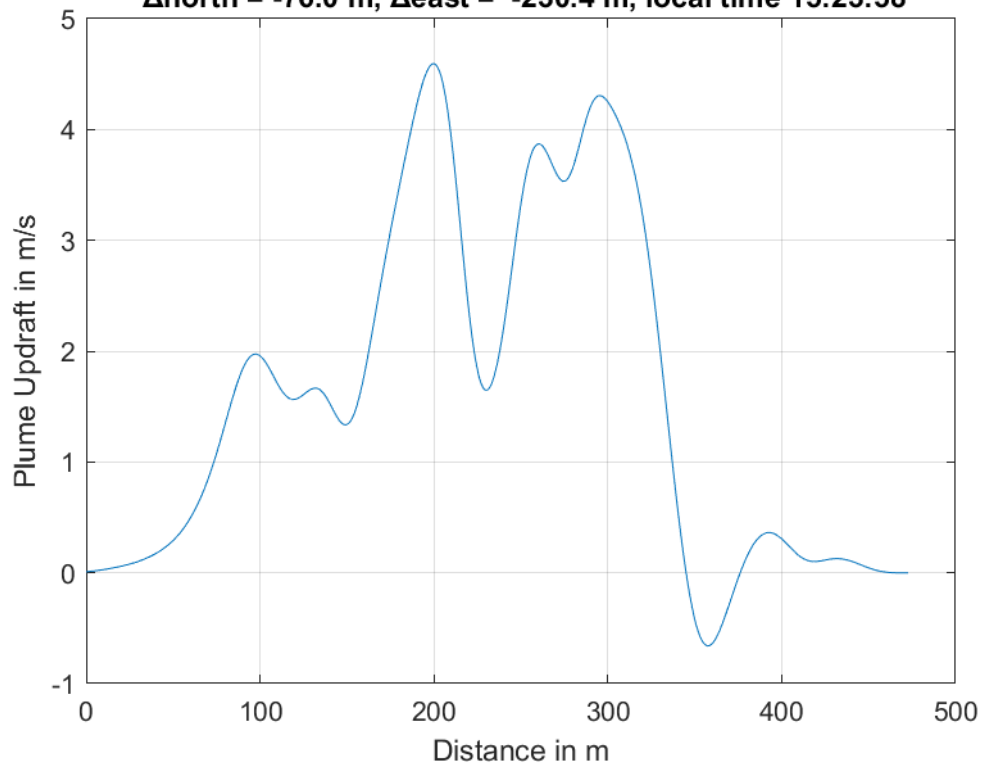




**Plume #4 at 321.2 m MSL, fly-through speed 55.0 m/s,
 $\Delta_{\text{north}} = -43.2$ m, $\Delta_{\text{east}} = -313.9$ m, local time 15:22:07**

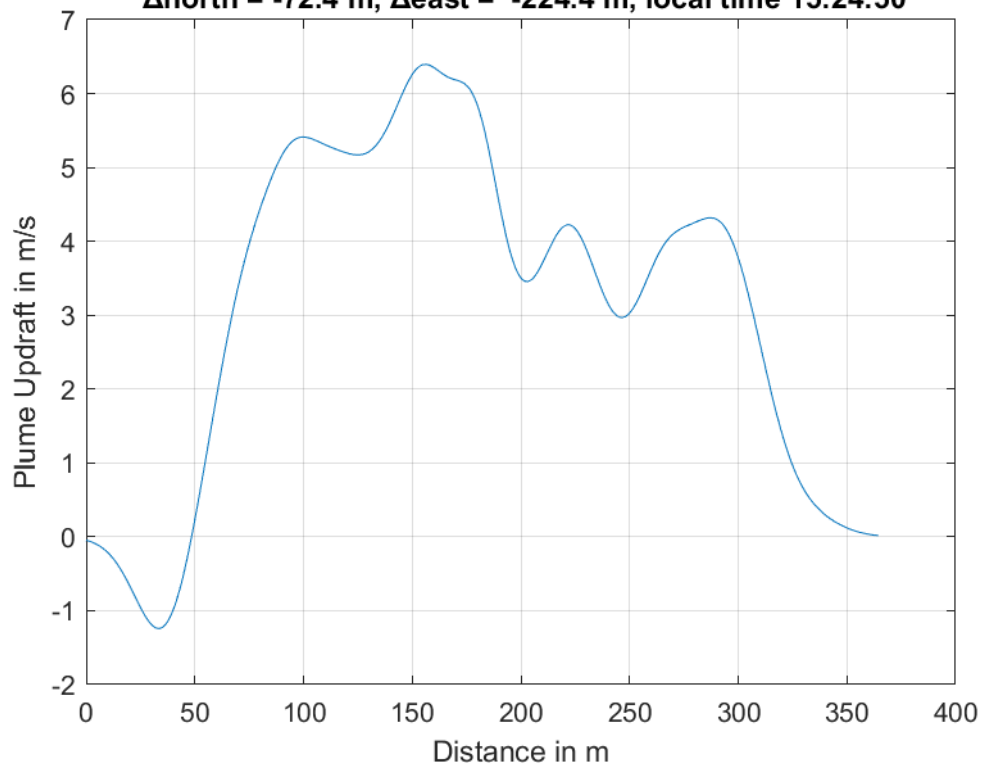


**Plume #5 at 304.5 m MSL, fly-through speed 57.0 m/s,
 $\Delta_{\text{north}} = -76.0$ m, $\Delta_{\text{east}} = -230.4$ m, local time 15:23:58**

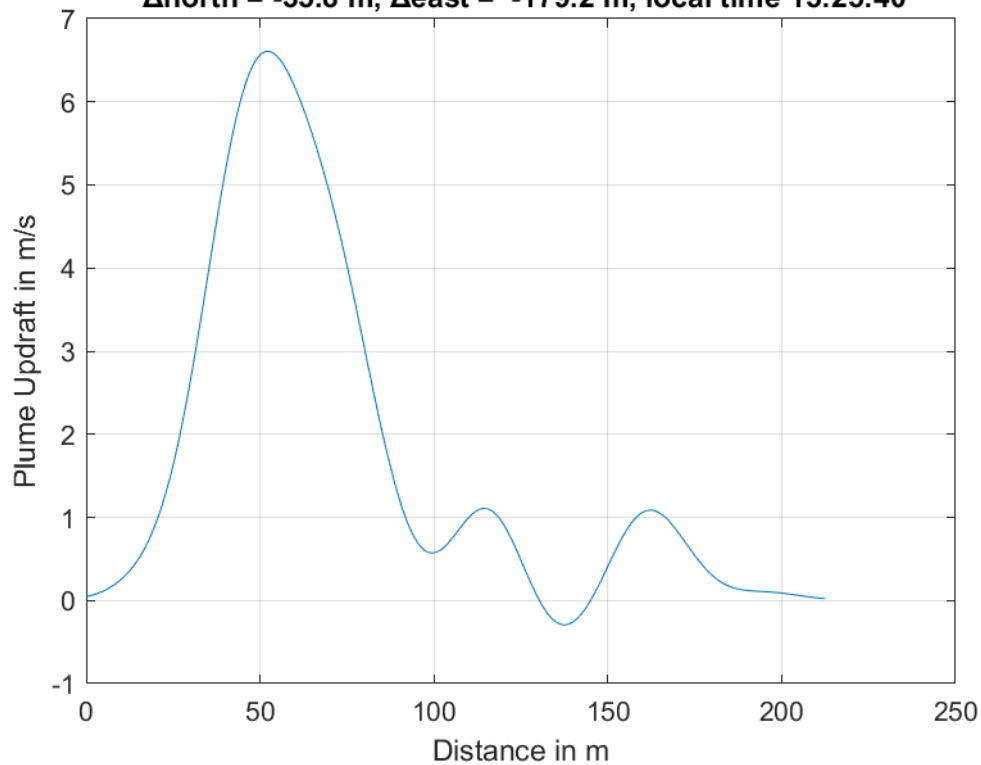




**Plume #6 at 315.3 m MSL, fly-through speed 57.0 m/s,
 $\Delta_{\text{north}} = -72.4$ m, $\Delta_{\text{east}} = -224.4$ m, local time 15:24:50**

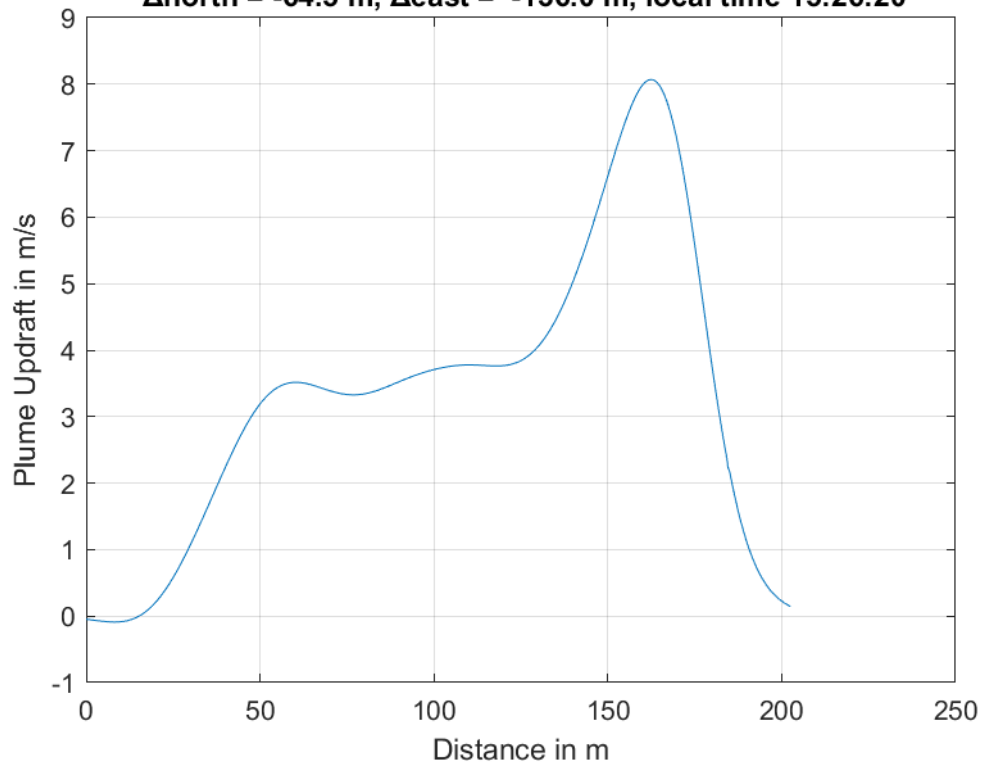


**Plume #7 at 312.9 m MSL, fly-through speed 56.0 m/s,
 $\Delta_{\text{north}} = -35.8$ m, $\Delta_{\text{east}} = -179.2$ m, local time 15:25:40**

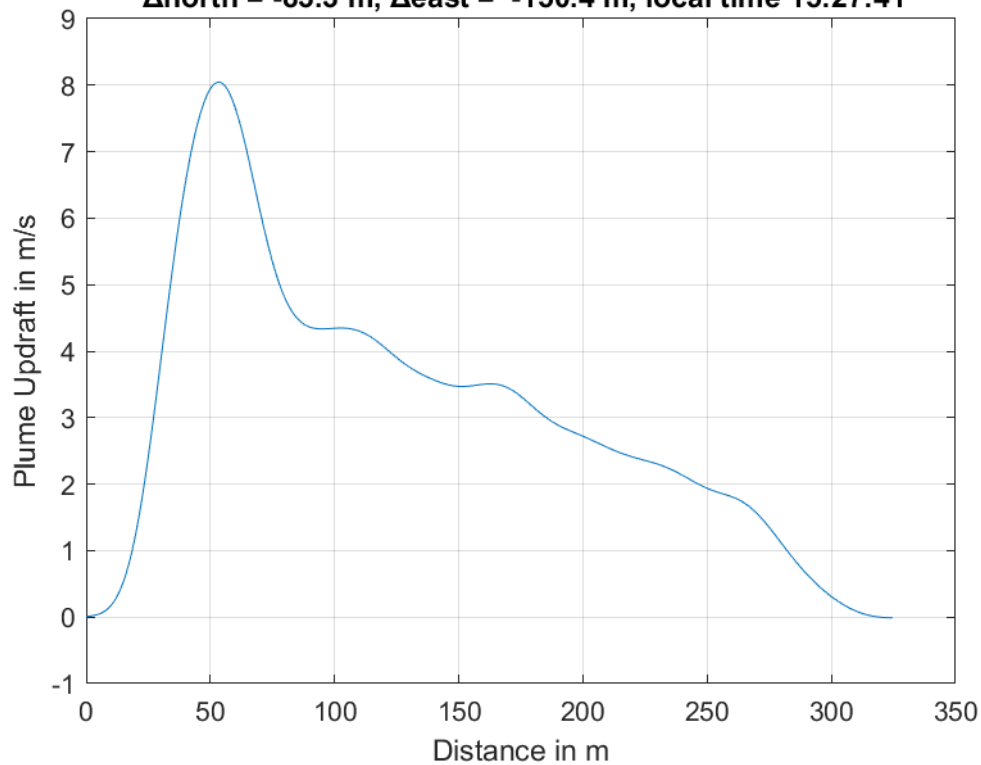




**Plume #8 at 290.1 m MSL, fly-through speed 58.0 m/s,
 $\Delta_{\text{north}} = -64.5$ m, $\Delta_{\text{east}} = -136.0$ m, local time 15:26:20**

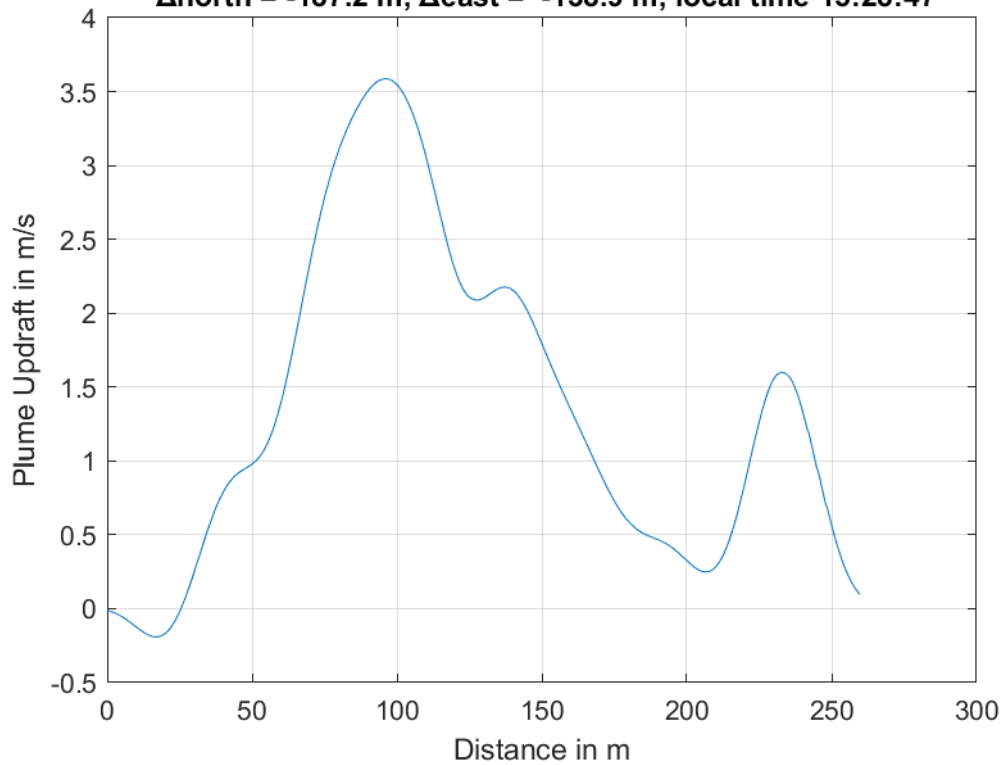


**Plume #9 at 305.6 m MSL, fly-through speed 58.0 m/s,
 $\Delta_{\text{north}} = -83.3$ m, $\Delta_{\text{east}} = -150.4$ m, local time 15:27:41**

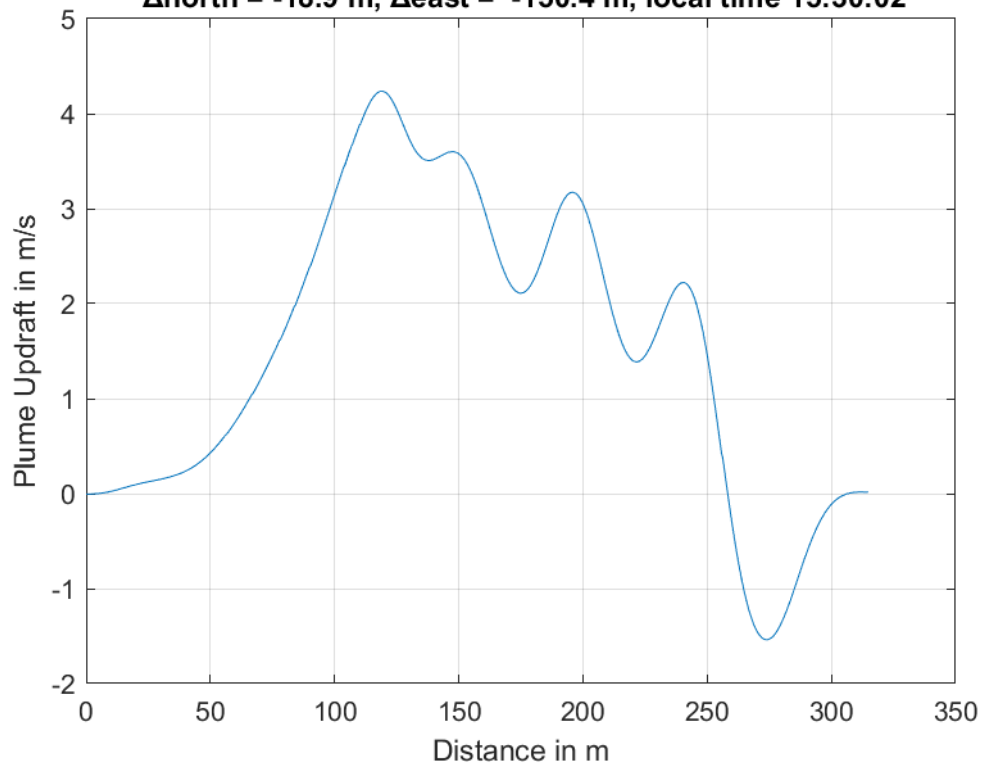




**Plume #10 at 269.6 m MSL, fly-through speed 51.0 m/s,
 $\Delta_{\text{north}} = -187.2$ m, $\Delta_{\text{east}} = -138.9$ m, local time 15:28:47**

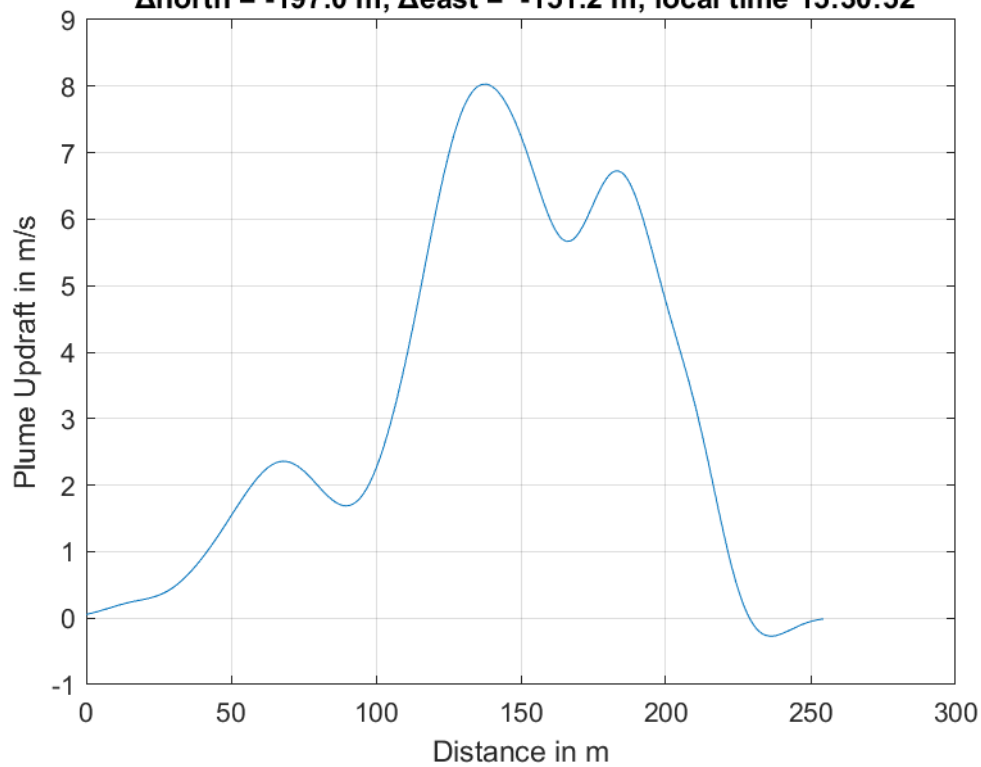


**Plume #11 at 296.7 m MSL, fly-through speed 47.0 m/s,
 $\Delta_{\text{north}} = -18.9$ m, $\Delta_{\text{east}} = -150.4$ m, local time 15:30:02**

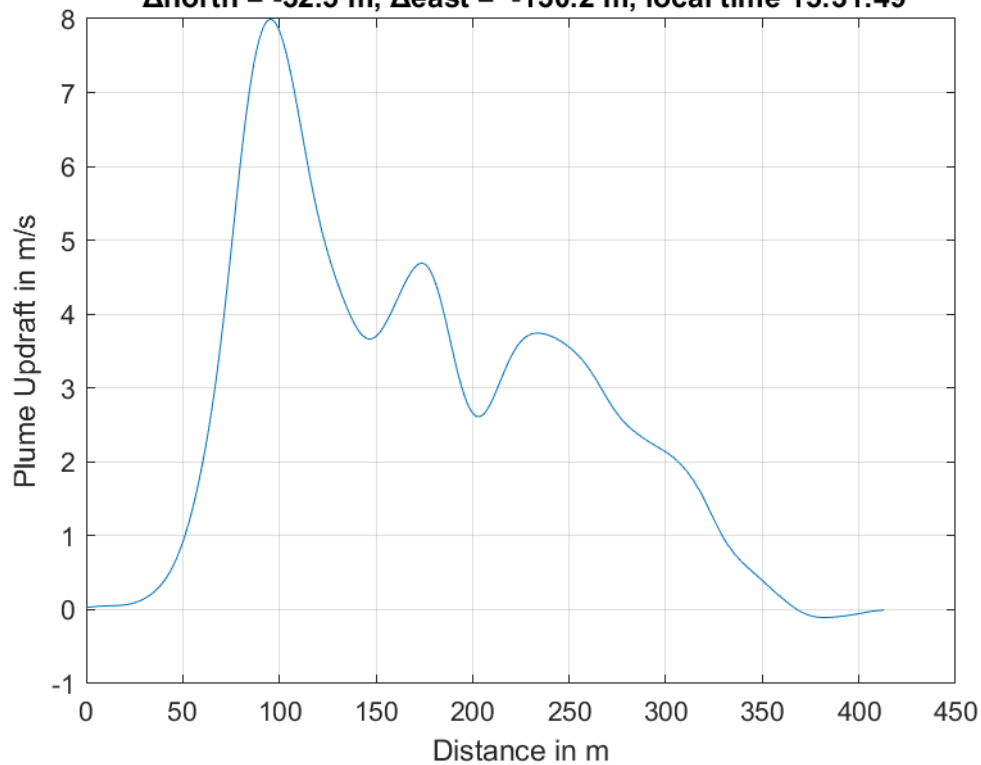




**Plume #12 at 296.0 m MSL, fly-through speed 49.0 m/s,
 $\Delta_{\text{north}} = -197.0$ m, $\Delta_{\text{east}} = -151.2$ m, local time 15:30:52**

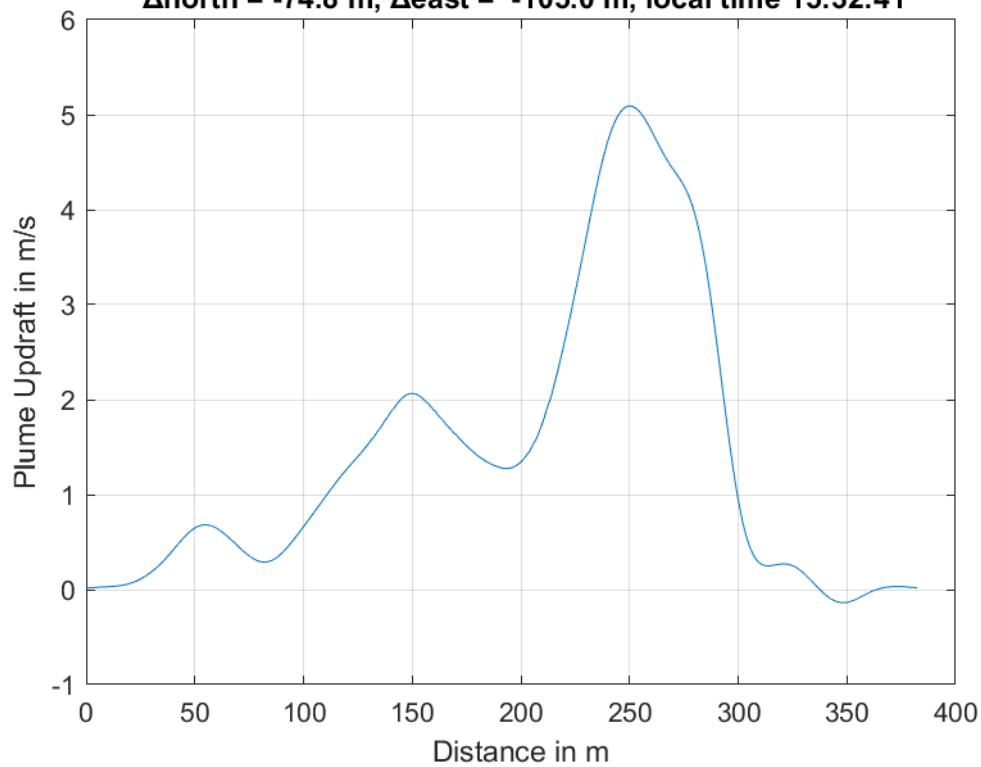


**Plume #13 at 281.1 m MSL, fly-through speed 53.0 m/s,
 $\Delta_{\text{north}} = -32.5$ m, $\Delta_{\text{east}} = -130.2$ m, local time 15:31:49**

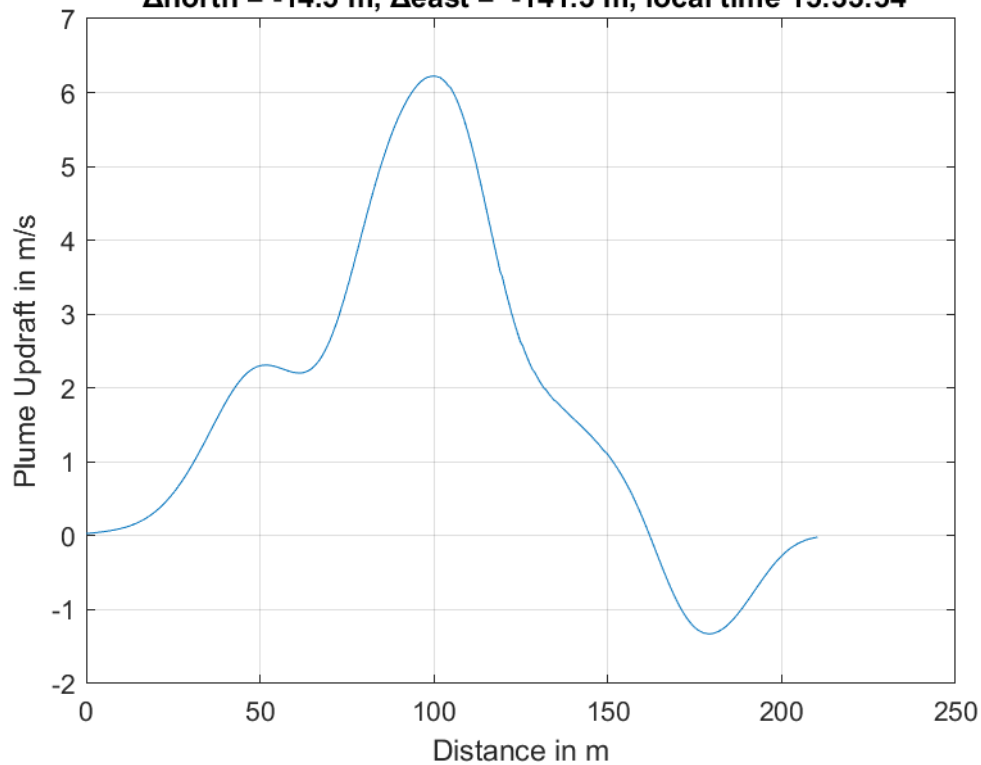




**Plume #14 at 225.4 m MSL, fly-through speed 51.0 m/s,
 $\Delta_{\text{north}} = -74.8$ m, $\Delta_{\text{east}} = -105.0$ m, local time 15:32:41**

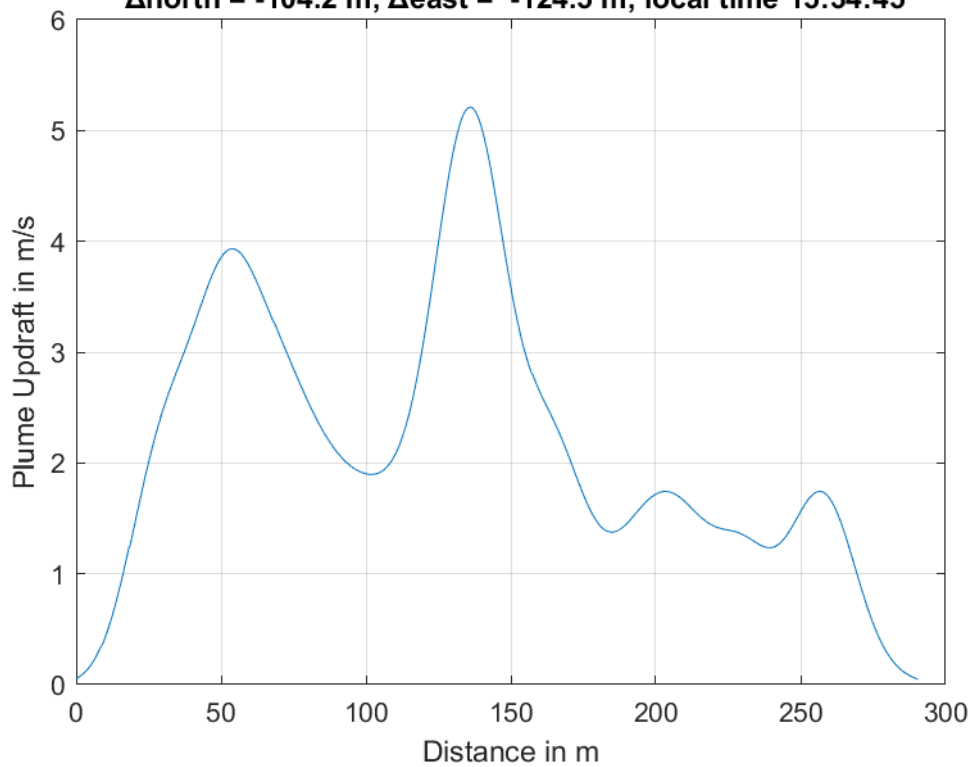


**Plume #15 at 238.4 m MSL, fly-through speed 49.0 m/s,
 $\Delta_{\text{north}} = -14.5$ m, $\Delta_{\text{east}} = -141.3$ m, local time 15:33:54**

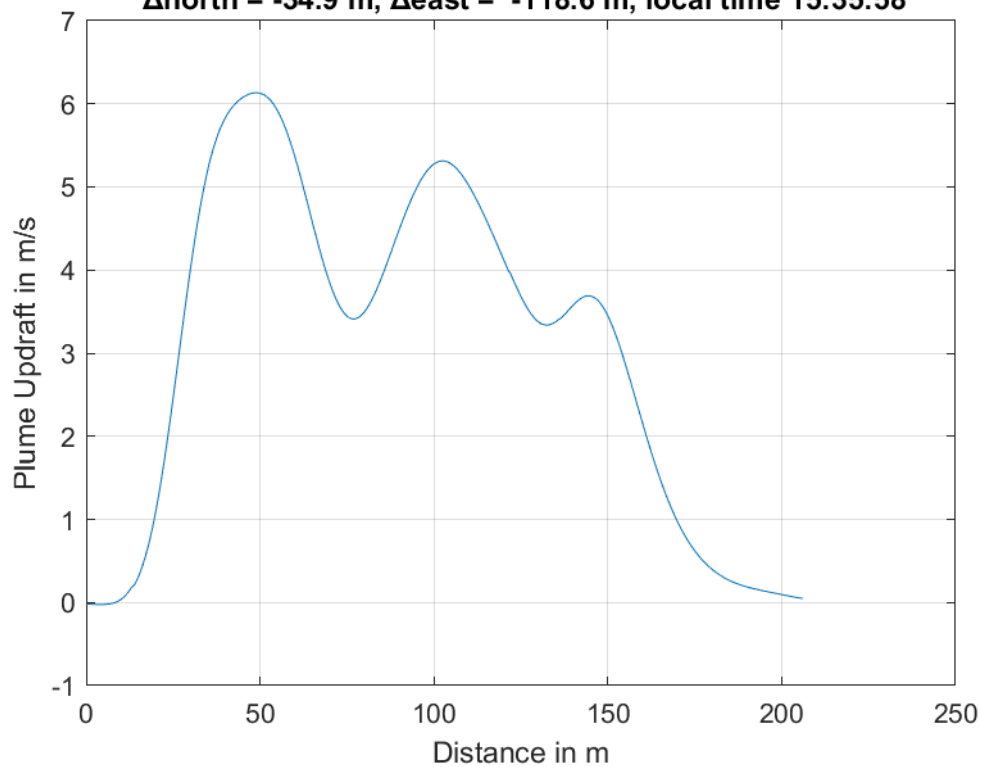




**Plume #16 at 240.9 m MSL, fly-through speed 51.0 m/s,
 $\Delta_{\text{north}} = -104.2$ m, $\Delta_{\text{east}} = -124.5$ m, local time 15:34:45**

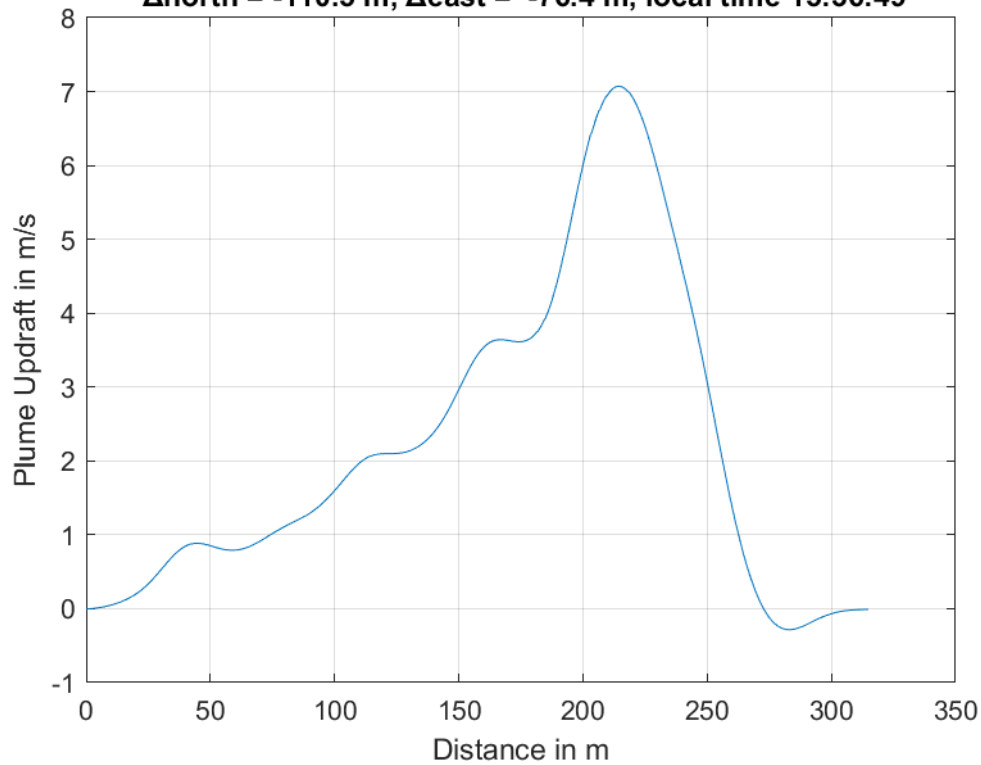


**Plume #17 at 256.4 m MSL, fly-through speed 48.0 m/s,
 $\Delta_{\text{north}} = -34.9$ m, $\Delta_{\text{east}} = -118.6$ m, local time 15:35:58**

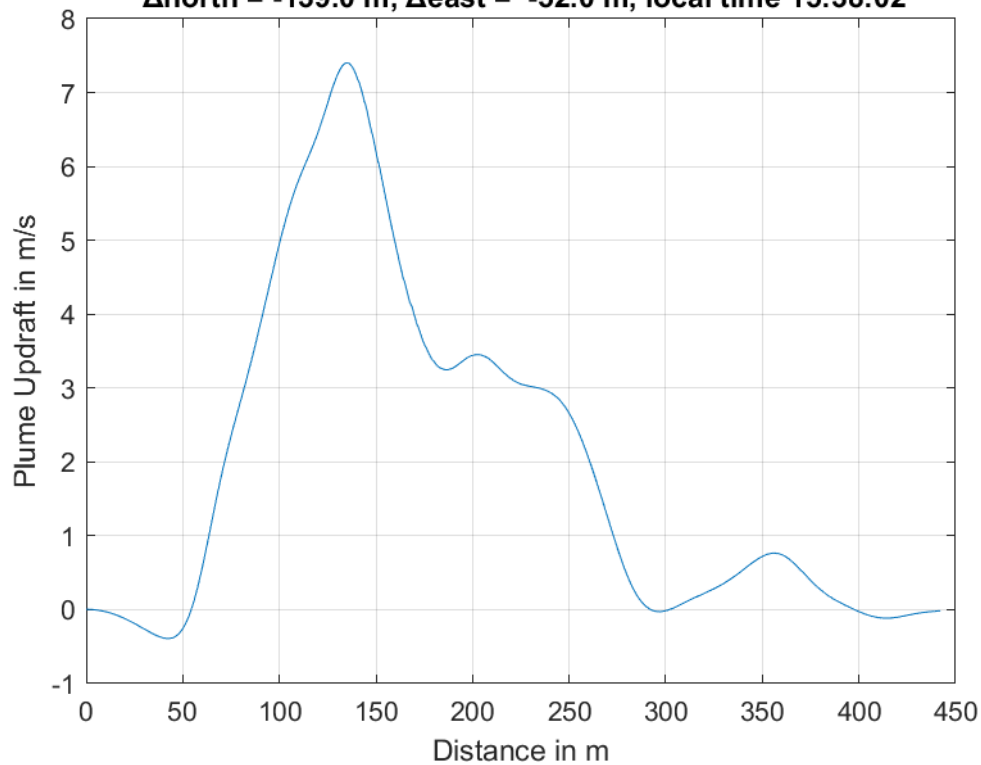




**Plume #18 at 249.6 m MSL, fly-through speed 50.0 m/s,
 $\Delta_{\text{north}} = -110.5$ m, $\Delta_{\text{east}} = -76.4$ m, local time 15:36:49**

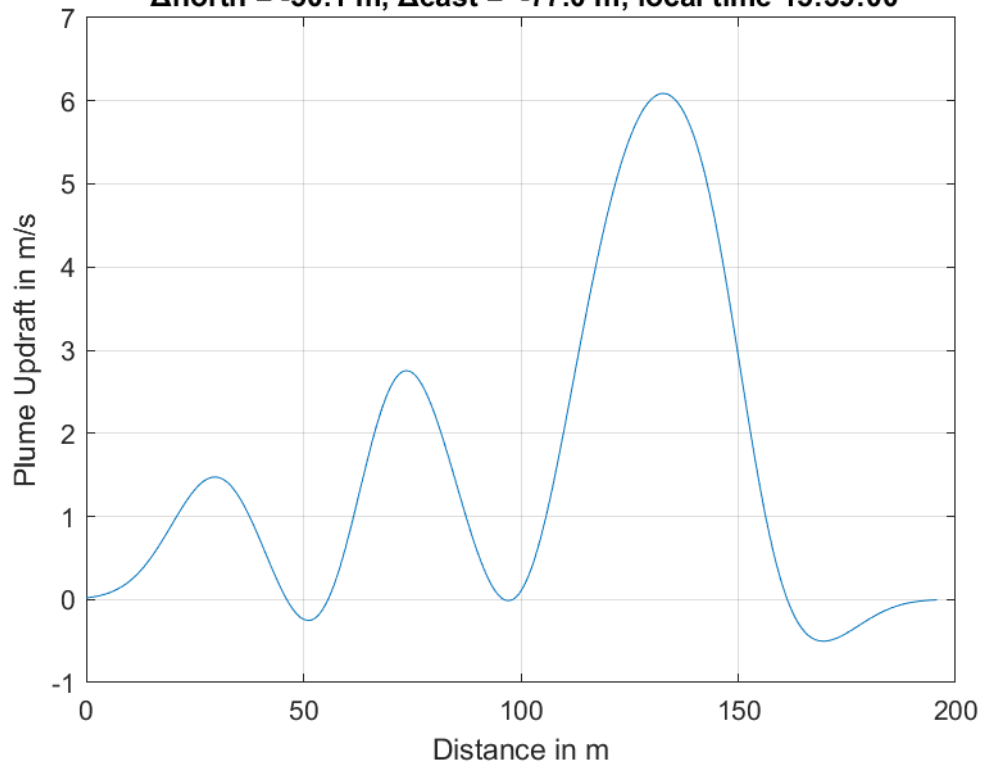


**Plume #19 at 198.6 m MSL, fly-through speed 56.0 m/s,
 $\Delta_{\text{north}} = -139.0$ m, $\Delta_{\text{east}} = -52.0$ m, local time 15:38:02**

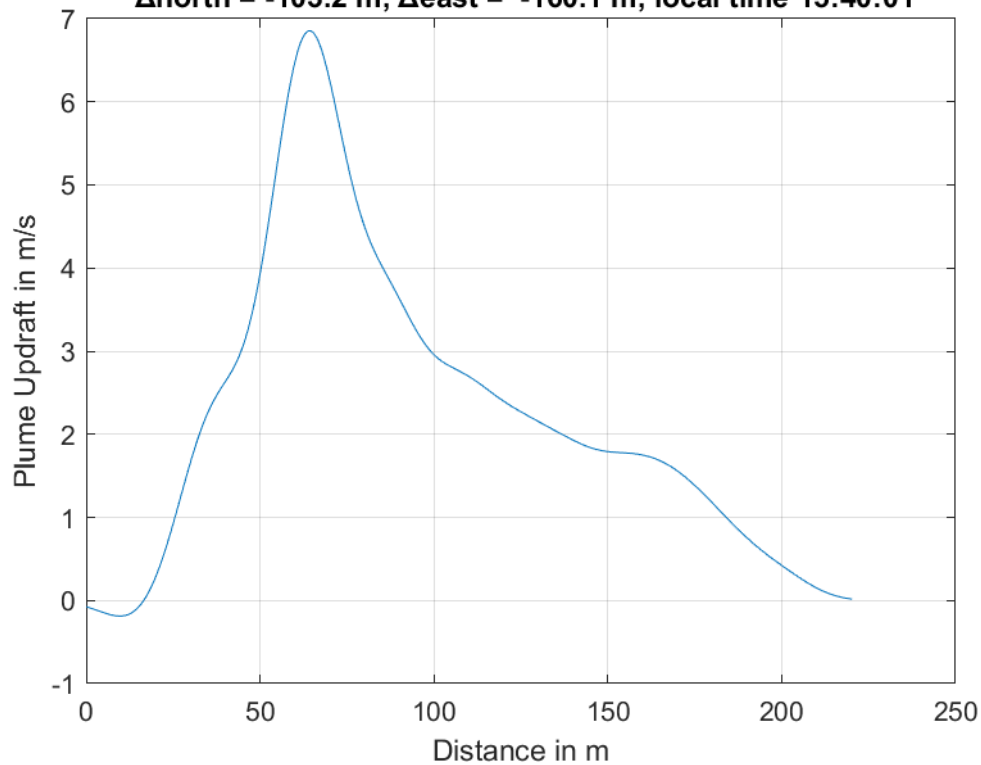




**Plume #20 at 217.1 m MSL, fly-through speed 49.0 m/s,
 $\Delta_{\text{north}} = -50.1$ m, $\Delta_{\text{east}} = -77.0$ m, local time 15:39:00**

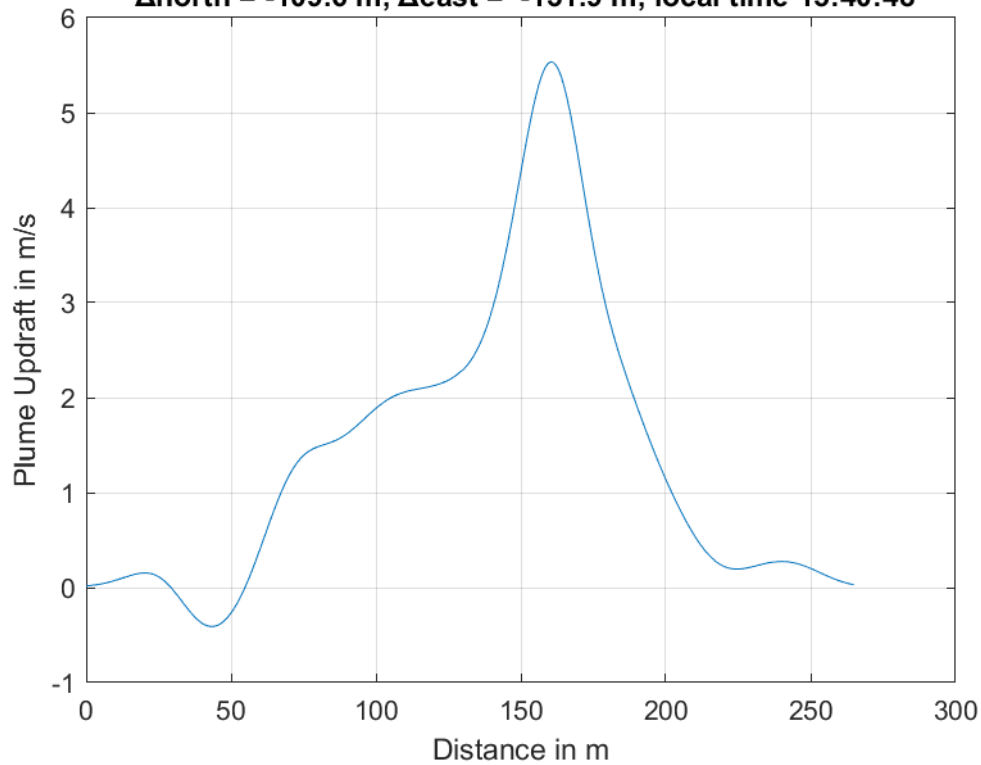


**Plume #21 at 258.9 m MSL, fly-through speed 45.0 m/s,
 $\Delta_{\text{north}} = -103.2$ m, $\Delta_{\text{east}} = -160.1$ m, local time 15:40:01**

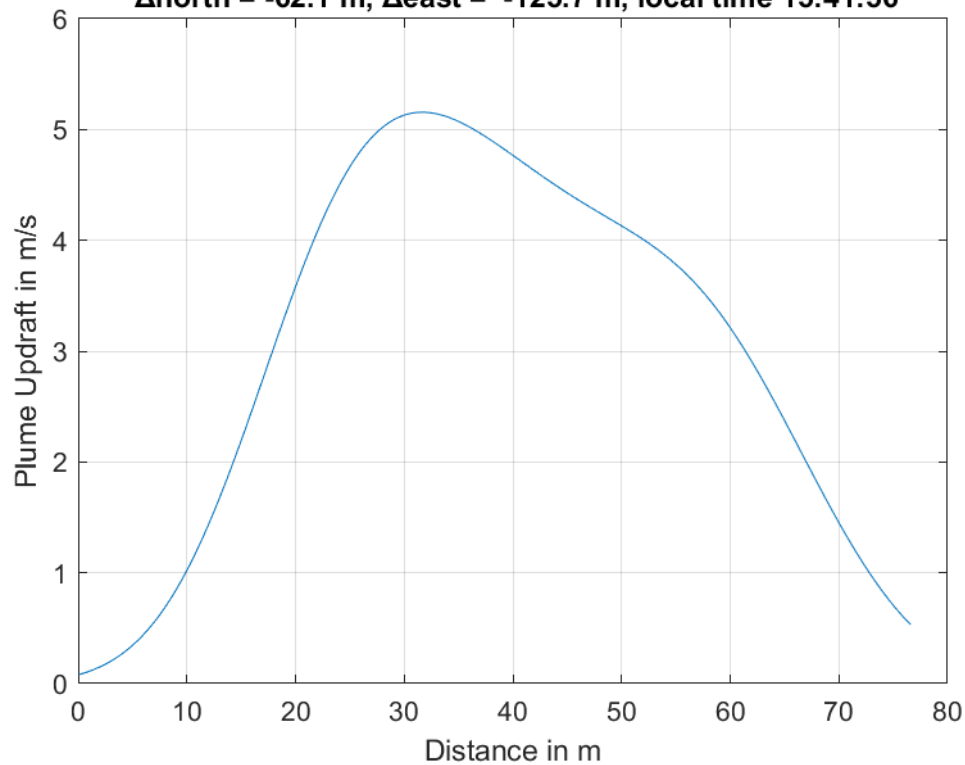




**Plume #22 at 232.0 m MSL, fly-through speed 53.0 m/s,
 $\Delta_{\text{north}} = -109.6$ m, $\Delta_{\text{east}} = -131.9$ m, local time 15:40:48**

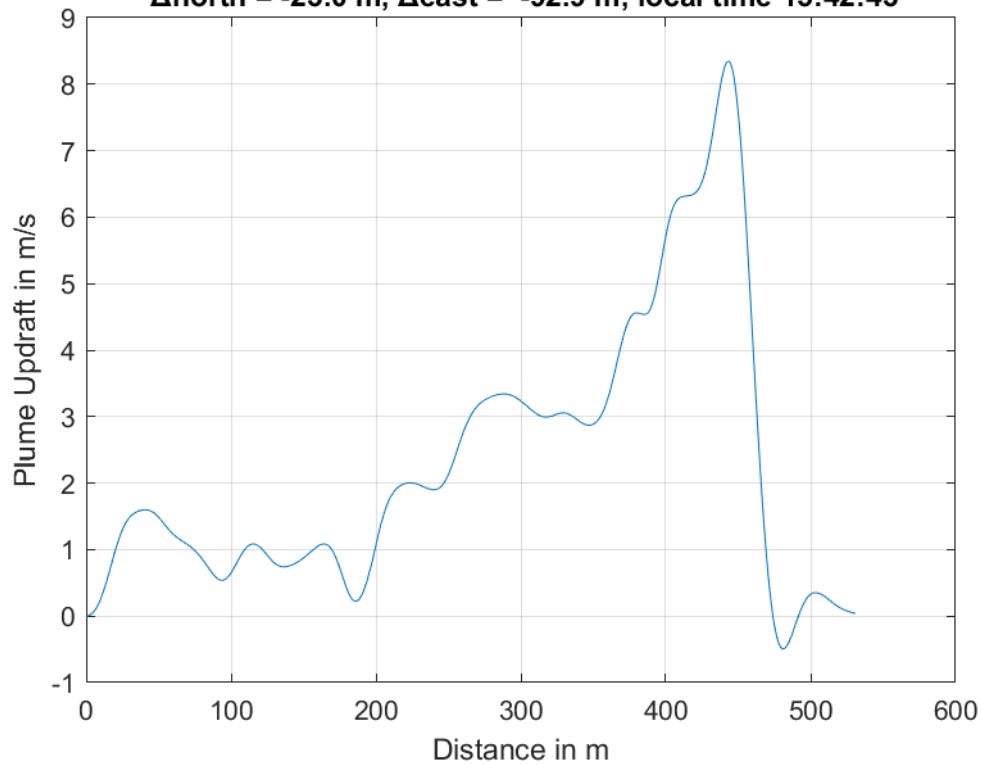


**Plume #23 at 197.3 m MSL, fly-through speed 48.0 m/s,
 $\Delta_{\text{north}} = -62.1$ m, $\Delta_{\text{east}} = -125.7$ m, local time 15:41:56**

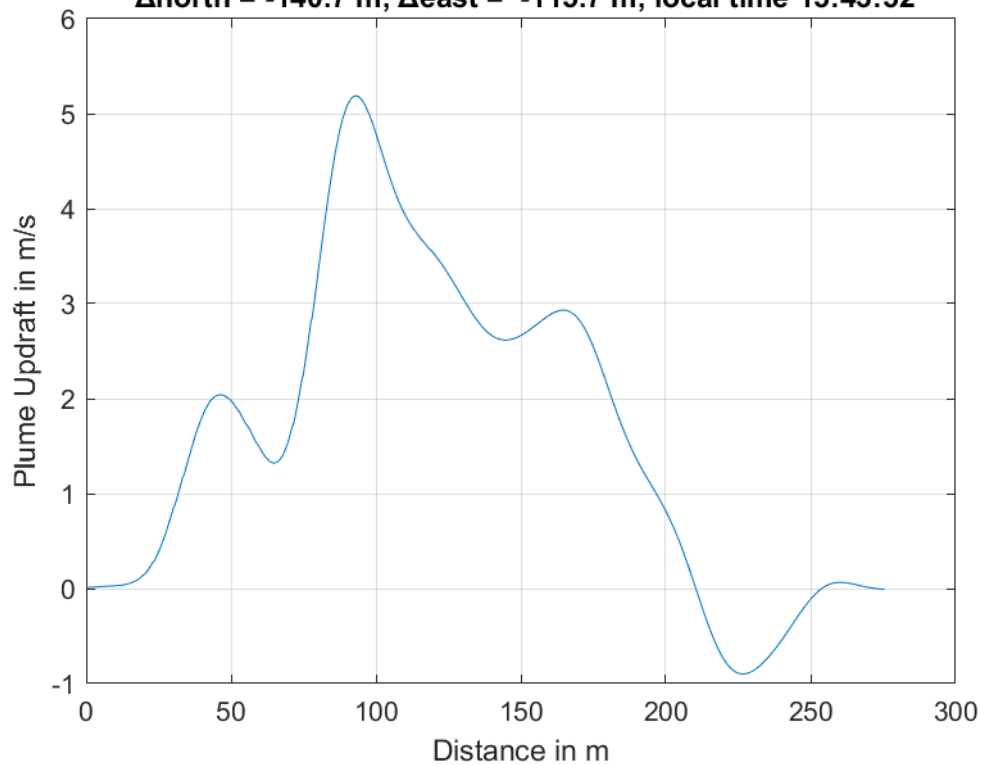




**Plume #24 at 210.1 m MSL, fly-through speed 47.0 m/s,
 $\Delta_{\text{north}} = -23.0$ m, $\Delta_{\text{east}} = -92.9$ m, local time 15:42:43**

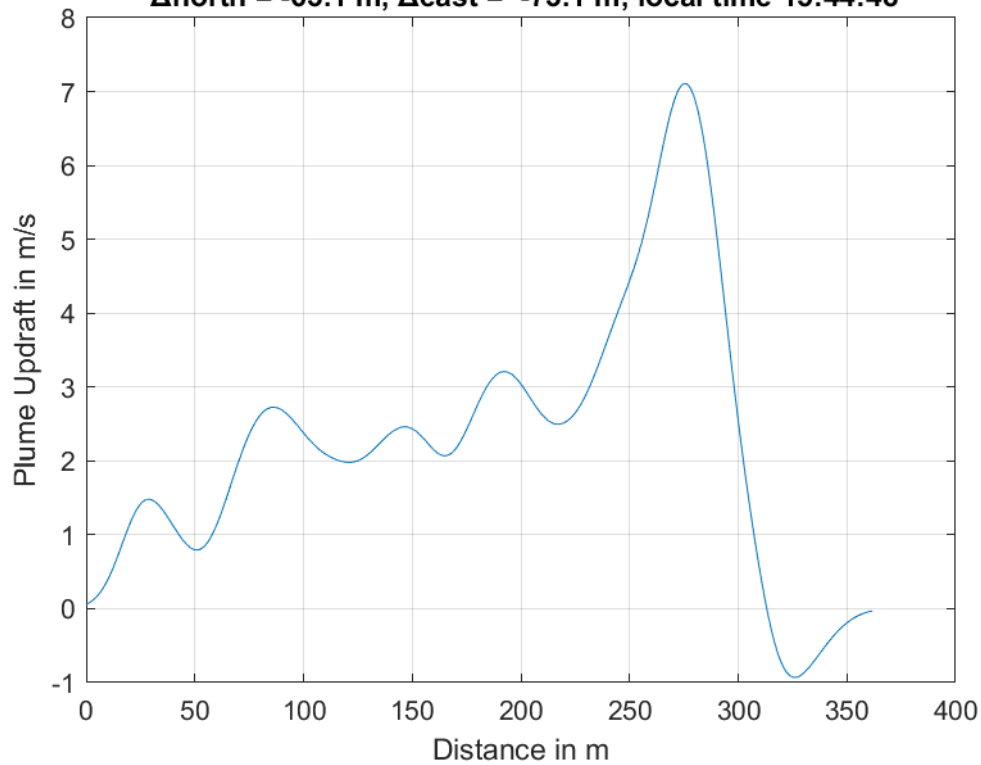


**Plume #25 at 240.1 m MSL, fly-through speed 52.0 m/s,
 $\Delta_{\text{north}} = -140.7$ m, $\Delta_{\text{east}} = -115.7$ m, local time 15:43:52**

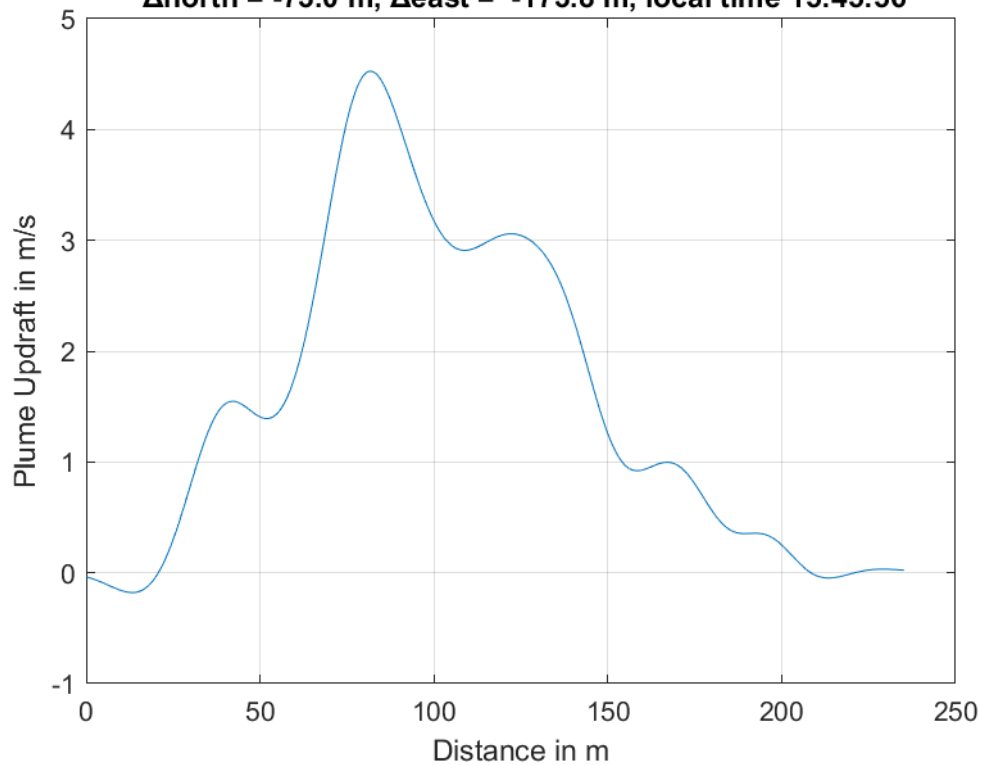




**Plume #26 at 242.4 m MSL, fly-through speed 51.0 m/s,
 $\Delta_{\text{north}} = -63.1$ m, $\Delta_{\text{east}} = -73.1$ m, local time 15:44:48**

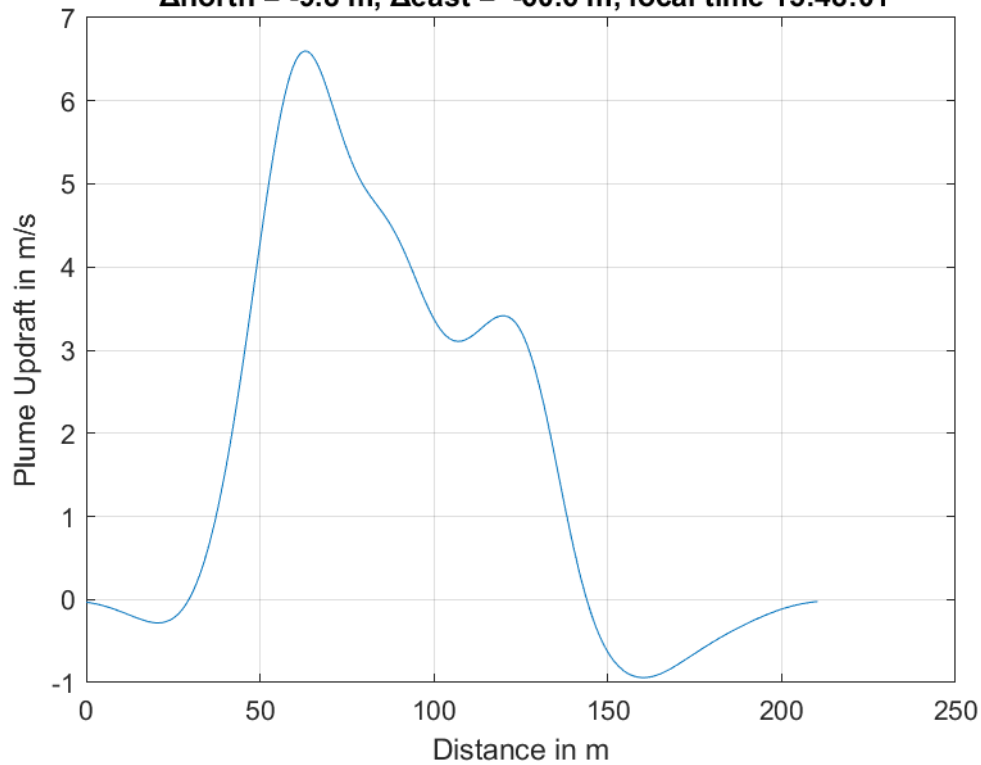


**Plume #27 at 249.4 m MSL, fly-through speed 49.0 m/s,
 $\Delta_{\text{north}} = -73.0$ m, $\Delta_{\text{east}} = -173.8$ m, local time 15:45:56**

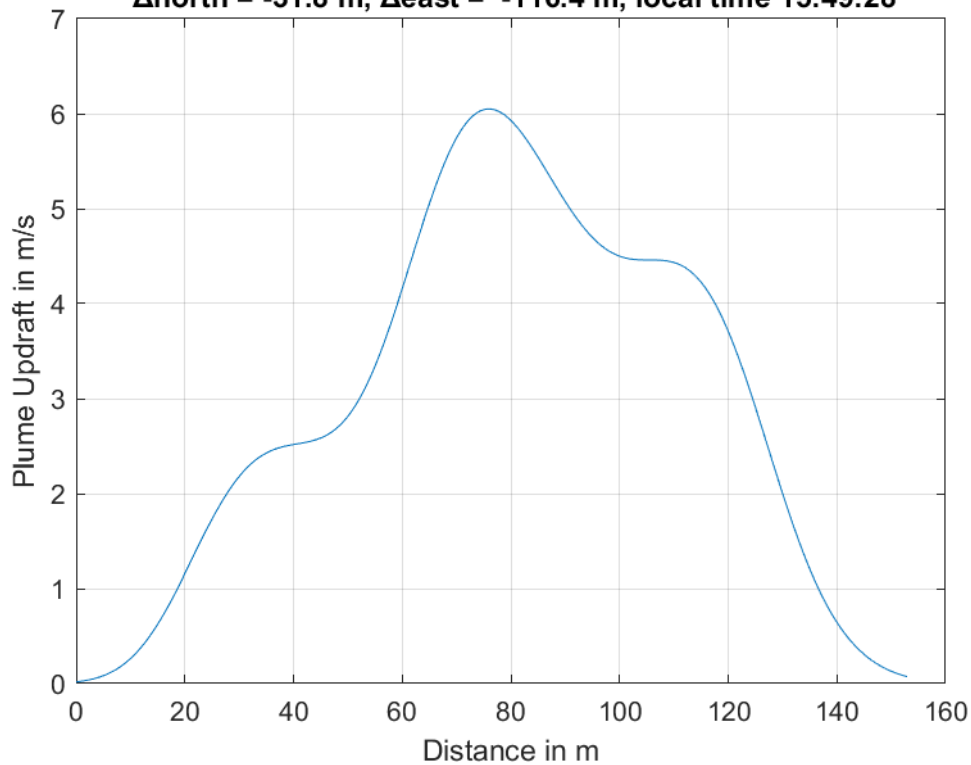




**Plume #28 at 219.4 m MSL, fly-through speed 54.0 m/s,
 $\Delta_{\text{north}} = -9.8$ m, $\Delta_{\text{east}} = -60.6$ m, local time 15:48:01**

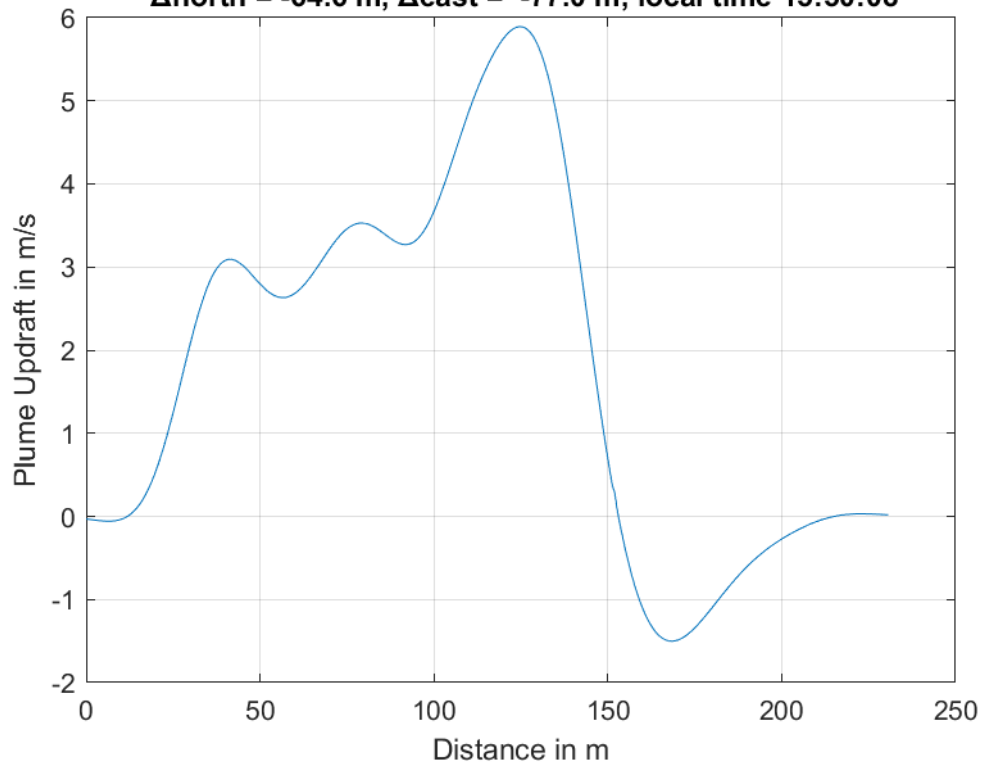


**Plume #29 at 214.1 m MSL, fly-through speed 51.0 m/s,
 $\Delta_{\text{north}} = -31.8$ m, $\Delta_{\text{east}} = -116.4$ m, local time 15:49:28**

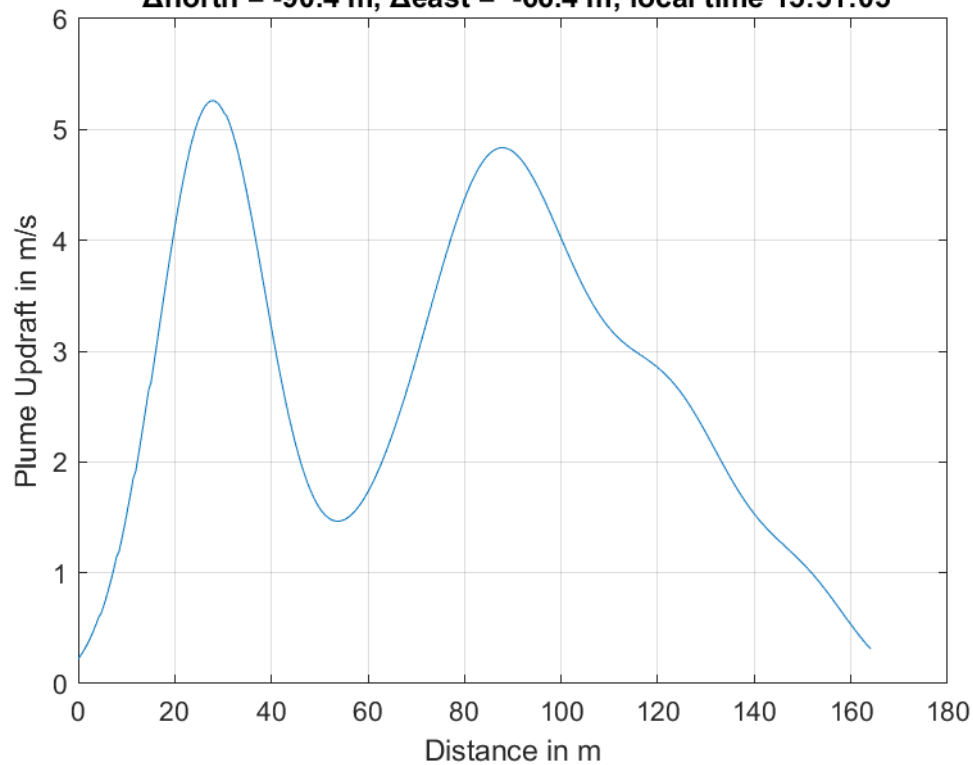




**Plume #30 at 203.0 m MSL, fly-through speed 55.0 m/s,
 $\Delta_{\text{north}} = -64.6$ m, $\Delta_{\text{east}} = -77.0$ m, local time 15:50:08**

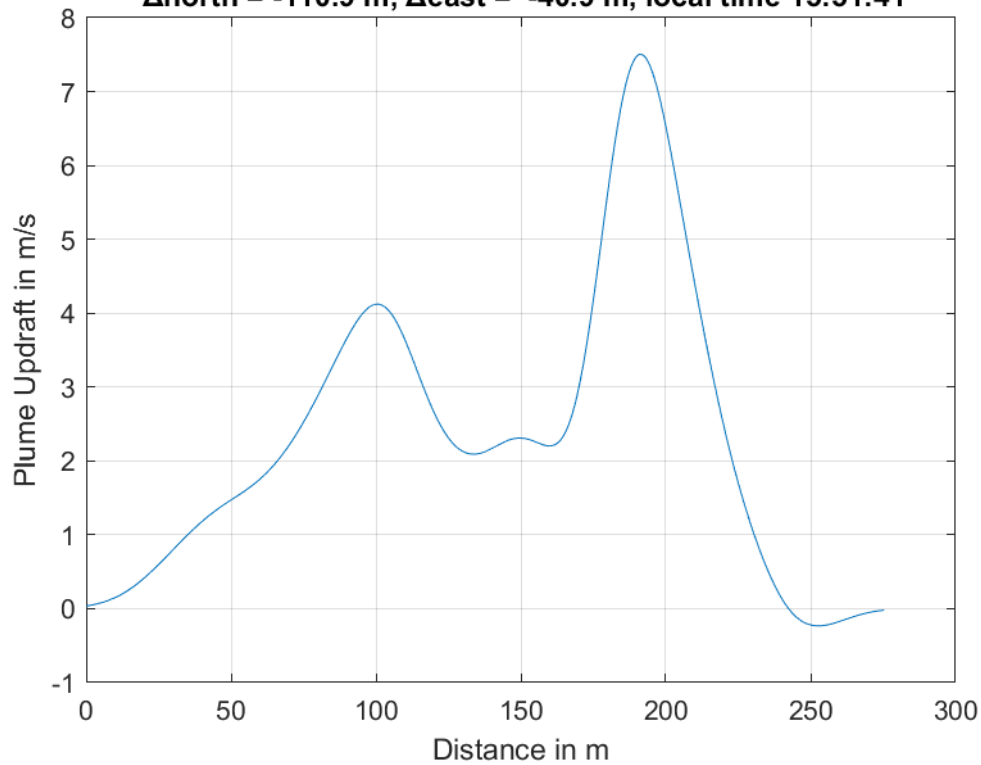


**Plume #31 at 206.8 m MSL, fly-through speed 53.0 m/s,
 $\Delta_{\text{north}} = -90.4$ m, $\Delta_{\text{east}} = -66.4$ m, local time 15:51:05**

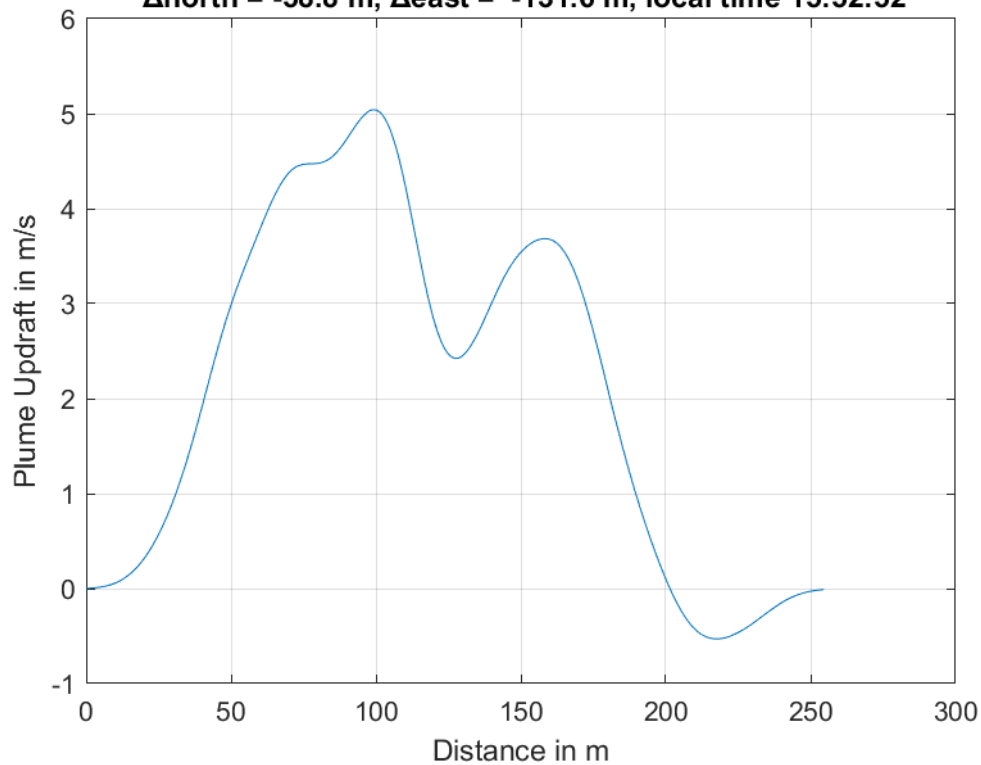




**Plume #32 at 213.7 m MSL, fly-through speed 52.0 m/s,
 Δ north = -110.9 m, Δ east = -40.9 m, local time 15:51:41**

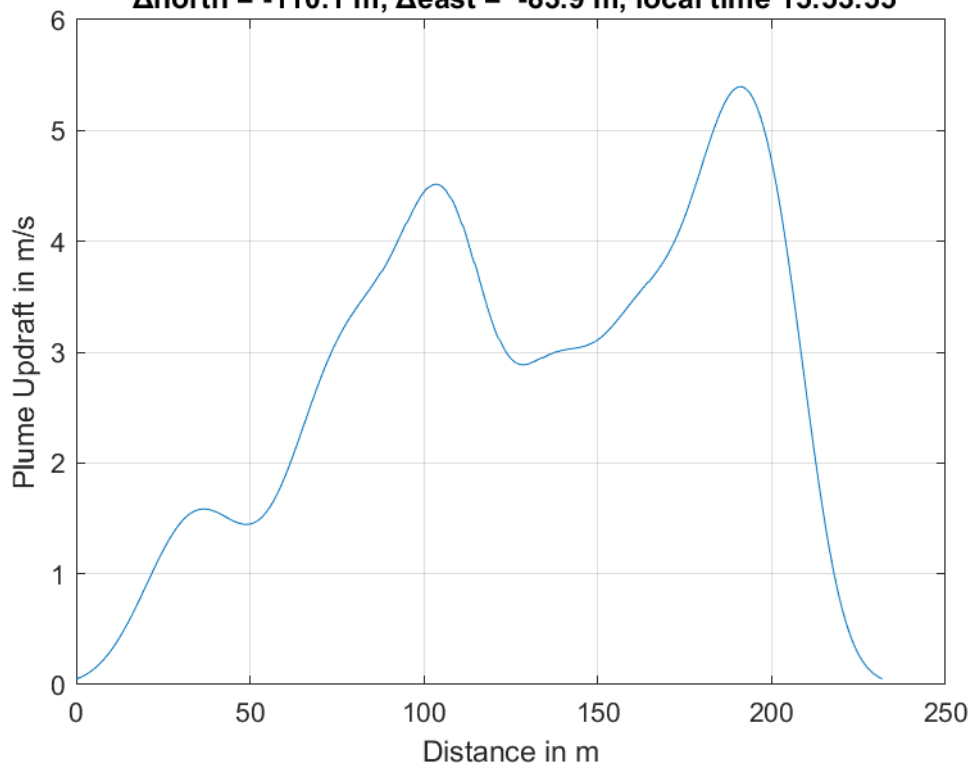


**Plume #33 at 212.5 m MSL, fly-through speed 52.0 m/s,
 Δ north = -58.8 m, Δ east = -131.6 m, local time 15:52:52**

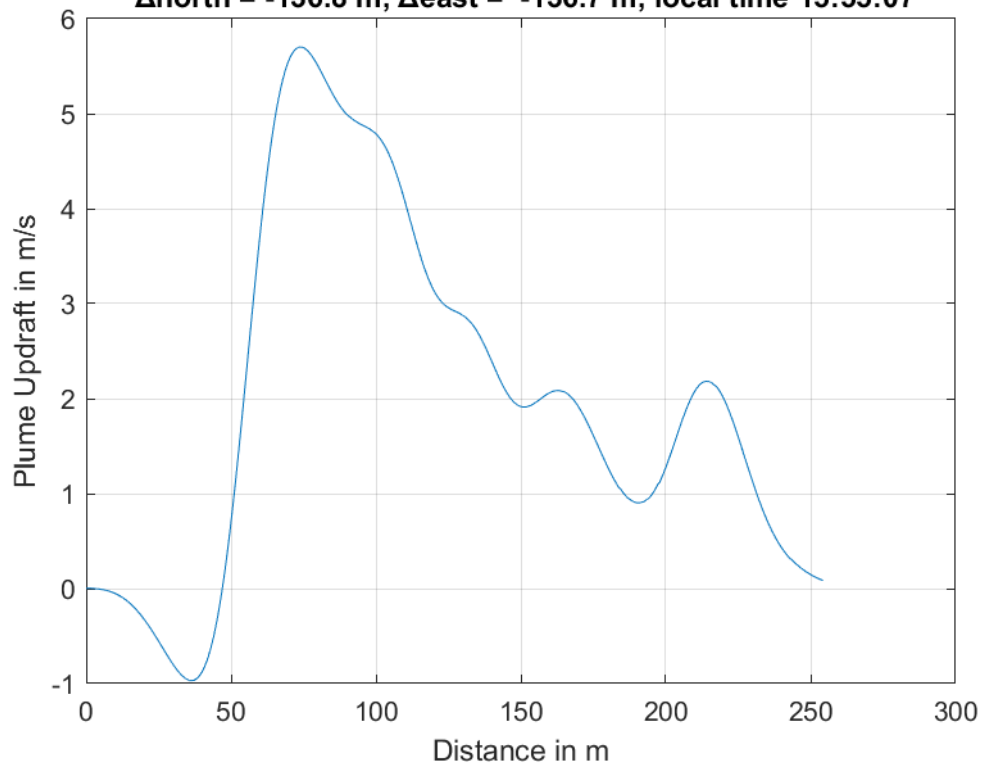




**Plume #34 at 287.5 m MSL, fly-through speed 54.0 m/s,
 $\Delta_{\text{north}} = -110.1$ m, $\Delta_{\text{east}} = -83.9$ m, local time 15:53:55**

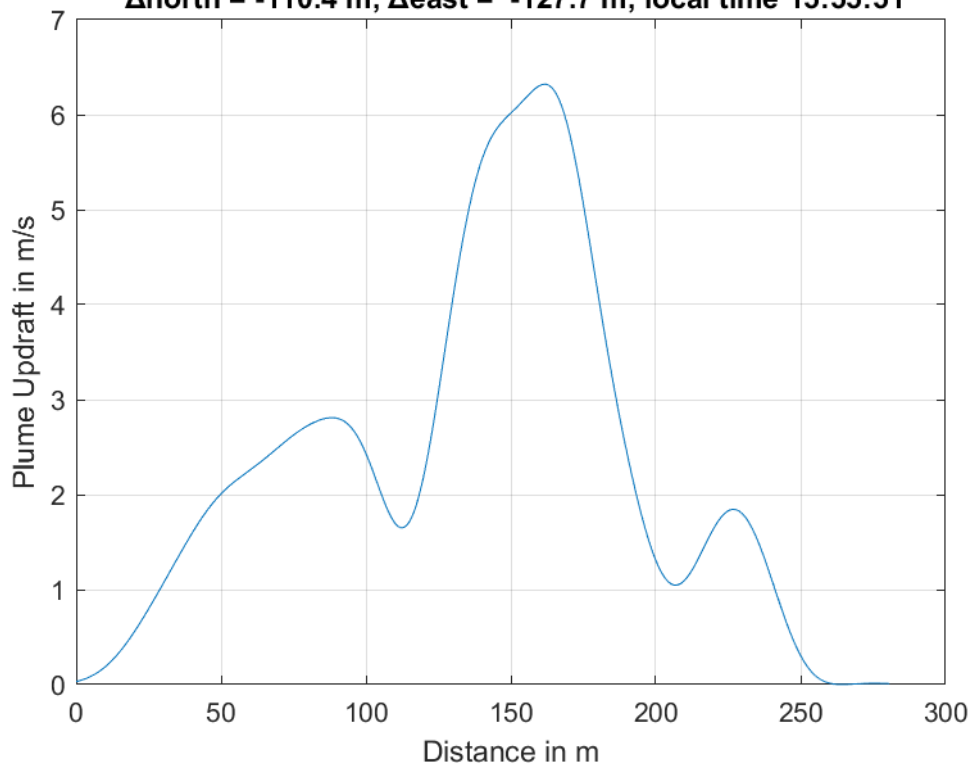


**Plume #35 at 279.7 m MSL, fly-through speed 53.0 m/s,
 $\Delta_{\text{north}} = -136.8$ m, $\Delta_{\text{east}} = -136.7$ m, local time 15:55:07**

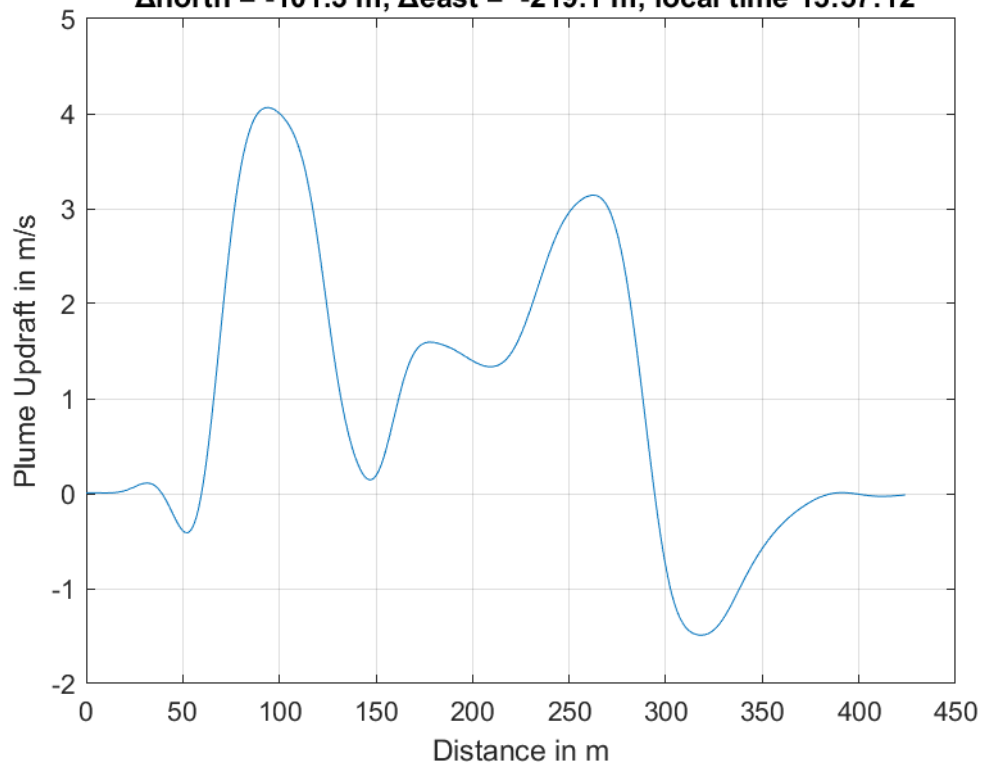




**Plume #36 at 265.4 m MSL, fly-through speed 53.0 m/s,
 $\Delta_{\text{north}} = -110.4$ m, $\Delta_{\text{east}} = -127.7$ m, local time 15:55:51**

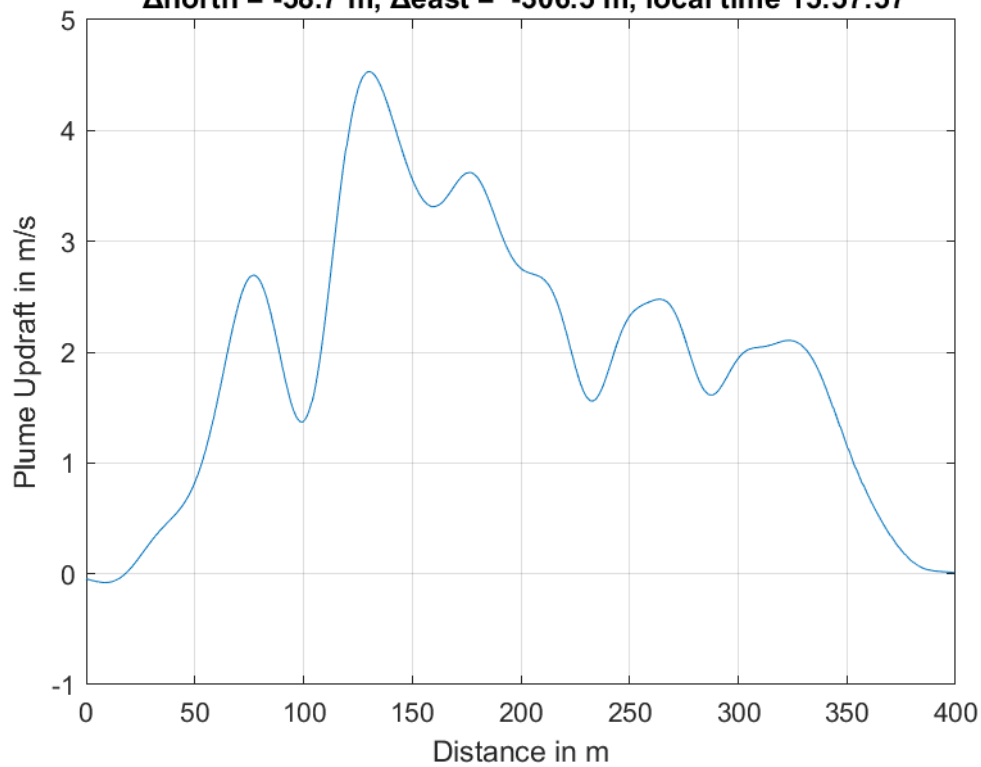


**Plume #37 at 310.1 m MSL, fly-through speed 53.0 m/s,
 $\Delta_{\text{north}} = -101.3$ m, $\Delta_{\text{east}} = -219.1$ m, local time 15:57:12**

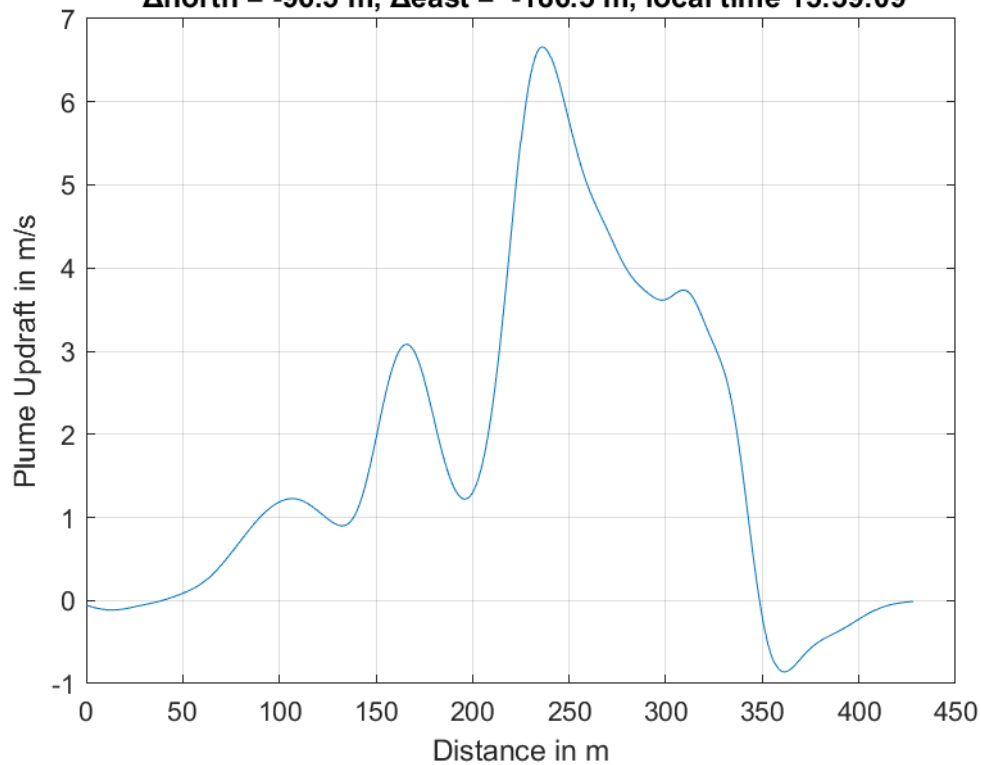




**Plume #38 at 310.1 m MSL, fly-through speed 54.0 m/s,
 $\Delta_{\text{north}} = -58.7$ m, $\Delta_{\text{east}} = -306.5$ m, local time 15:57:57**

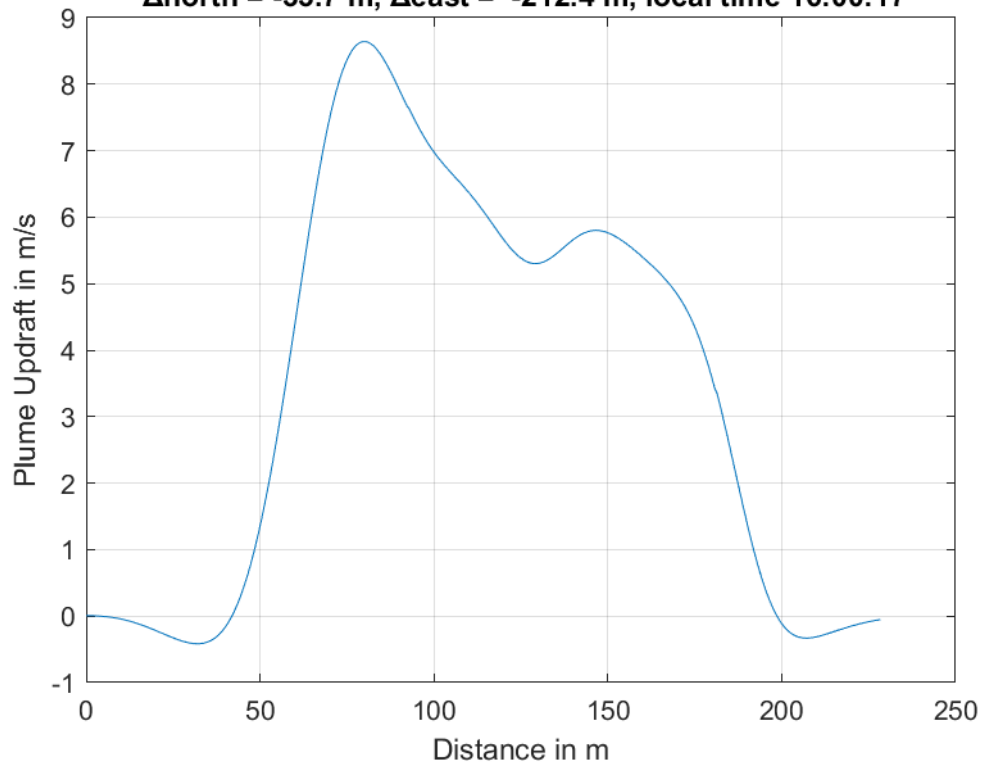


**Plume #39 at 292.0 m MSL, fly-through speed 51.0 m/s,
 $\Delta_{\text{north}} = -96.5$ m, $\Delta_{\text{east}} = -186.5$ m, local time 15:59:09**

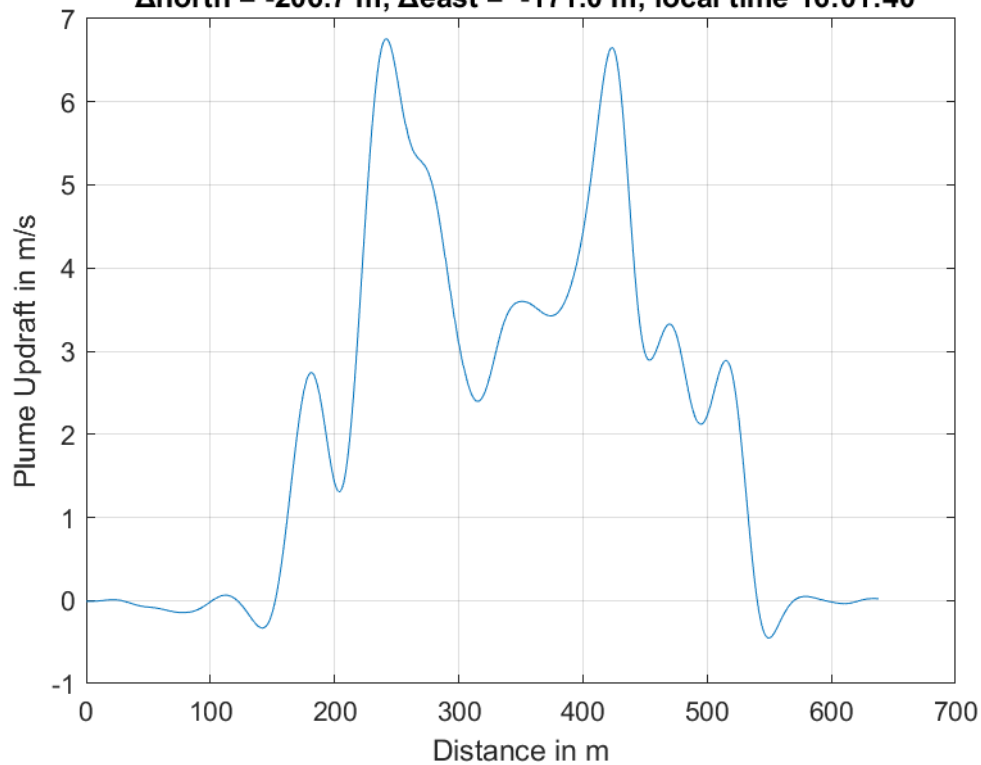




**Plume #40 at 298.9 m MSL, fly-through speed 52.0 m/s,
 $\Delta_{\text{north}} = -33.7$ m, $\Delta_{\text{east}} = -212.4$ m, local time 16:00:17**

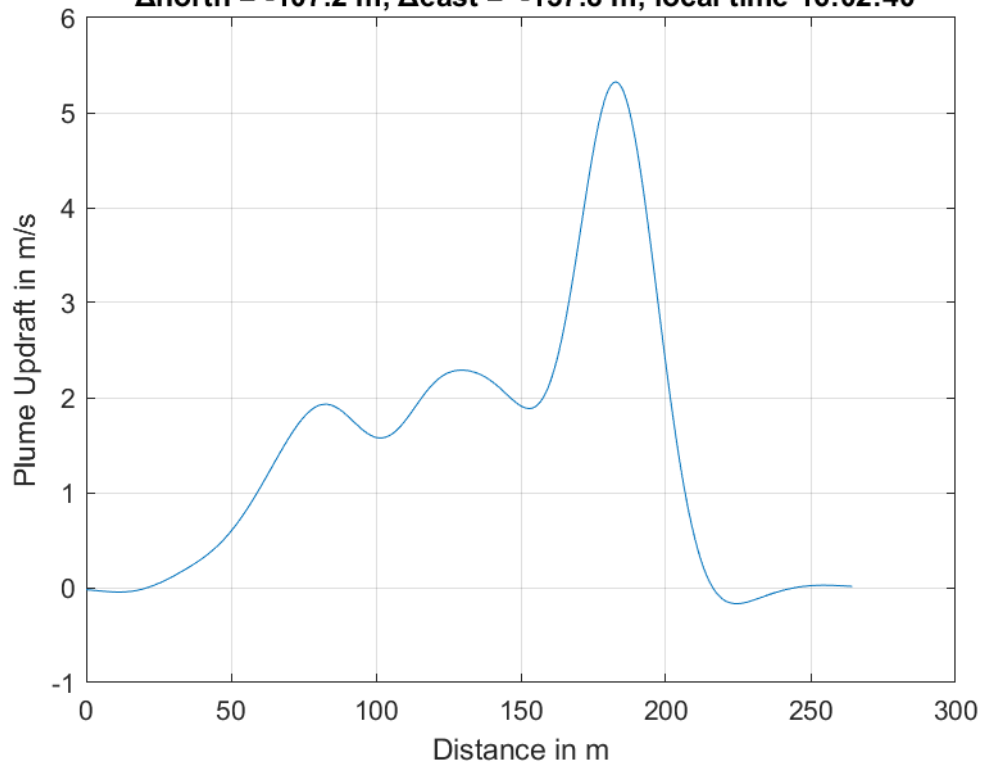


**Plume #41 at 348.7 m MSL, fly-through speed 57.0 m/s,
 $\Delta_{\text{north}} = -206.7$ m, $\Delta_{\text{east}} = -171.0$ m, local time 16:01:40**

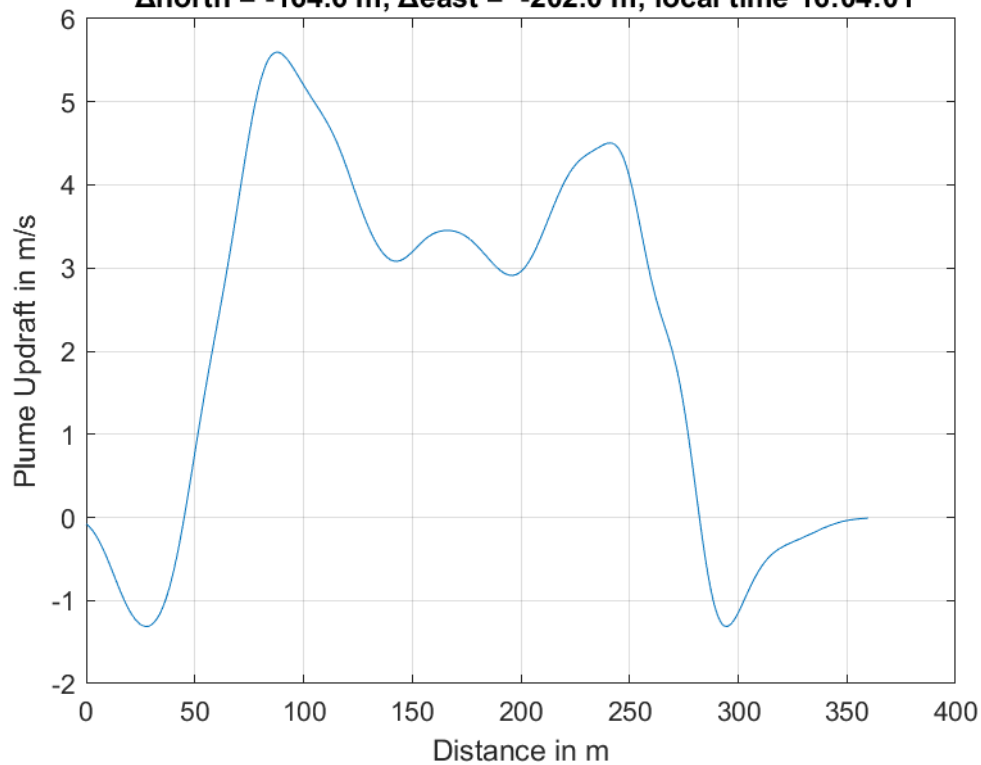




**Plume #42 at 340.3 m MSL, fly-through speed 54.0 m/s,
 $\Delta_{\text{north}} = -107.2$ m, $\Delta_{\text{east}} = -137.8$ m, local time 16:02:40**

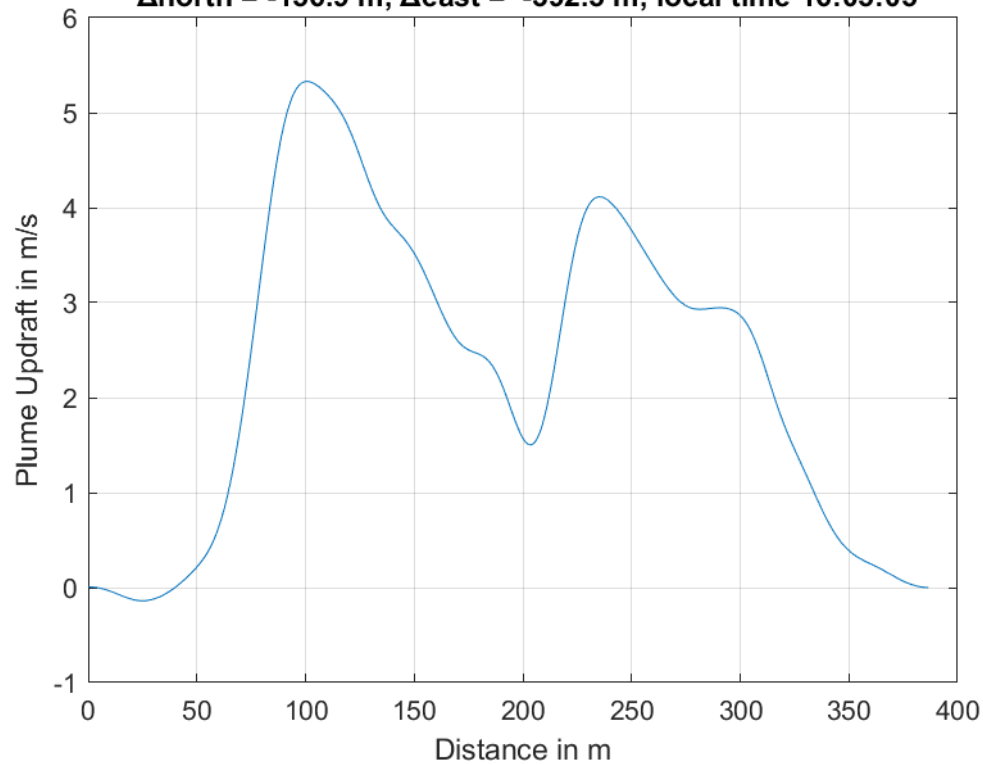


**Plume #43 at 346.7 m MSL, fly-through speed 50.0 m/s,
 $\Delta_{\text{north}} = -164.6$ m, $\Delta_{\text{east}} = -202.0$ m, local time 16:04:01**



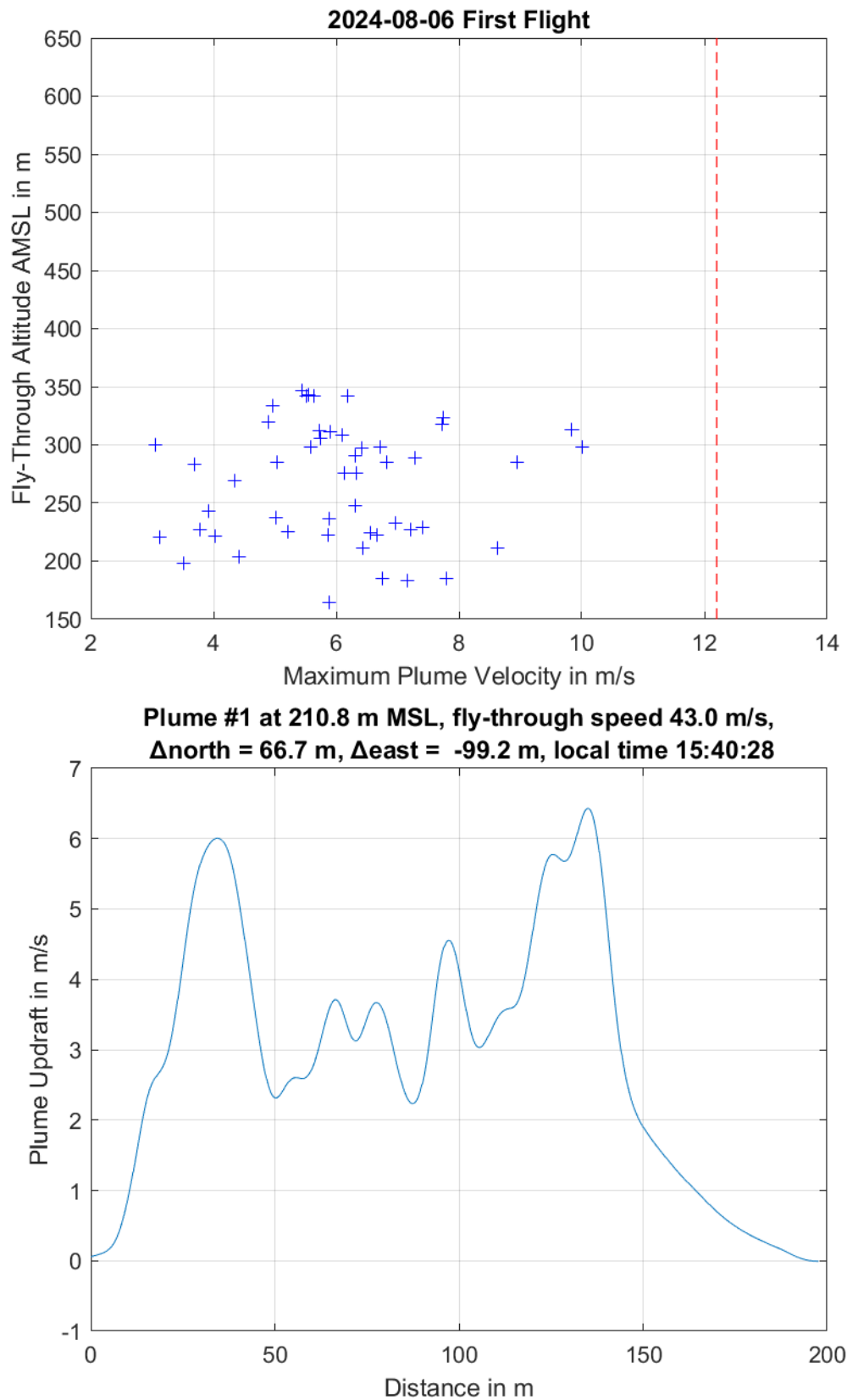


**Plume #44 at 368.8 m MSL, fly-through speed 53.0 m/s,
 $\Delta_{\text{north}} = -156.9$ m, $\Delta_{\text{east}} = -392.5$ m, local time 16:05:05**



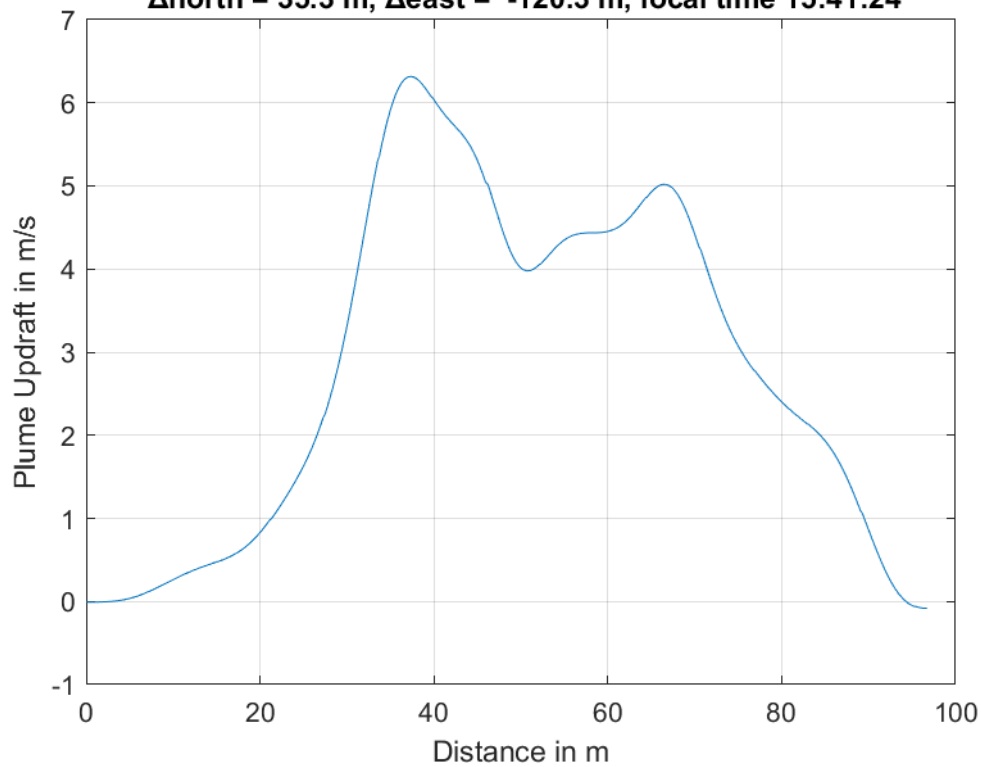


7 Measured Plumes: 2024-08-06 Flight

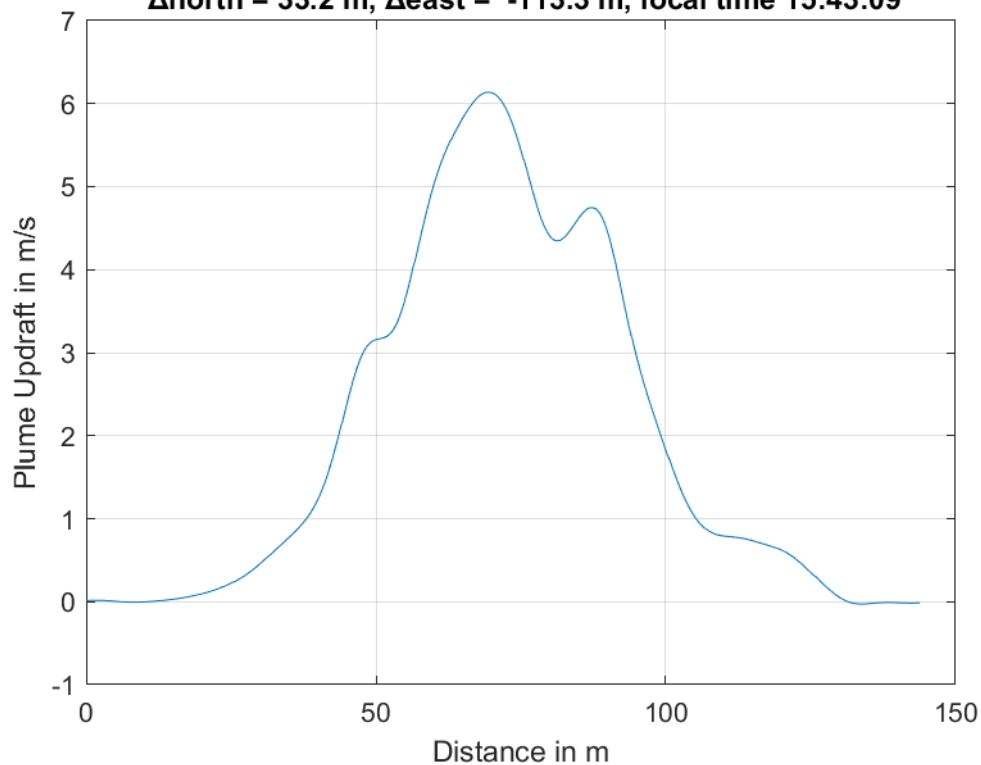




**Plume #2 at 247.4 m MSL, fly-through speed 44.0 m/s,
 $\Delta_{\text{north}} = 35.3$ m, $\Delta_{\text{east}} = -120.3$ m, local time 15:41:24**

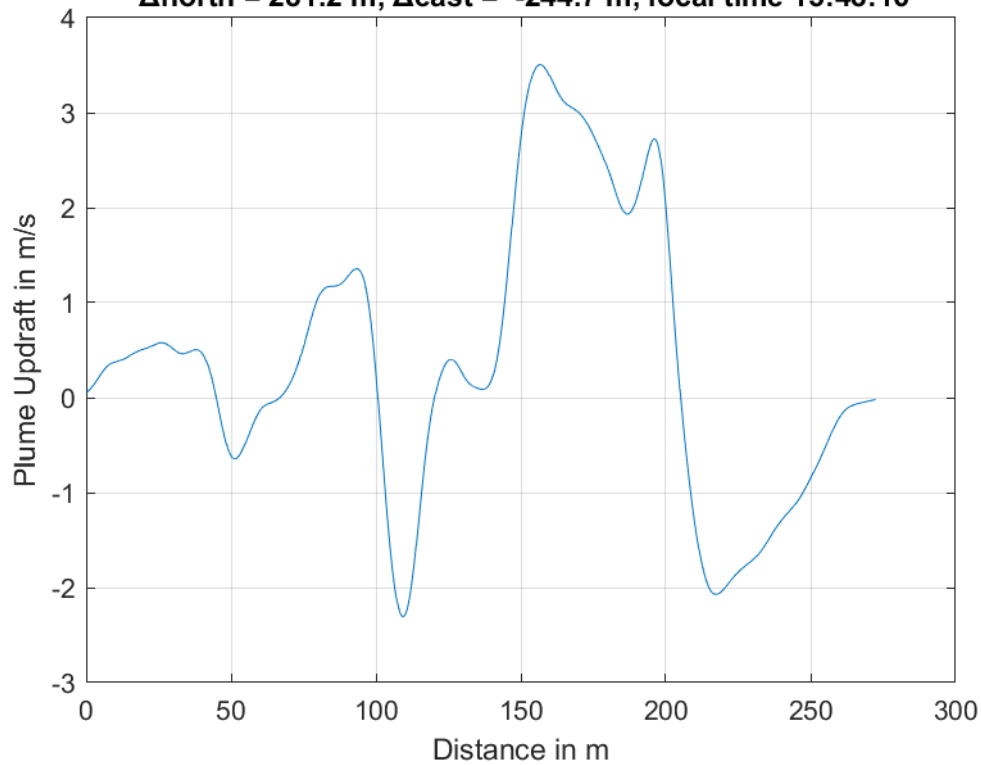


**Plume #3 at 275.7 m MSL, fly-through speed 45.0 m/s,
 $\Delta_{\text{north}} = 33.2$ m, $\Delta_{\text{east}} = -113.3$ m, local time 15:43:09**

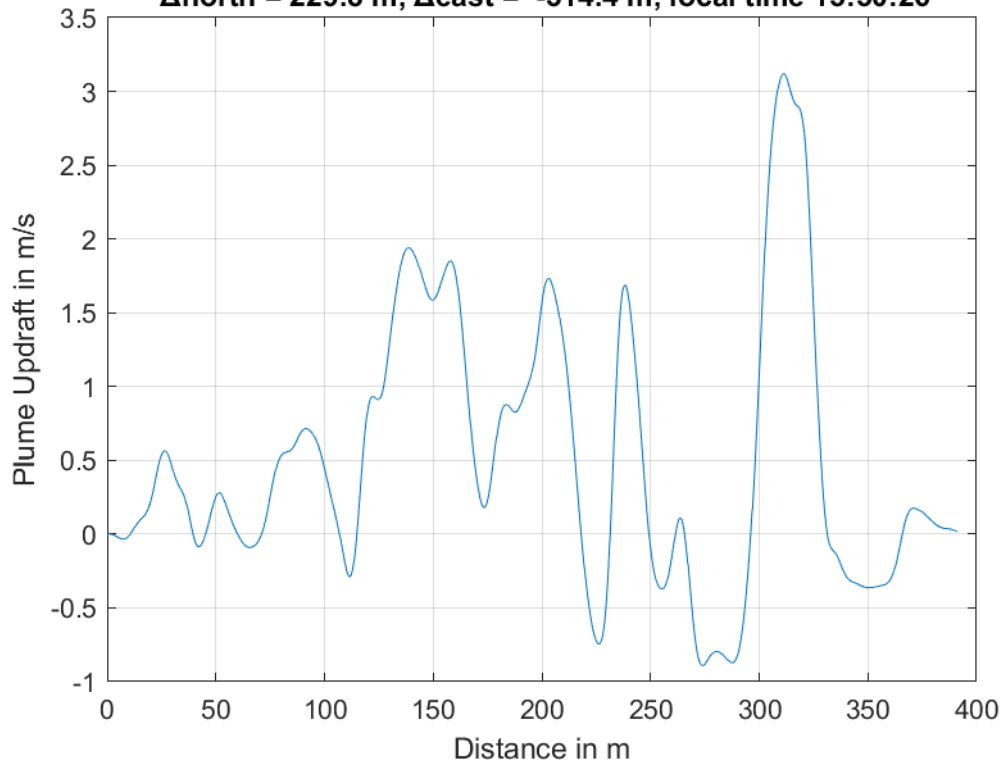




**Plume #4 at 198.2 m MSL, fly-through speed 47.0 m/s,
 Δ north = 281.2 m, Δ east = -244.7 m, local time 15:48:16**

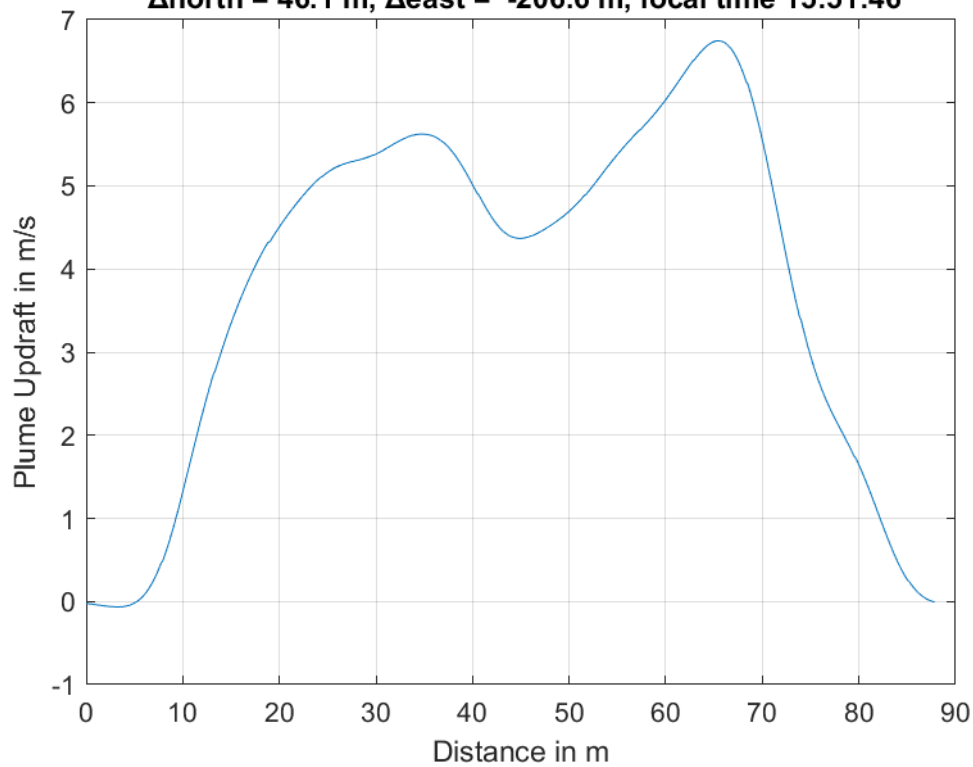


**Plume #5 at 221.0 m MSL, fly-through speed 43.0 m/s,
 Δ north = 229.8 m, Δ east = -314.4 m, local time 15:50:26**

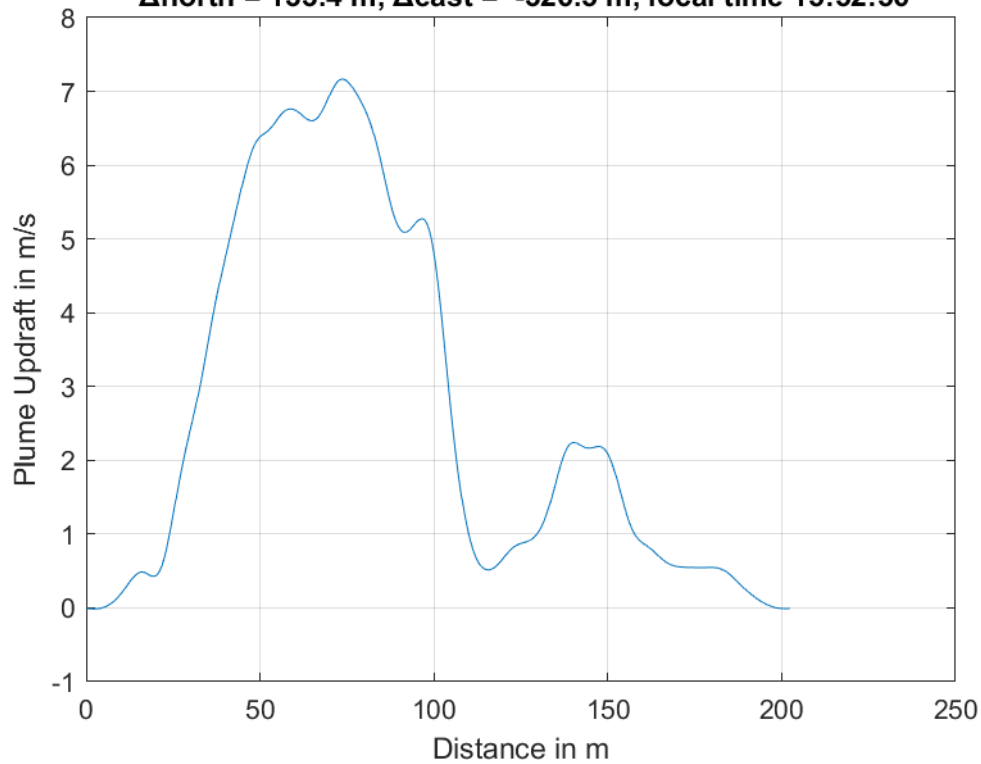




**Plume #6 at 185.2 m MSL, fly-through speed 40.0 m/s,
 $\Delta_{\text{north}} = 46.1$ m, $\Delta_{\text{east}} = -206.6$ m, local time 15:51:46**

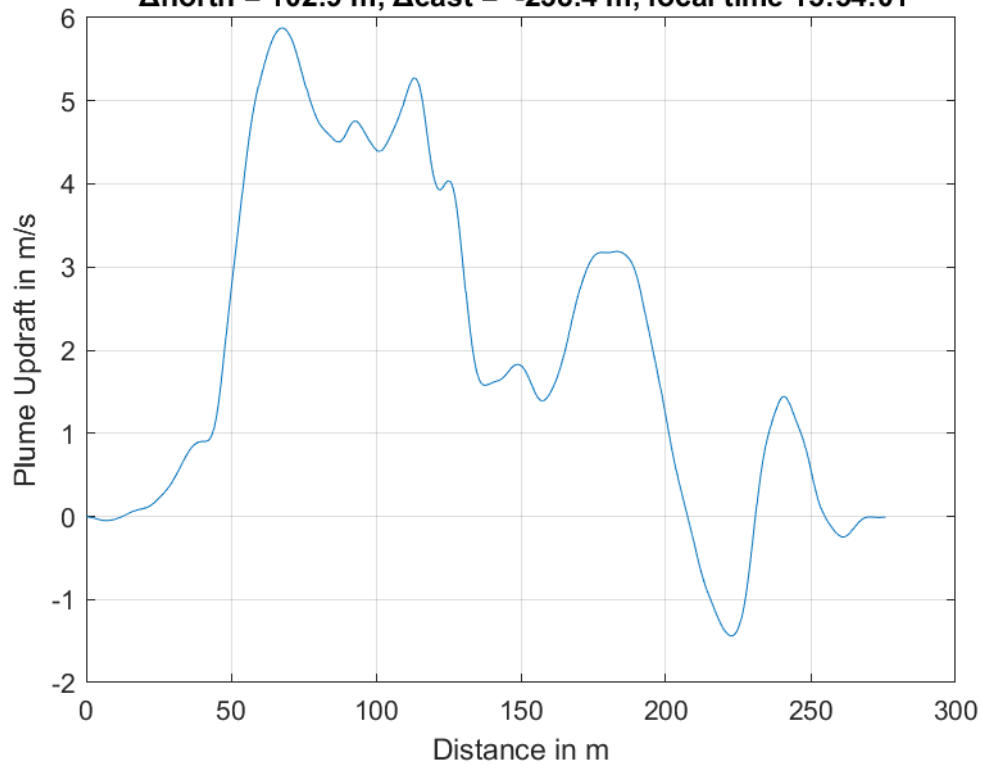


**Plume #7 at 182.9 m MSL, fly-through speed 45.0 m/s,
 $\Delta_{\text{north}} = 133.4$ m, $\Delta_{\text{east}} = -326.5$ m, local time 15:52:56**

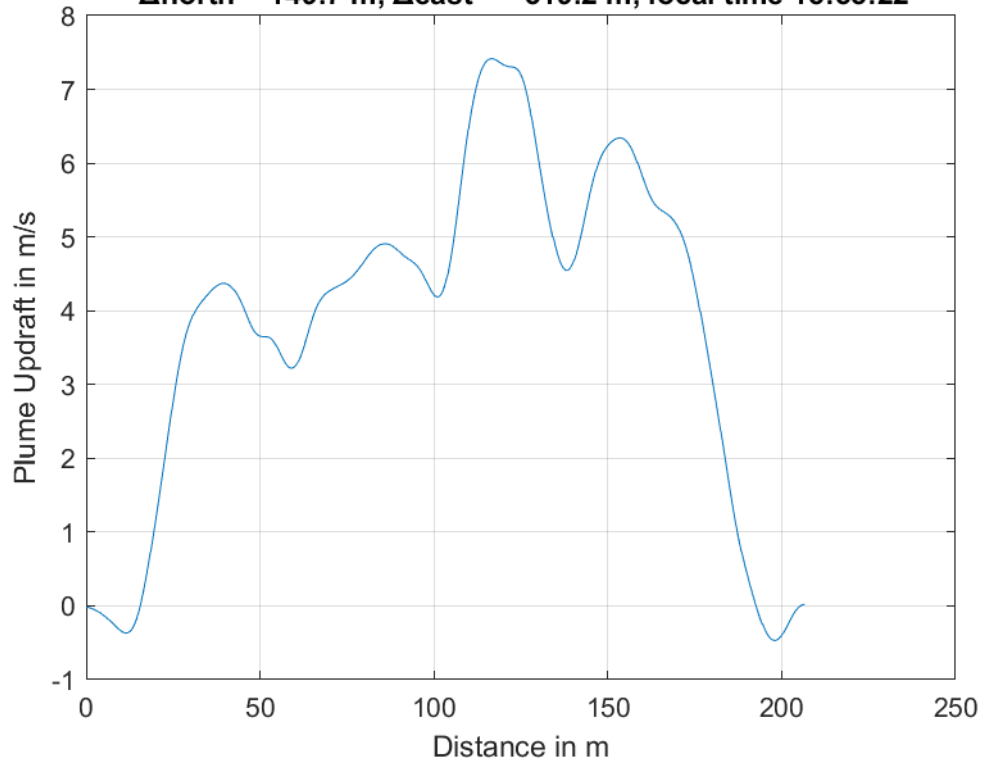




**Plume #8 at 164.6 m MSL, fly-through speed 40.0 m/s,
 Δ north = 102.9 m, Δ east = -238.4 m, local time 15:54:01**

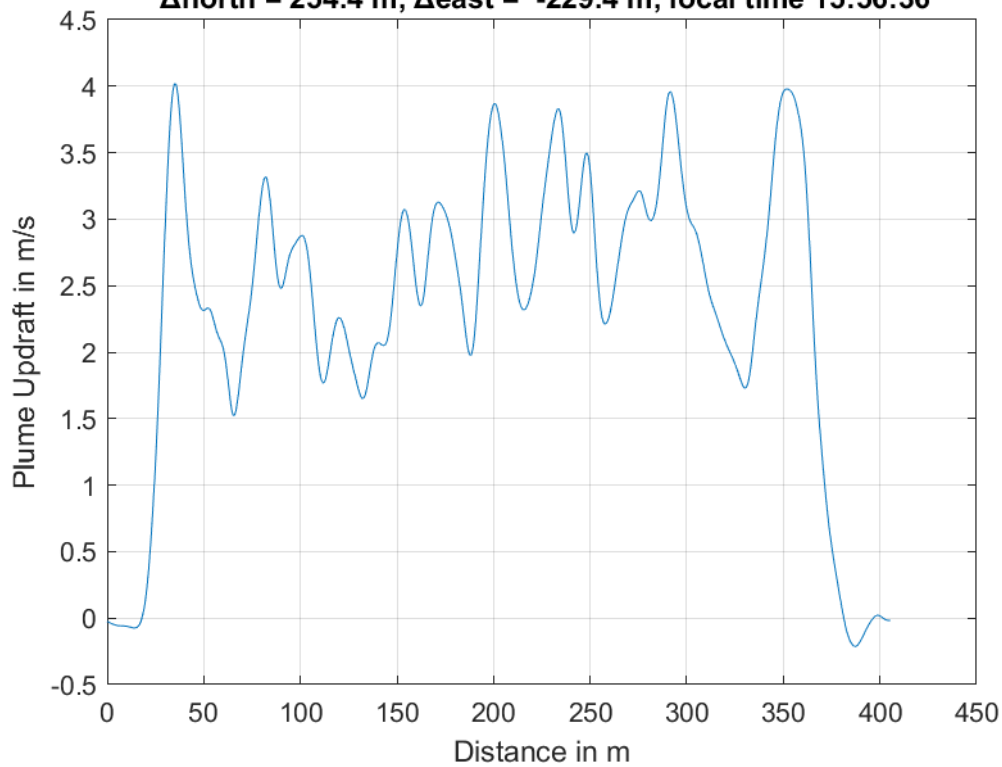


**Plume #9 at 228.8 m MSL, fly-through speed 44.0 m/s,
 Δ north = 149.7 m, Δ east = -319.2 m, local time 15:55:22**

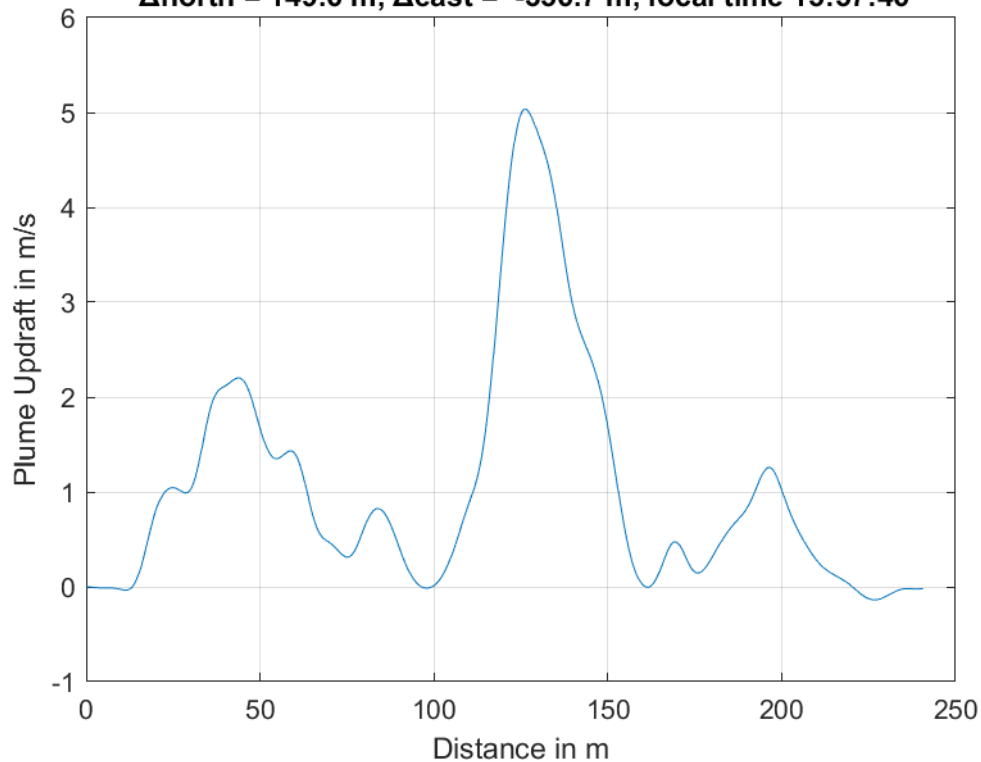




**Plume #10 at 221.4 m MSL, fly-through speed 39.0 m/s,
 $\Delta_{\text{north}} = 254.4$ m, $\Delta_{\text{east}} = -229.4$ m, local time 15:56:36**

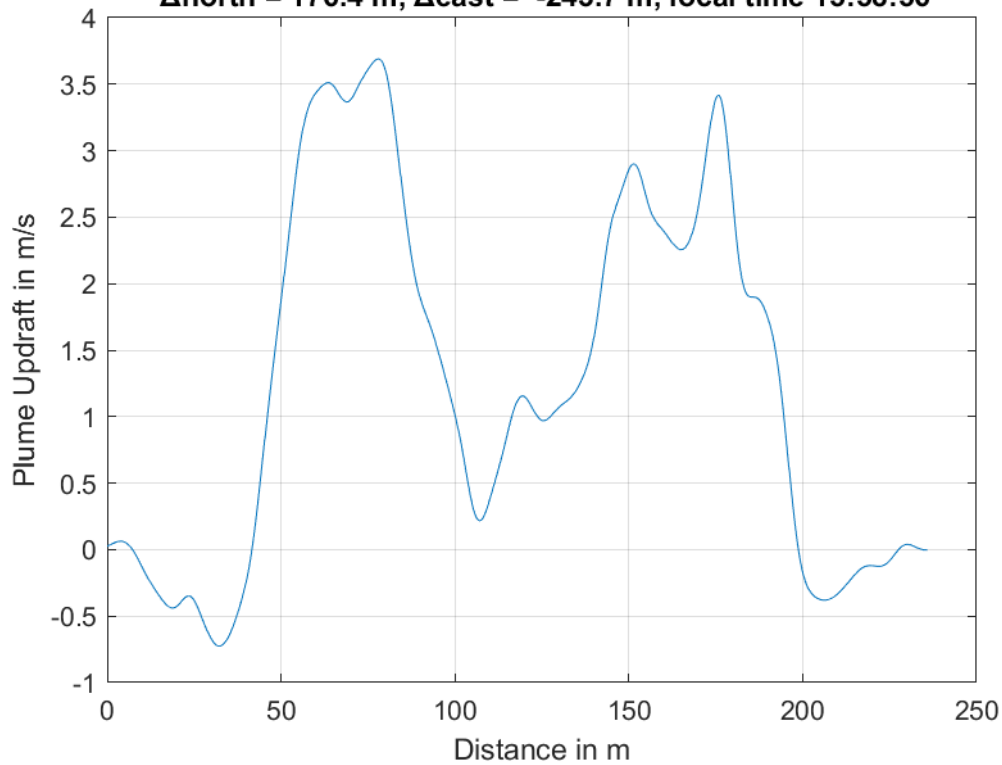


**Plume #11 at 285.4 m MSL, fly-through speed 43.0 m/s,
 $\Delta_{\text{north}} = 149.6$ m, $\Delta_{\text{east}} = -356.7$ m, local time 15:57:46**

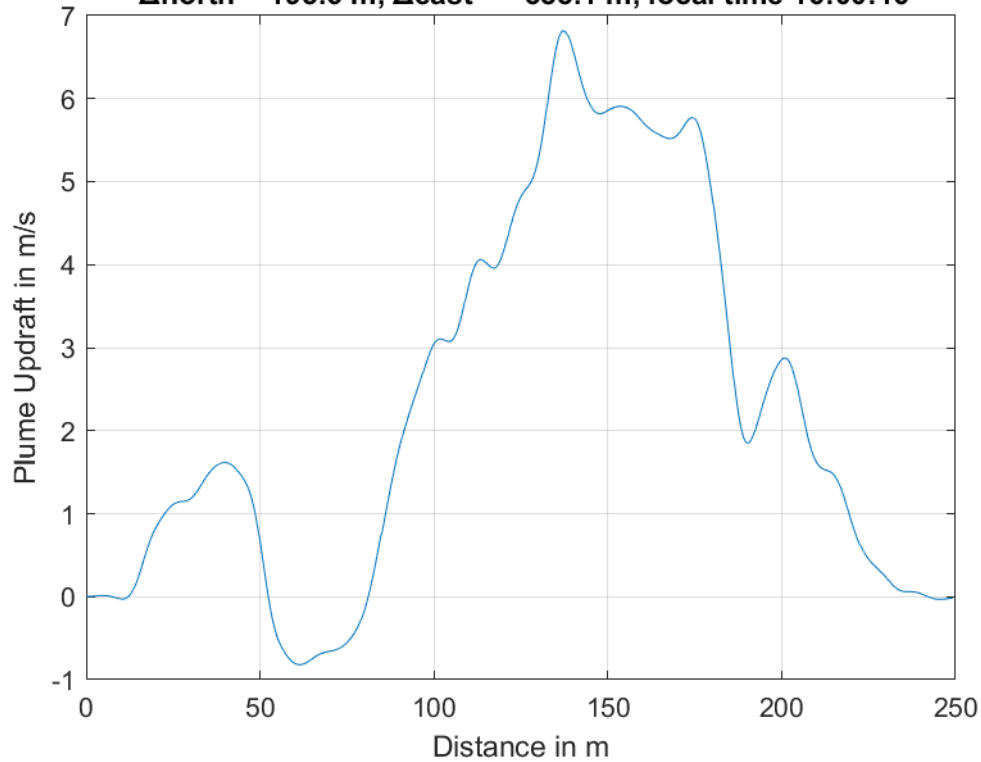




**Plume #12 at 283.0 m MSL, fly-through speed 40.0 m/s,
 $\Delta_{\text{north}} = 176.4$ m, $\Delta_{\text{east}} = -243.7$ m, local time 15:58:56**

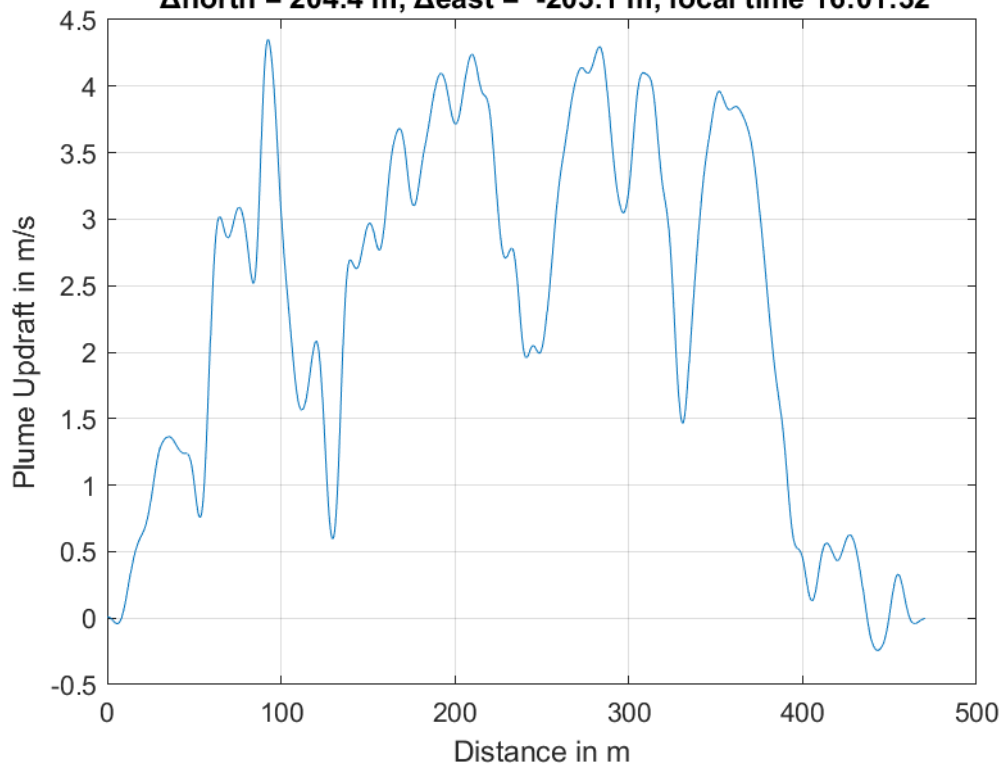


**Plume #13 at 285.3 m MSL, fly-through speed 43.0 m/s,
 $\Delta_{\text{north}} = 195.6$ m, $\Delta_{\text{east}} = -385.1$ m, local time 16:00:16**

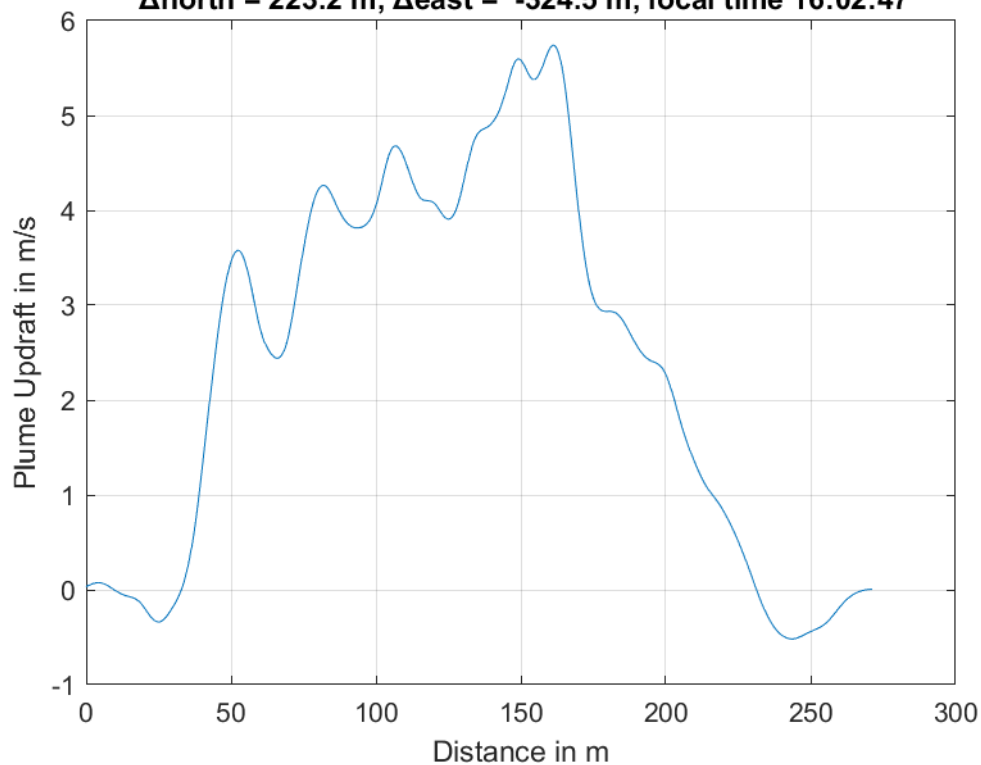




**Plume #14 at 269.2 m MSL, fly-through speed 42.0 m/s,
 $\Delta_{\text{north}} = 204.4$ m, $\Delta_{\text{east}} = -203.1$ m, local time 16:01:32**

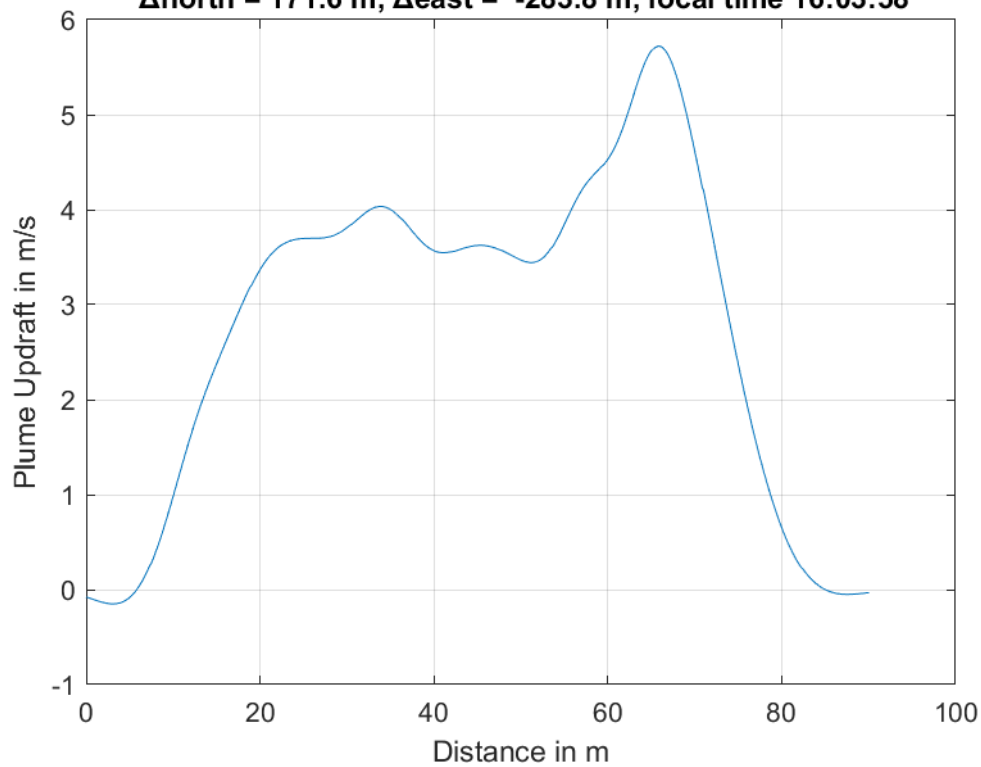


**Plume #15 at 305.6 m MSL, fly-through speed 46.0 m/s,
 $\Delta_{\text{north}} = 223.2$ m, $\Delta_{\text{east}} = -324.5$ m, local time 16:02:47**

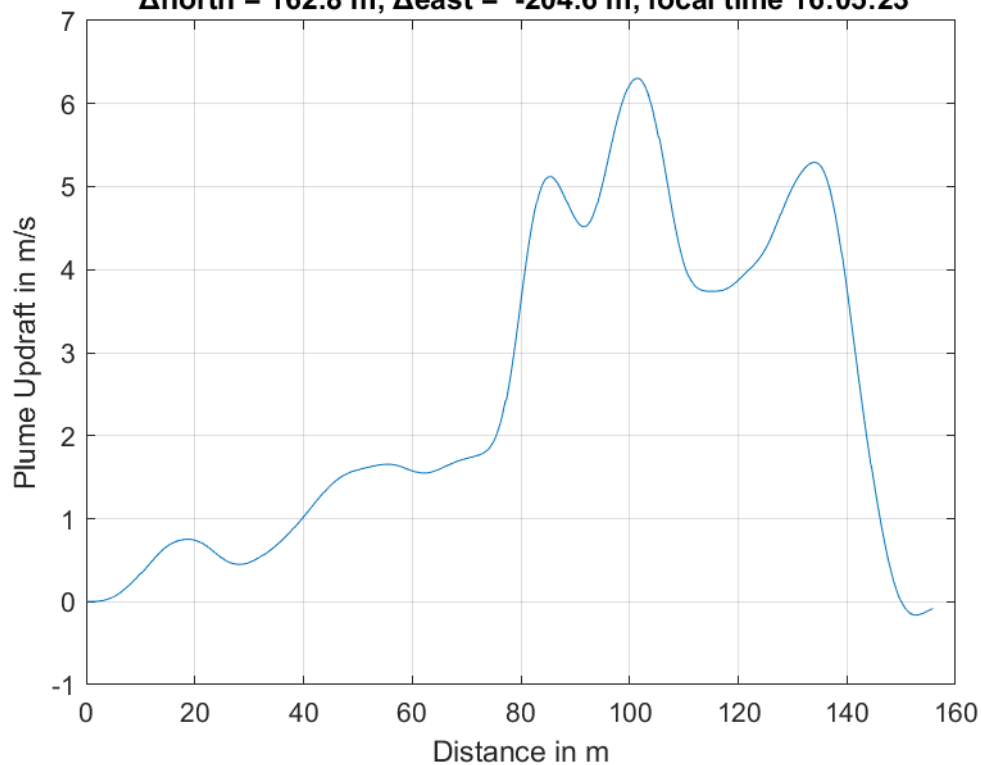




**Plume #16 at 312.0 m MSL, fly-through speed 41.0 m/s,
 $\Delta_{\text{north}} = 171.6$ m, $\Delta_{\text{east}} = -283.8$ m, local time 16:03:58**

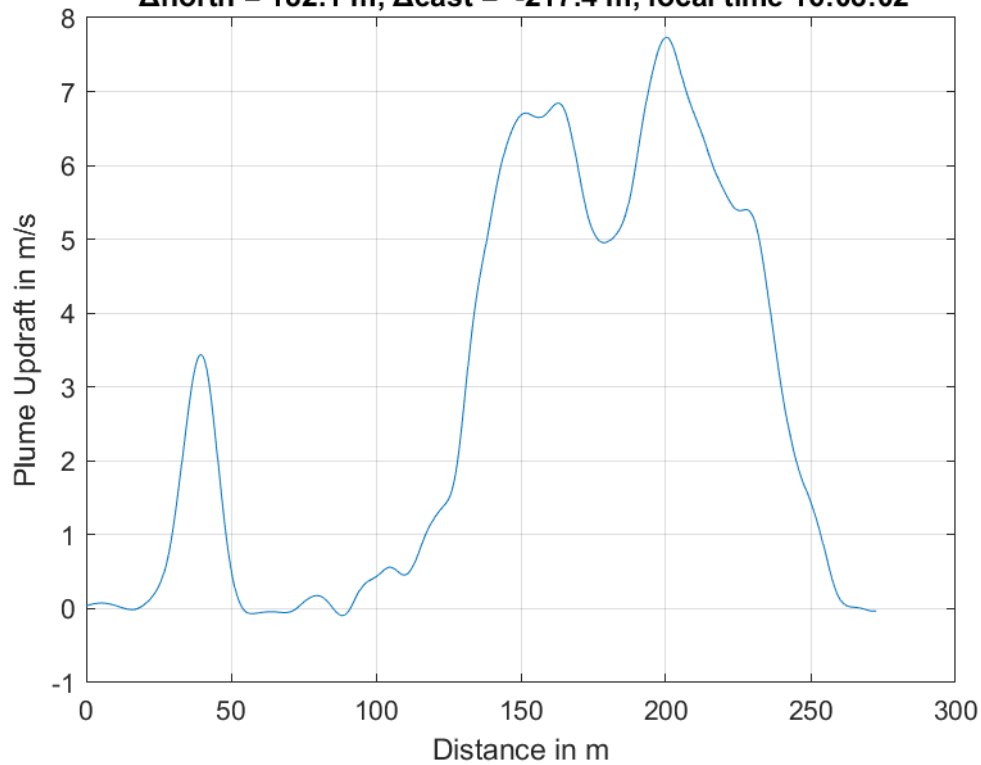


**Plume #17 at 290.4 m MSL, fly-through speed 40.0 m/s,
 $\Delta_{\text{north}} = 162.8$ m, $\Delta_{\text{east}} = -204.6$ m, local time 16:05:23**

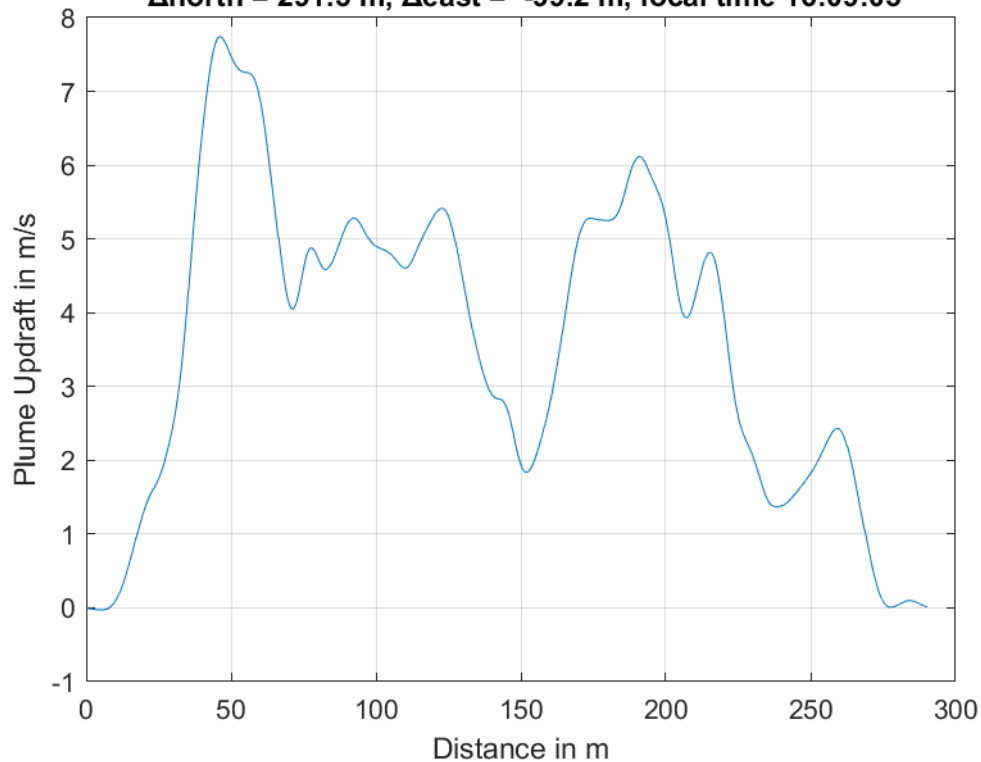




**Plume #18 at 318.1 m MSL, fly-through speed 44.0 m/s,
 $\Delta_{\text{north}} = 182.1$ m, $\Delta_{\text{east}} = -217.4$ m, local time 16:08:02**

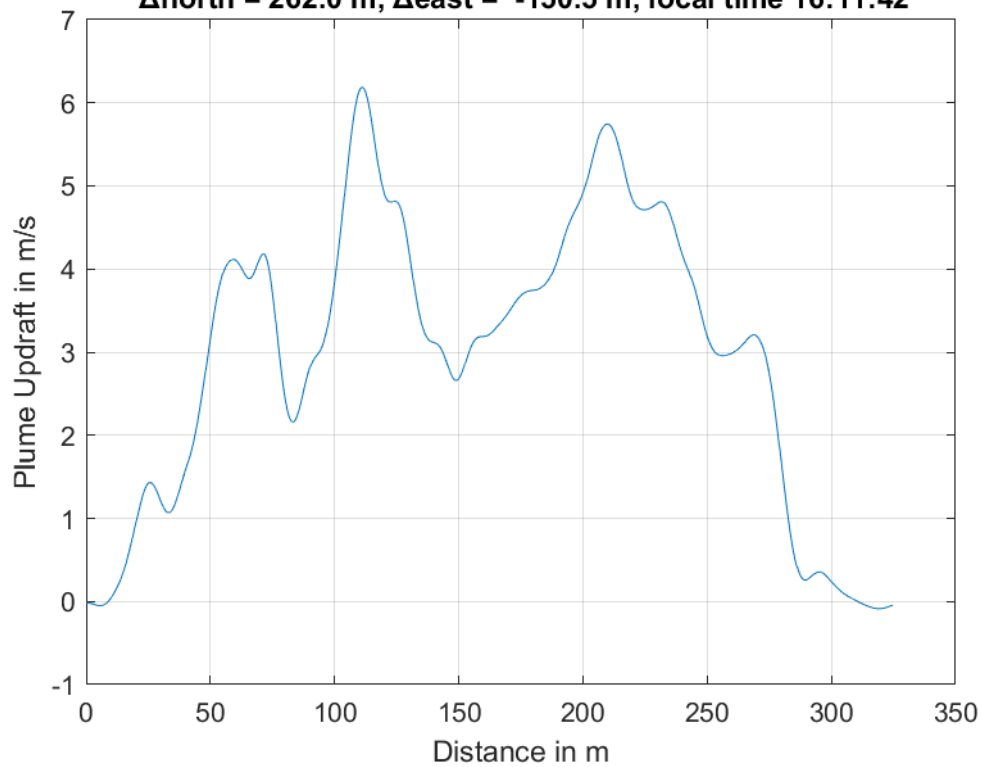


**Plume #19 at 322.9 m MSL, fly-through speed 44.0 m/s,
 $\Delta_{\text{north}} = 291.3$ m, $\Delta_{\text{east}} = -99.2$ m, local time 16:09:05**

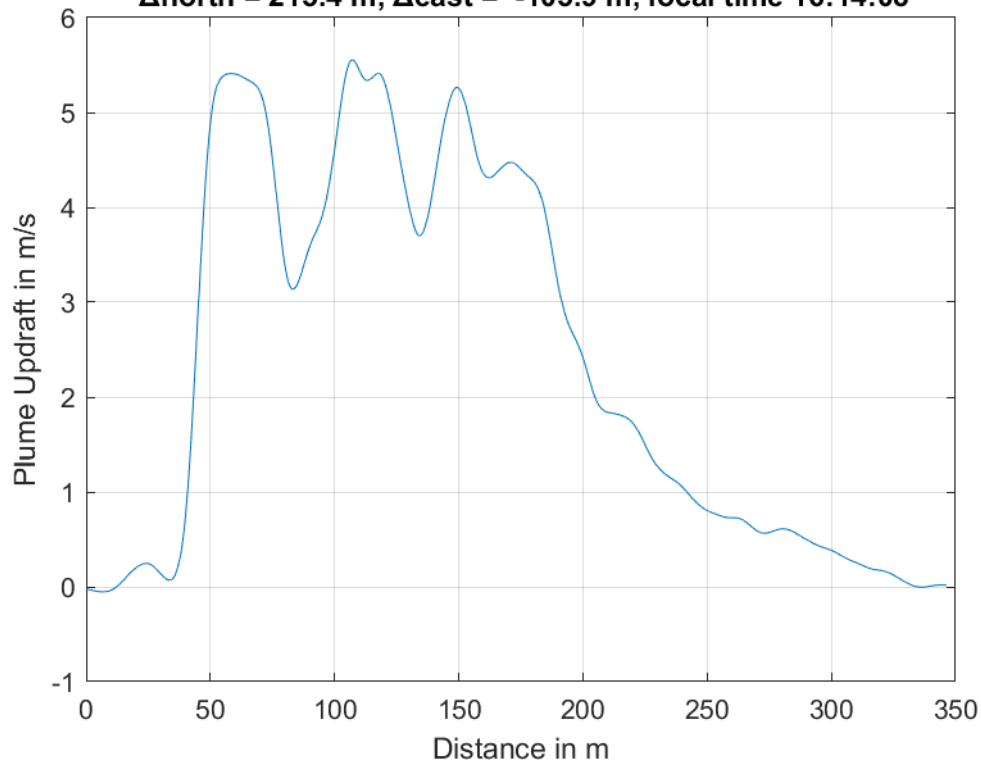




**Plume #20 at 342.1 m MSL, fly-through speed 50.0 m/s,
 Δ north = 262.0 m, Δ east = -150.5 m, local time 16:11:42**

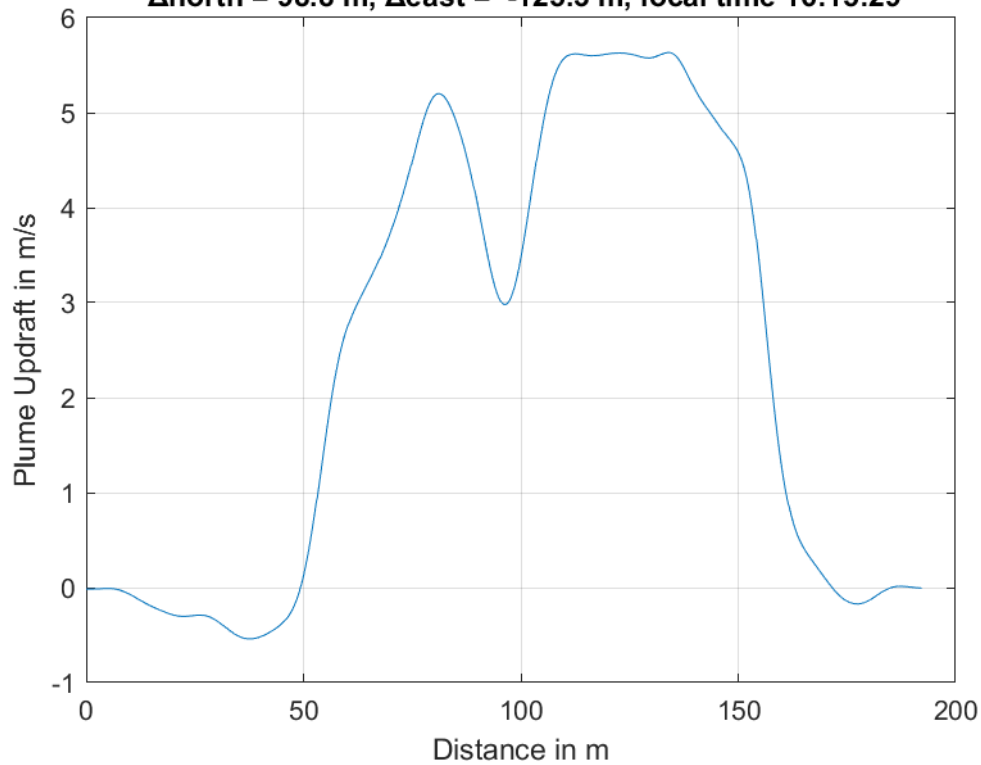


**Plume #21 at 343.1 m MSL, fly-through speed 55.0 m/s,
 Δ north = 215.4 m, Δ east = -105.9 m, local time 16:14:08**

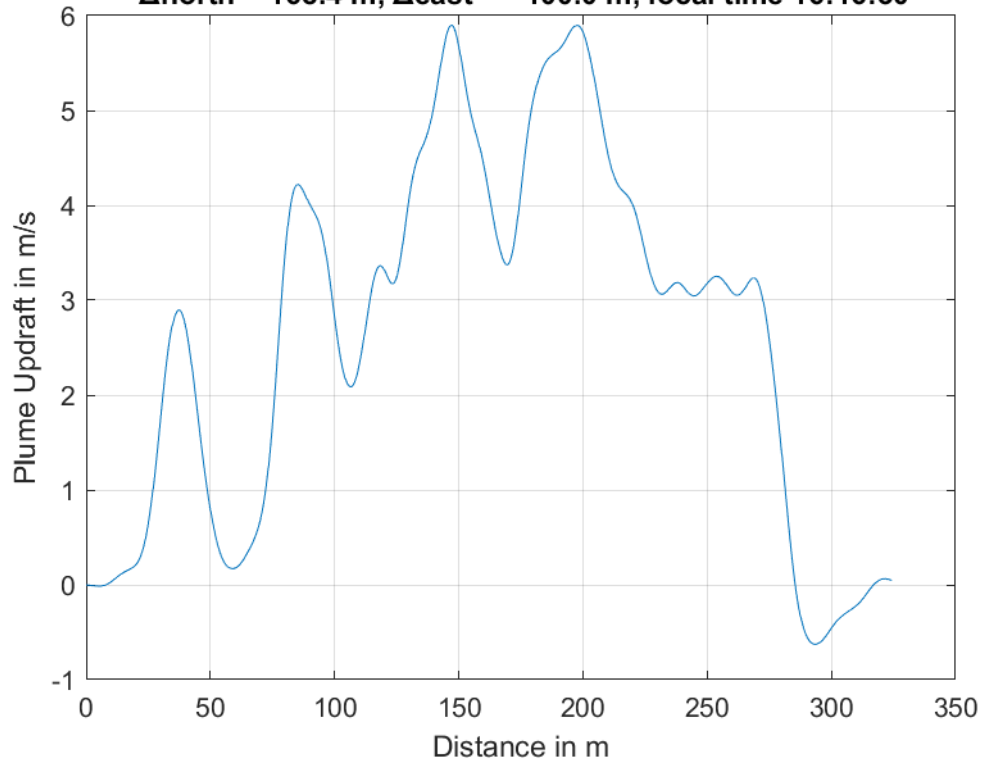




**Plume #22 at 341.9 m MSL, fly-through speed 52.0 m/s,
 $\Delta_{\text{north}} = 98.8$ m, $\Delta_{\text{east}} = -125.3$ m, local time 16:15:29**

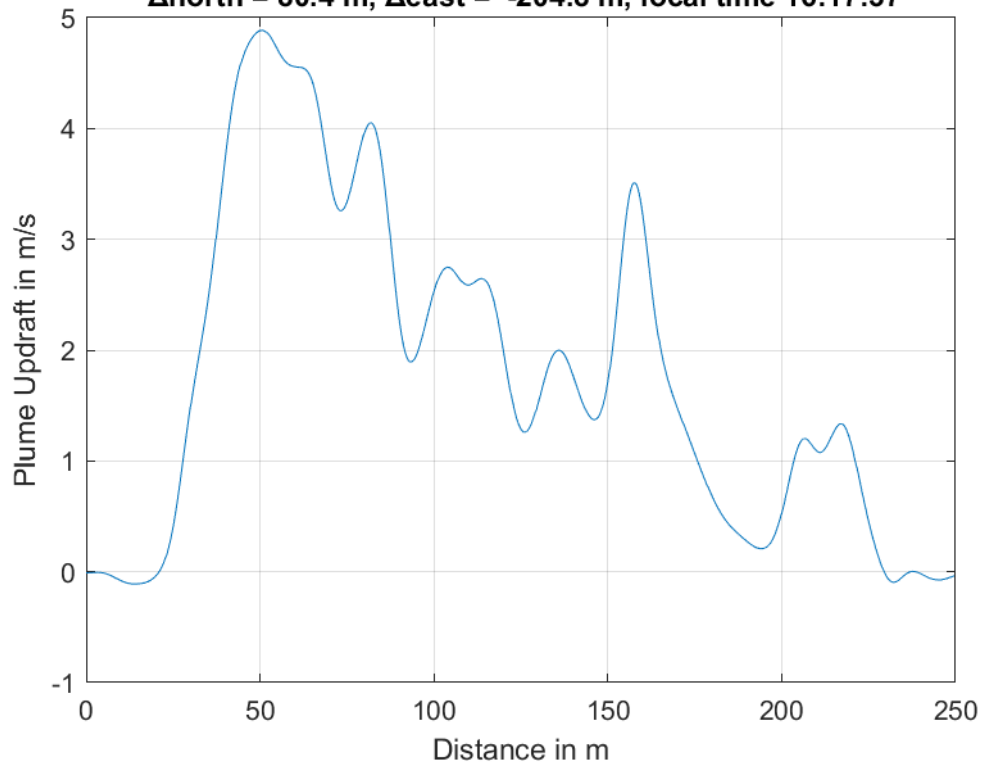


**Plume #23 at 311.5 m MSL, fly-through speed 55.0 m/s,
 $\Delta_{\text{north}} = 168.4$ m, $\Delta_{\text{east}} = -100.0$ m, local time 16:16:30**

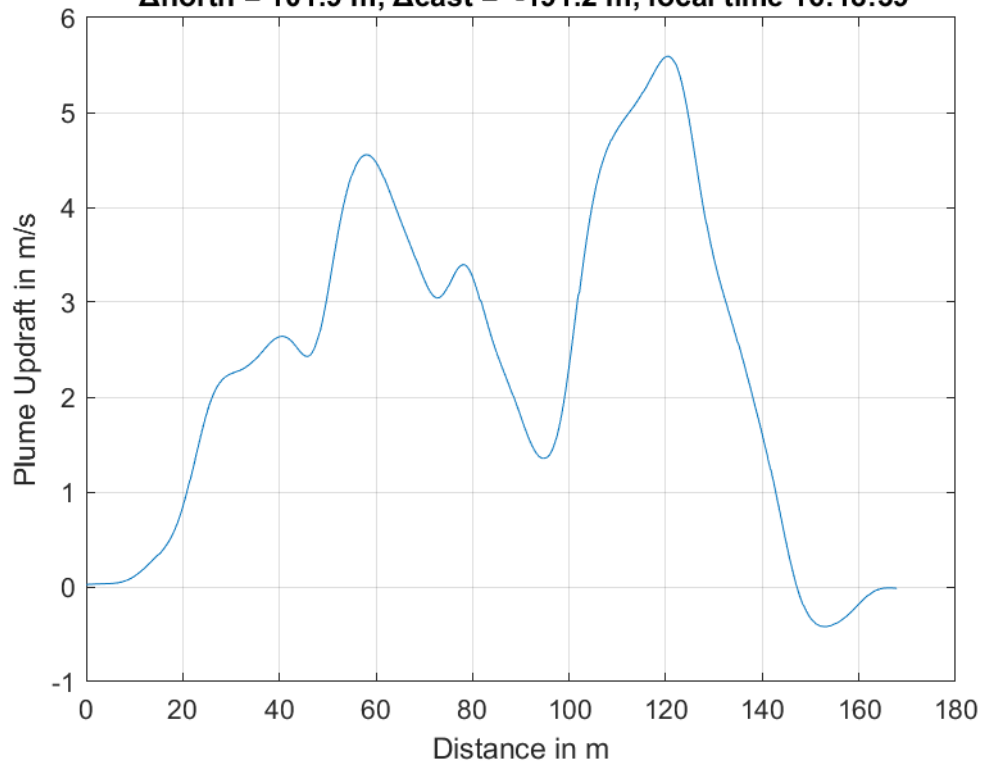




**Plume #24 at 319.9 m MSL, fly-through speed 51.0 m/s,
 $\Delta_{\text{north}} = 80.4$ m, $\Delta_{\text{east}} = -204.8$ m, local time 16:17:37**

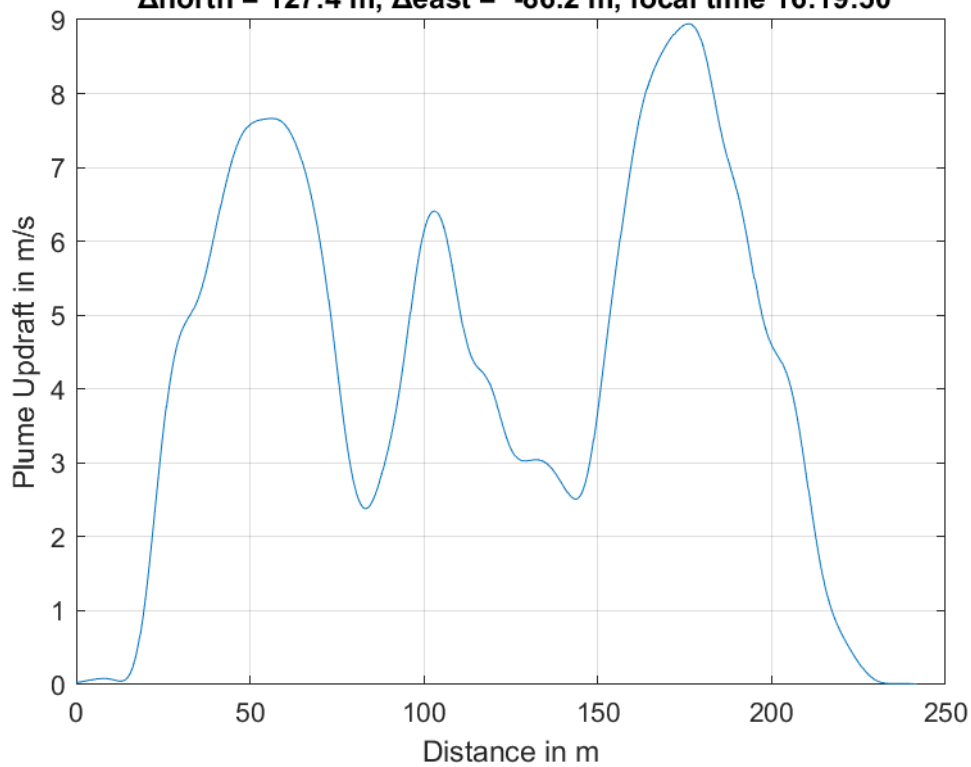


**Plume #25 at 297.7 m MSL, fly-through speed 48.0 m/s,
 $\Delta_{\text{north}} = 101.9$ m, $\Delta_{\text{east}} = -191.2$ m, local time 16:18:39**

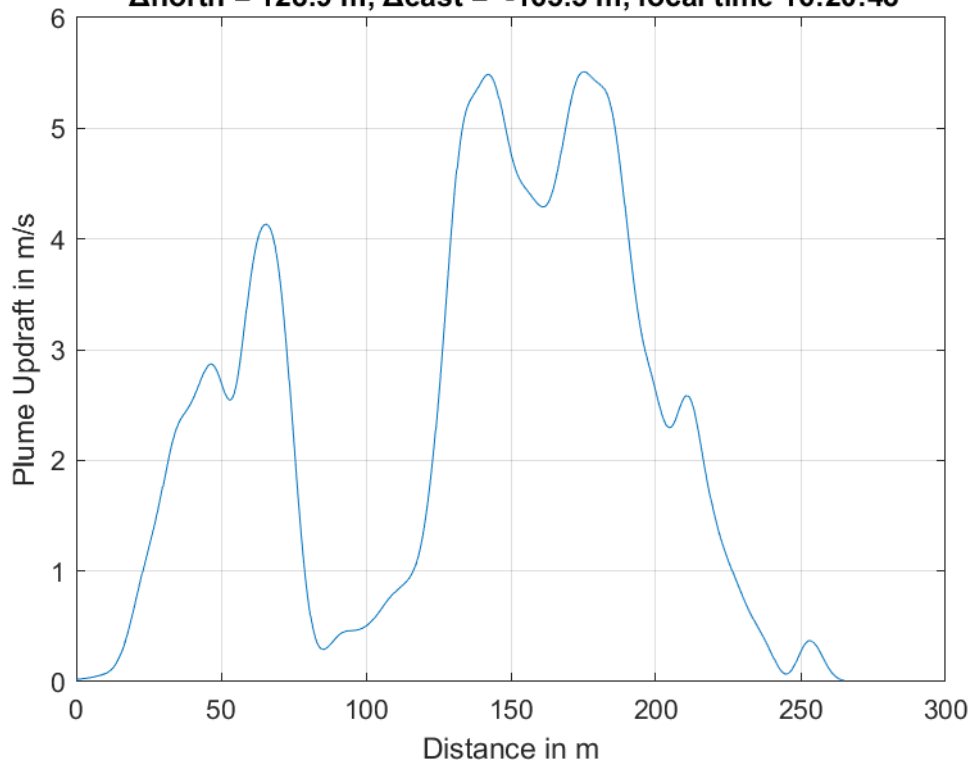




**Plume #26 at 284.9 m MSL, fly-through speed 55.0 m/s,
 $\Delta_{\text{north}} = 127.4$ m, $\Delta_{\text{east}} = -86.2$ m, local time 16:19:50**

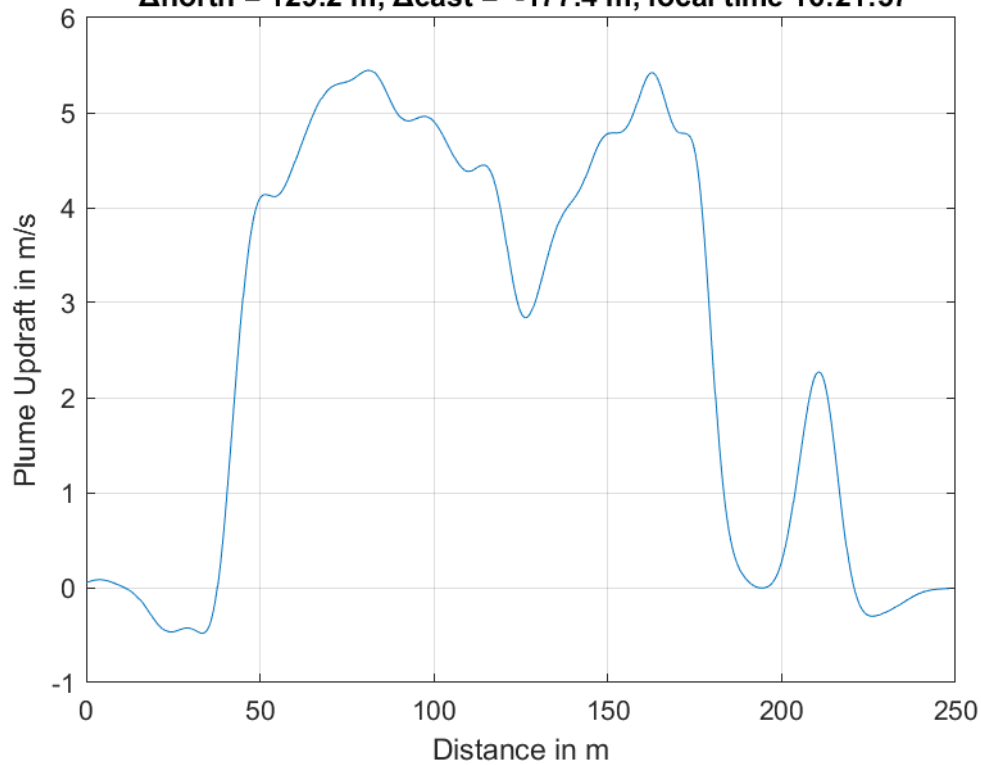


**Plume #27 at 342.1 m MSL, fly-through speed 52.0 m/s,
 $\Delta_{\text{north}} = 128.9$ m, $\Delta_{\text{east}} = -165.5$ m, local time 16:20:48**

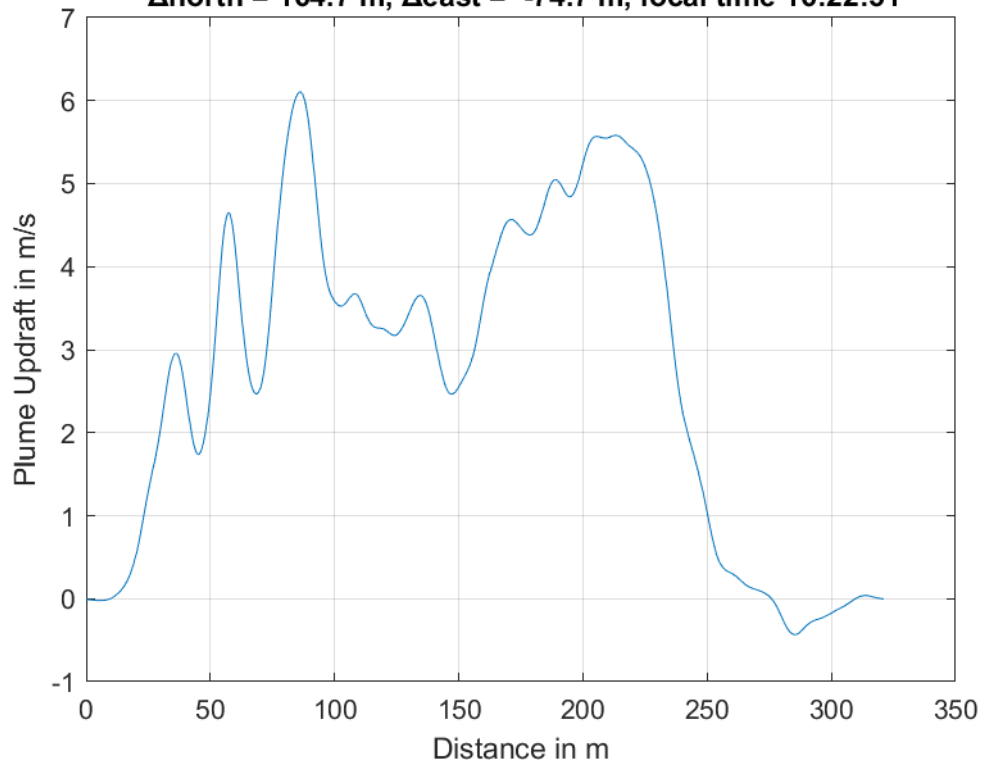




**Plume #28 at 347.2 m MSL, fly-through speed 54.0 m/s,
 $\Delta_{\text{north}} = 129.2$ m, $\Delta_{\text{east}} = -177.4$ m, local time 16:21:57**

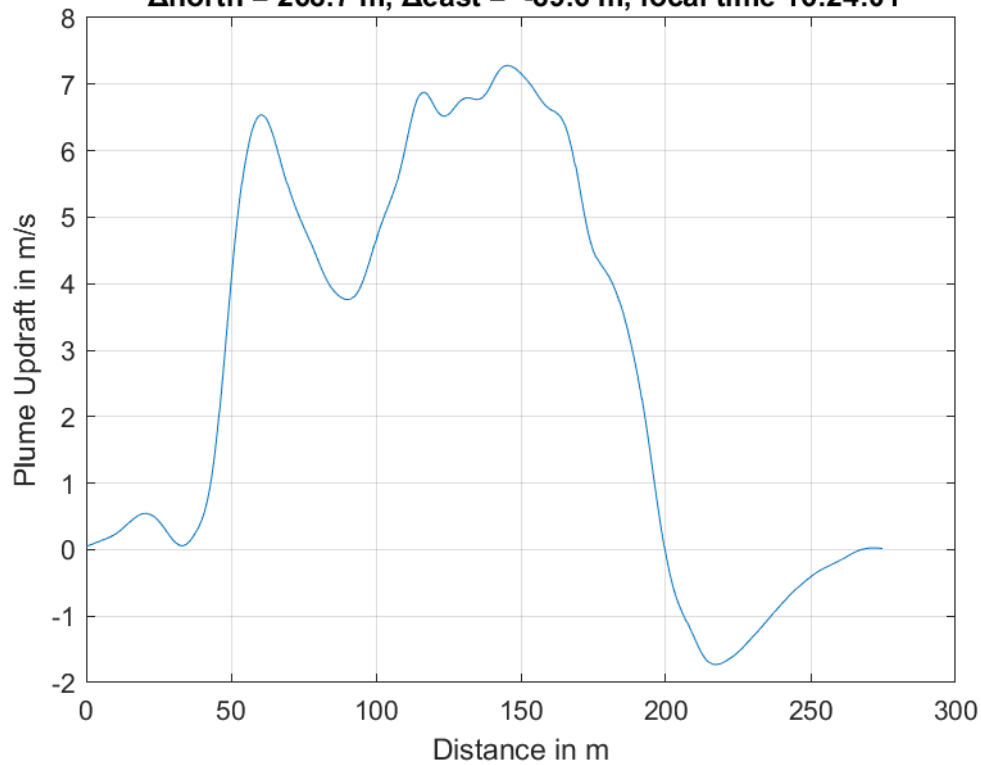


**Plume #29 at 308.3 m MSL, fly-through speed 51.0 m/s,
 $\Delta_{\text{north}} = 164.7$ m, $\Delta_{\text{east}} = -74.7$ m, local time 16:22:51**

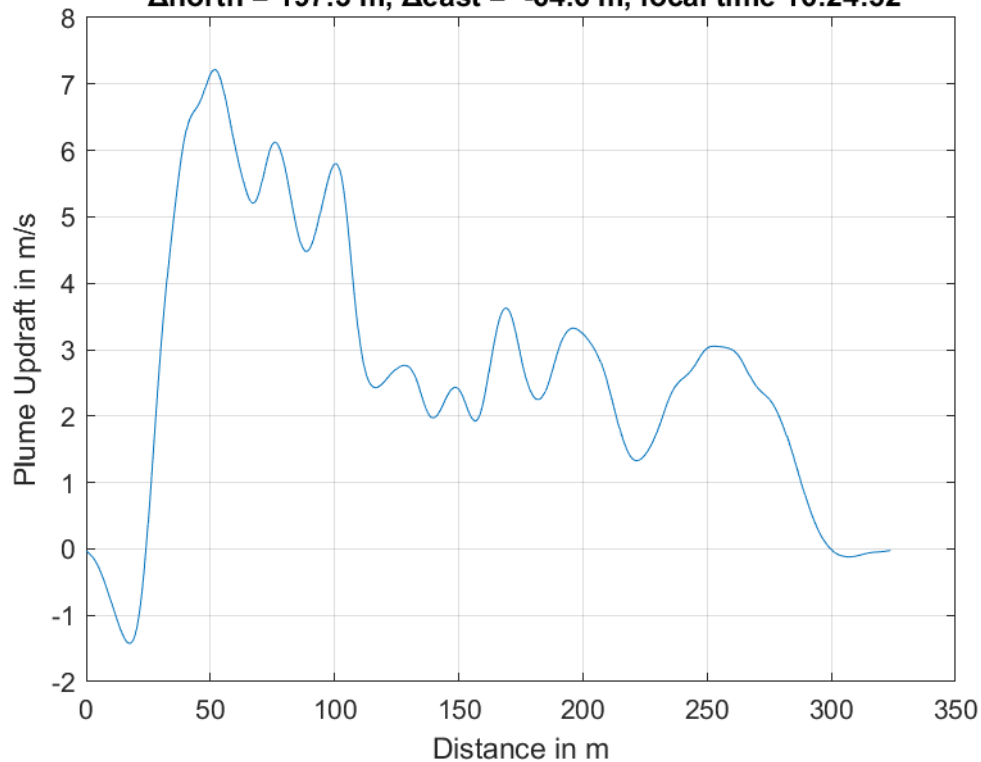




**Plume #30 at 288.5 m MSL, fly-through speed 55.0 m/s,
 $\Delta_{\text{north}} = 268.7$ m, $\Delta_{\text{east}} = -89.6$ m, local time 16:24:01**

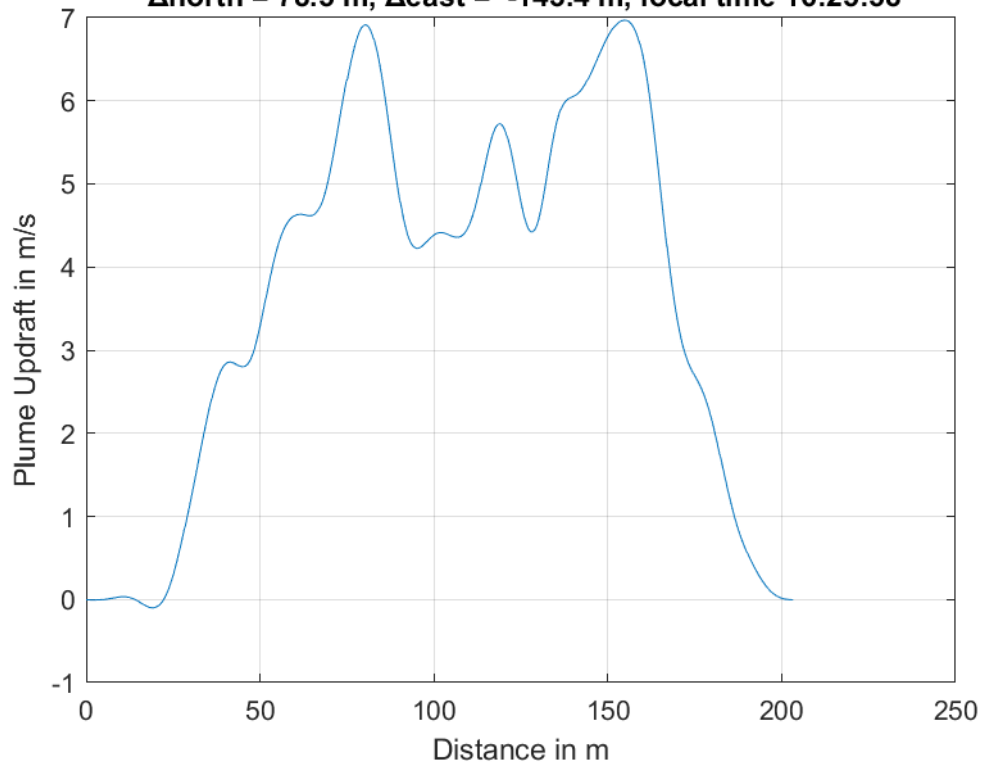


**Plume #31 at 227.5 m MSL, fly-through speed 54.0 m/s,
 $\Delta_{\text{north}} = 197.3$ m, $\Delta_{\text{east}} = -64.6$ m, local time 16:24:52**

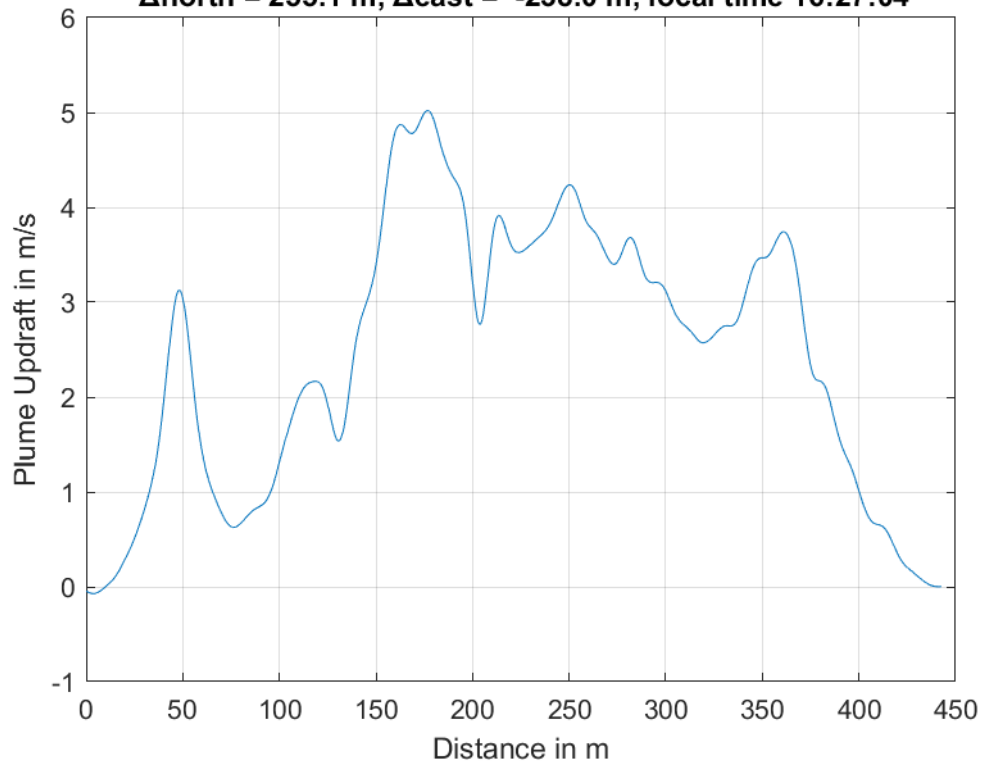




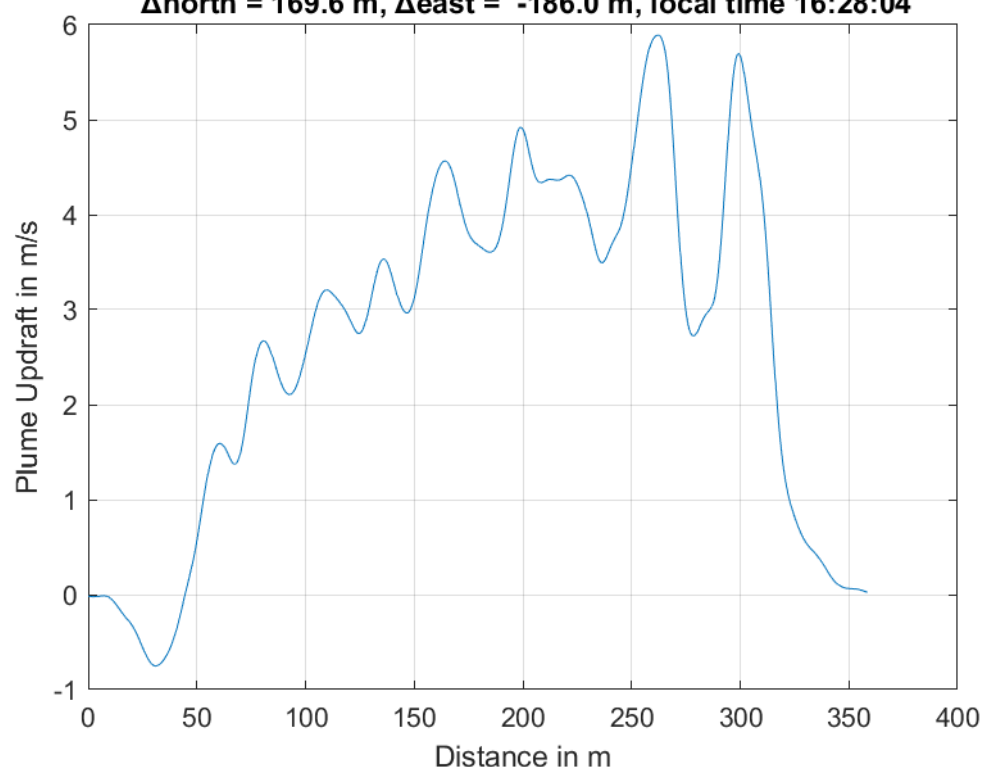
**Plume #32 at 232.8 m MSL, fly-through speed 55.0 m/s,
 $\Delta_{\text{north}} = 78.5$ m, $\Delta_{\text{east}} = -143.4$ m, local time 16:25:58**



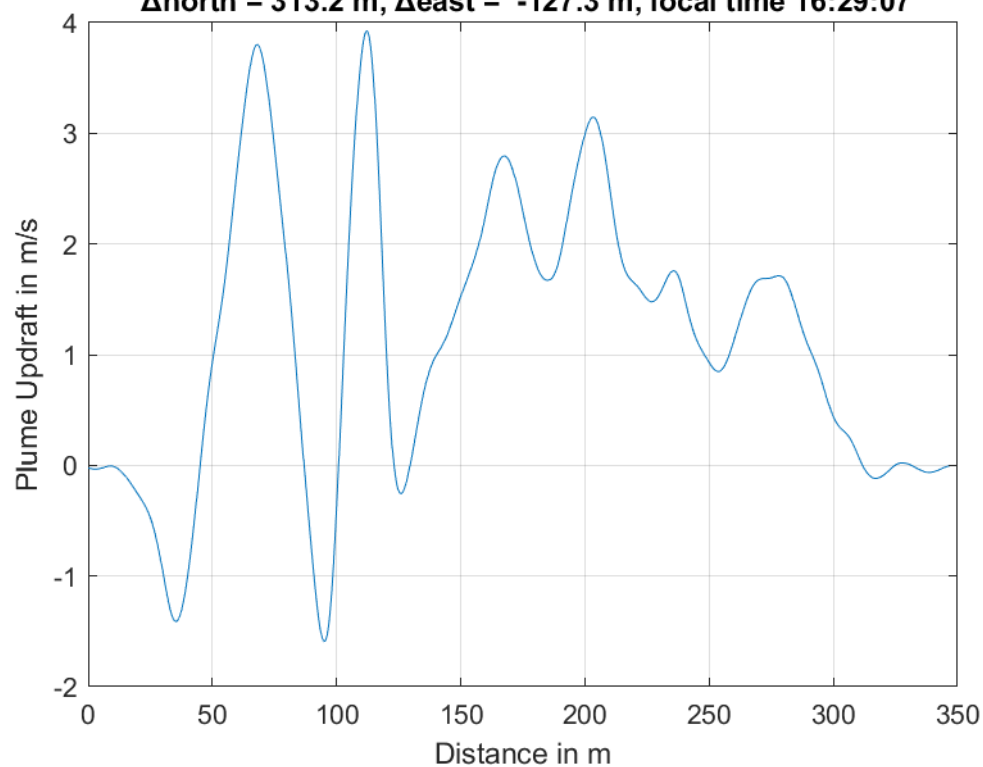
**Plume #33 at 237.0 m MSL, fly-through speed 54.0 m/s,
 $\Delta_{\text{north}} = 255.1$ m, $\Delta_{\text{east}} = -238.0$ m, local time 16:27:04**



**Plume #34 at 236.1 m MSL, fly-through speed 52.0 m/s,
 $\Delta_{\text{north}} = 169.6$ m, $\Delta_{\text{east}} = -186.0$ m, local time 16:28:04**

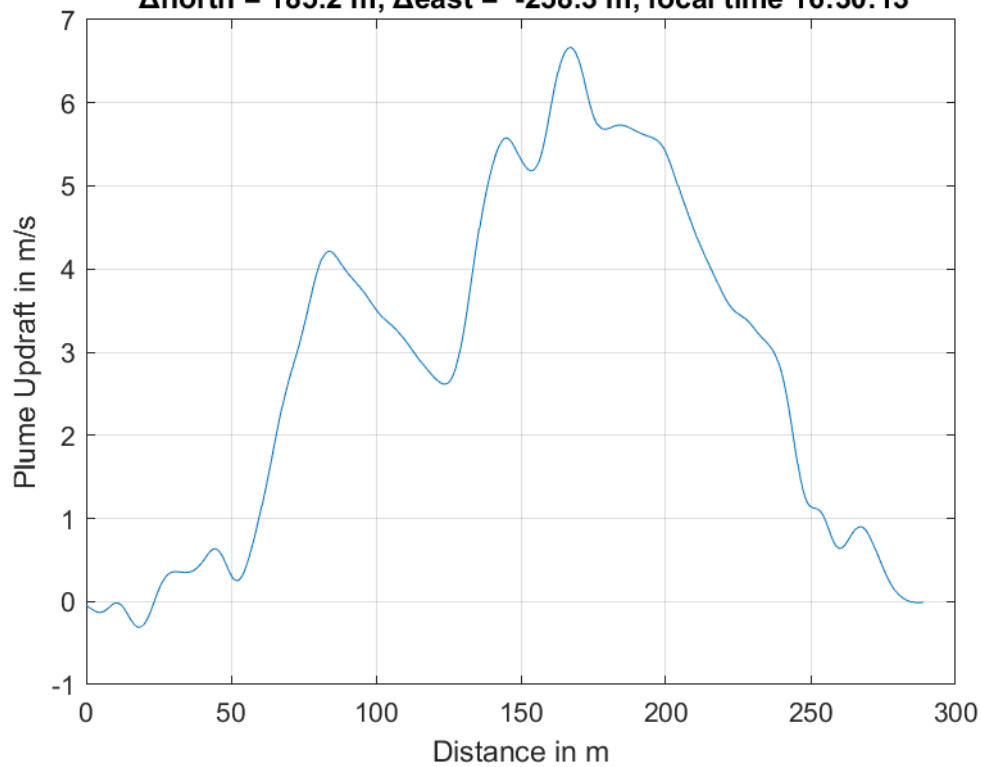


**Plume #35 at 243.1 m MSL, fly-through speed 51.0 m/s,
 $\Delta_{\text{north}} = 313.2$ m, $\Delta_{\text{east}} = -127.3$ m, local time 16:29:07**

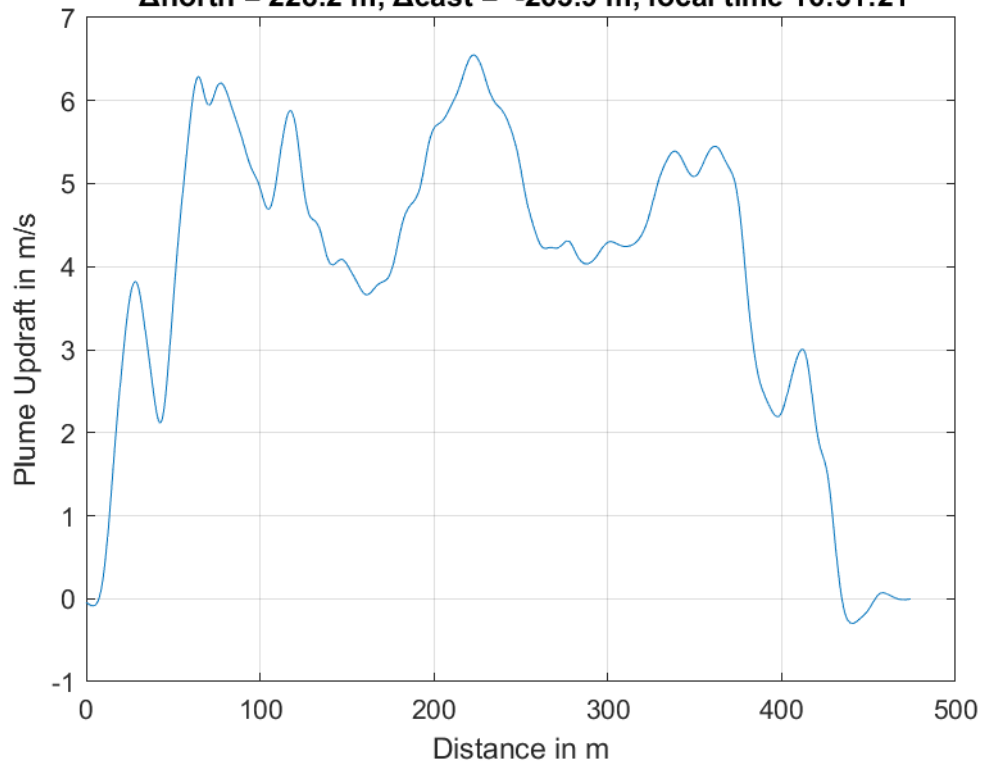




**Plume #36 at 222.1 m MSL, fly-through speed 49.0 m/s,
 $\Delta_{\text{north}} = 185.2$ m, $\Delta_{\text{east}} = -258.3$ m, local time 16:30:13**

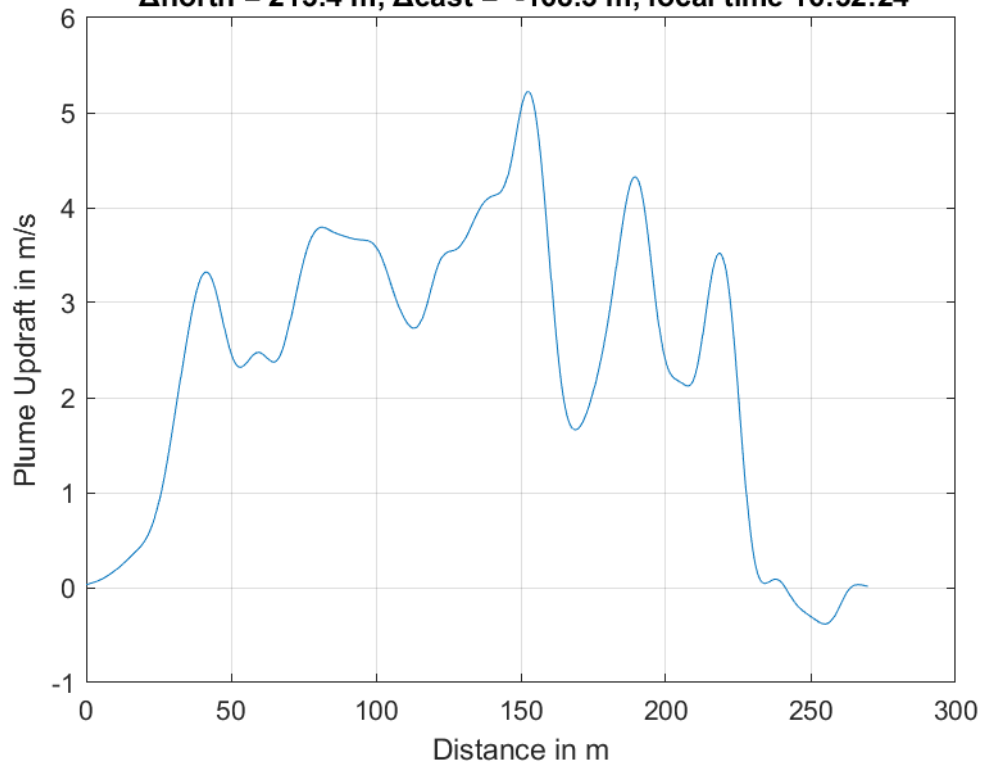


**Plume #37 at 224.3 m MSL, fly-through speed 51.0 m/s,
 $\Delta_{\text{north}} = 228.2$ m, $\Delta_{\text{east}} = -263.9$ m, local time 16:31:21**

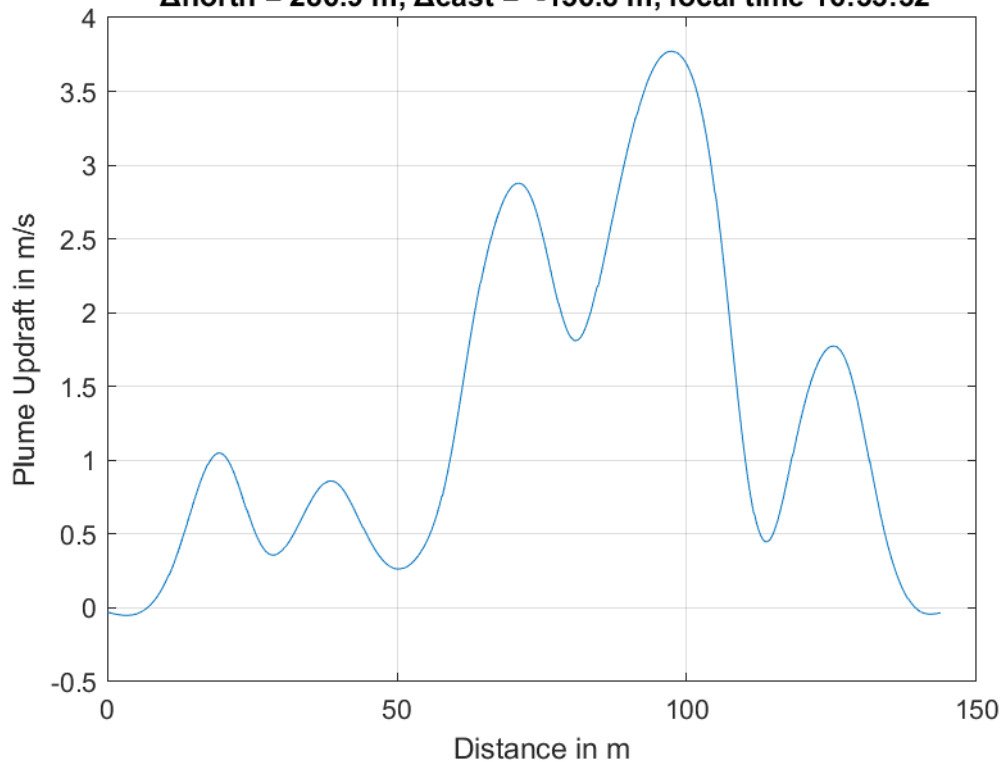




**Plume #38 at 225.3 m MSL, fly-through speed 54.0 m/s,
 $\Delta_{\text{north}} = 213.4$ m, $\Delta_{\text{east}} = -168.3$ m, local time 16:32:24**

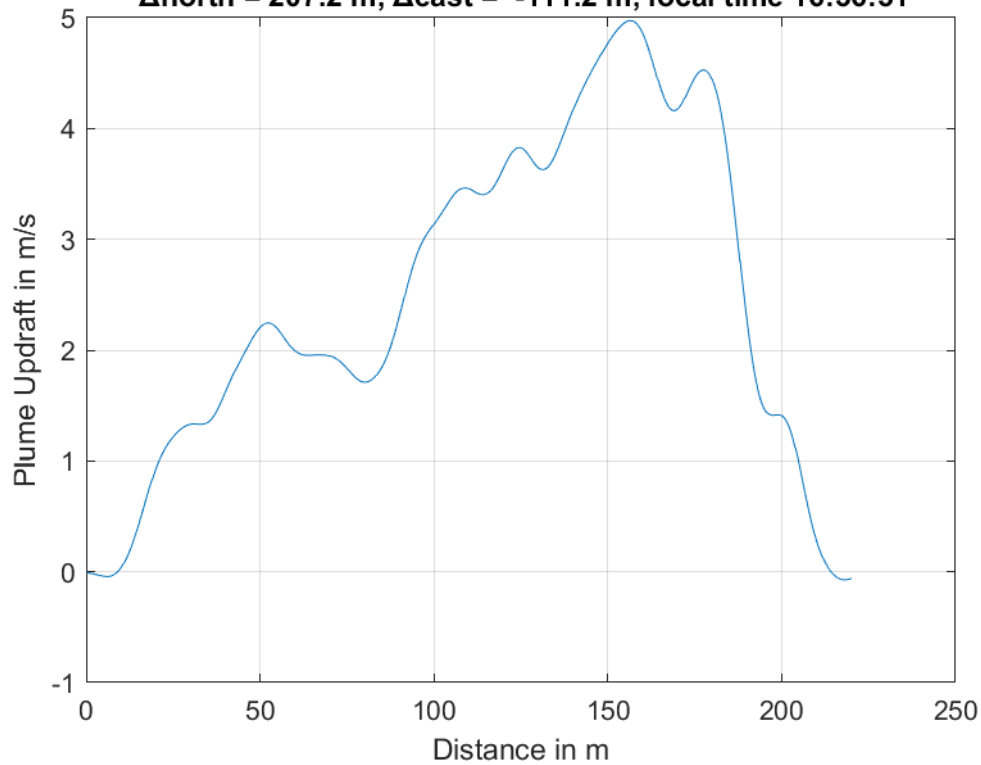


**Plume #39 at 227.3 m MSL, fly-through speed 48.0 m/s,
 $\Delta_{\text{north}} = 286.9$ m, $\Delta_{\text{east}} = -156.8$ m, local time 16:33:32**

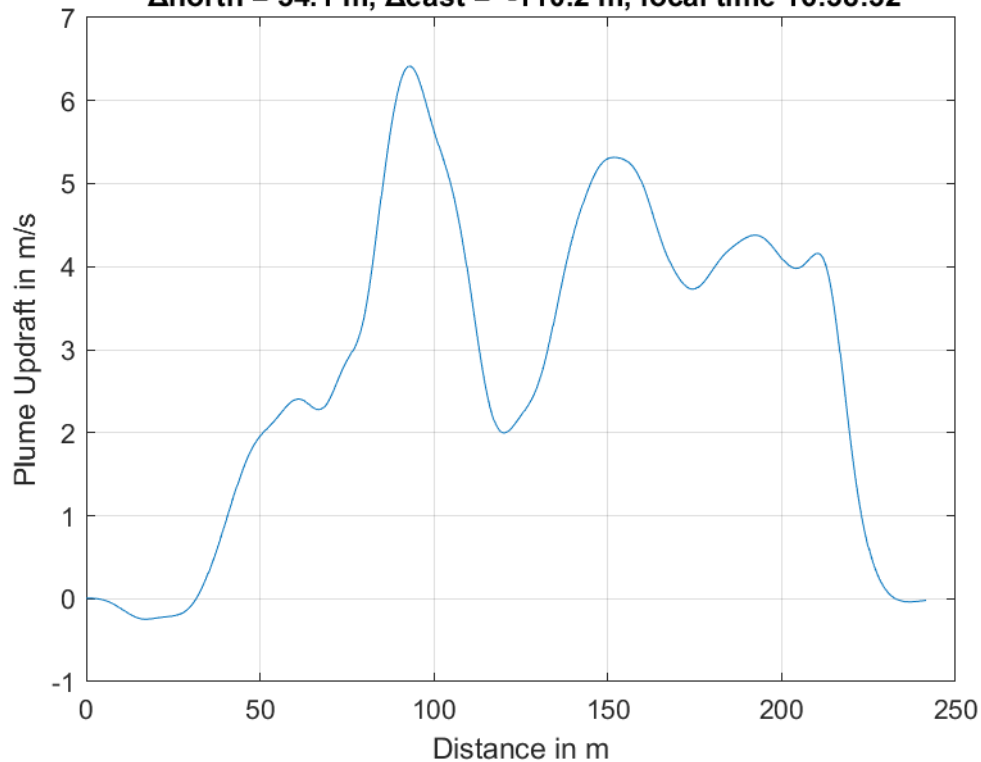




**Plume #40 at 333.8 m MSL, fly-through speed 58.0 m/s,
 $\Delta_{\text{north}} = 207.2$ m, $\Delta_{\text{east}} = -111.2$ m, local time 16:36:51**

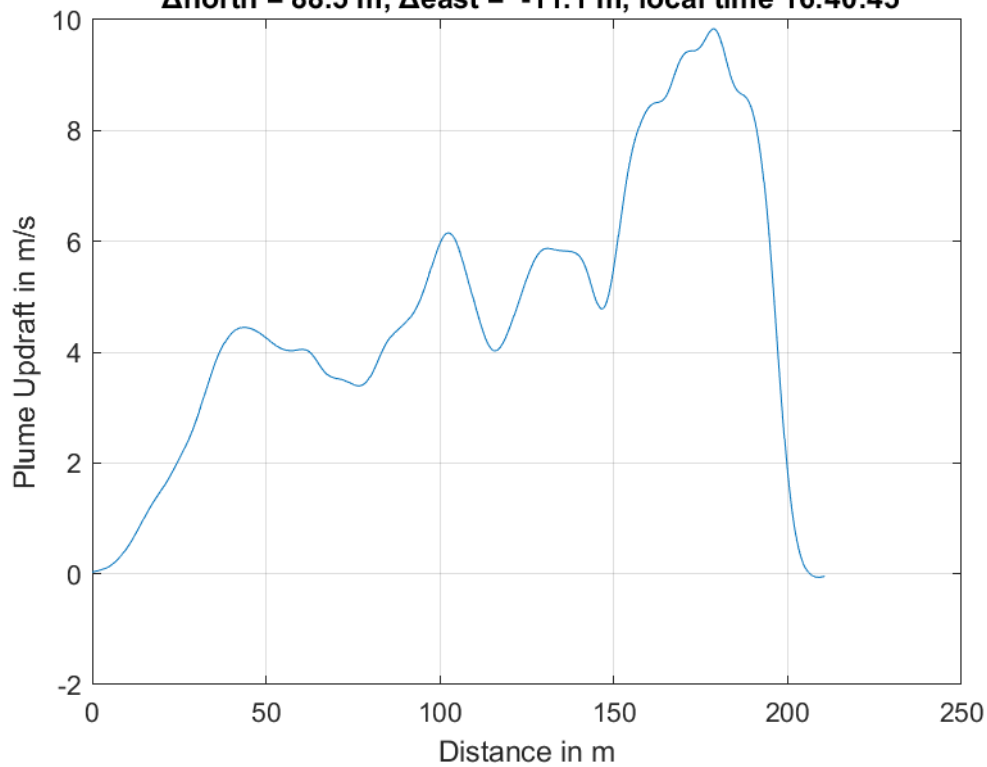


**Plume #41 at 297.3 m MSL, fly-through speed 59.0 m/s,
 $\Delta_{\text{north}} = 54.1$ m, $\Delta_{\text{east}} = -110.2$ m, local time 16:38:32**

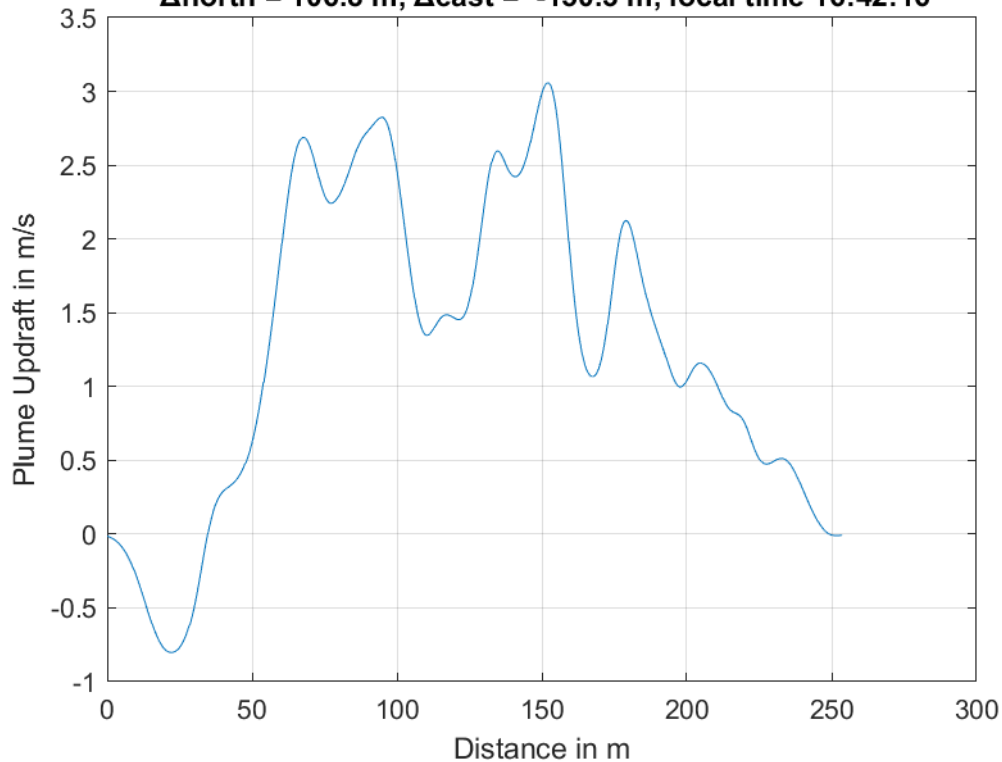




**Plume #42 at 312.6 m MSL, fly-through speed 43.0 m/s,
 $\Delta_{\text{north}} = 88.5$ m, $\Delta_{\text{east}} = -11.1$ m, local time 16:40:45**

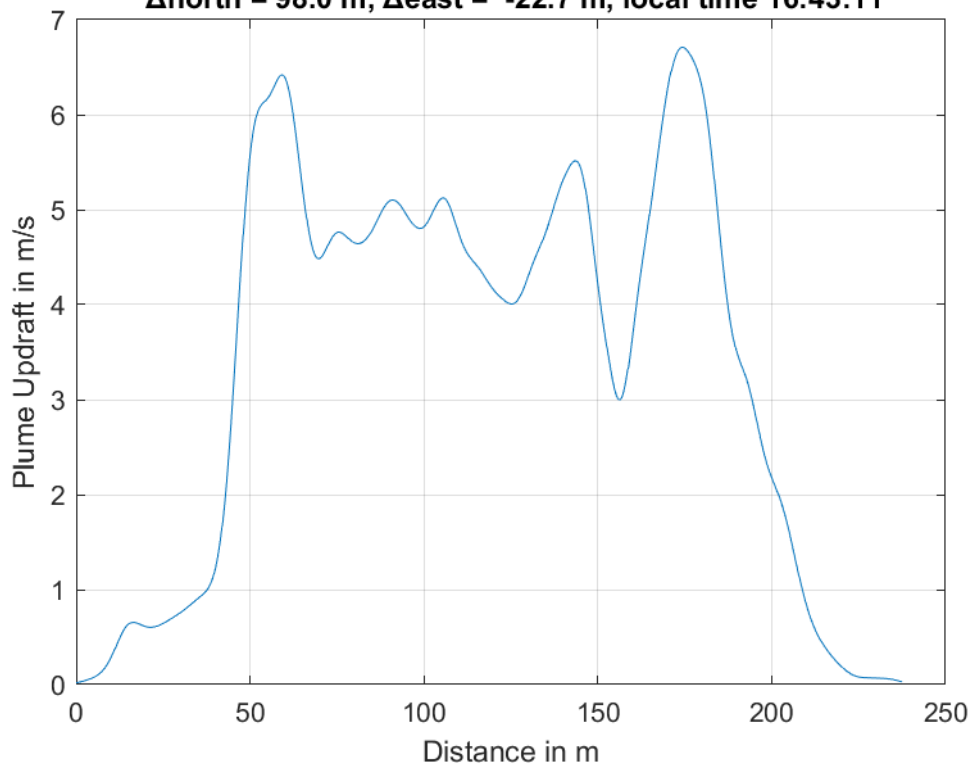


**Plume #43 at 300.2 m MSL, fly-through speed 47.0 m/s,
 $\Delta_{\text{north}} = 106.8$ m, $\Delta_{\text{east}} = -150.3$ m, local time 16:42:16**

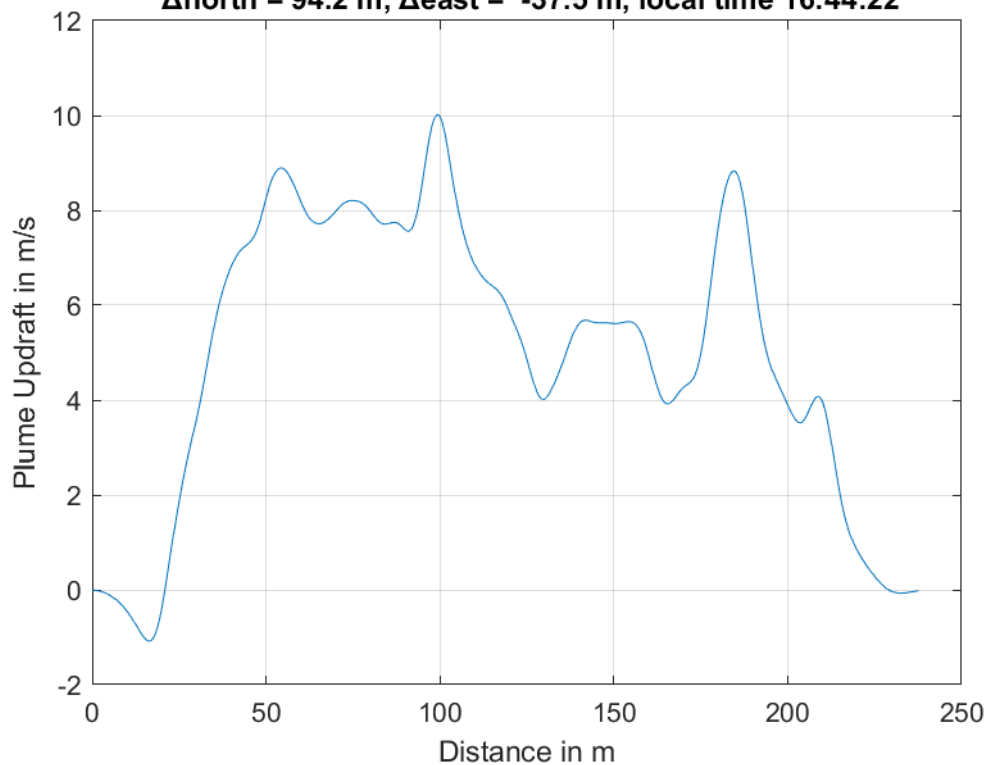




**Plume #44 at 297.7 m MSL, fly-through speed 44.0 m/s,
 $\Delta_{\text{north}} = 98.0$ m, $\Delta_{\text{east}} = -22.7$ m, local time 16:43:11**

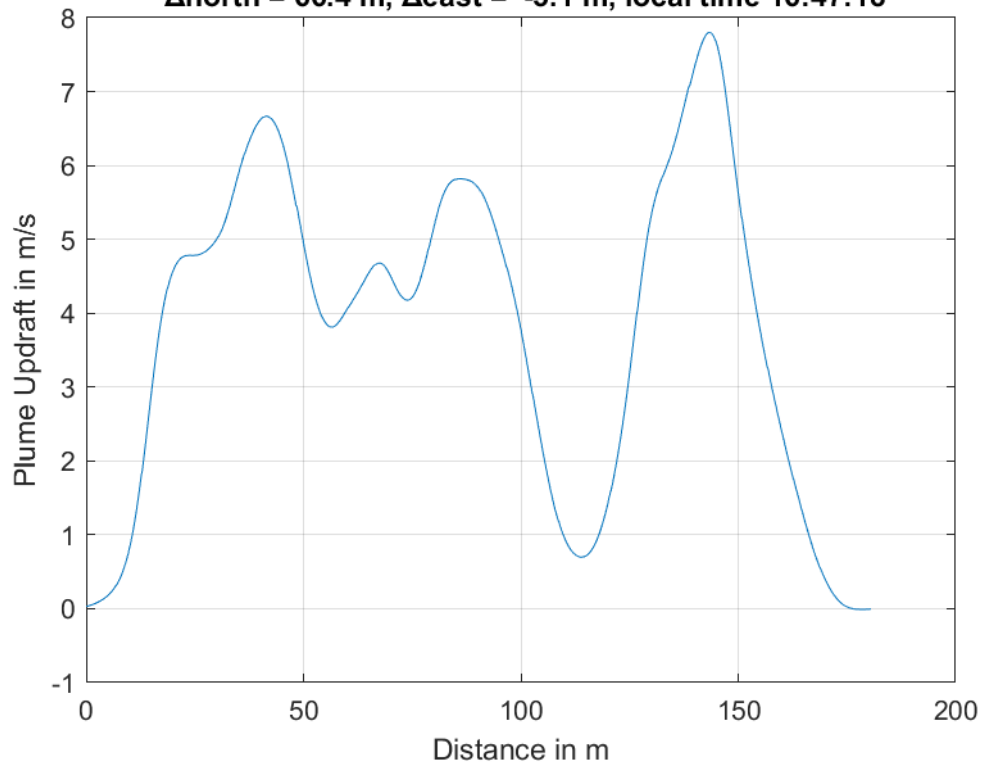


**Plume #45 at 298.6 m MSL, fly-through speed 41.0 m/s,
 $\Delta_{\text{north}} = 94.2$ m, $\Delta_{\text{east}} = -37.5$ m, local time 16:44:22**

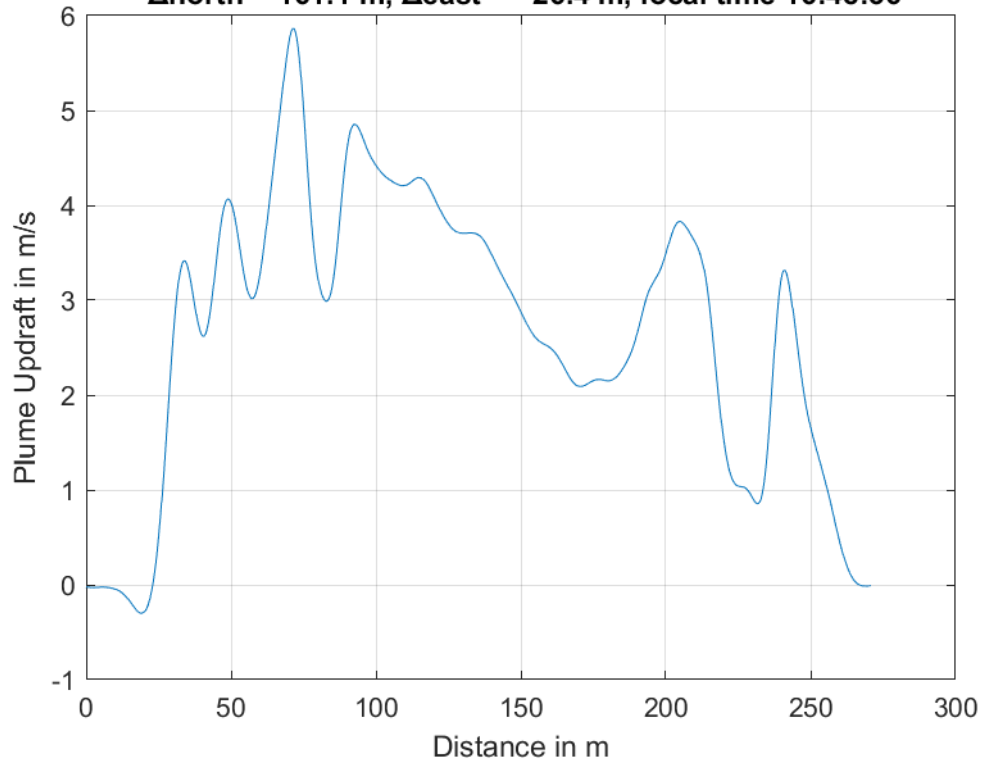




**Plume #46 at 185.0 m MSL, fly-through speed 43.0 m/s,
 $\Delta_{\text{north}} = 66.4$ m, $\Delta_{\text{east}} = -5.1$ m, local time 16:47:18**

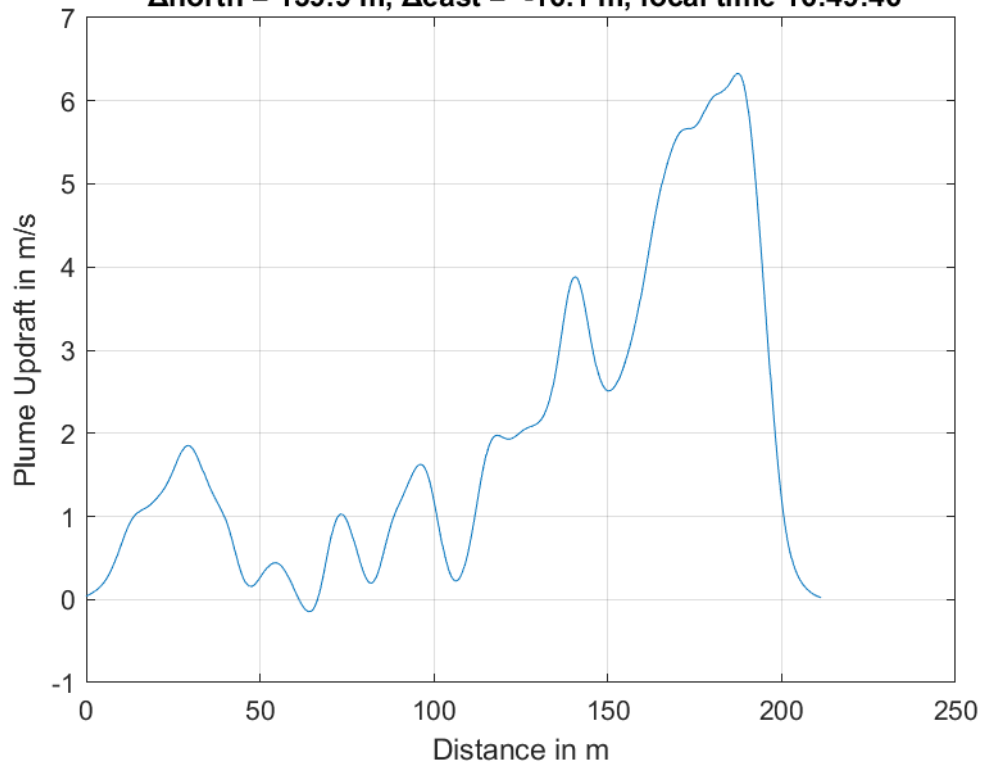


**Plume #47 at 222.7 m MSL, fly-through speed 43.0 m/s,
 $\Delta_{\text{north}} = 161.1$ m, $\Delta_{\text{east}} = -26.4$ m, local time 16:48:36**

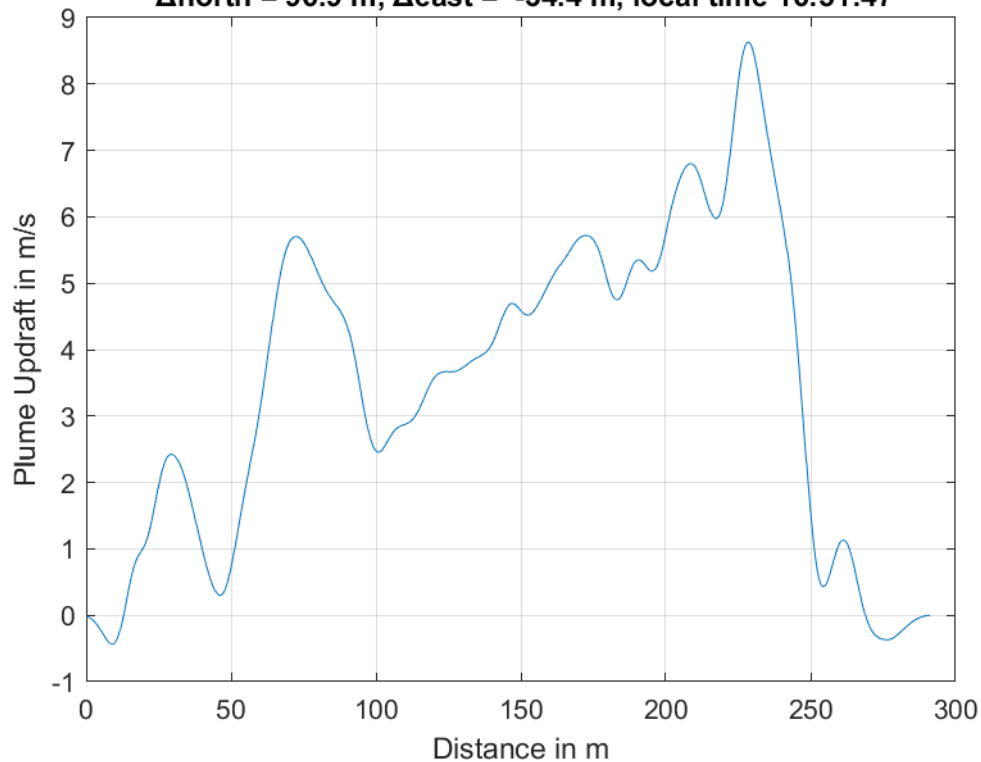




**Plume #48 at 276.1 m MSL, fly-through speed 45.0 m/s,
 Δ north = 139.9 m, Δ east = -16.1 m, local time 16:49:46**

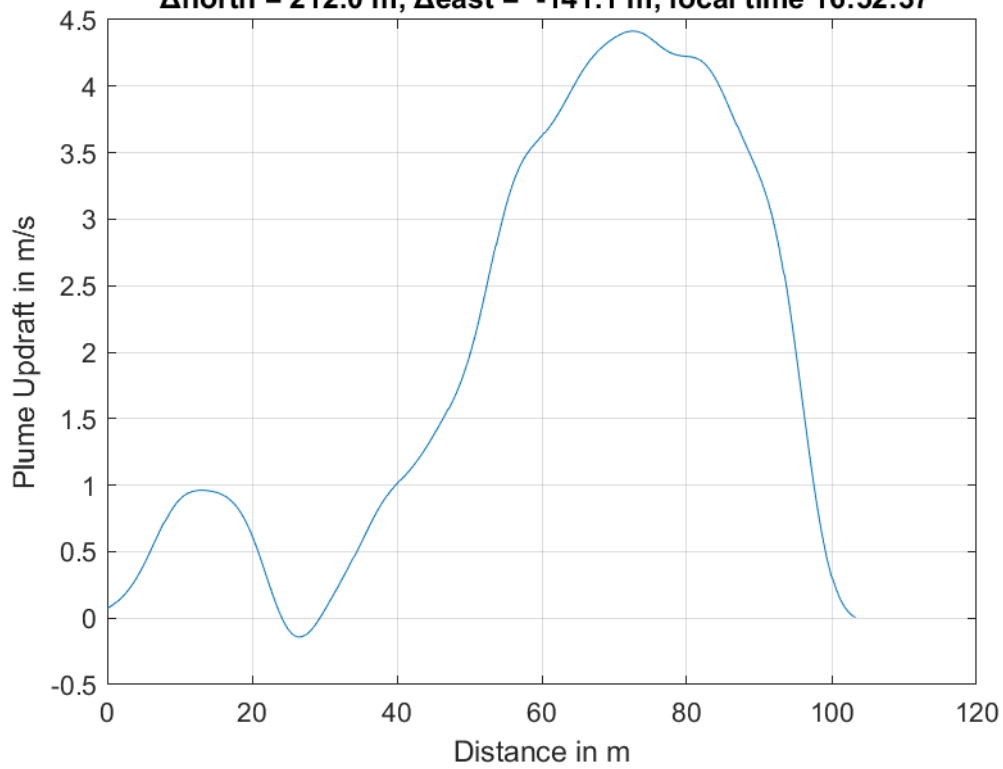


**Plume #49 at 210.9 m MSL, fly-through speed 47.0 m/s,
 Δ north = 96.9 m, Δ east = -34.4 m, local time 16:51:47**



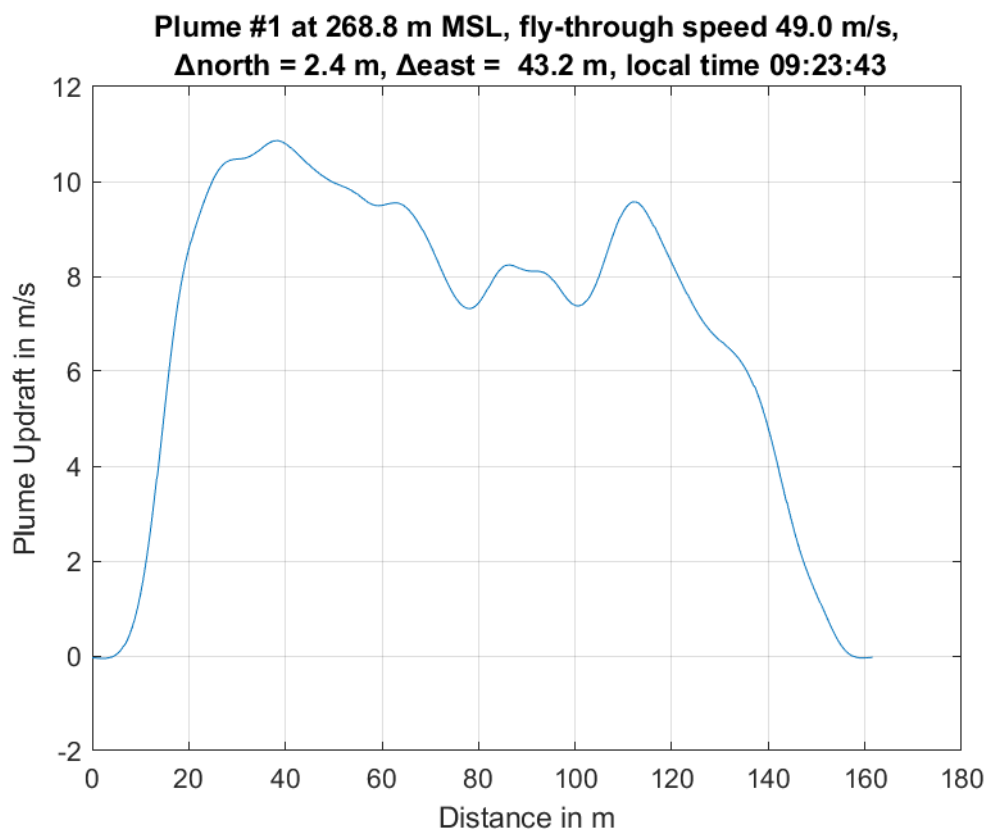
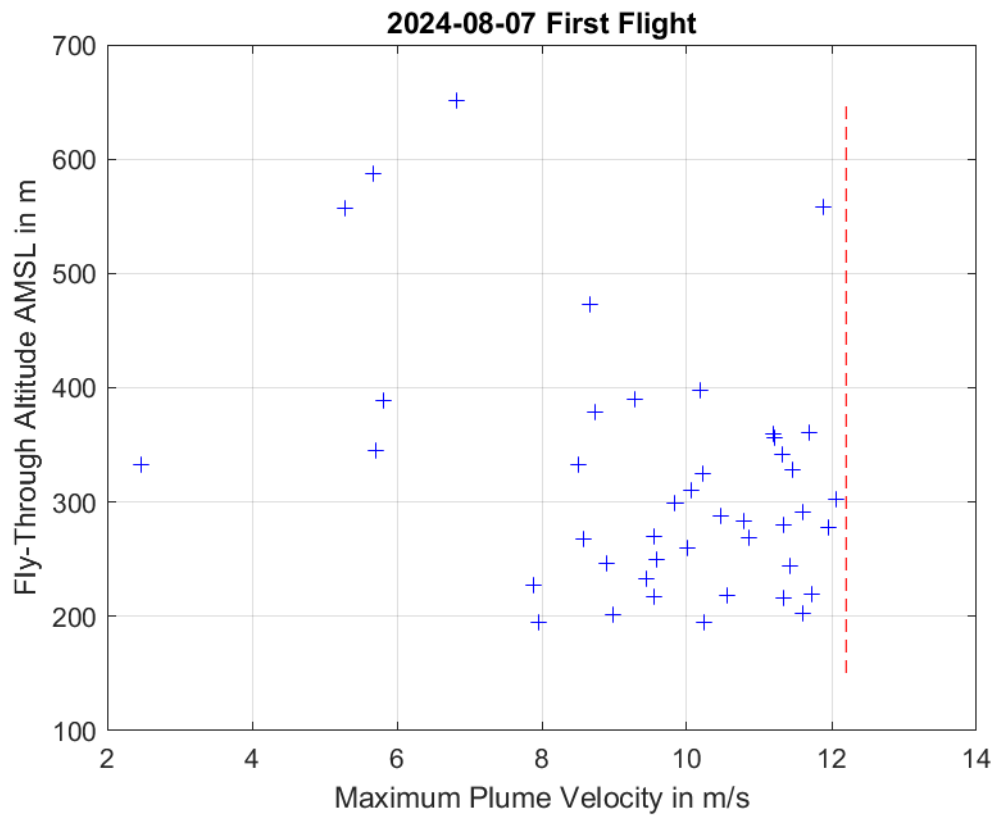


**Plume #50 at 203.6 m MSL, fly-through speed 47.0 m/s,
 $\Delta_{\text{north}} = 212.0$ m, $\Delta_{\text{east}} = -141.1$ m, local time 16:52:37**



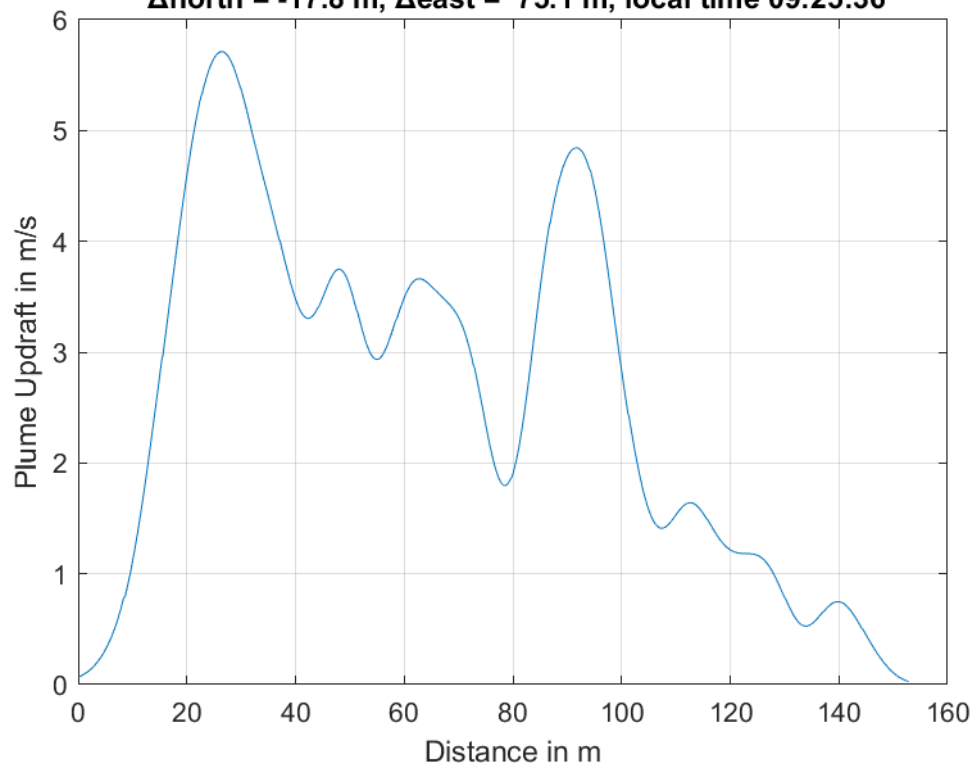


8 Measured Plumes: 2024-08-07 First Flight

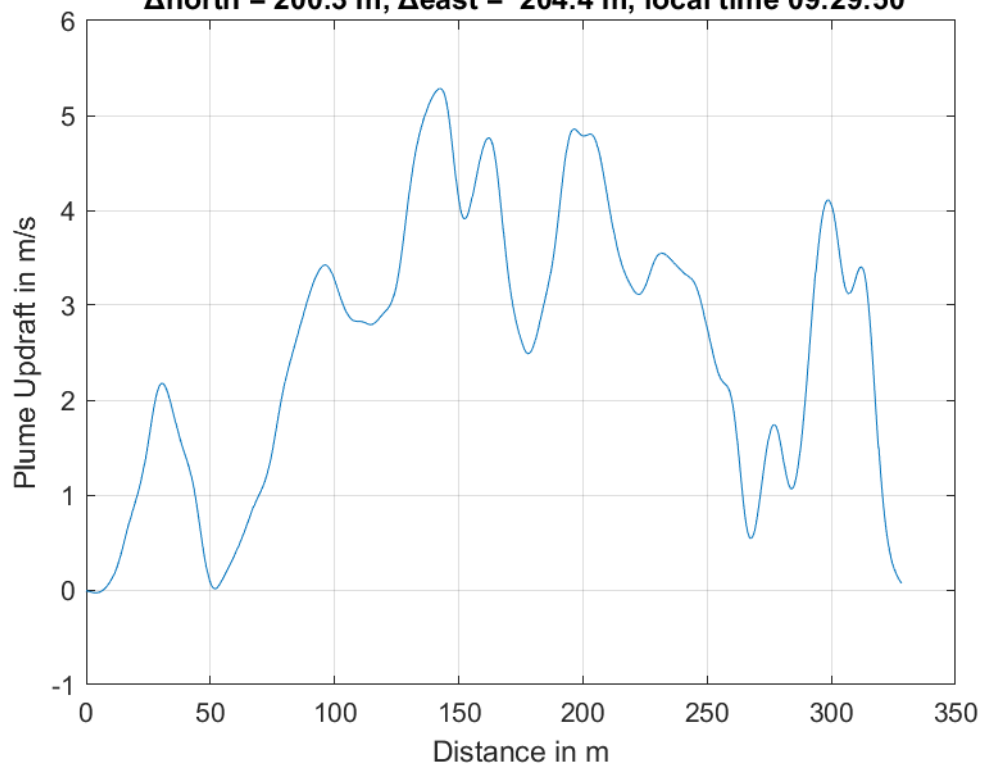




**Plume #2 at 345.4 m MSL, fly-through speed 51.0 m/s,
 $\Delta_{\text{north}} = -17.8$ m, $\Delta_{\text{east}} = 75.1$ m, local time 09:25:36**

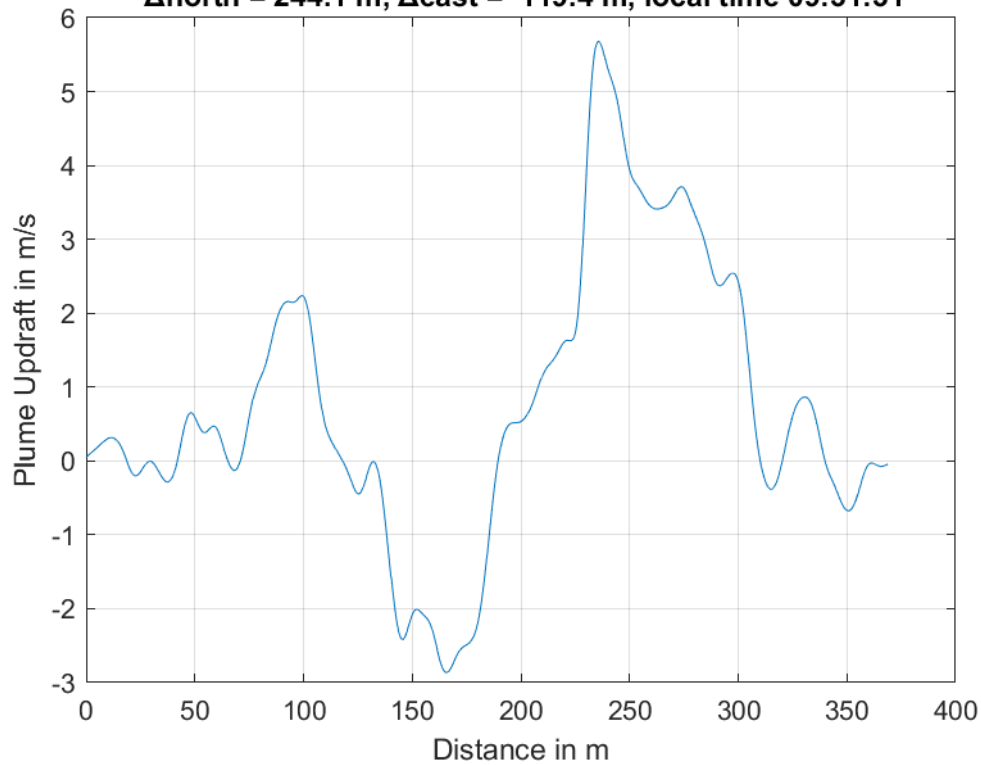


**Plume #3 at 556.9 m MSL, fly-through speed 45.0 m/s,
 $\Delta_{\text{north}} = 200.3$ m, $\Delta_{\text{east}} = 204.4$ m, local time 09:29:50**

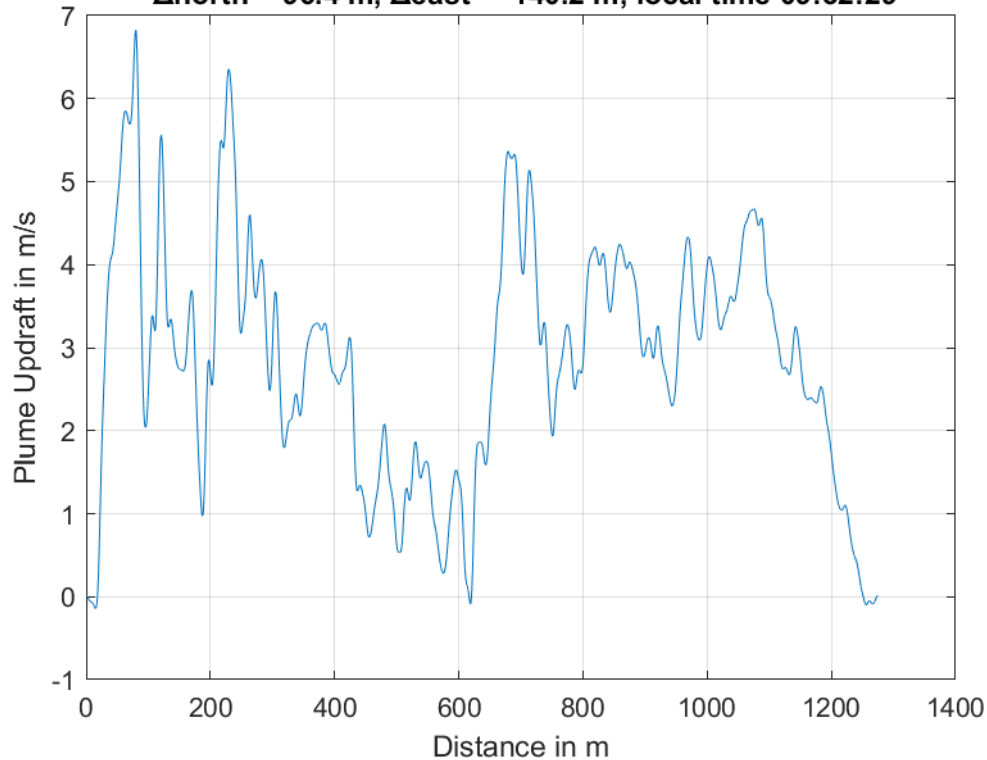




**Plume #4 at 587.3 m MSL, fly-through speed 45.0 m/s,
 $\Delta_{\text{north}} = 244.1$ m, $\Delta_{\text{east}} = 119.4$ m, local time 09:31:31**

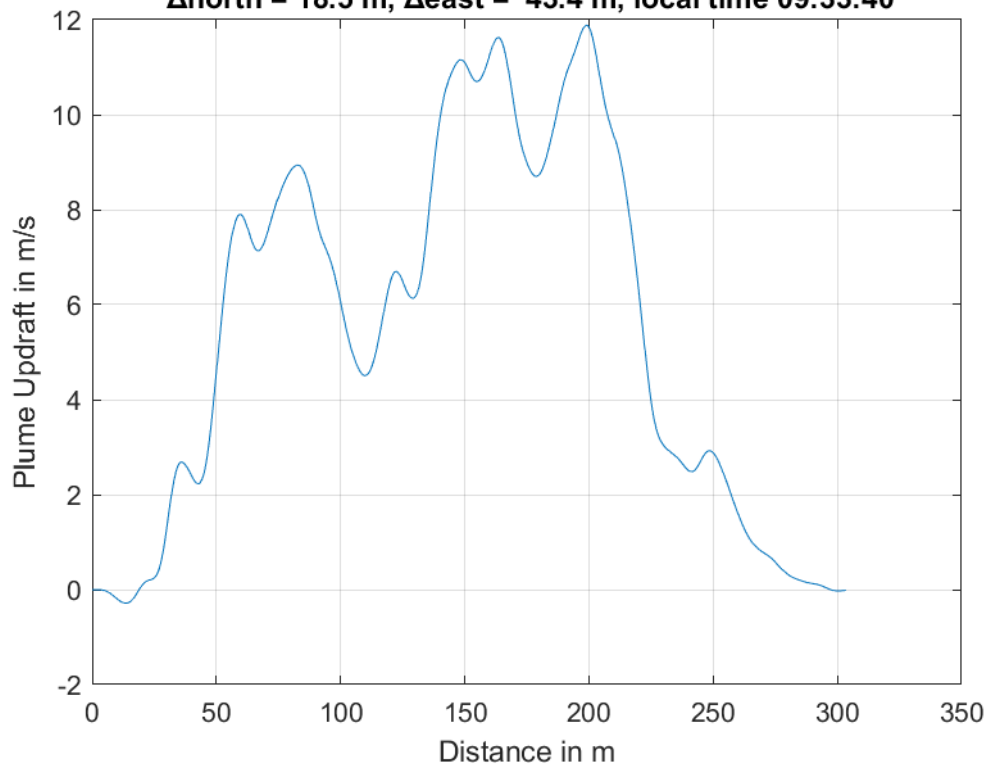


**Plume #5 at 651.6 m MSL, fly-through speed 44.0 m/s,
 $\Delta_{\text{north}} = 96.4$ m, $\Delta_{\text{east}} = 140.2$ m, local time 09:32:29**

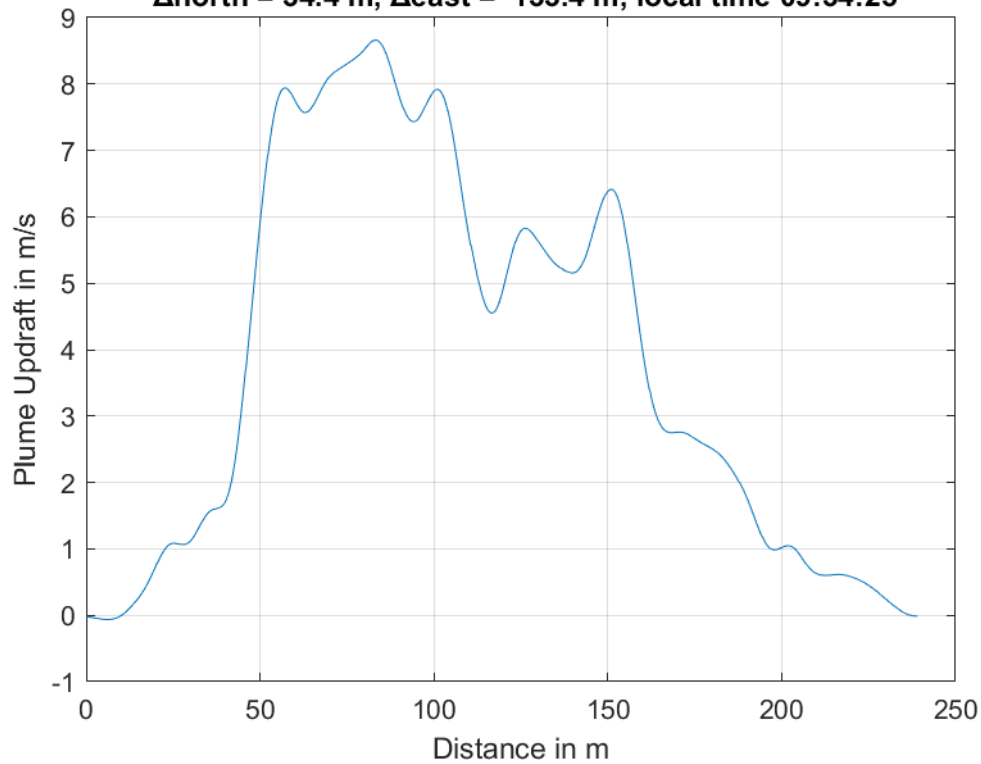




**Plume #6 at 557.6 m MSL, fly-through speed 44.0 m/s,
 $\Delta_{\text{north}} = 18.5$ m, $\Delta_{\text{east}} = 43.4$ m, local time 09:33:40**

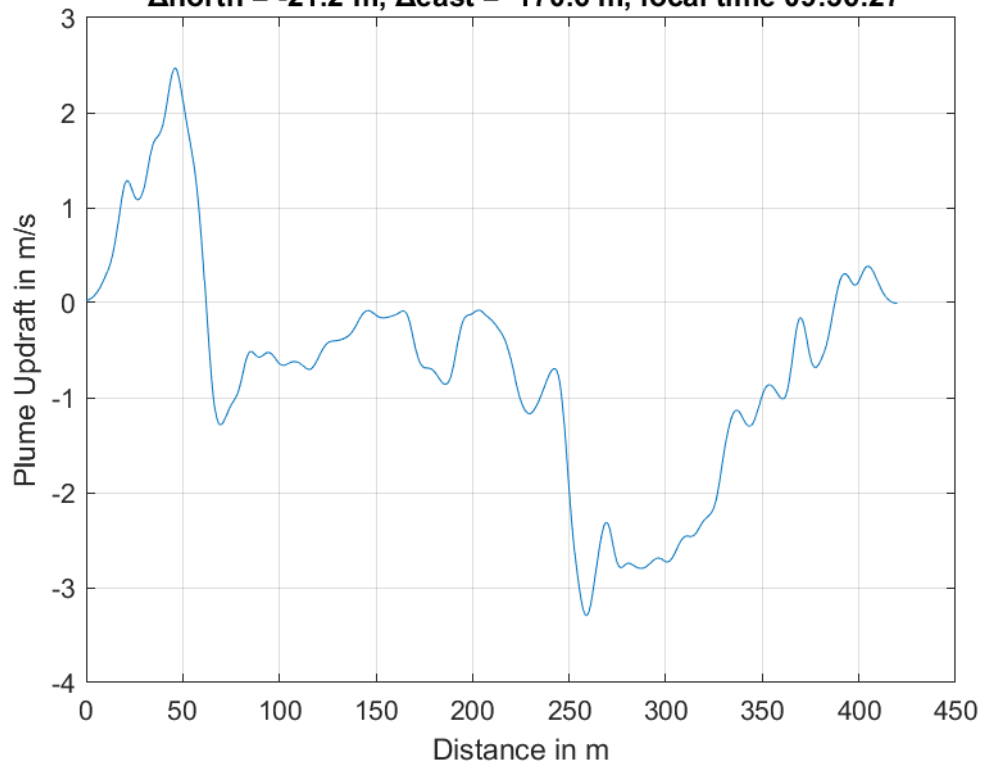


**Plume #7 at 473.1 m MSL, fly-through speed 46.0 m/s,
 $\Delta_{\text{north}} = 34.4$ m, $\Delta_{\text{east}} = 133.4$ m, local time 09:34:25**

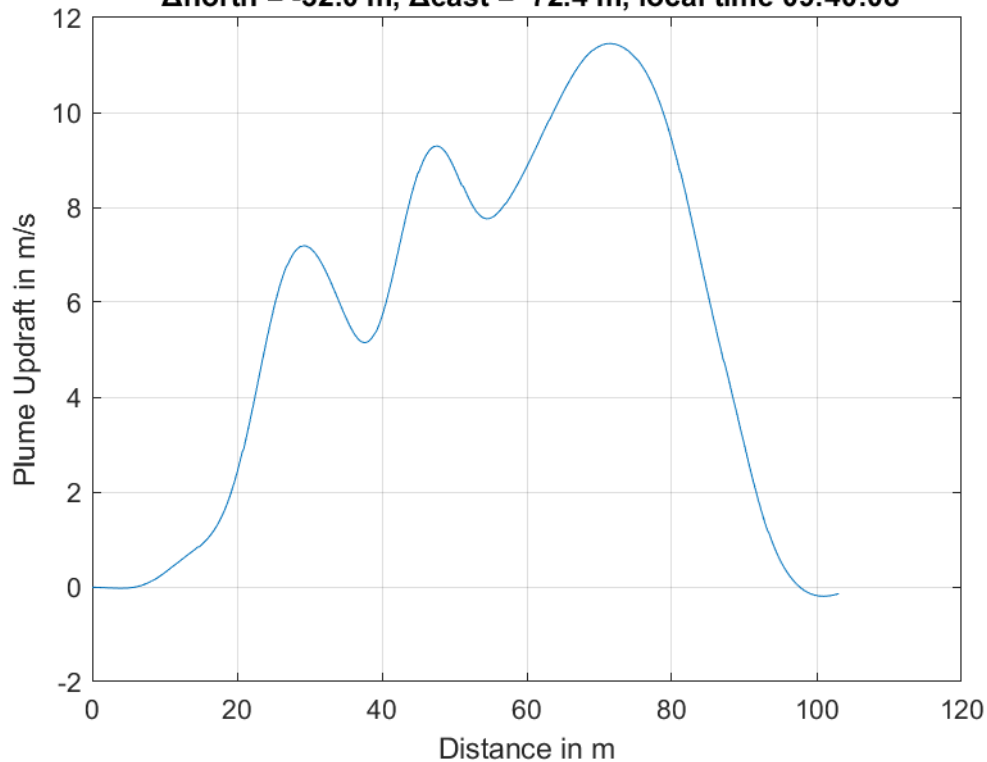




**Plume #8 at 333.2 m MSL, fly-through speed 40.0 m/s,
 $\Delta_{\text{north}} = -21.2$ m, $\Delta_{\text{east}} = 170.6$ m, local time 09:36:27**

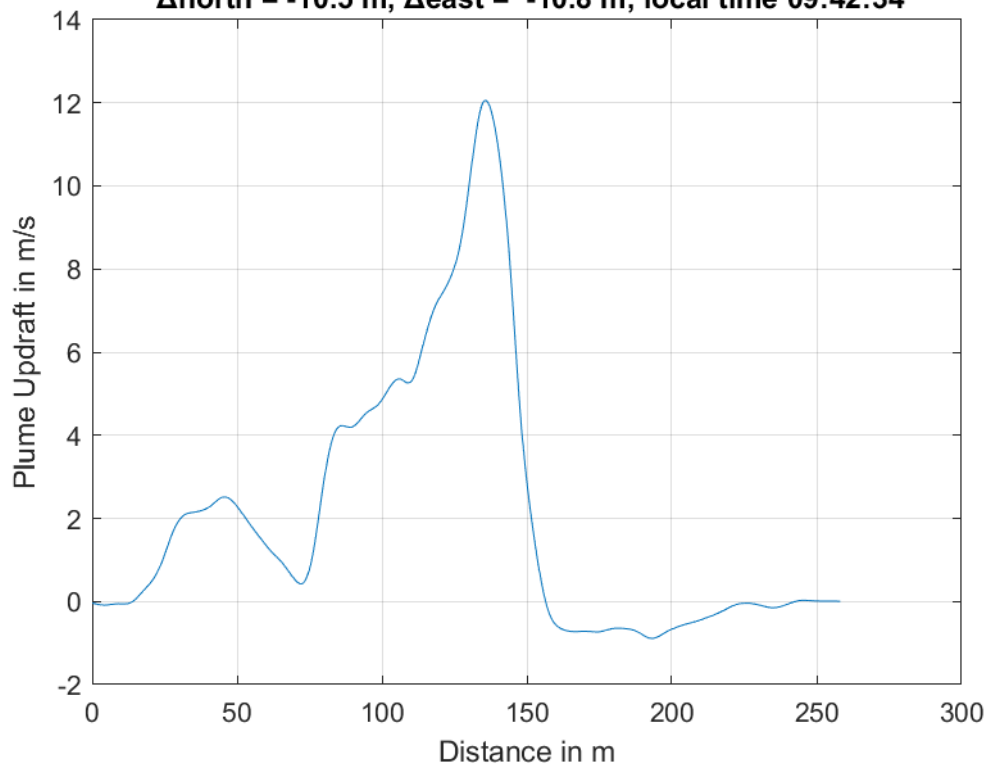


**Plume #9 at 328.5 m MSL, fly-through speed 43.0 m/s,
 $\Delta_{\text{north}} = -32.0$ m, $\Delta_{\text{east}} = 72.4$ m, local time 09:40:08**

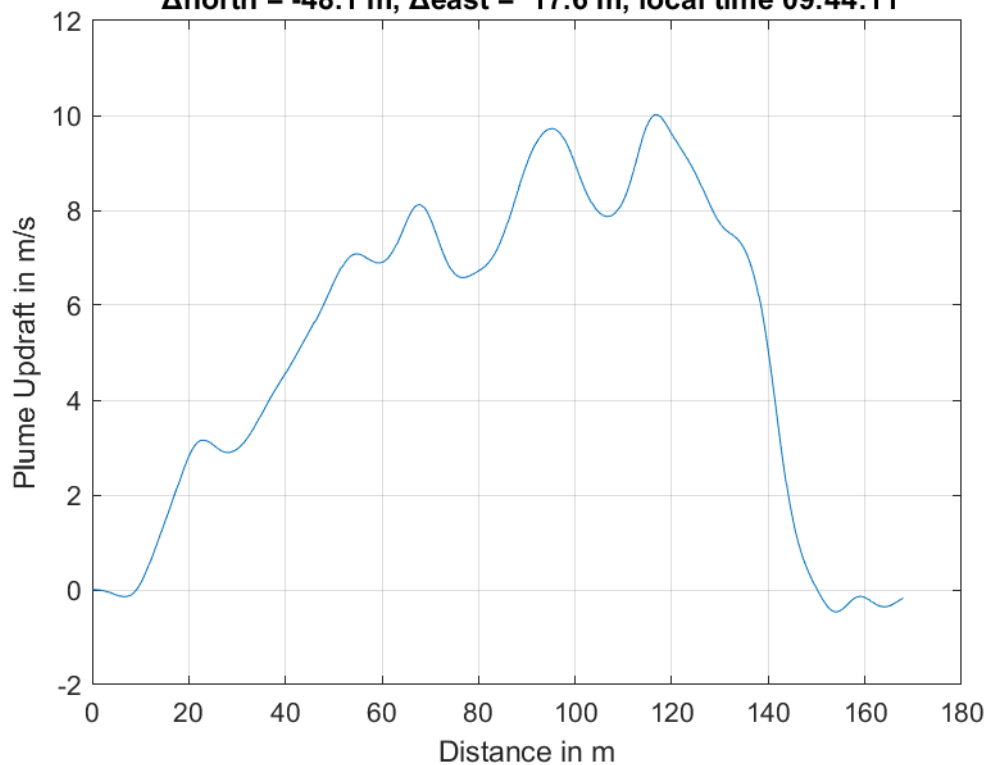




**Plume #10 at 302.8 m MSL, fly-through speed 41.0 m/s,
 $\Delta_{\text{north}} = -10.5$ m, $\Delta_{\text{east}} = -10.8$ m, local time 09:42:34**

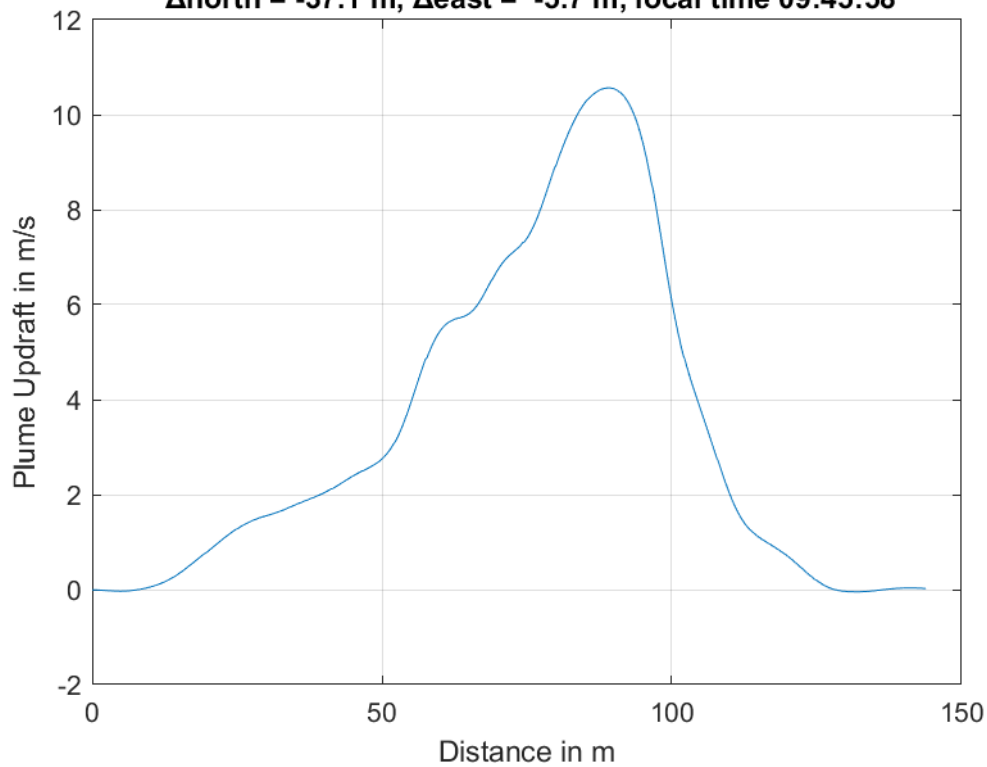


**Plume #11 at 259.5 m MSL, fly-through speed 41.0 m/s,
 $\Delta_{\text{north}} = -48.1$ m, $\Delta_{\text{east}} = 17.6$ m, local time 09:44:11**

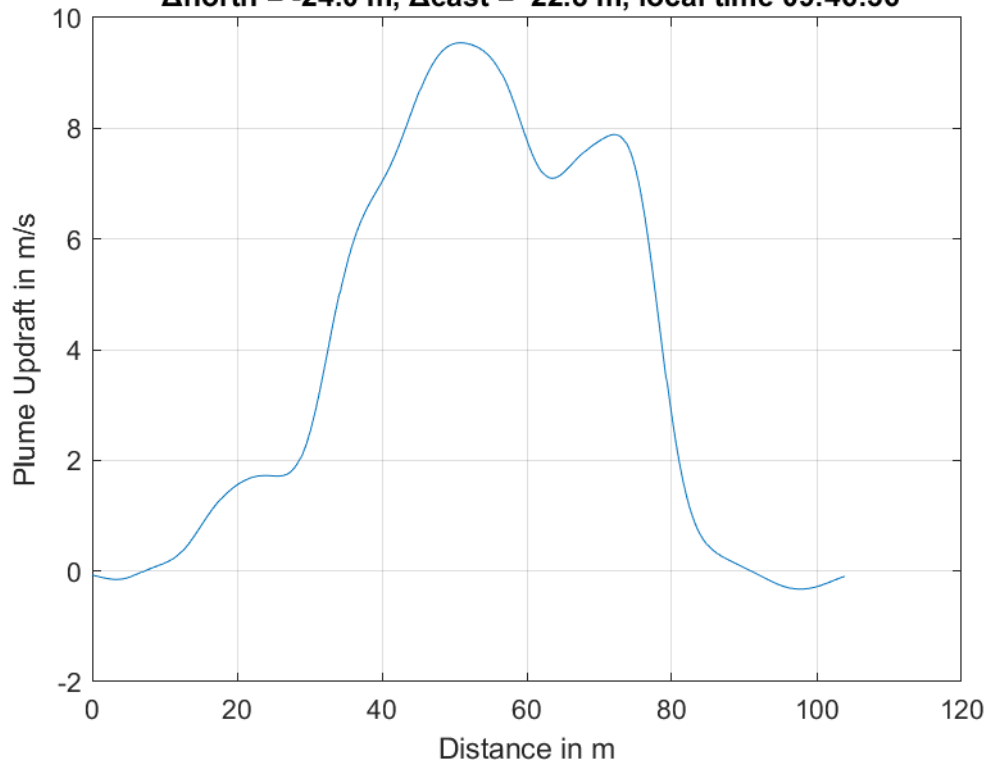




**Plume #12 at 218.1 m MSL, fly-through speed 40.0 m/s,
 $\Delta_{\text{north}} = -37.1$ m, $\Delta_{\text{east}} = -5.7$ m, local time 09:45:58**

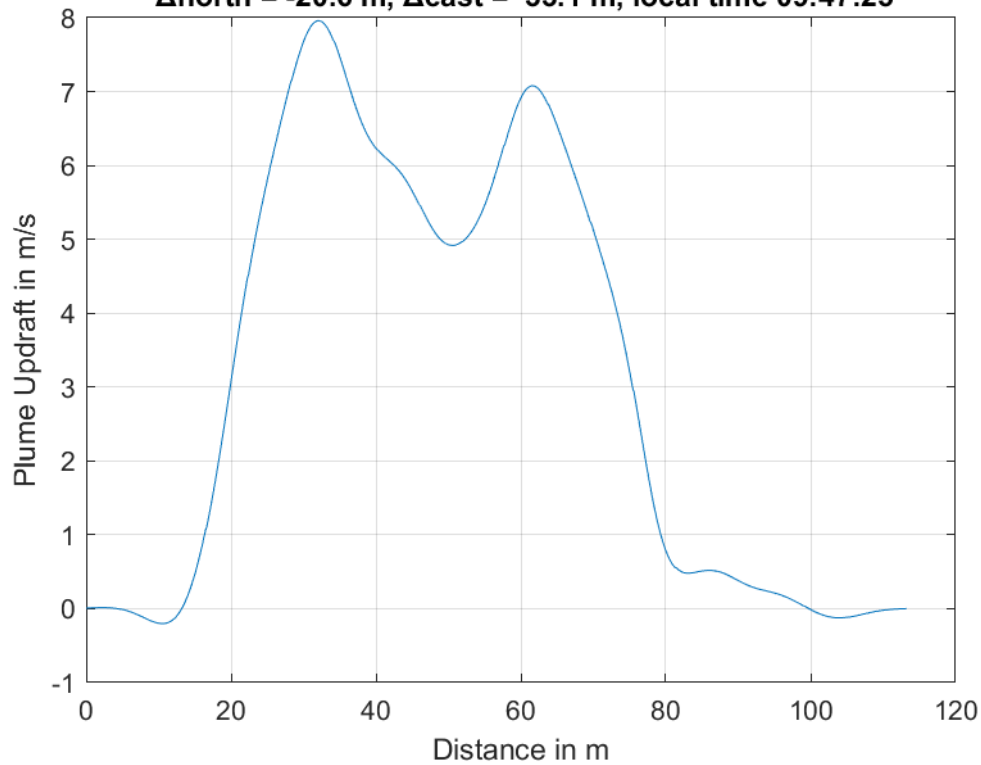


**Plume #13 at 216.9 m MSL, fly-through speed 40.0 m/s,
 $\Delta_{\text{north}} = -24.0$ m, $\Delta_{\text{east}} = 22.8$ m, local time 09:46:36**

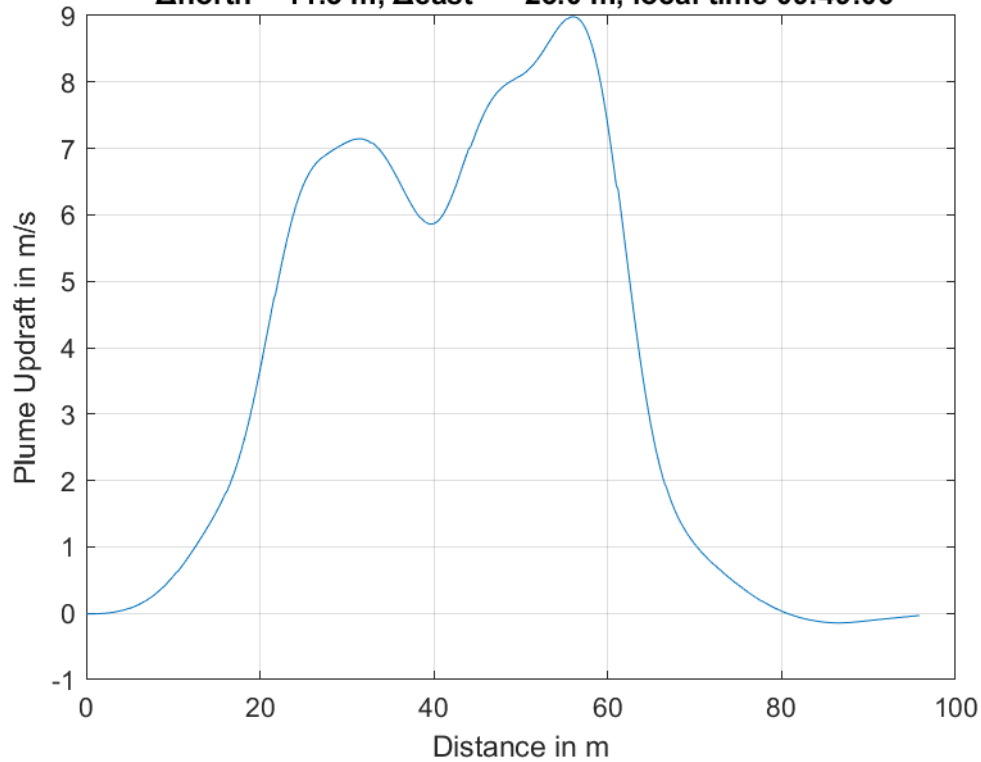




**Plume #14 at 194.2 m MSL, fly-through speed 42.0 m/s,
 $\Delta_{\text{north}} = -20.6$ m, $\Delta_{\text{east}} = 33.1$ m, local time 09:47:25**

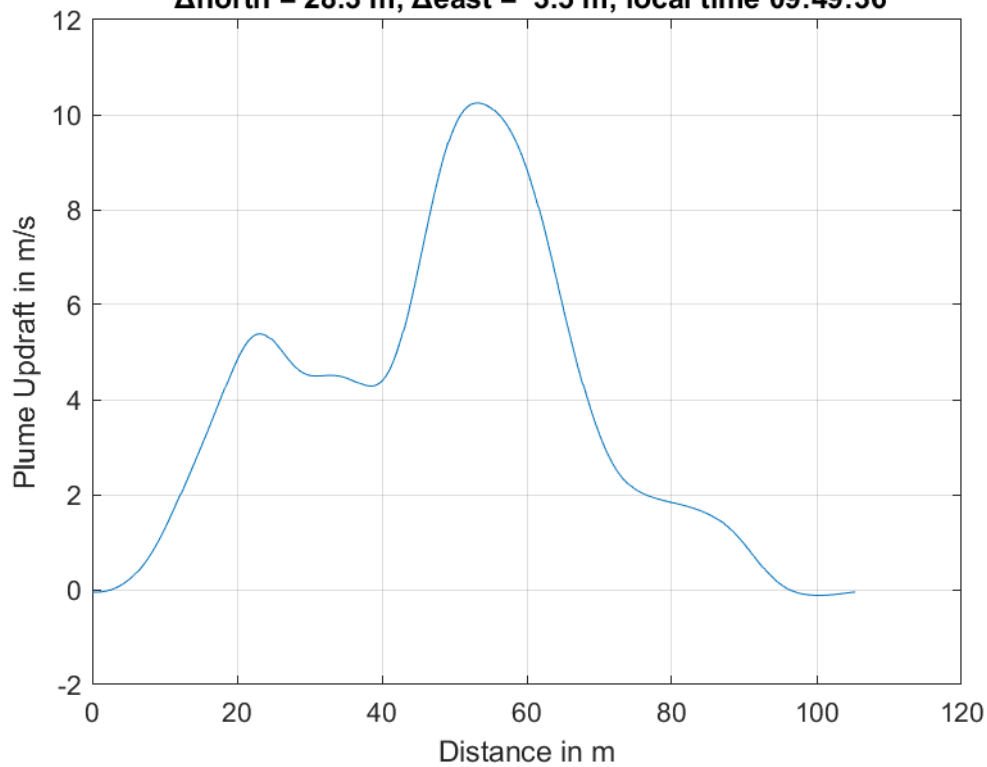


**Plume #15 at 202.0 m MSL, fly-through speed 40.0 m/s,
 $\Delta_{\text{north}} = 11.3$ m, $\Delta_{\text{east}} = -23.0$ m, local time 09:49:06**

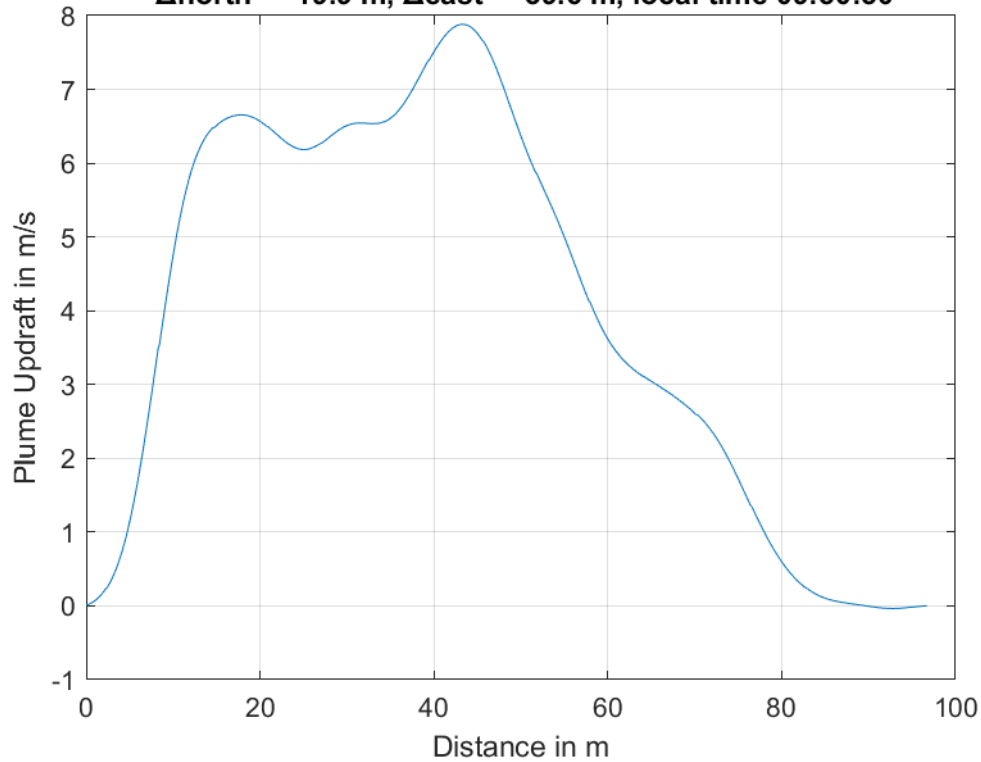




**Plume #16 at 194.3 m MSL, fly-through speed 44.0 m/s,
 $\Delta_{\text{north}} = 28.3$ m, $\Delta_{\text{east}} = 3.5$ m, local time 09:49:36**

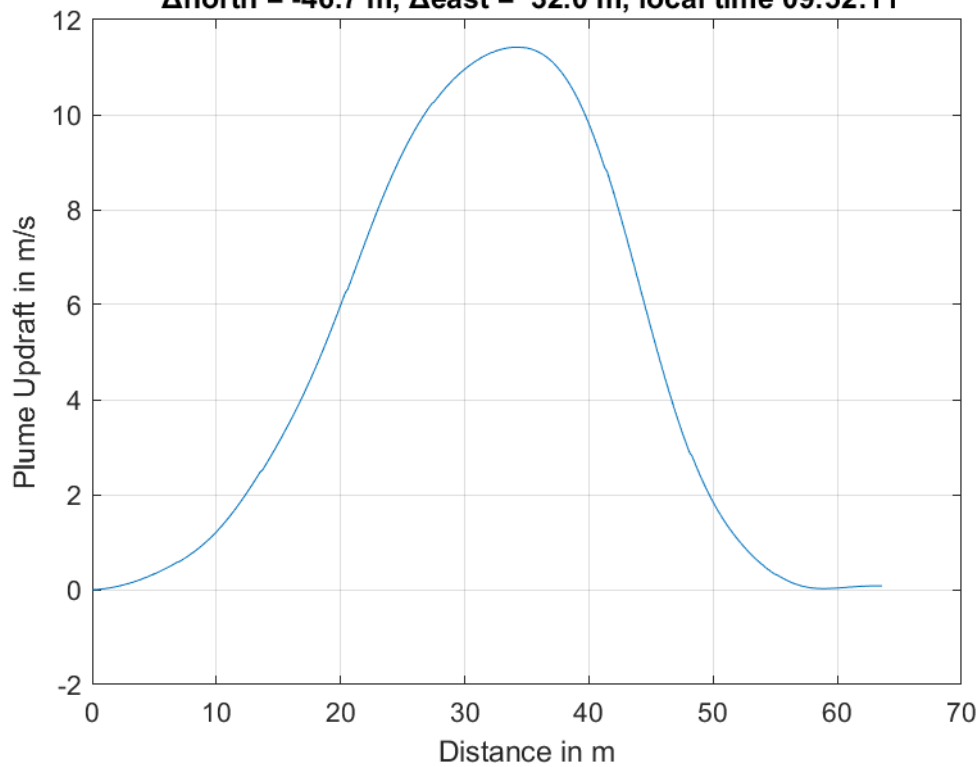


**Plume #17 at 227.1 m MSL, fly-through speed 44.0 m/s,
 $\Delta_{\text{north}} = -19.9$ m, $\Delta_{\text{east}} = 39.6$ m, local time 09:50:50**

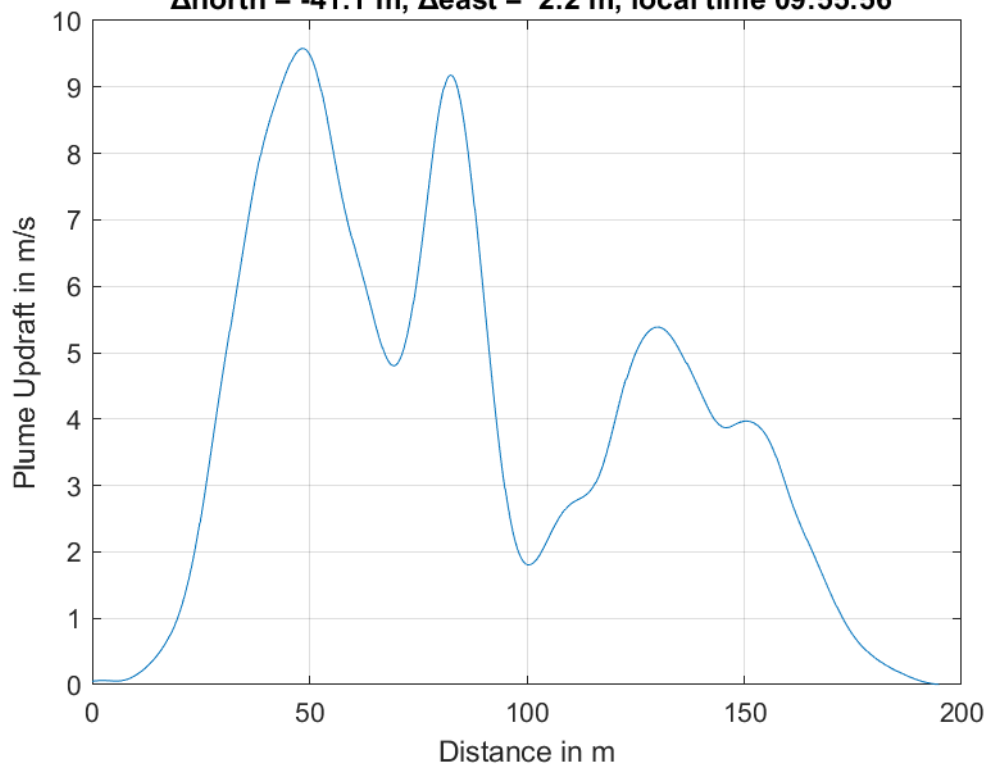




**Plume #18 at 243.7 m MSL, fly-through speed 49.0 m/s,
 $\Delta_{\text{north}} = -46.7$ m, $\Delta_{\text{east}} = 32.0$ m, local time 09:52:11**

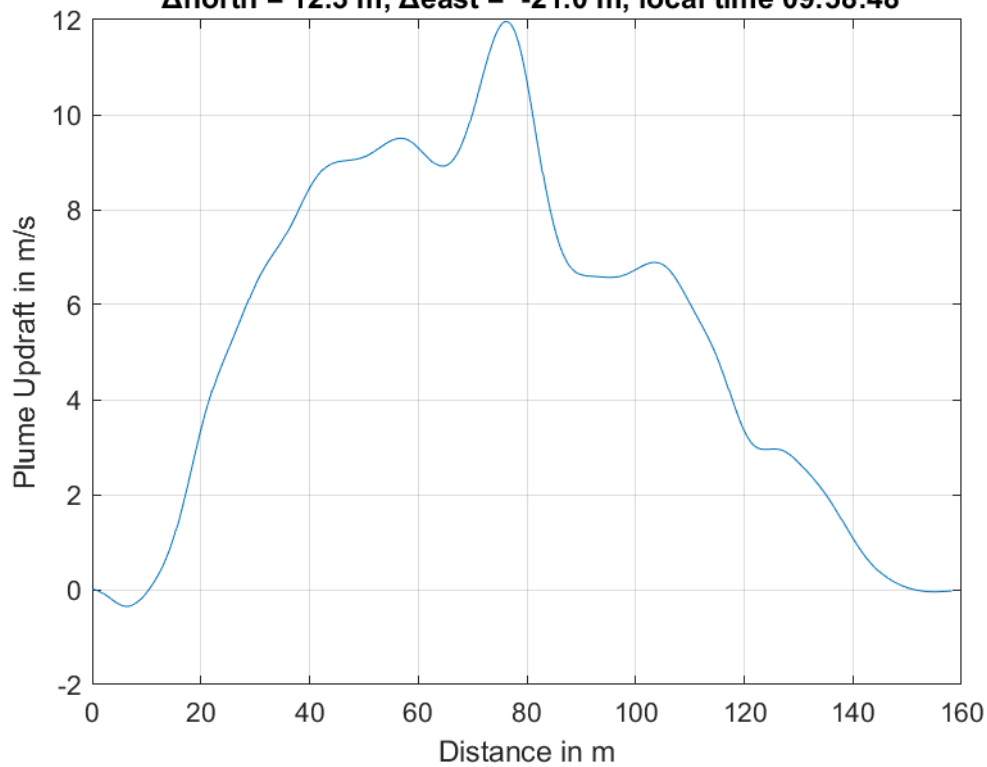


**Plume #19 at 249.7 m MSL, fly-through speed 50.0 m/s,
 $\Delta_{\text{north}} = -41.1$ m, $\Delta_{\text{east}} = 2.2$ m, local time 09:55:56**

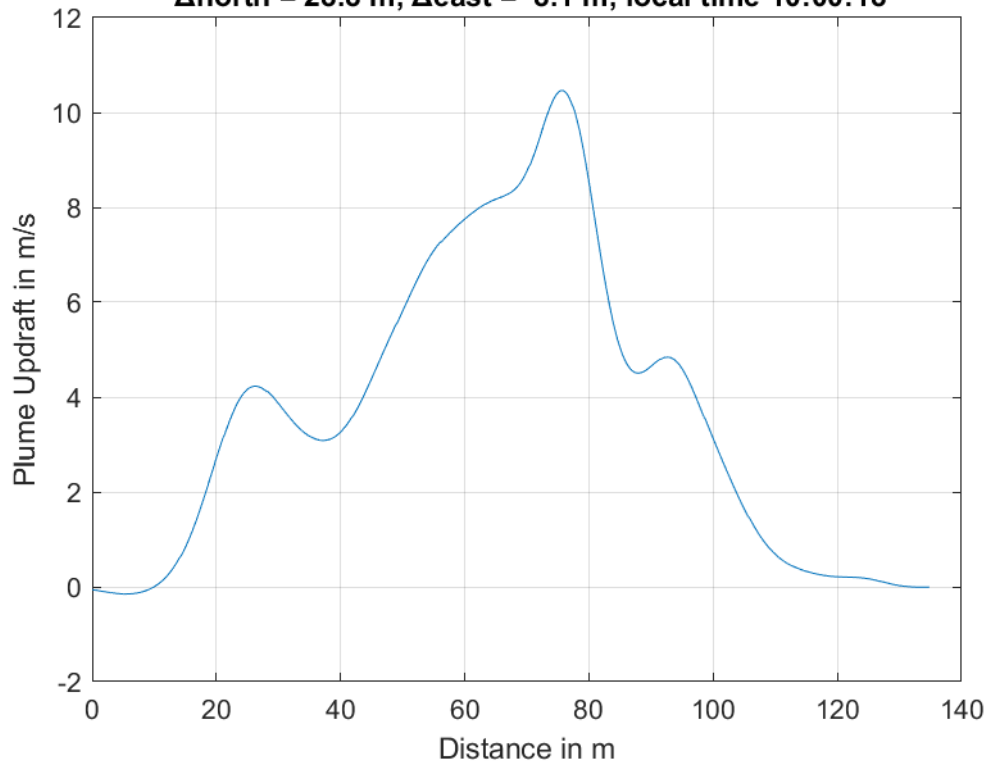




**Plume #20 at 277.7 m MSL, fly-through speed 48.0 m/s,
 $\Delta_{\text{north}} = 12.3$ m, $\Delta_{\text{east}} = -21.0$ m, local time 09:58:48**

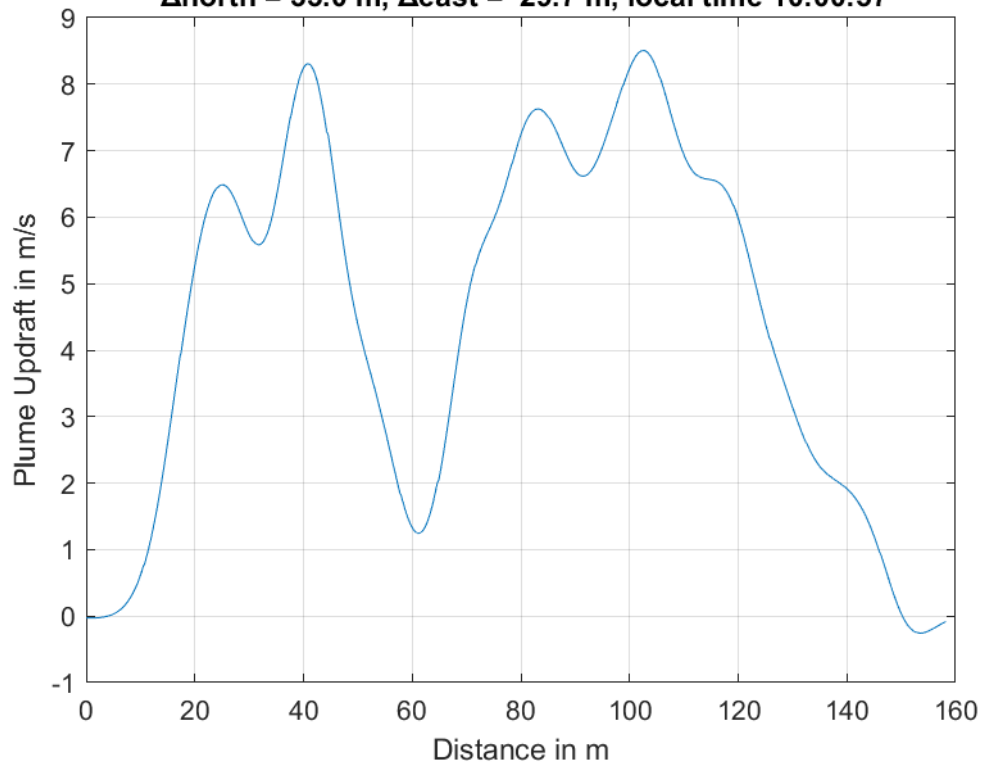


**Plume #21 at 288.3 m MSL, fly-through speed 50.0 m/s,
 $\Delta_{\text{north}} = 28.8$ m, $\Delta_{\text{east}} = 8.1$ m, local time 10:00:18**

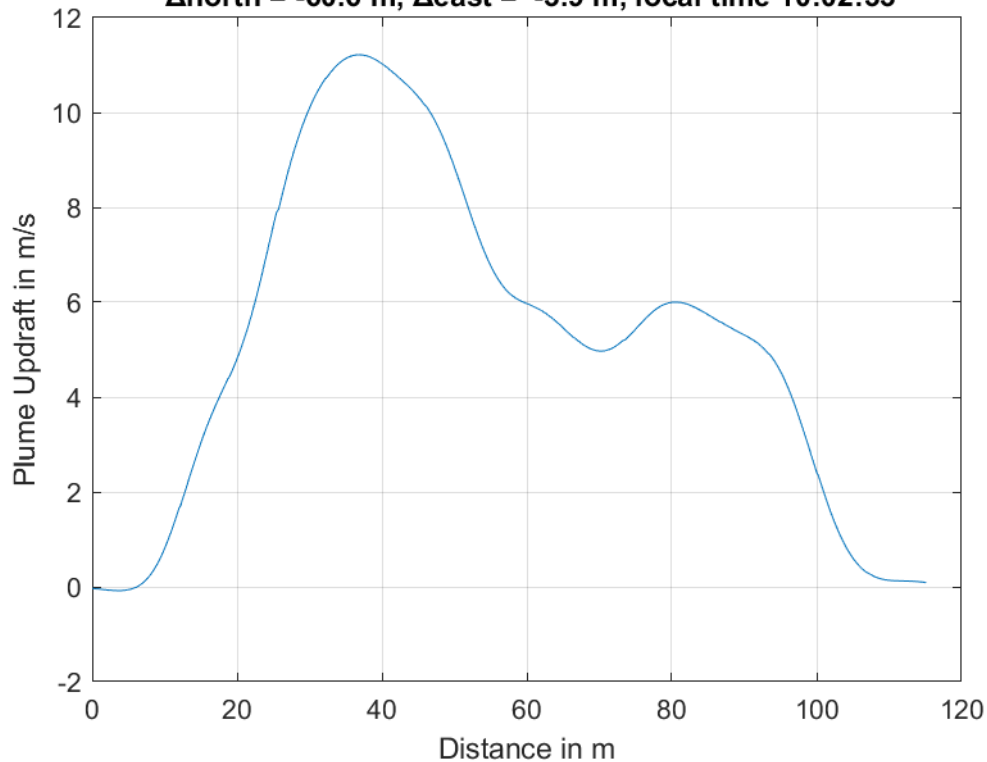




**Plume #22 at 333.2 m MSL, fly-through speed 48.0 m/s,
 $\Delta_{\text{north}} = 33.0$ m, $\Delta_{\text{east}} = 29.7$ m, local time 10:00:57**

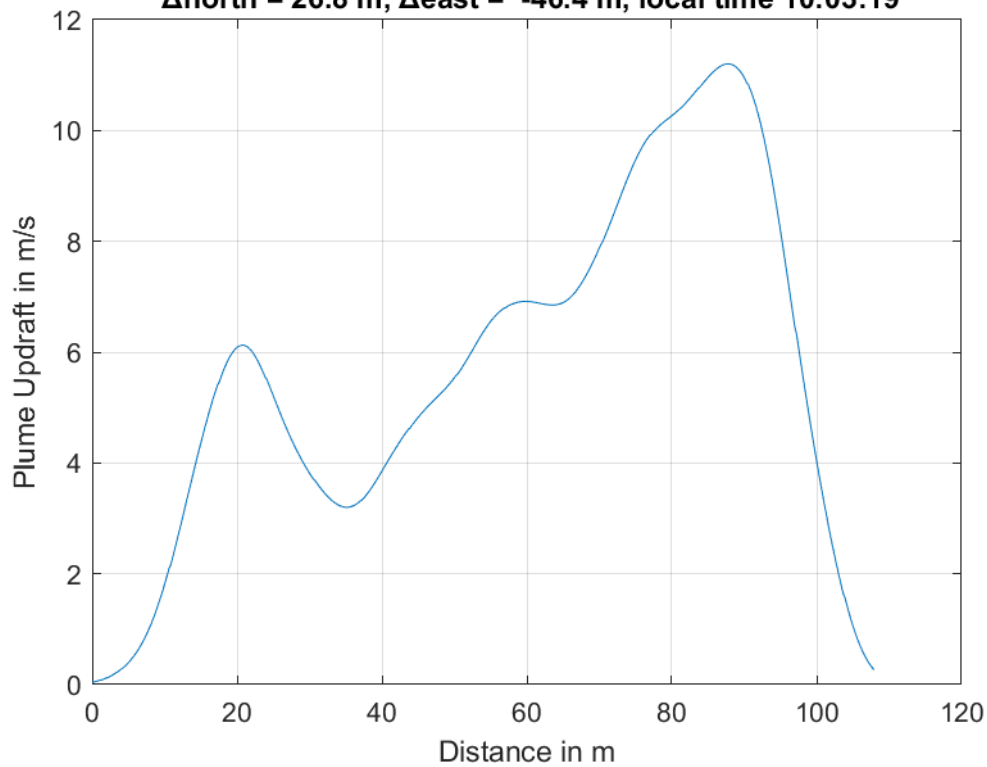


**Plume #23 at 356.8 m MSL, fly-through speed 48.0 m/s,
 $\Delta_{\text{north}} = -60.6$ m, $\Delta_{\text{east}} = -3.9$ m, local time 10:02:33**

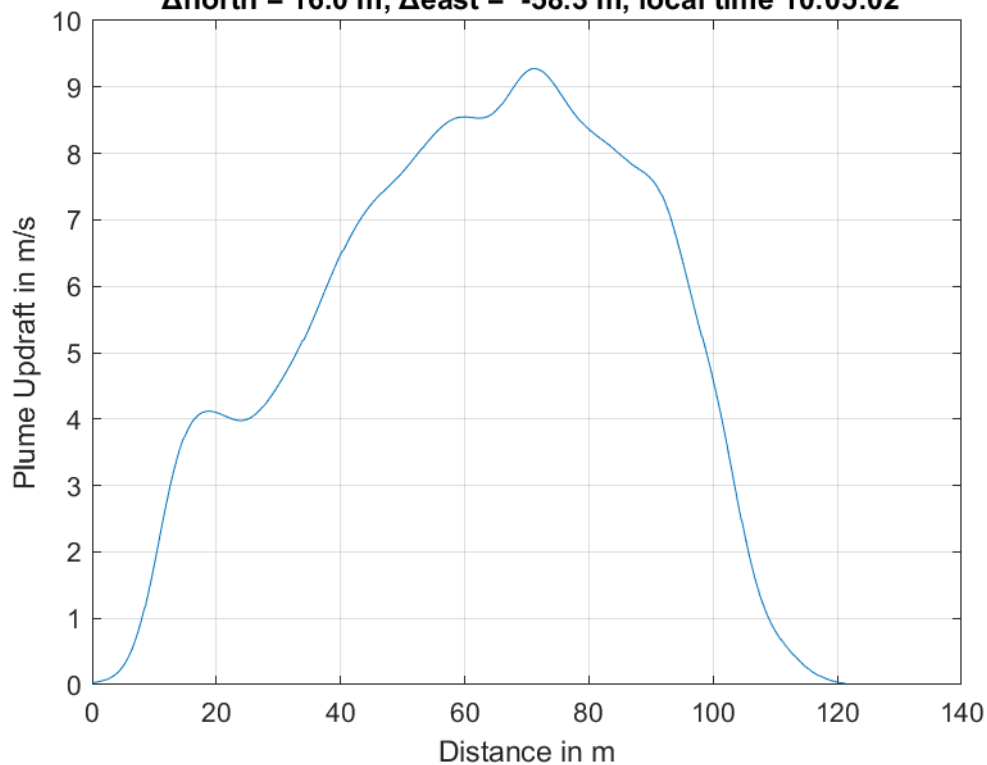




**Plume #24 at 360.1 m MSL, fly-through speed 47.0 m/s,
 $\Delta_{\text{north}} = 26.8$ m, $\Delta_{\text{east}} = -46.4$ m, local time 10:03:19**

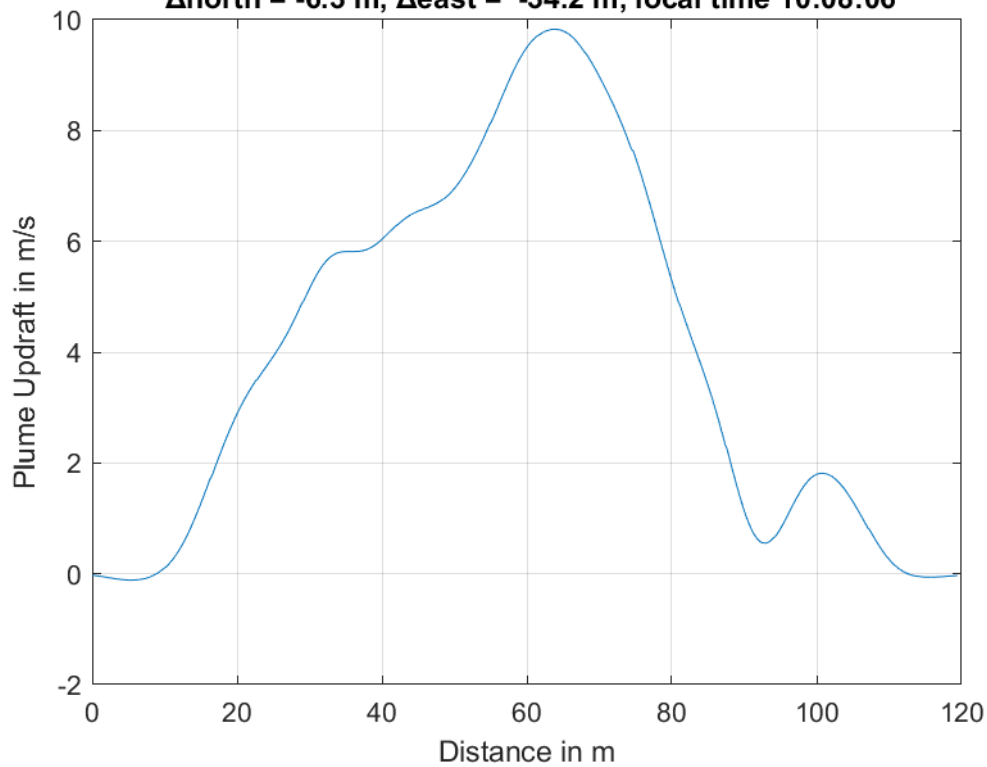


**Plume #25 at 389.6 m MSL, fly-through speed 45.0 m/s,
 $\Delta_{\text{north}} = 16.0$ m, $\Delta_{\text{east}} = -58.3$ m, local time 10:05:02**

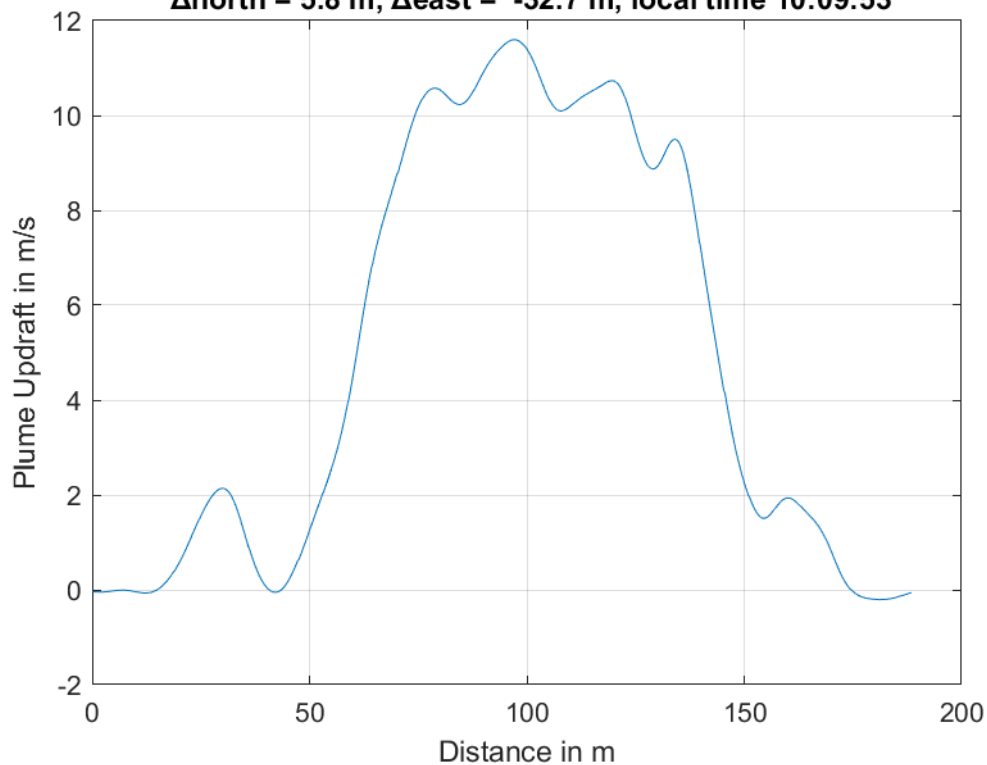




**Plume #26 at 299.1 m MSL, fly-through speed 46.0 m/s,
 $\Delta_{\text{north}} = -6.3$ m, $\Delta_{\text{east}} = -34.2$ m, local time 10:08:06**

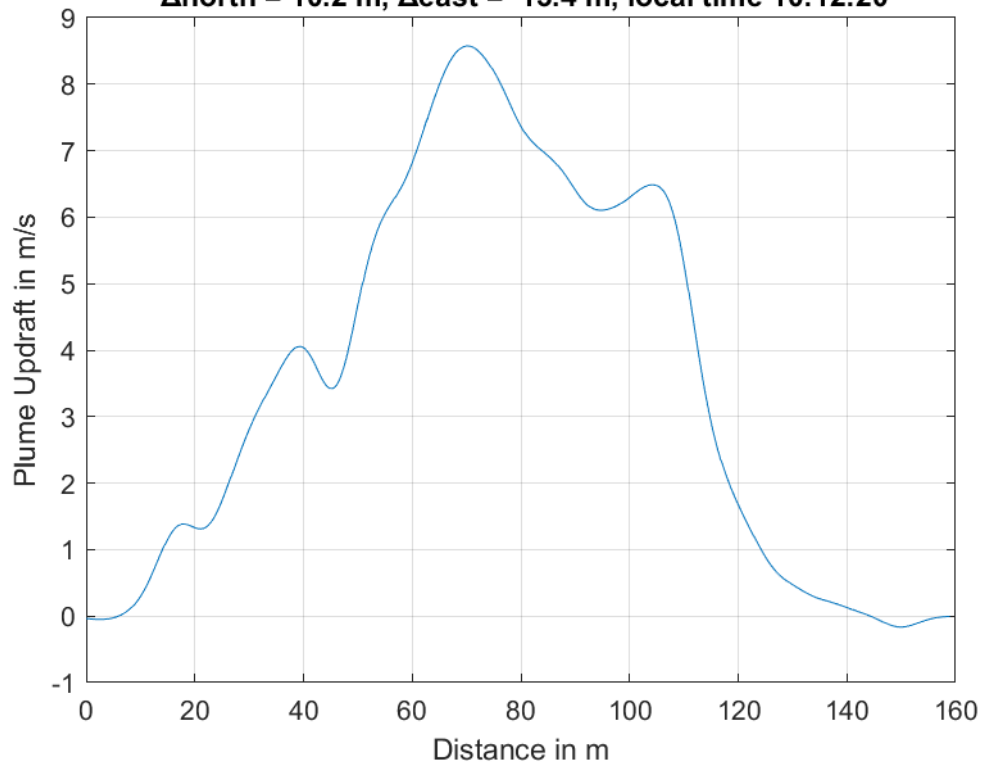


**Plume #27 at 290.9 m MSL, fly-through speed 41.0 m/s,
 $\Delta_{\text{north}} = 5.8$ m, $\Delta_{\text{east}} = -32.7$ m, local time 10:09:53**

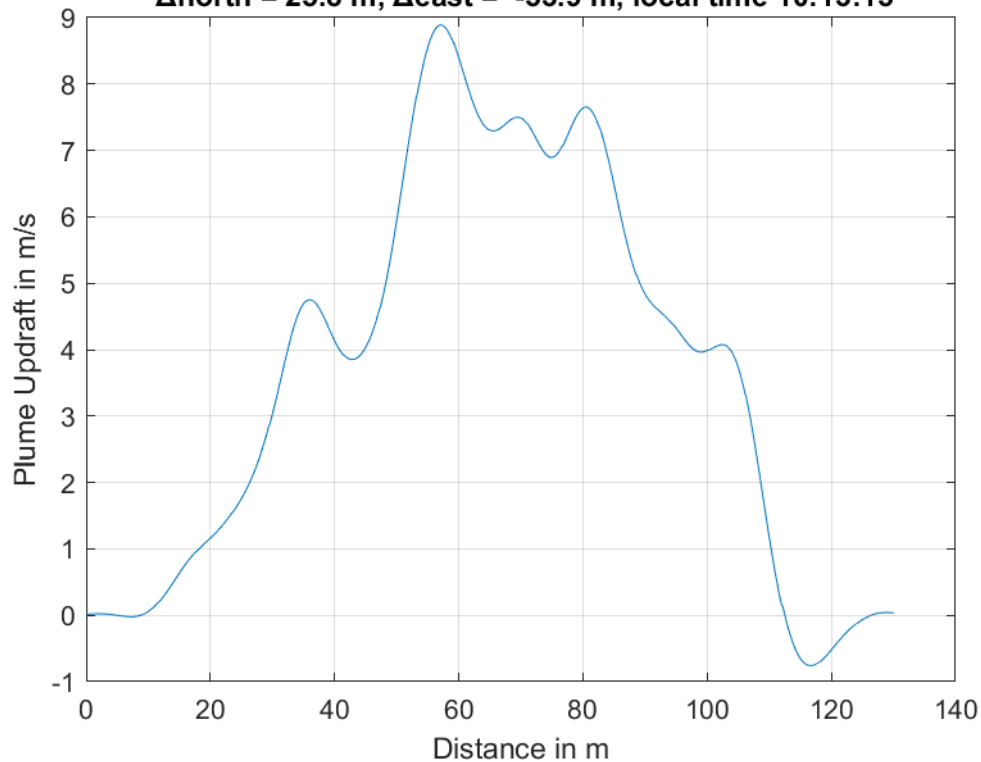




**Plume #28 at 267.2 m MSL, fly-through speed 43.0 m/s,
 $\Delta_{\text{north}} = 10.2$ m, $\Delta_{\text{east}} = 13.4$ m, local time 10:12:20**

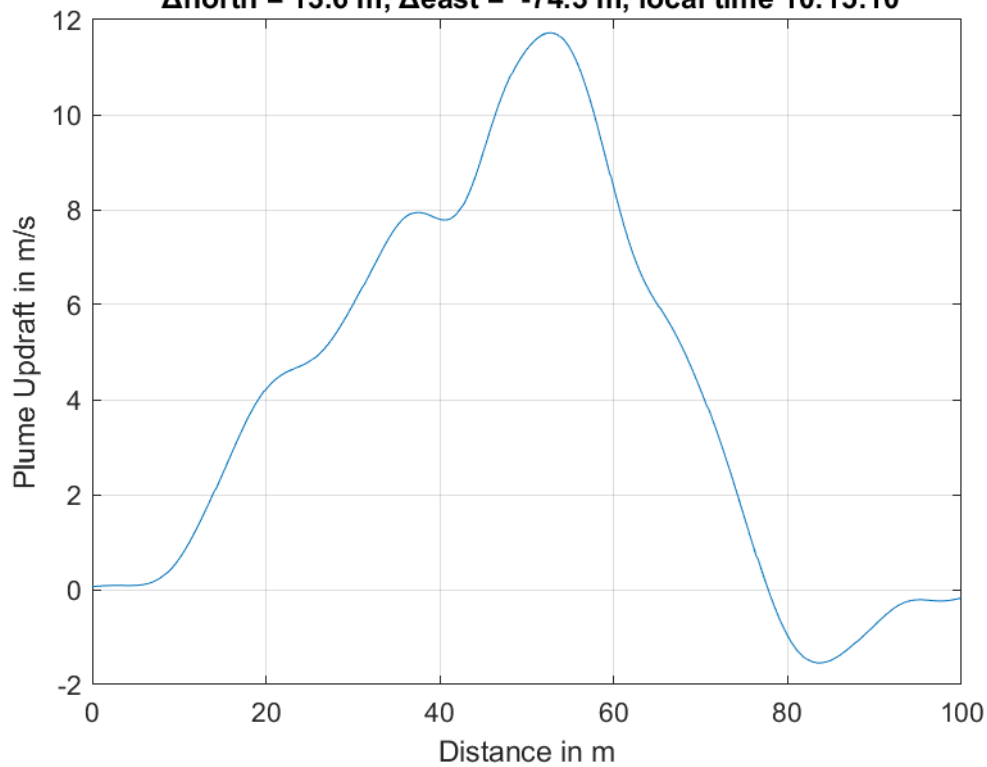


**Plume #29 at 246.1 m MSL, fly-through speed 42.0 m/s,
 $\Delta_{\text{north}} = 25.8$ m, $\Delta_{\text{east}} = -53.9$ m, local time 10:13:15**

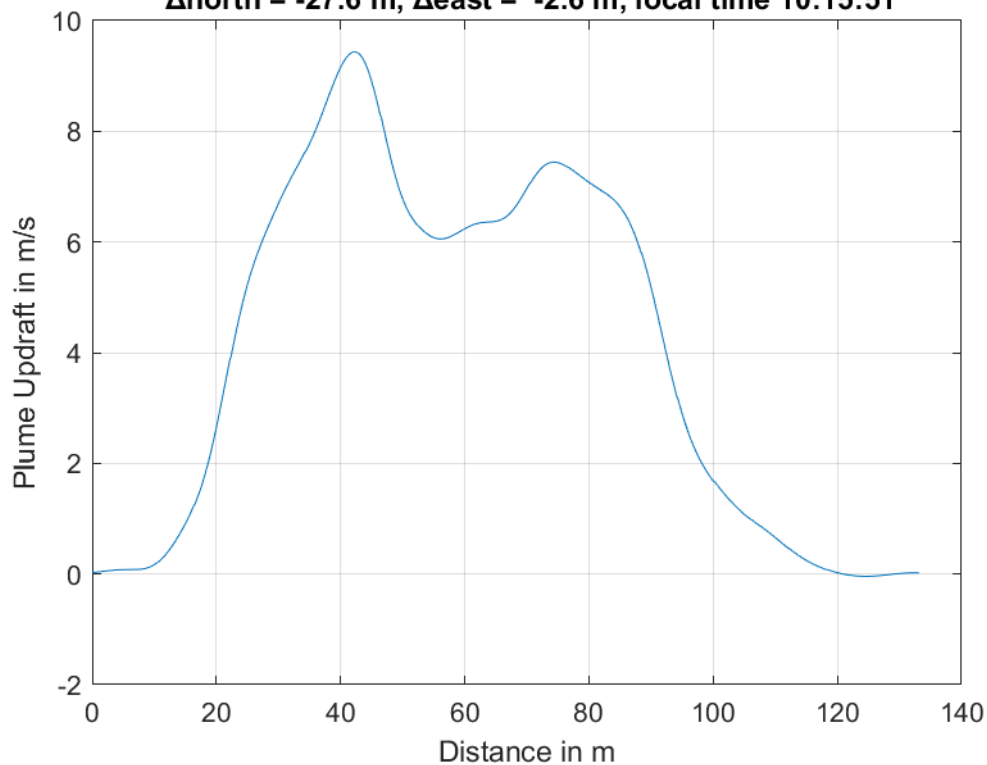




**Plume #30 at 219.4 m MSL, fly-through speed 40.0 m/s,
 $\Delta_{\text{north}} = 13.6$ m, $\Delta_{\text{east}} = -74.3$ m, local time 10:15:10**

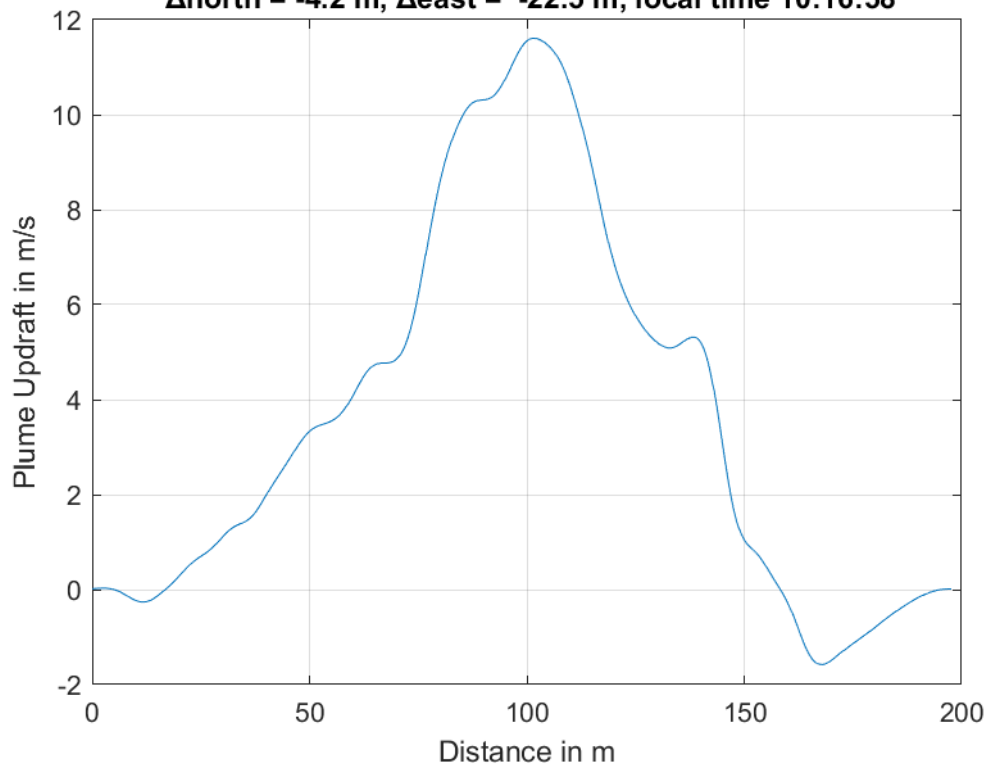


**Plume #31 at 232.3 m MSL, fly-through speed 43.0 m/s,
 $\Delta_{\text{north}} = -27.6$ m, $\Delta_{\text{east}} = -2.6$ m, local time 10:15:51**

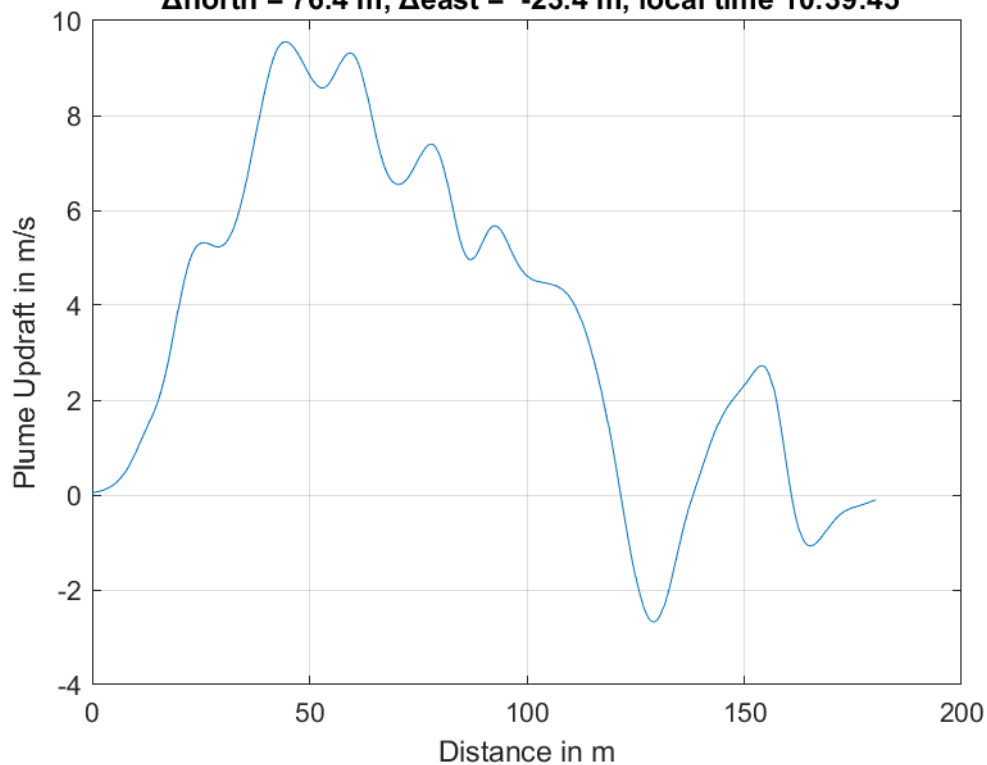




**Plume #32 at 203.0 m MSL, fly-through speed 43.0 m/s,
 $\Delta_{\text{north}} = -4.2$ m, $\Delta_{\text{east}} = -22.5$ m, local time 10:16:58**

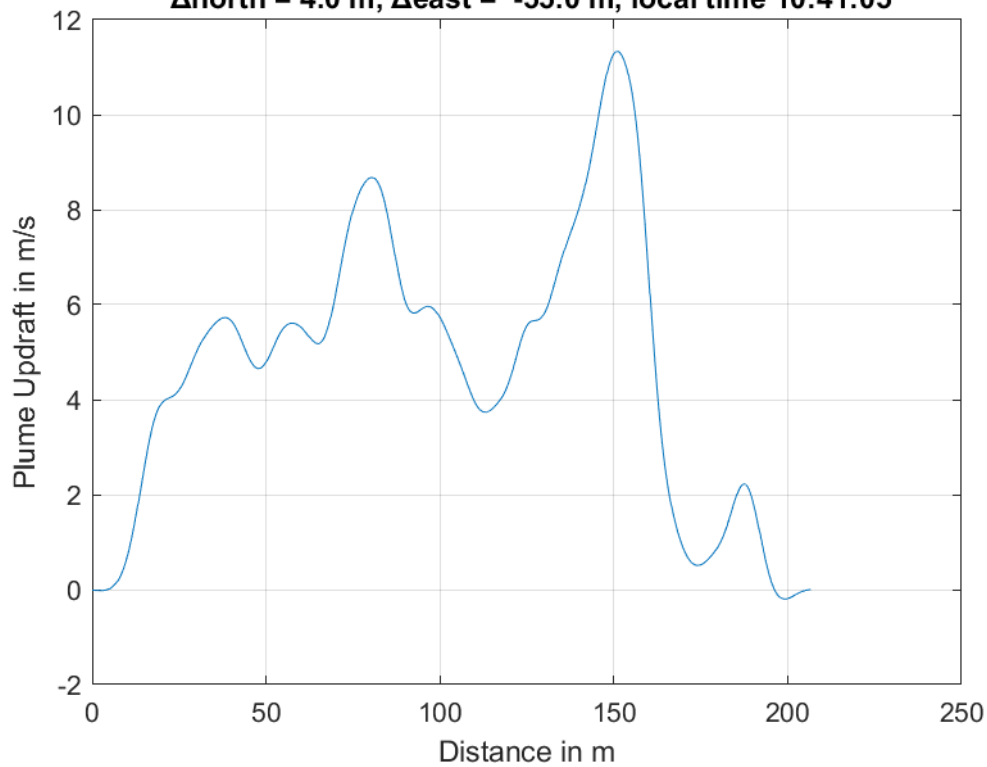


**Plume #33 at 270.0 m MSL, fly-through speed 44.0 m/s,
 $\Delta_{\text{north}} = 76.4$ m, $\Delta_{\text{east}} = -23.4$ m, local time 10:39:45**

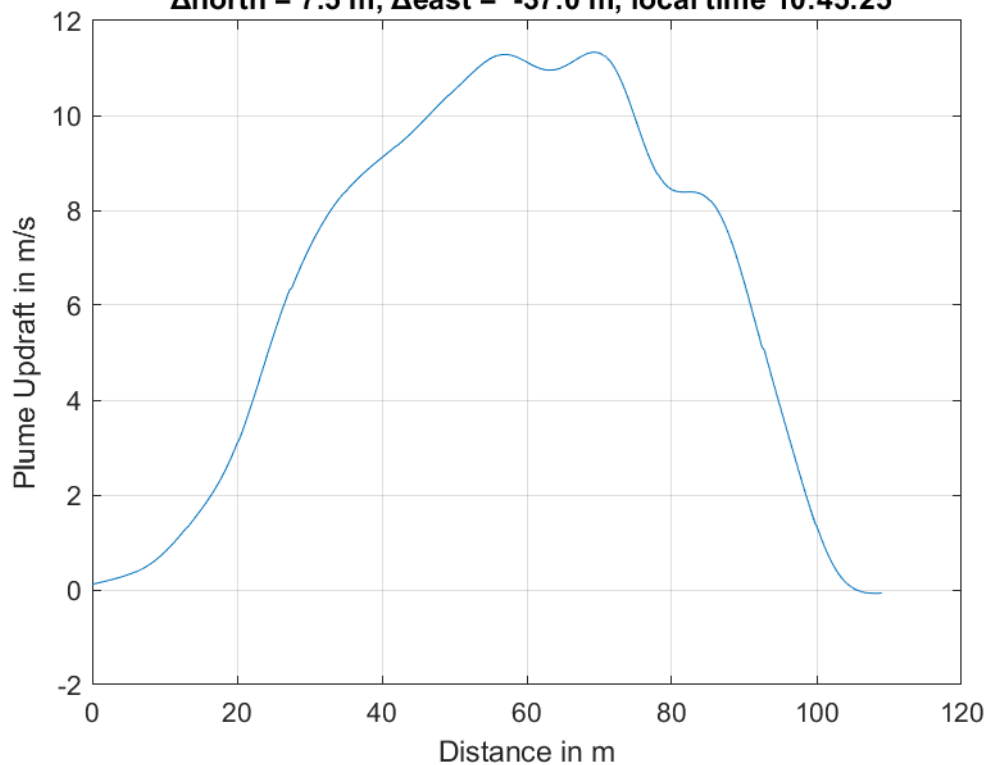




**Plume #34 at 279.5 m MSL, fly-through speed 44.0 m/s,
 $\Delta_{\text{north}} = 4.0$ m, $\Delta_{\text{east}} = -55.0$ m, local time 10:41:05**

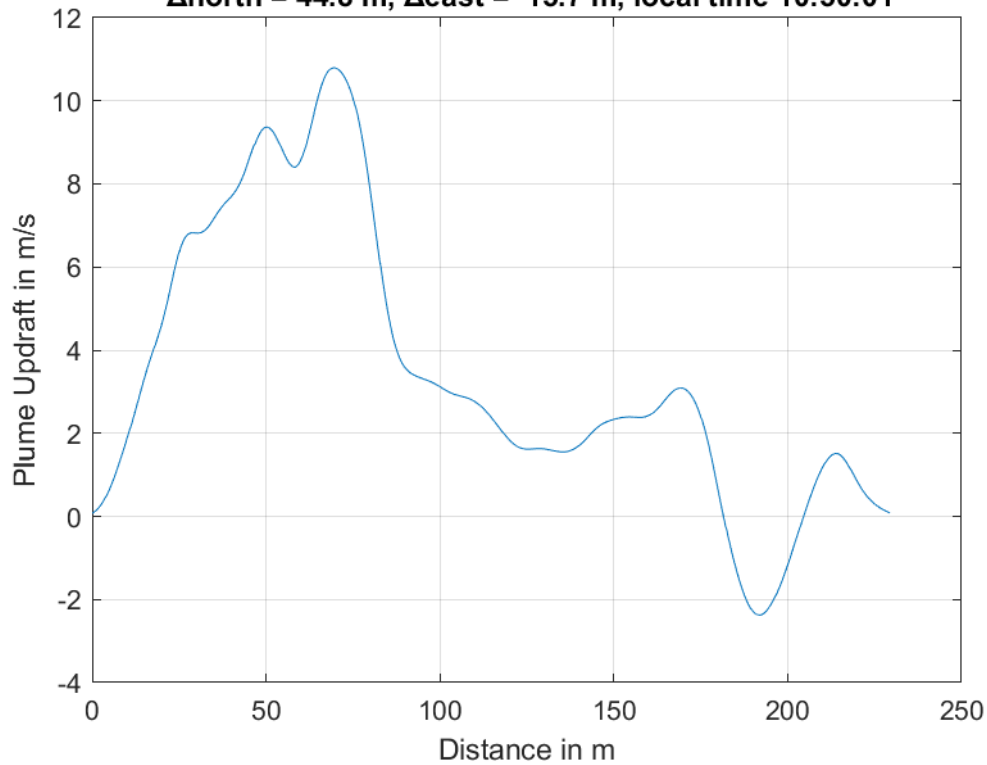


**Plume #35 at 215.9 m MSL, fly-through speed 52.0 m/s,
 $\Delta_{\text{north}} = 7.5$ m, $\Delta_{\text{east}} = -37.0$ m, local time 10:45:25**

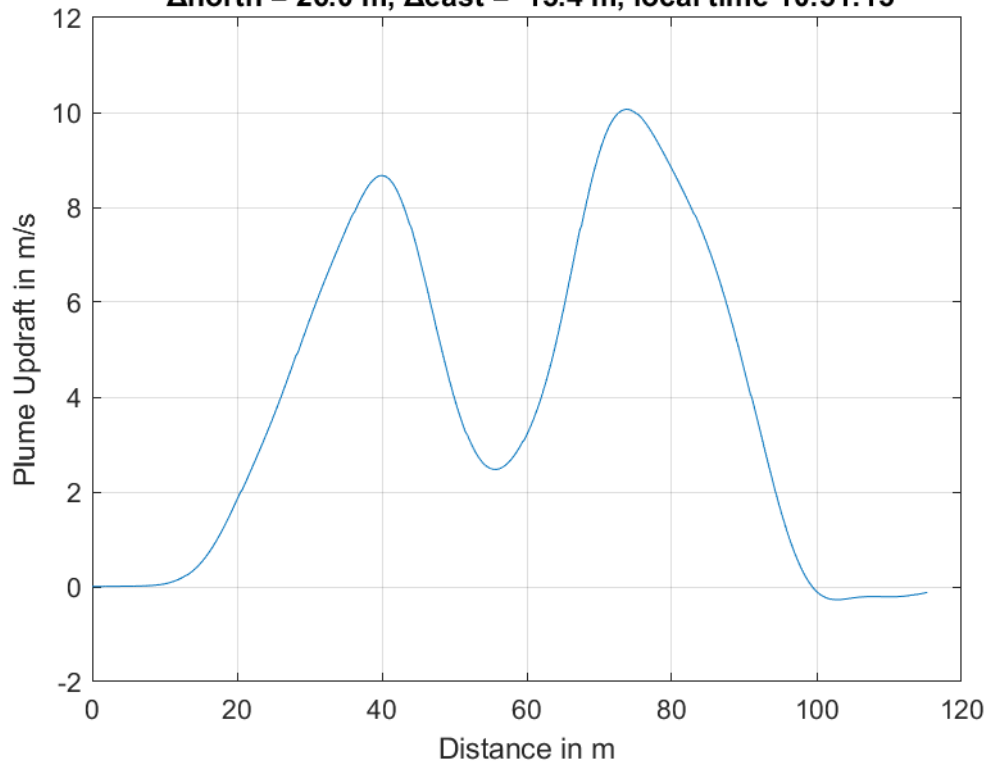




**Plume #36 at 283.0 m MSL, fly-through speed 51.0 m/s,
 $\Delta_{\text{north}} = 44.8$ m, $\Delta_{\text{east}} = 15.7$ m, local time 10:50:01**

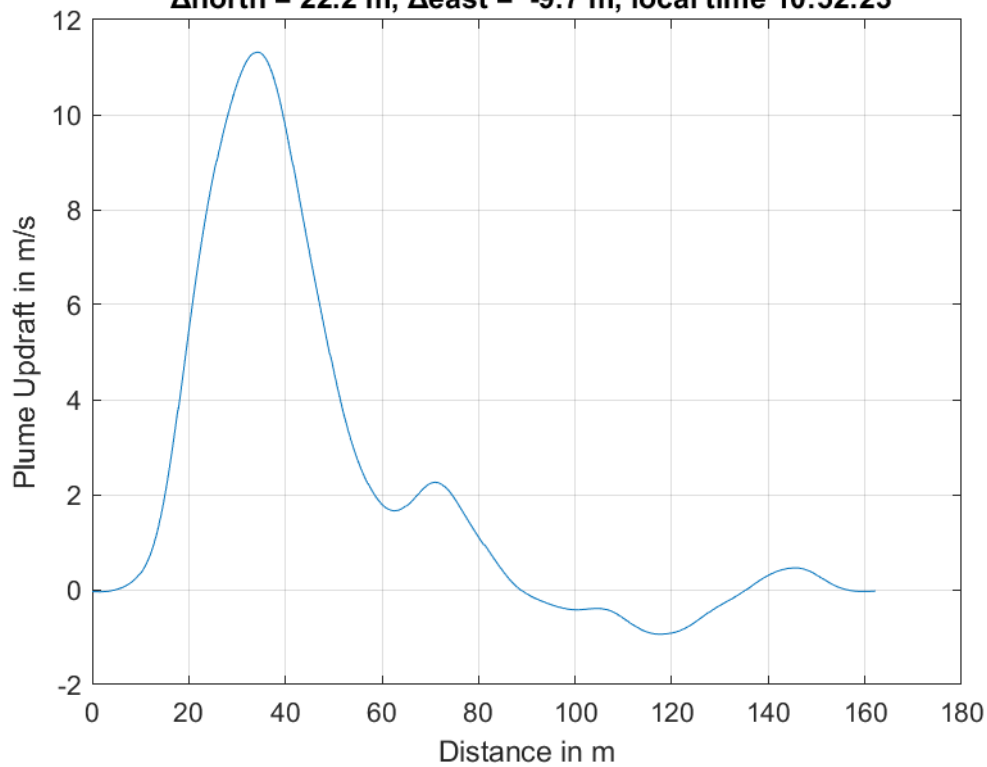


**Plume #37 at 310.5 m MSL, fly-through speed 55.0 m/s,
 $\Delta_{\text{north}} = 26.0$ m, $\Delta_{\text{east}} = 15.4$ m, local time 10:51:15**

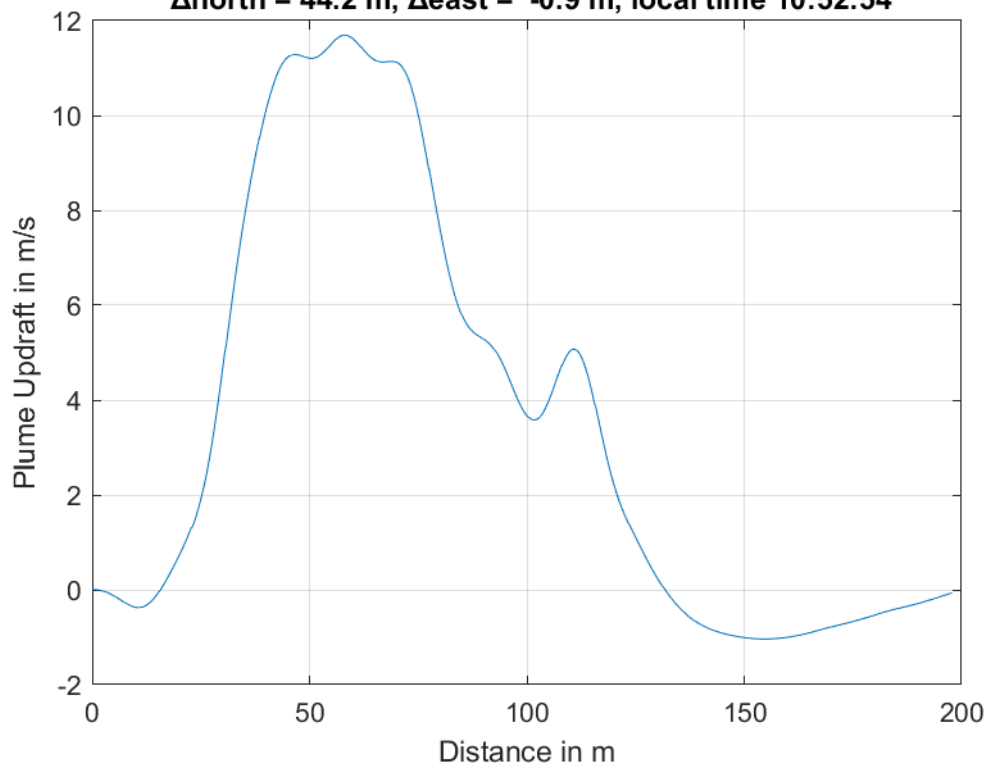




**Plume #38 at 341.2 m MSL, fly-through speed 56.0 m/s,
 $\Delta_{\text{north}} = 22.2$ m, $\Delta_{\text{east}} = -9.7$ m, local time 10:52:23**

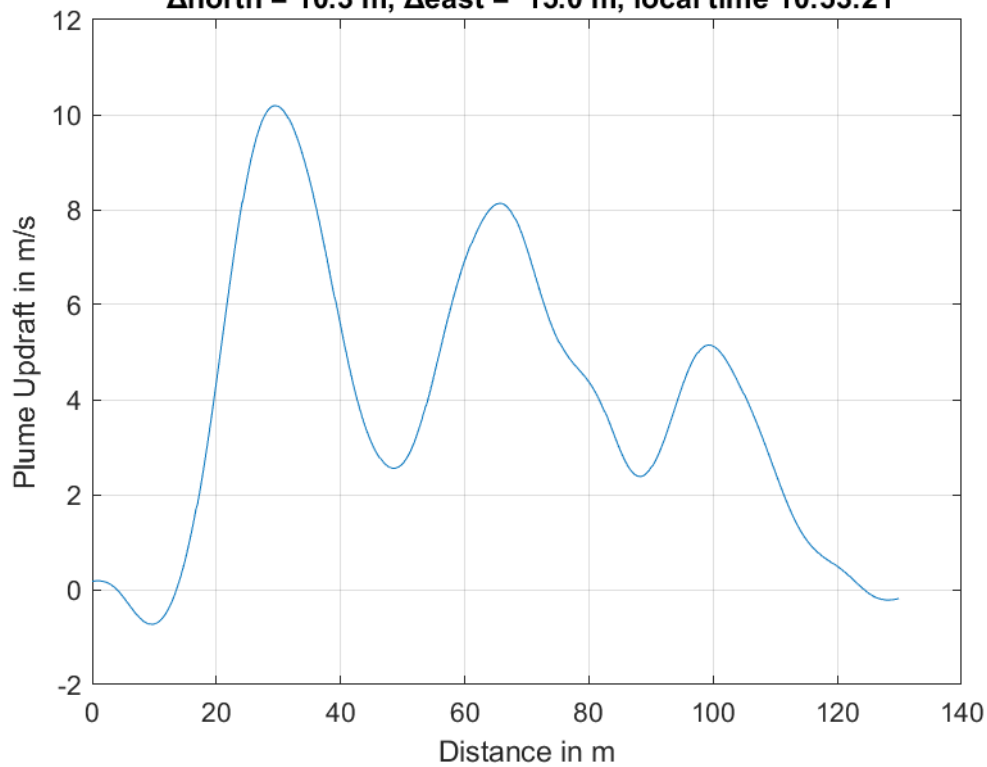


**Plume #39 at 360.7 m MSL, fly-through speed 55.0 m/s,
 $\Delta_{\text{north}} = 44.2$ m, $\Delta_{\text{east}} = -0.9$ m, local time 10:52:54**

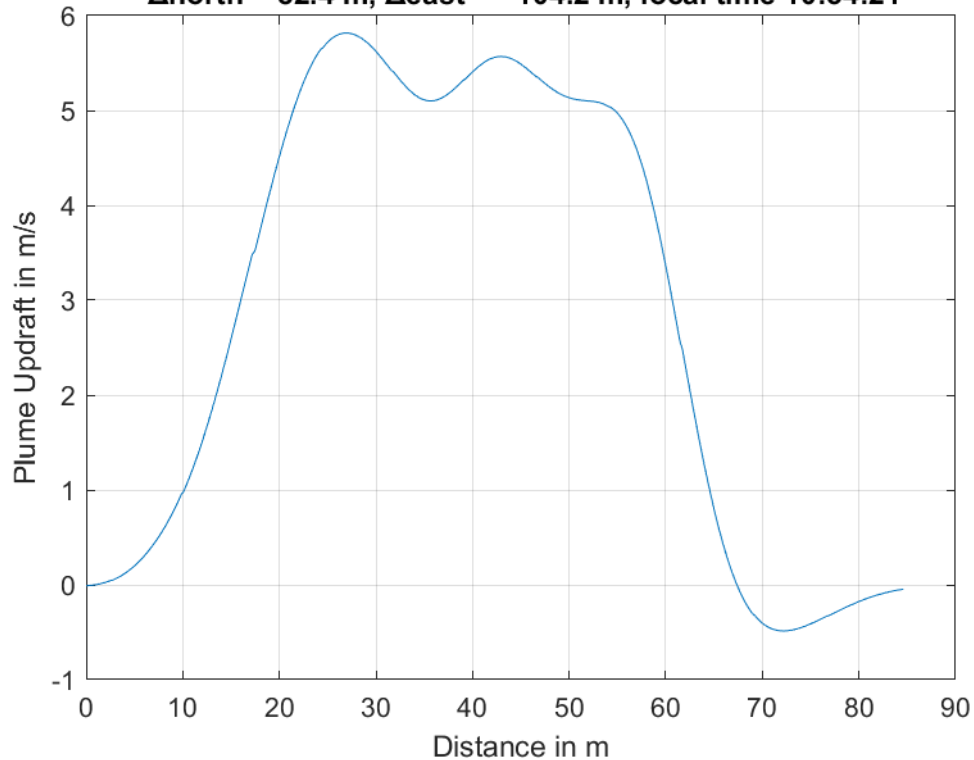




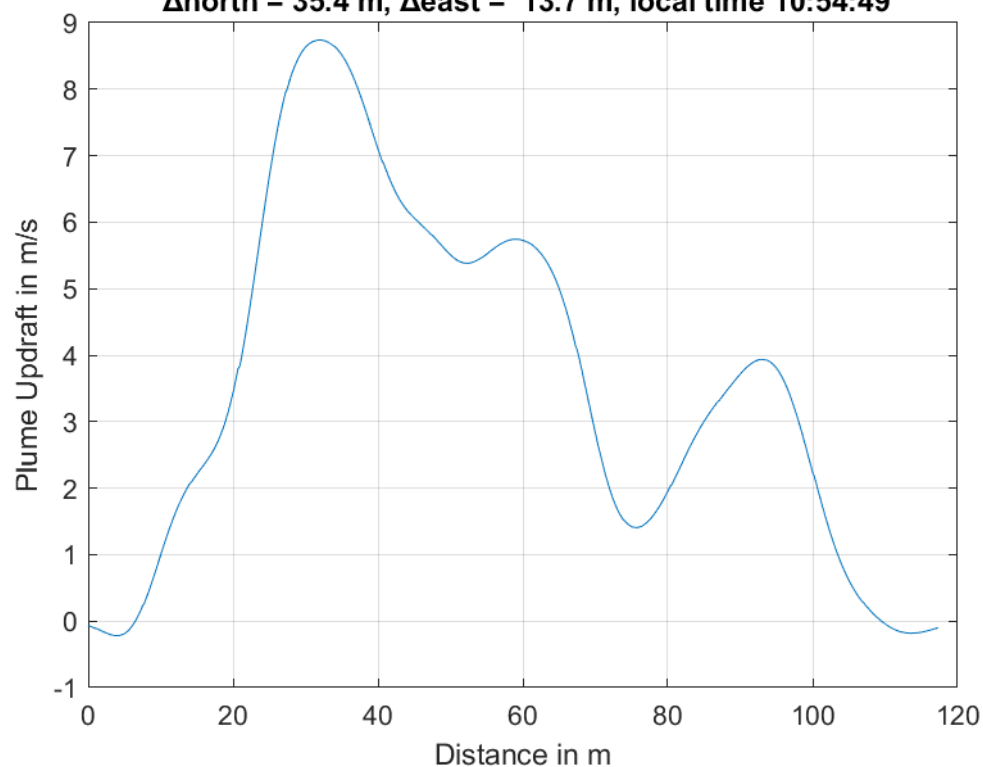
**Plume #40 at 398.2 m MSL, fly-through speed 52.0 m/s,
 $\Delta_{\text{north}} = 10.3$ m, $\Delta_{\text{east}} = 15.0$ m, local time 10:53:21**



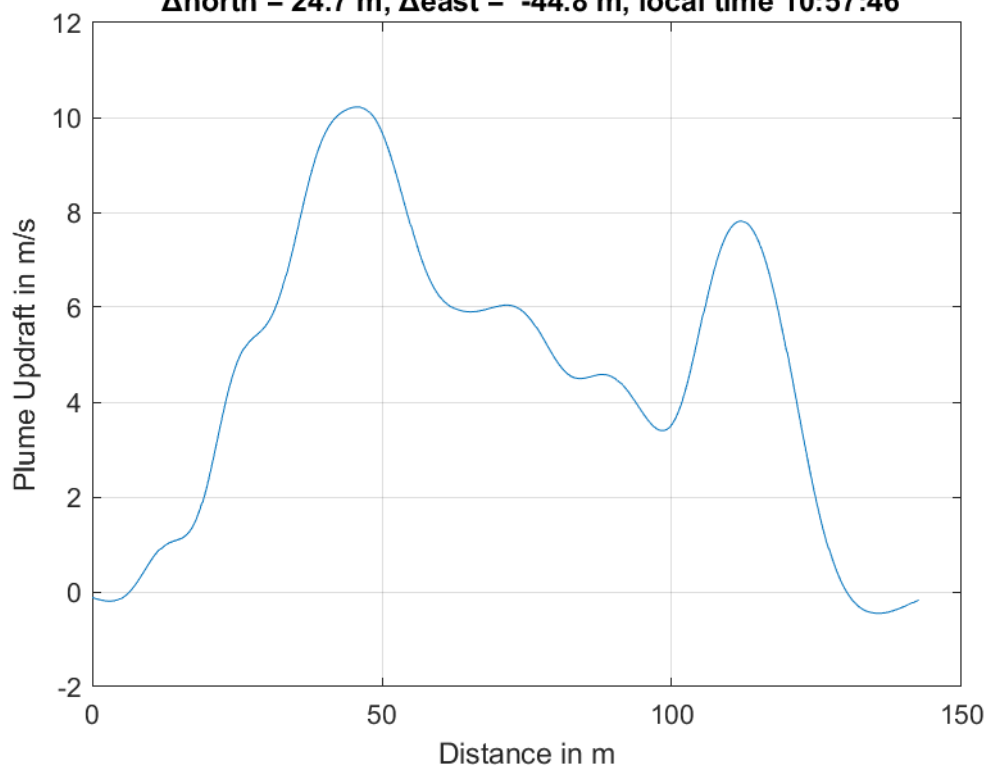
**Plume #41 at 389.3 m MSL, fly-through speed 53.0 m/s,
 $\Delta_{\text{north}} = 82.4$ m, $\Delta_{\text{east}} = -104.2$ m, local time 10:54:21**



**Plume #42 at 379.1 m MSL, fly-through speed 47.0 m/s,
 $\Delta_{\text{north}} = 35.4$ m, $\Delta_{\text{east}} = 13.7$ m, local time 10:54:49**

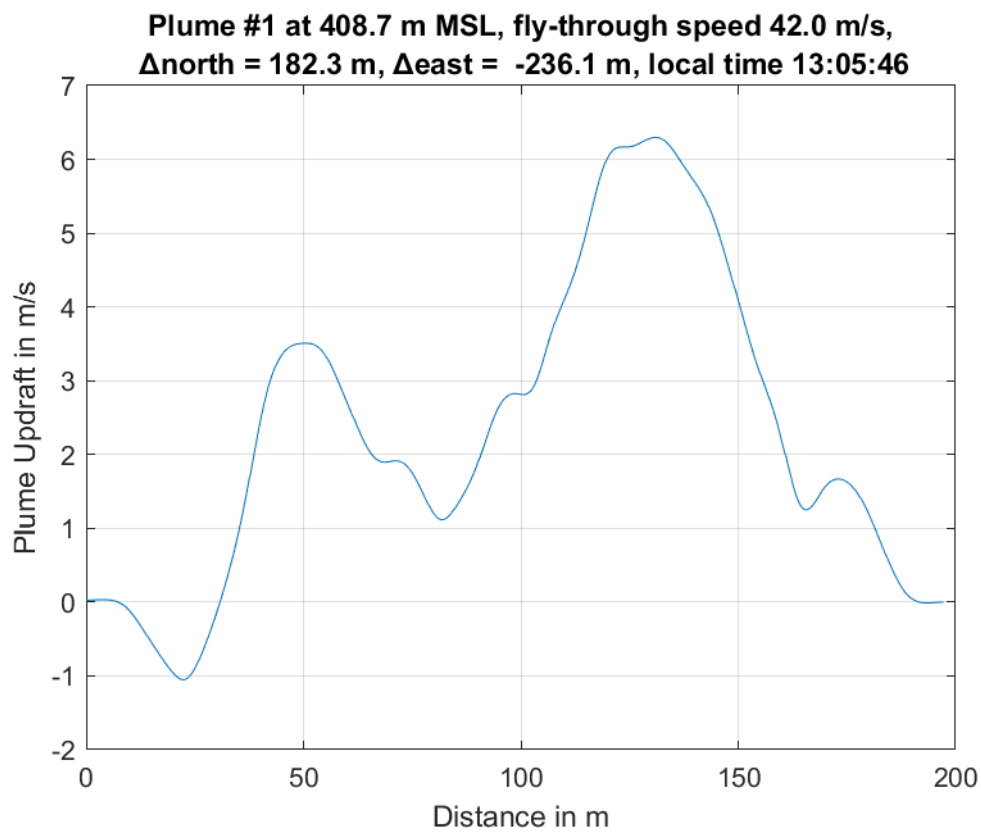
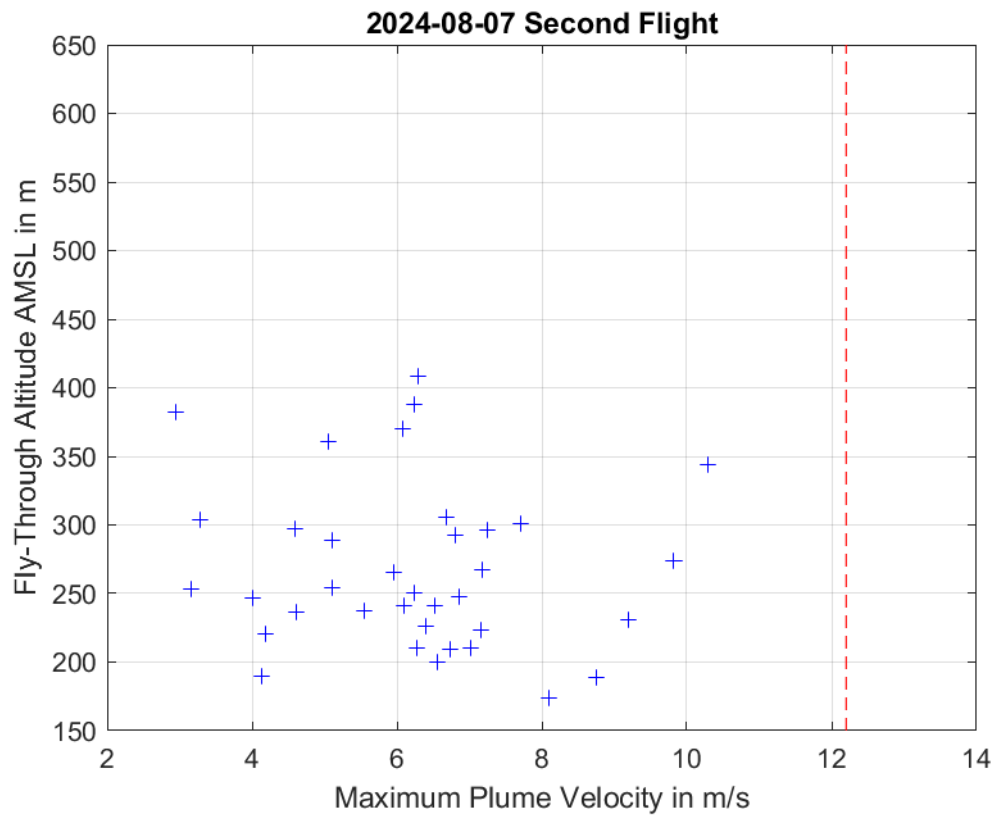


**Plume #43 at 325.3 m MSL, fly-through speed 51.0 m/s,
 $\Delta_{\text{north}} = 24.7$ m, $\Delta_{\text{east}} = -44.8$ m, local time 10:57:46**



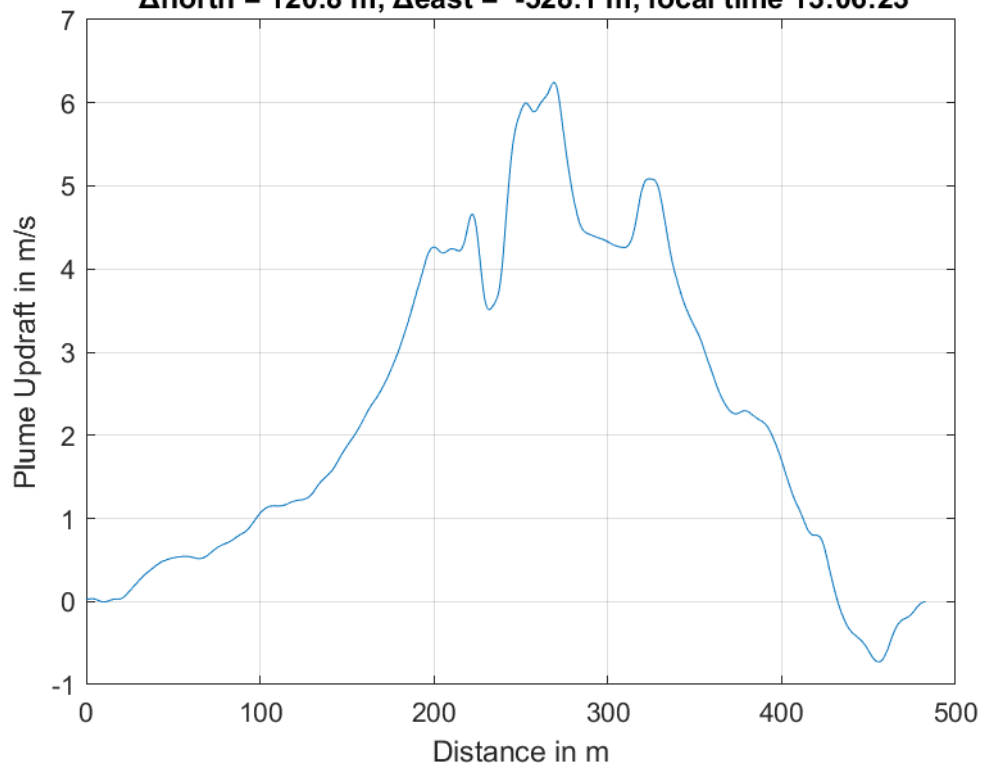


9 Measured Plumes: 2024-08-07 Second Flight

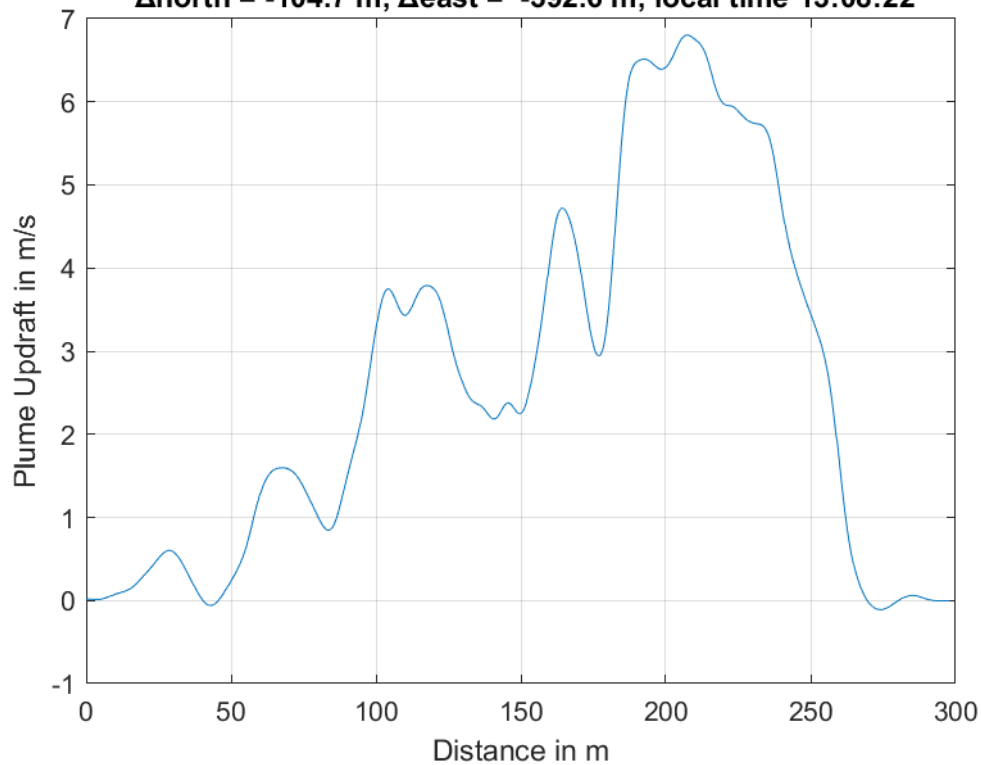




**Plume #2 at 387.9 m MSL, fly-through speed 46.0 m/s,
 Δ north = 120.8 m, Δ east = -528.1 m, local time 13:06:23**

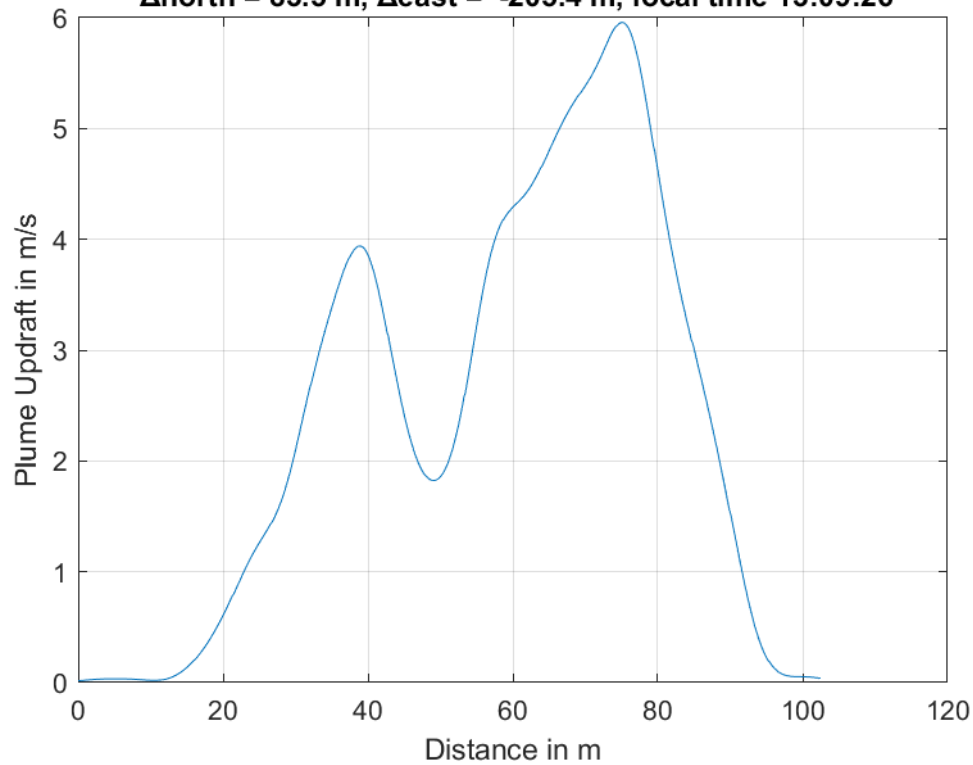


**Plume #3 at 292.7 m MSL, fly-through speed 42.0 m/s,
 Δ north = -104.7 m, Δ east = -392.6 m, local time 13:08:22**

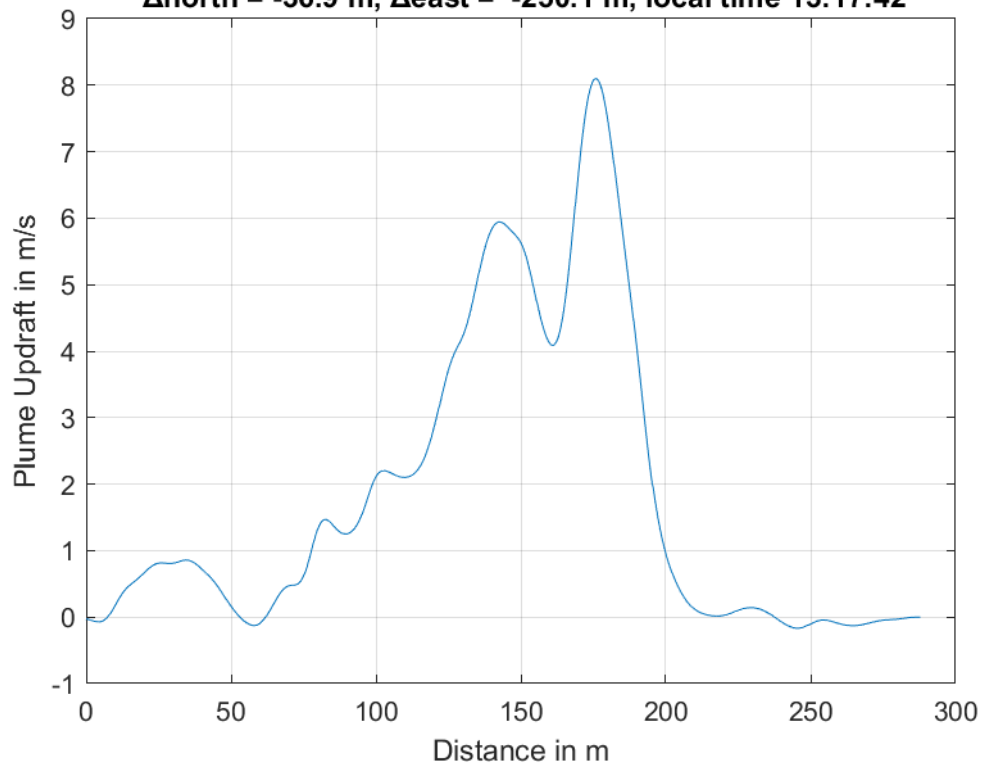




**Plume #4 at 265.4 m MSL, fly-through speed 38.0 m/s,
 $\Delta_{\text{north}} = 83.5$ m, $\Delta_{\text{east}} = -205.4$ m, local time 13:09:26**

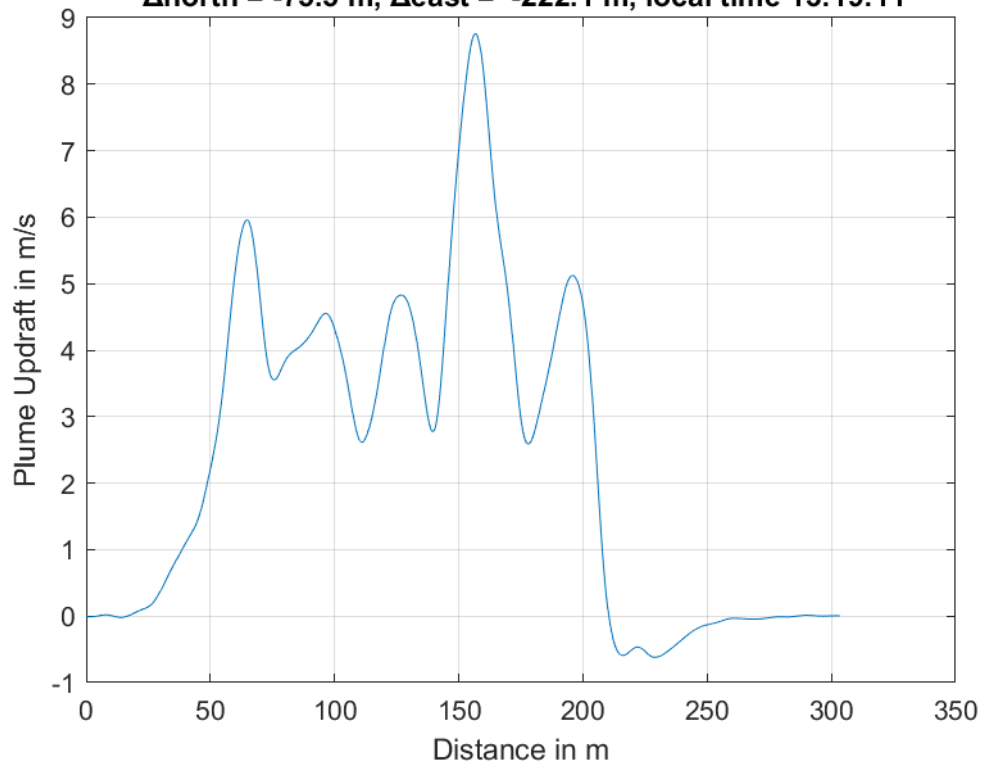


**Plume #5 at 173.8 m MSL, fly-through speed 48.0 m/s,
 $\Delta_{\text{north}} = -36.9$ m, $\Delta_{\text{east}} = -250.1$ m, local time 13:17:42**

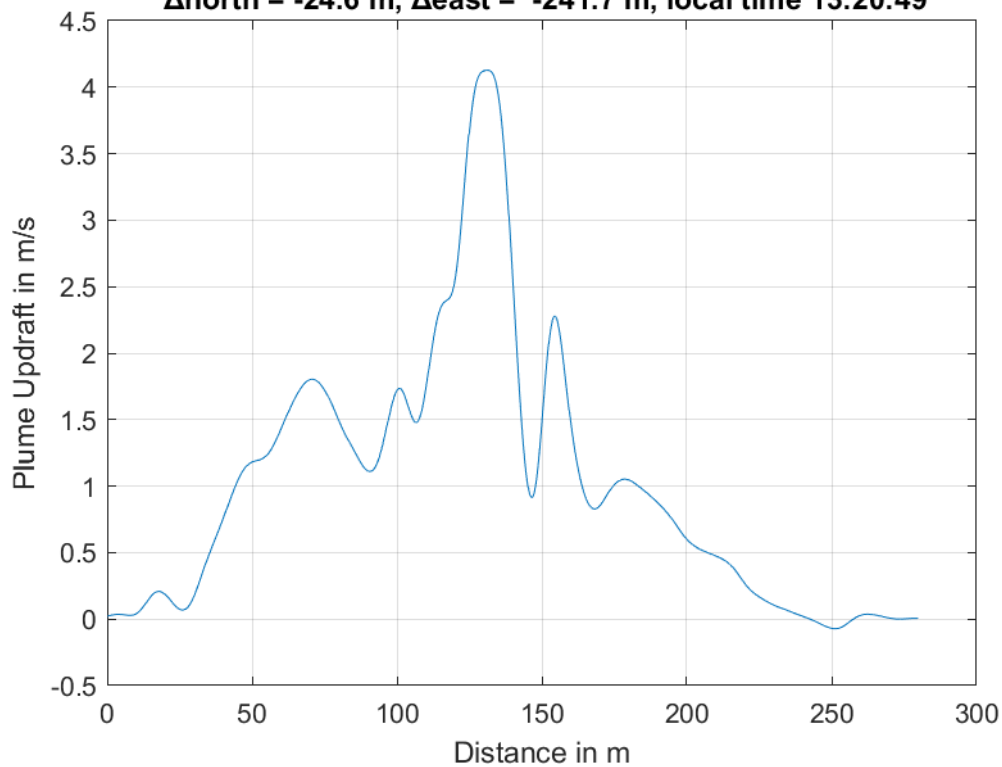




**Plume #6 at 188.9 m MSL, fly-through speed 46.0 m/s,
 $\Delta_{\text{north}} = -75.5$ m, $\Delta_{\text{east}} = -222.1$ m, local time 13:19:11**

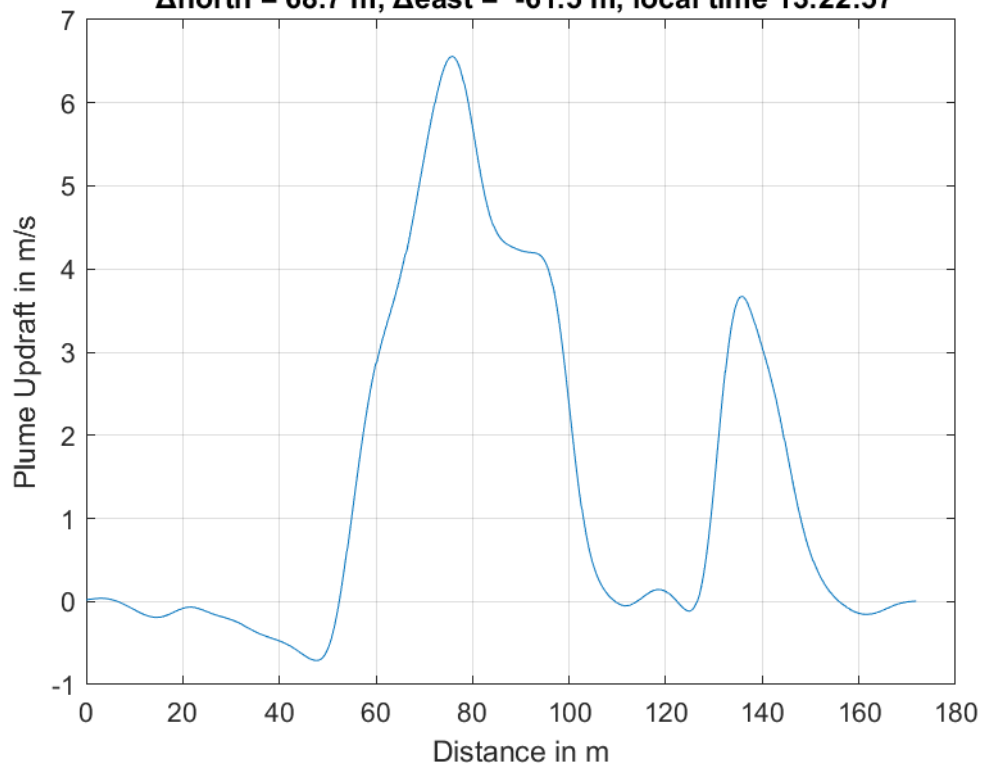


**Plume #7 at 189.7 m MSL, fly-through speed 50.0 m/s,
 $\Delta_{\text{north}} = -24.6$ m, $\Delta_{\text{east}} = -241.7$ m, local time 13:20:49**

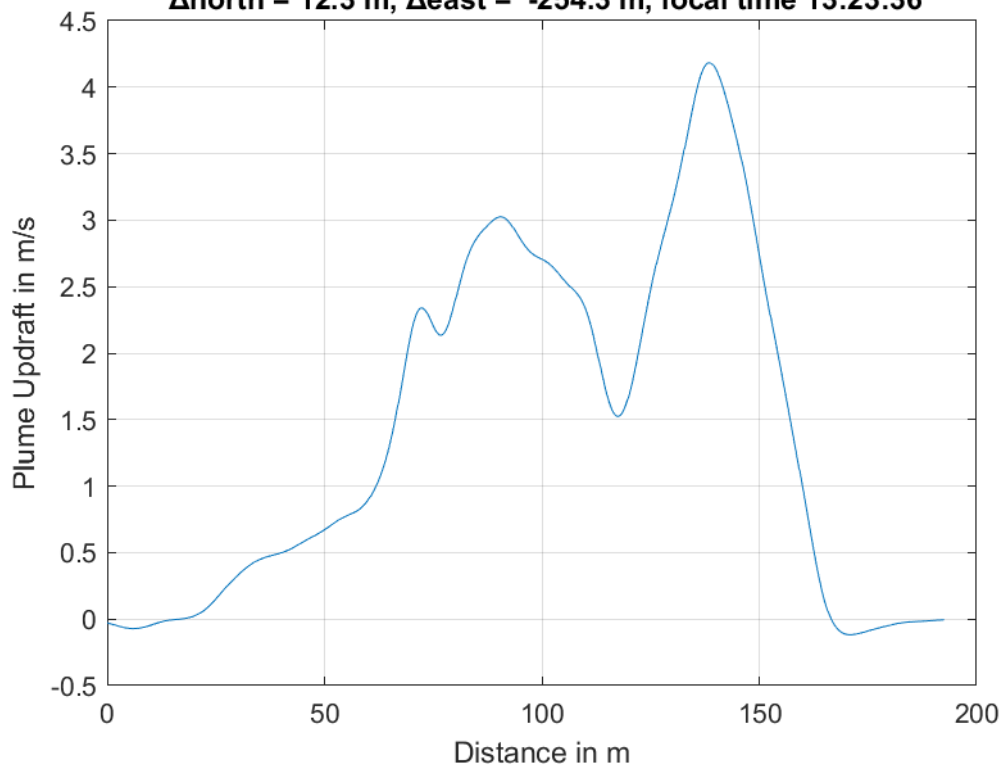




**Plume #8 at 199.9 m MSL, fly-through speed 43.0 m/s,
 $\Delta_{\text{north}} = 68.7$ m, $\Delta_{\text{east}} = -61.5$ m, local time 13:22:57**

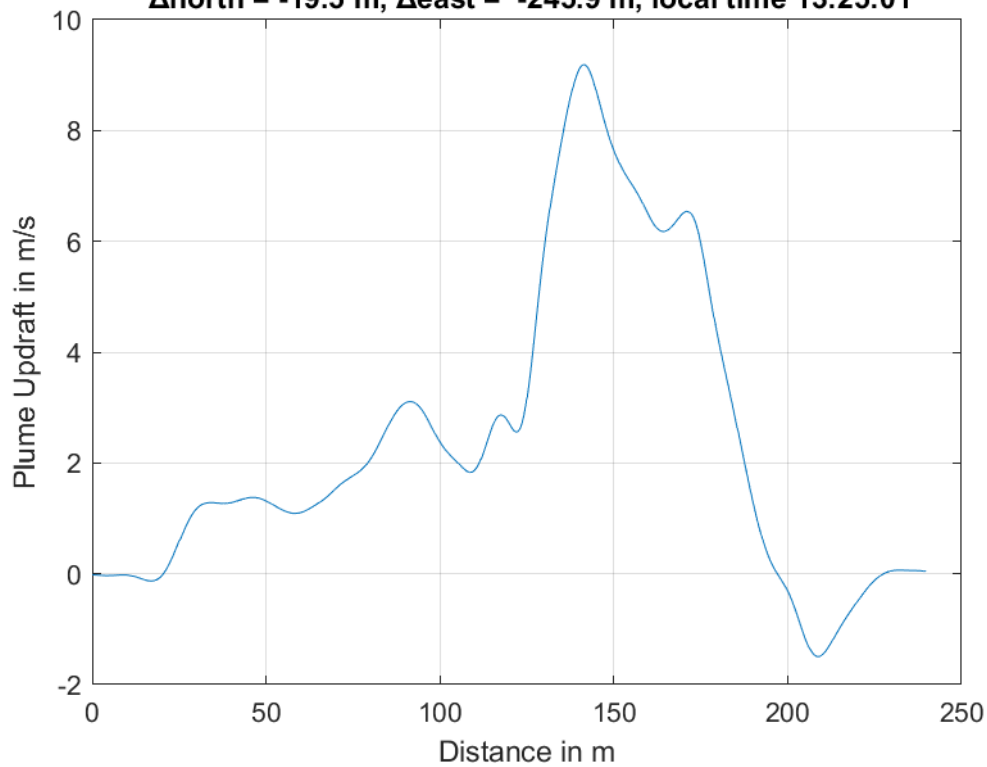


**Plume #9 at 220.9 m MSL, fly-through speed 47.0 m/s,
 $\Delta_{\text{north}} = 12.3$ m, $\Delta_{\text{east}} = -254.3$ m, local time 13:23:36**

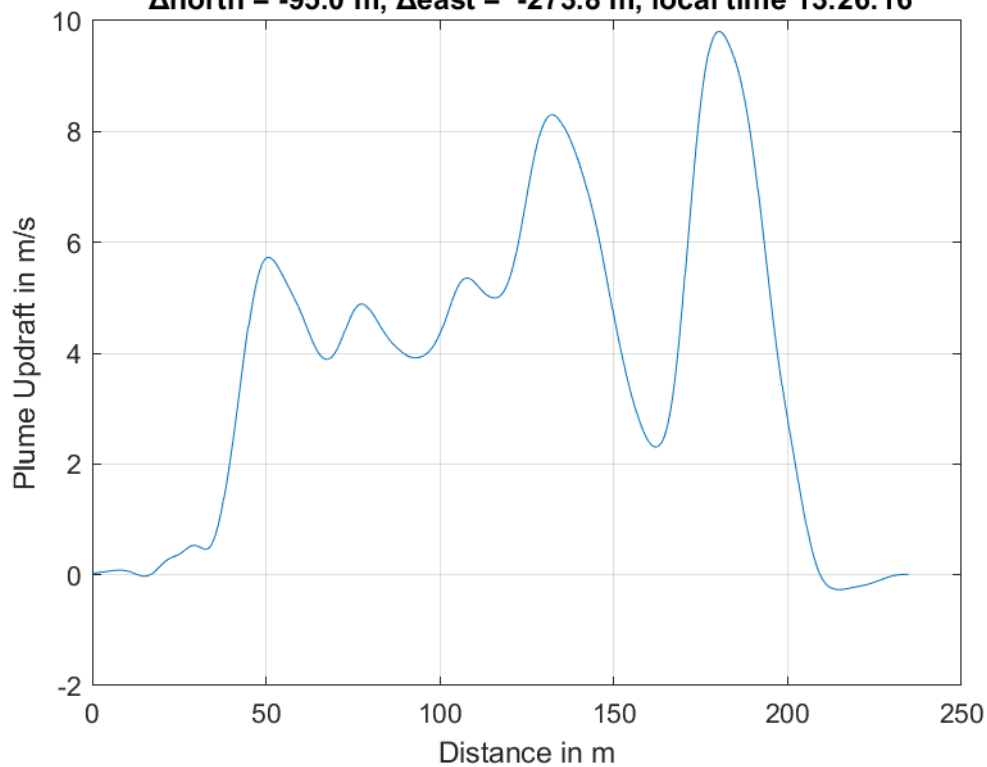




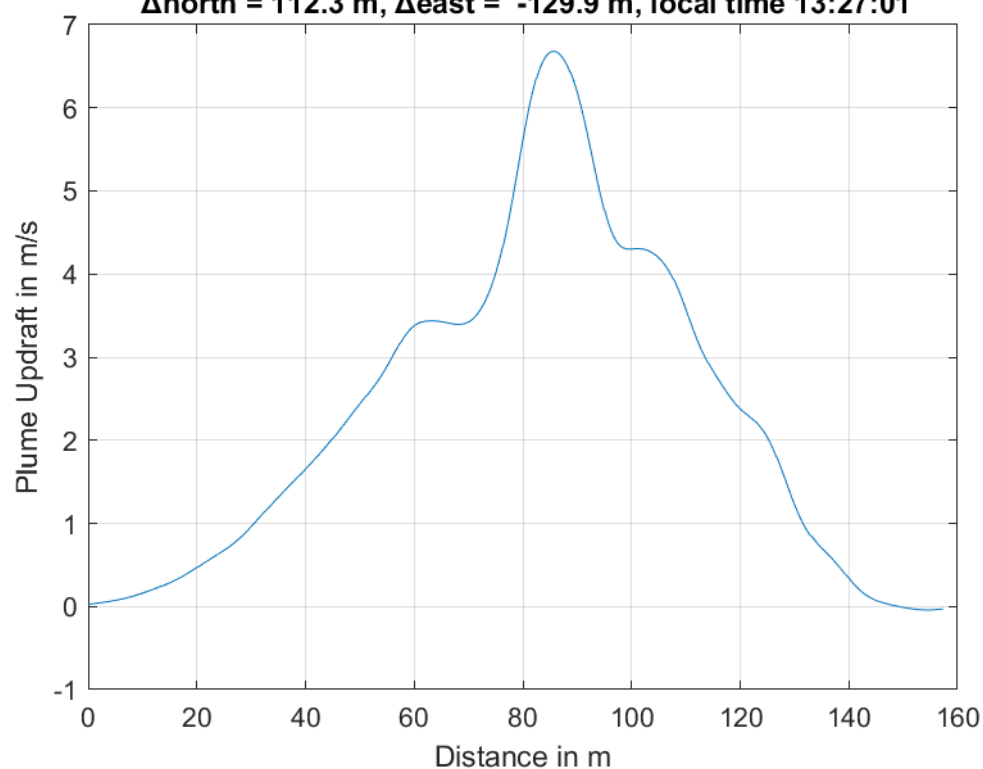
**Plume #10 at 230.6 m MSL, fly-through speed 48.0 m/s,
 $\Delta_{\text{north}} = -19.5$ m, $\Delta_{\text{east}} = -245.9$ m, local time 13:25:01**



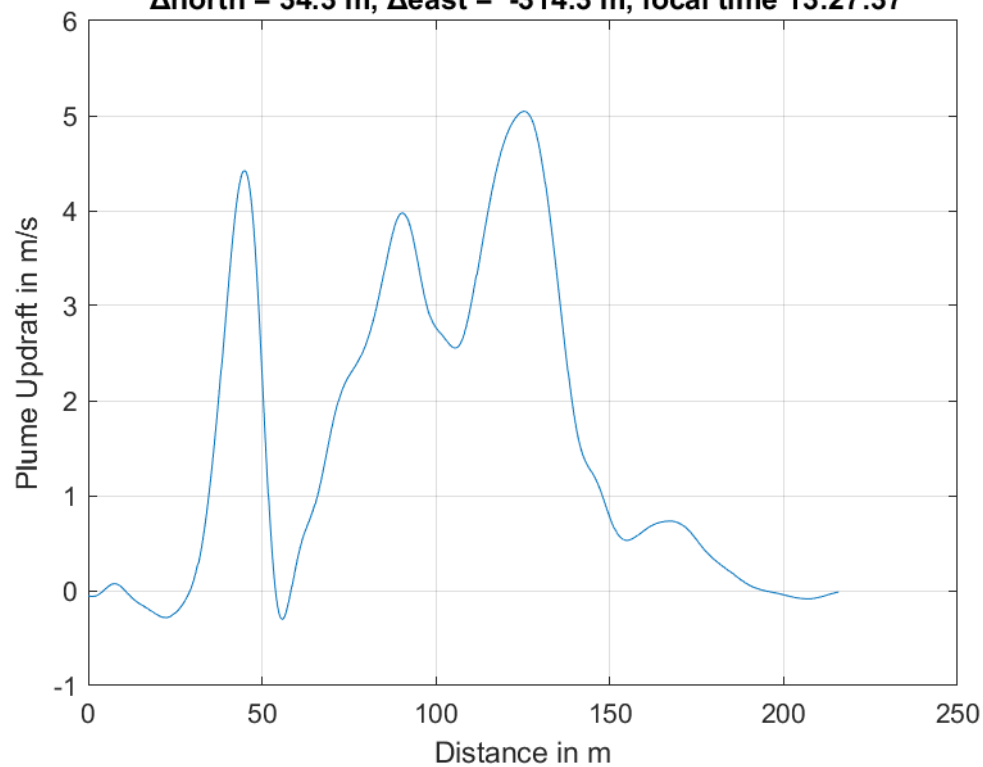
**Plume #11 at 273.7 m MSL, fly-through speed 50.0 m/s,
 $\Delta_{\text{north}} = -95.0$ m, $\Delta_{\text{east}} = -273.8$ m, local time 13:26:16**



**Plume #12 at 306.0 m MSL, fly-through speed 45.0 m/s,
 $\Delta_{\text{north}} = 112.3$ m, $\Delta_{\text{east}} = -129.9$ m, local time 13:27:01**

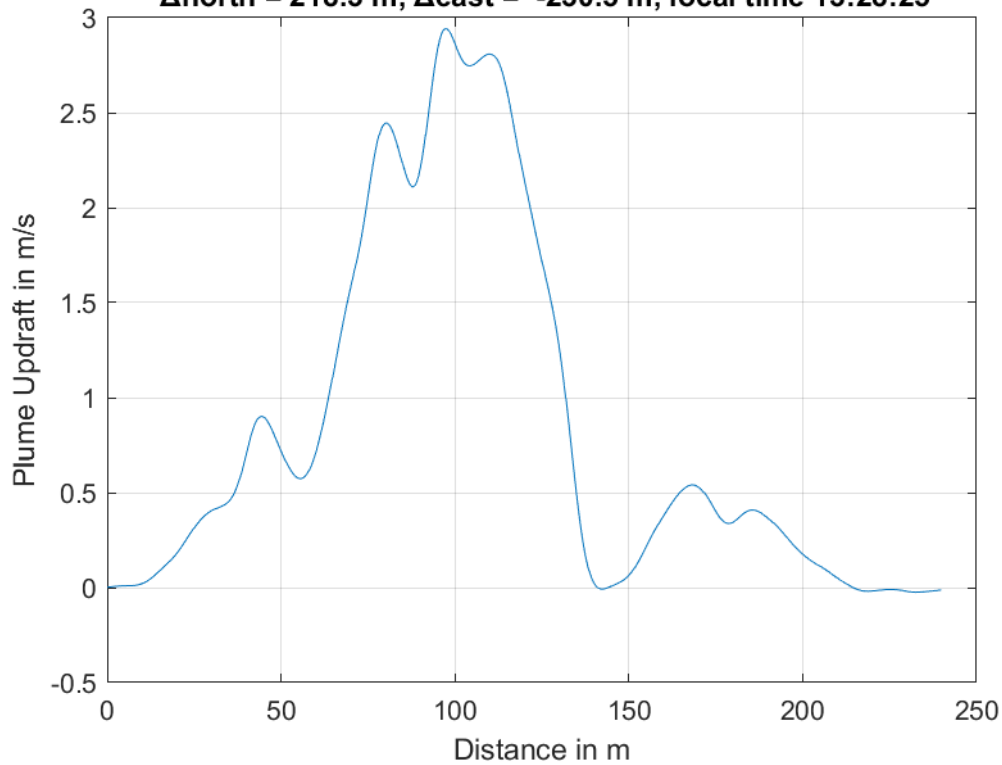


**Plume #13 at 360.9 m MSL, fly-through speed 48.0 m/s,
 $\Delta_{\text{north}} = 34.3$ m, $\Delta_{\text{east}} = -314.3$ m, local time 13:27:37**

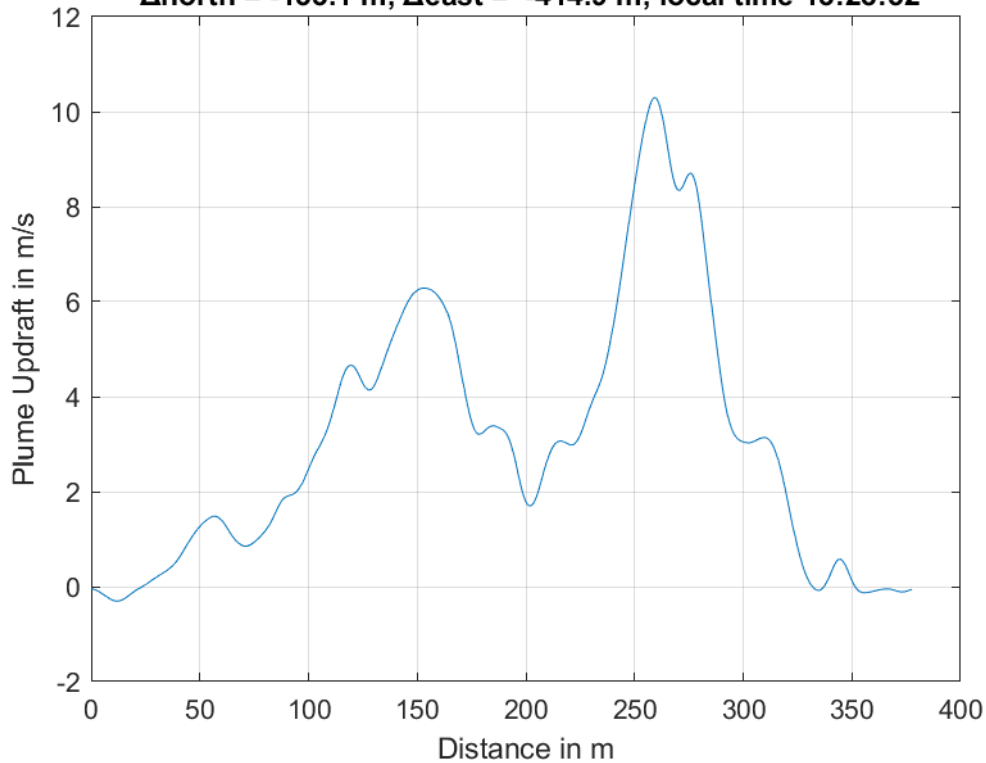




**Plume #14 at 381.8 m MSL, fly-through speed 48.0 m/s,
 $\Delta_{\text{north}} = 218.3$ m, $\Delta_{\text{east}} = -230.5$ m, local time 13:28:25**

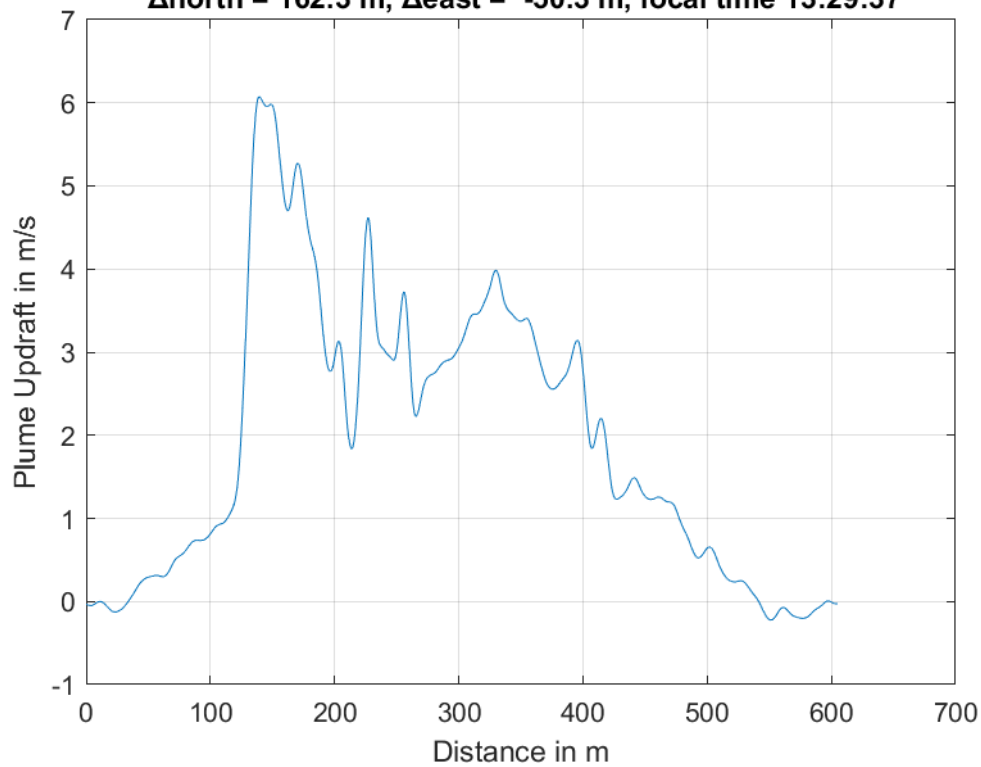


**Plume #15 at 344.0 m MSL, fly-through speed 54.0 m/s,
 $\Delta_{\text{north}} = -133.1$ m, $\Delta_{\text{east}} = -414.9$ m, local time 13:28:52**

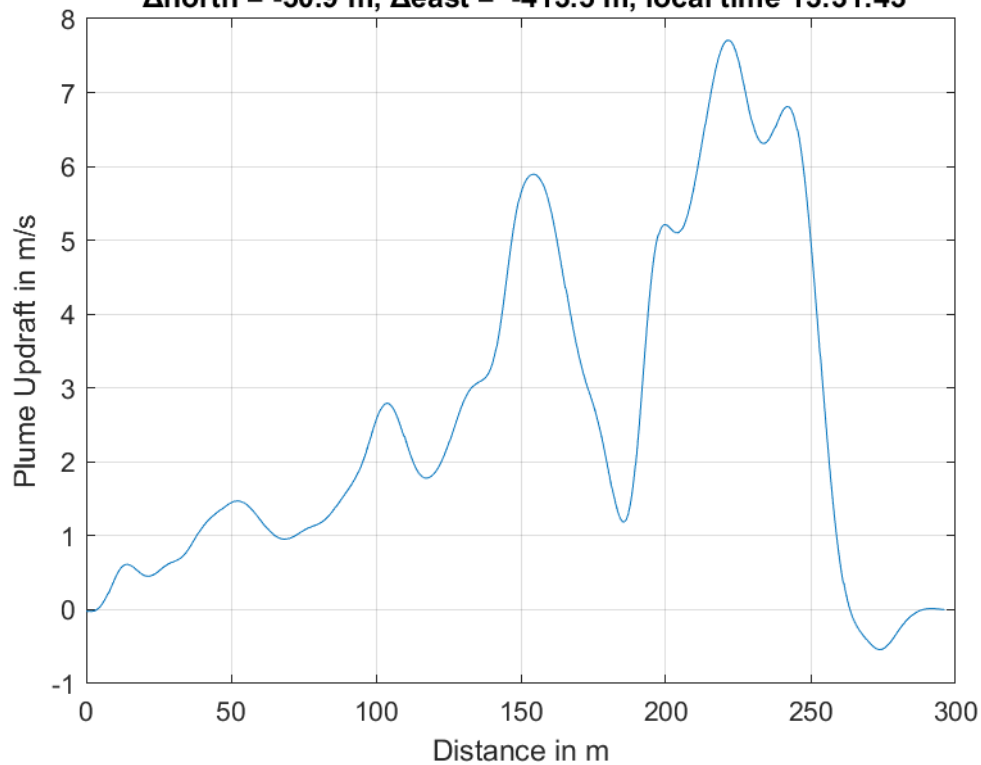




**Plume #16 at 370.1 m MSL, fly-through speed 50.0 m/s,
 $\Delta_{\text{north}} = 162.3$ m, $\Delta_{\text{east}} = -50.3$ m, local time 13:29:37**

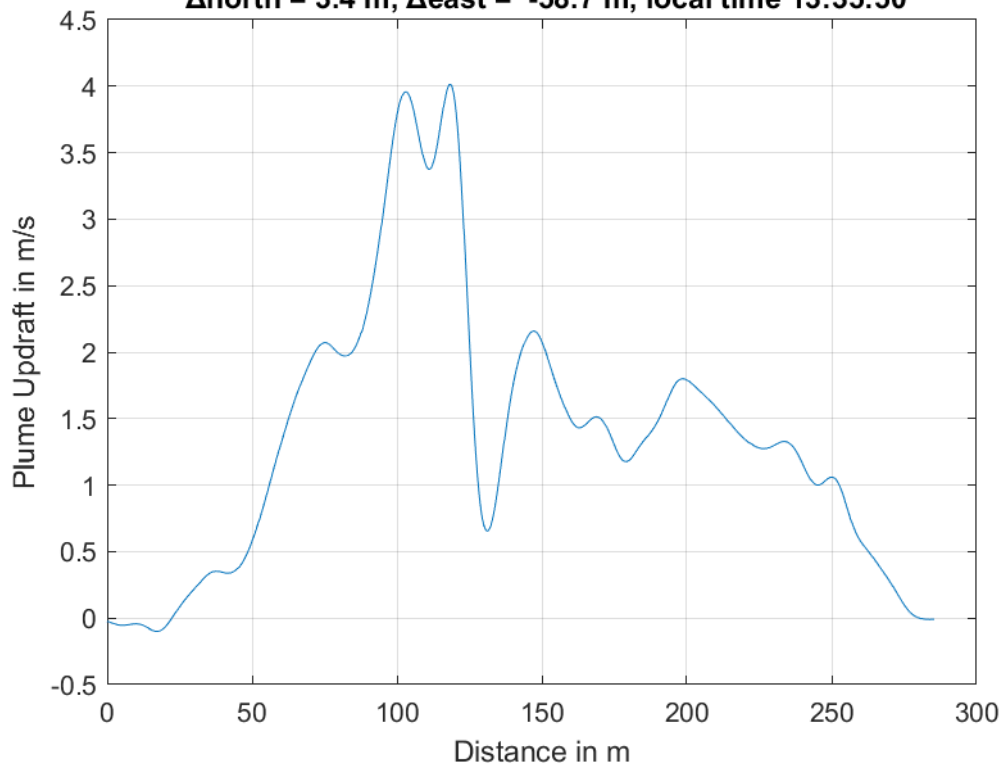


**Plume #17 at 300.7 m MSL, fly-through speed 57.0 m/s,
 $\Delta_{\text{north}} = -50.9$ m, $\Delta_{\text{east}} = -413.5$ m, local time 13:31:43**

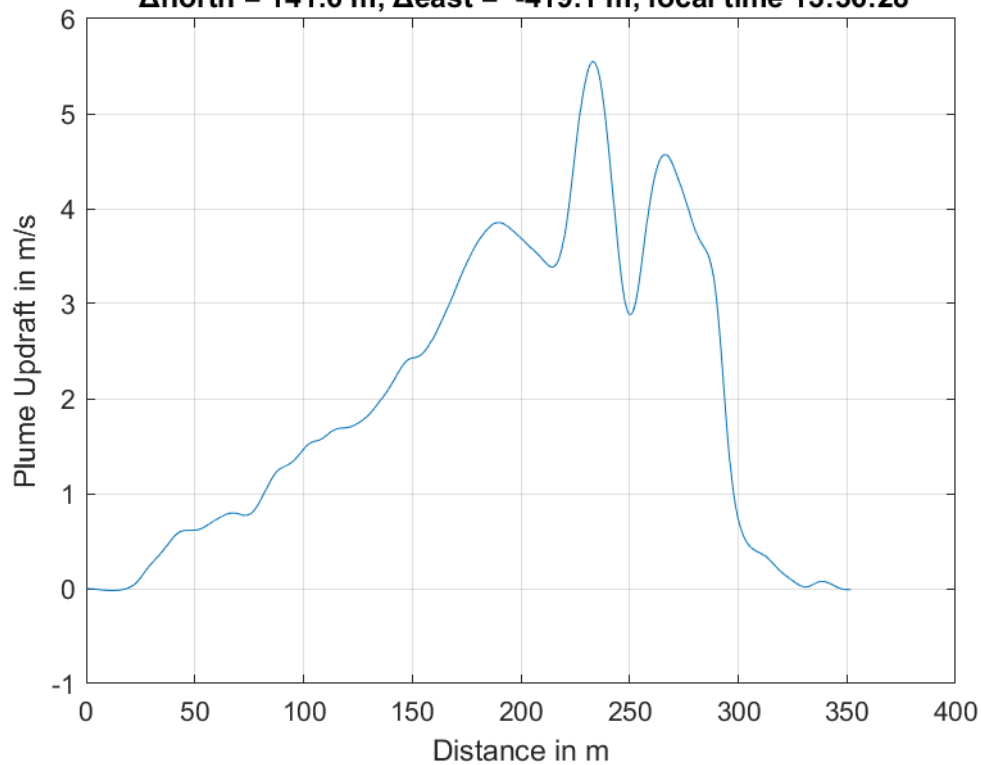




**Plume #18 at 247.0 m MSL, fly-through speed 51.0 m/s,
 $\Delta_{\text{north}} = 3.4$ m, $\Delta_{\text{east}} = -58.7$ m, local time 13:35:50**

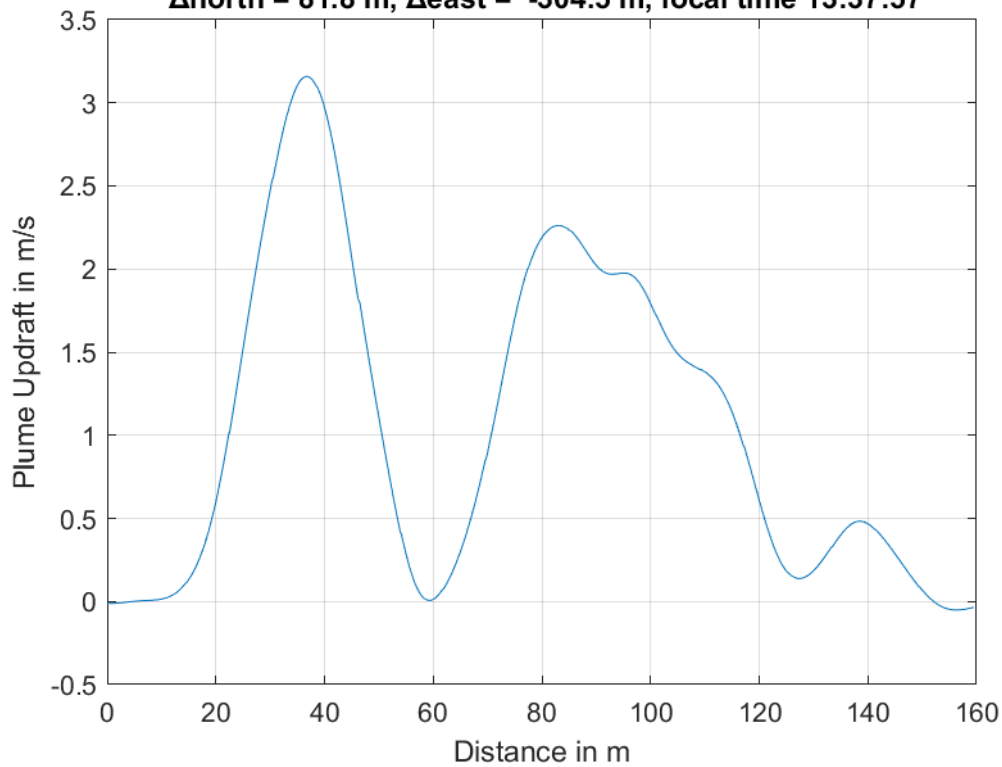


**Plume #19 at 237.8 m MSL, fly-through speed 55.0 m/s,
 $\Delta_{\text{north}} = 141.6$ m, $\Delta_{\text{east}} = -419.1$ m, local time 13:36:28**

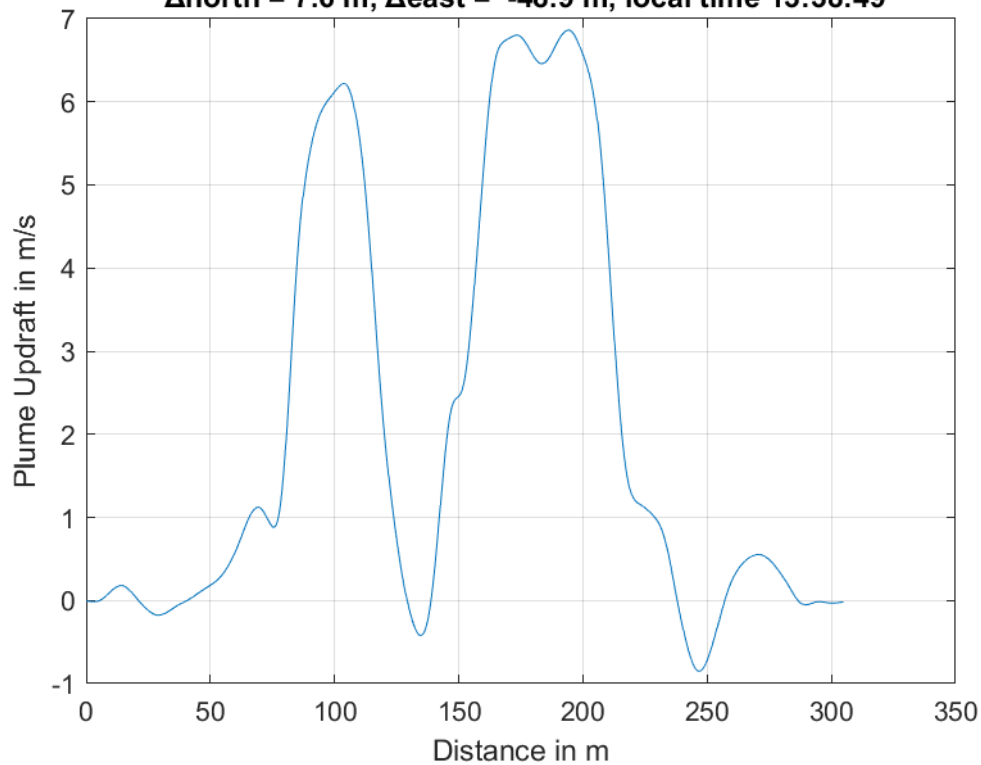




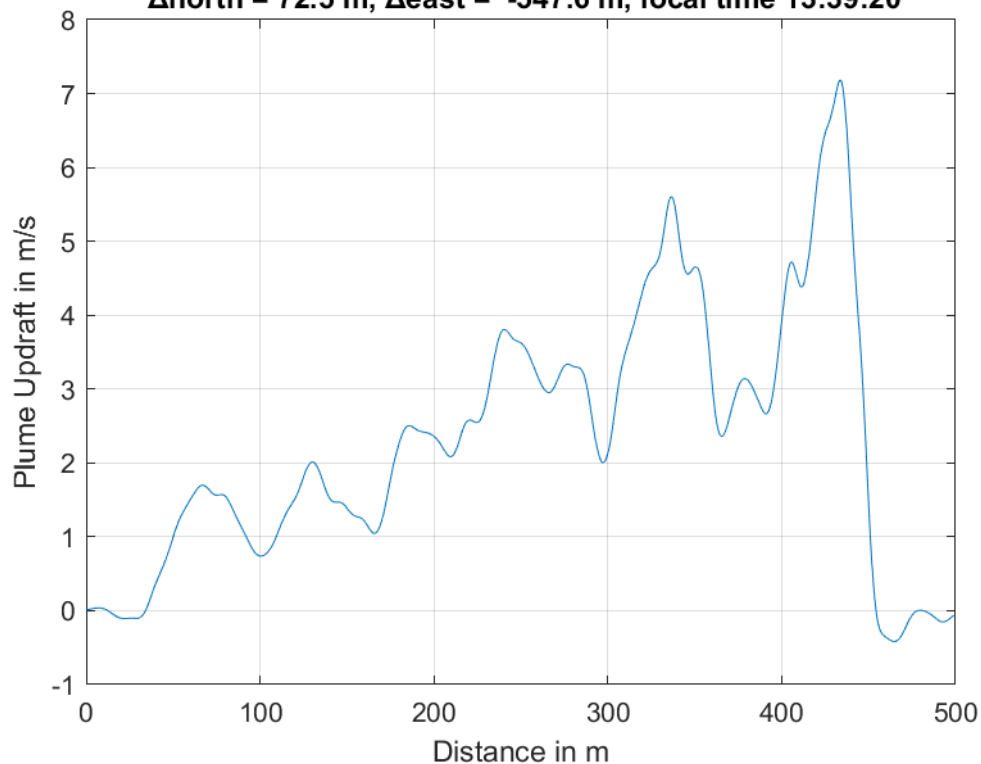
**Plume #20 at 253.0 m MSL, fly-through speed 57.0 m/s,
 $\Delta_{\text{north}} = 81.8$ m, $\Delta_{\text{east}} = -304.5$ m, local time 13:37:57**



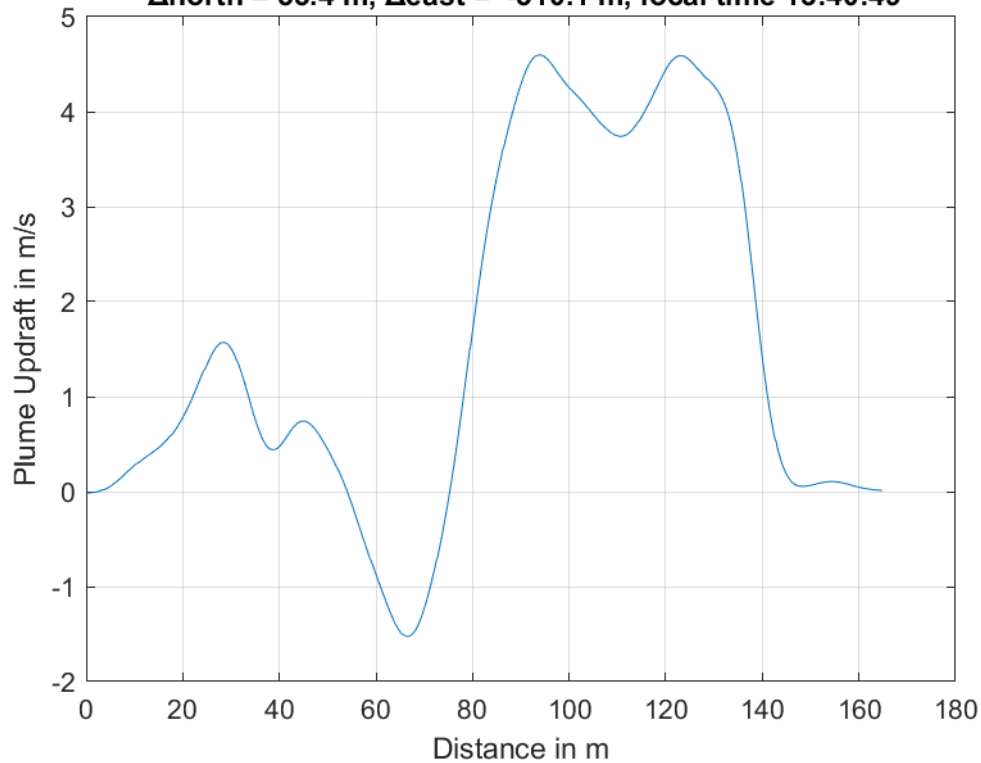
**Plume #21 at 247.8 m MSL, fly-through speed 50.0 m/s,
 $\Delta_{\text{north}} = 7.6$ m, $\Delta_{\text{east}} = -48.9$ m, local time 13:38:49**



**Plume #22 at 267.6 m MSL, fly-through speed 52.0 m/s,
 $\Delta_{\text{north}} = 72.5$ m, $\Delta_{\text{east}} = -547.6$ m, local time 13:39:20**

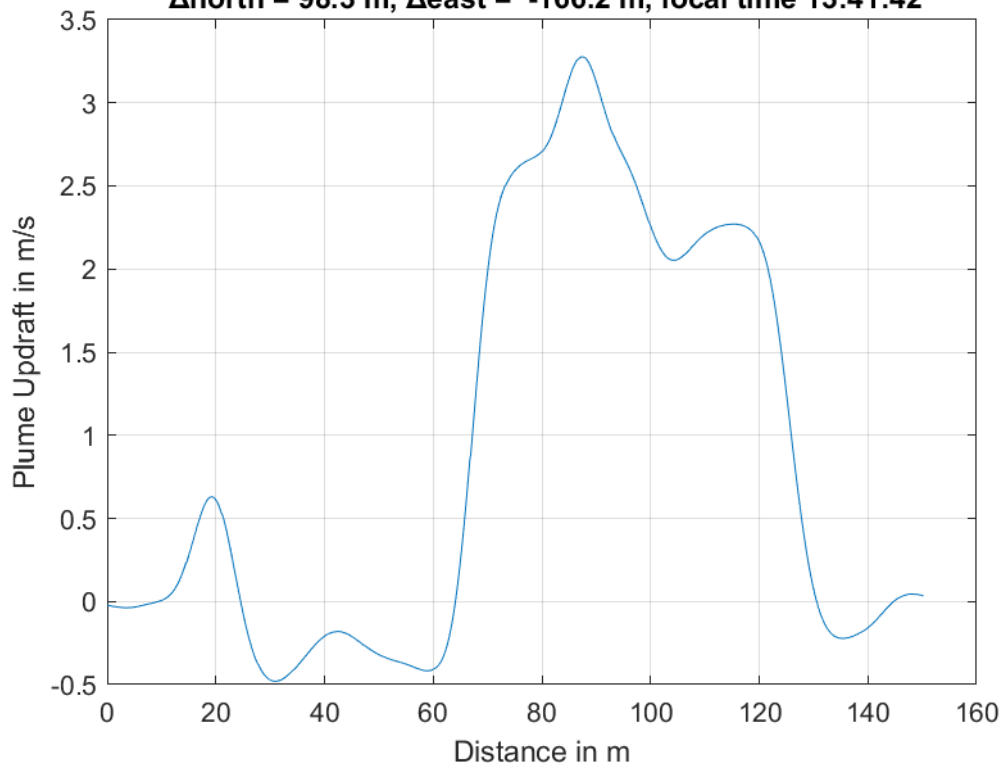


**Plume #23 at 297.6 m MSL, fly-through speed 50.0 m/s,
 $\Delta_{\text{north}} = 53.4$ m, $\Delta_{\text{east}} = -310.1$ m, local time 13:40:49**

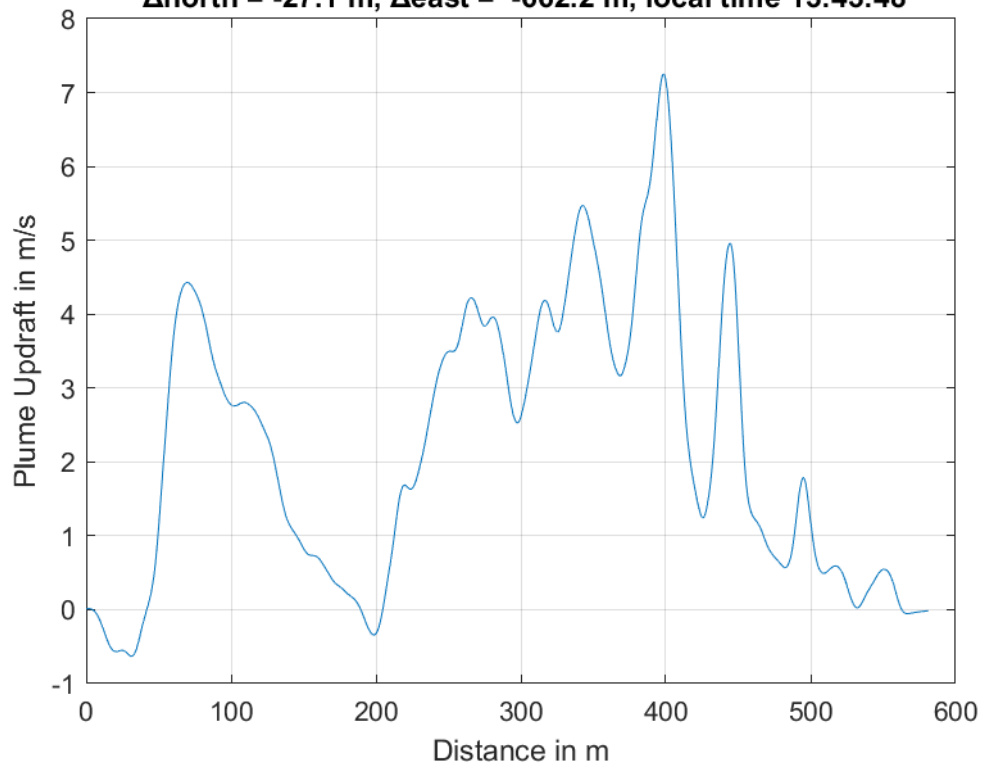




**Plume #24 at 303.4 m MSL, fly-through speed 47.0 m/s,
 $\Delta_{\text{north}} = 98.3$ m, $\Delta_{\text{east}} = -166.2$ m, local time 13:41:42**

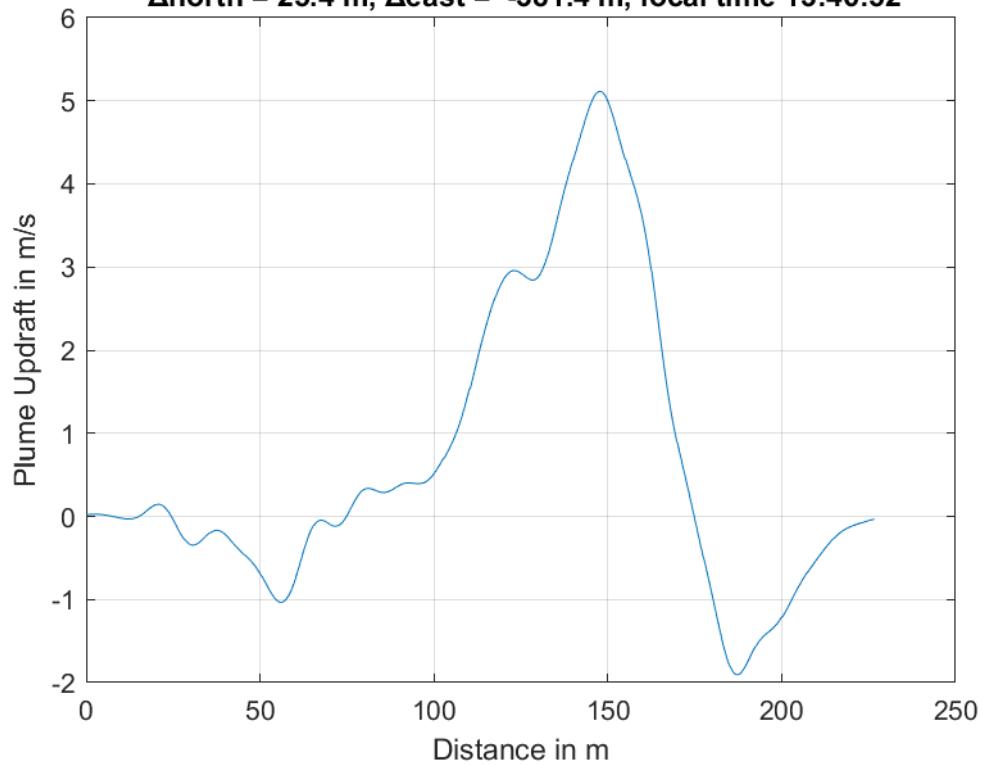


**Plume #25 at 295.9 m MSL, fly-through speed 51.0 m/s,
 $\Delta_{\text{north}} = -27.1$ m, $\Delta_{\text{east}} = -662.2$ m, local time 13:43:48**

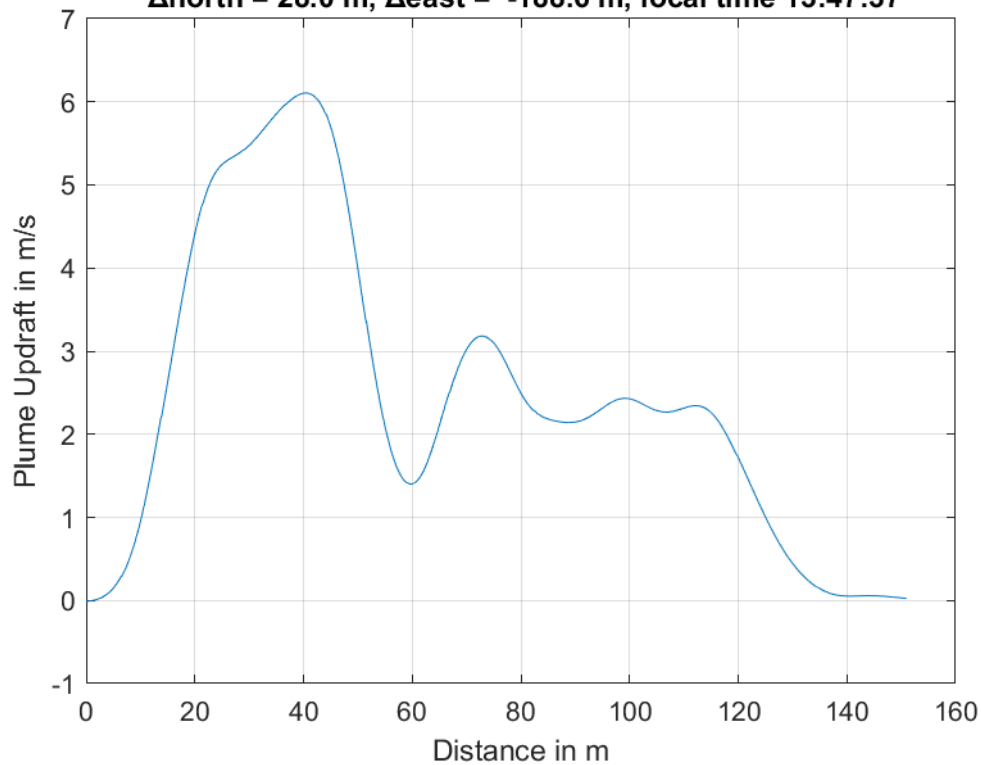




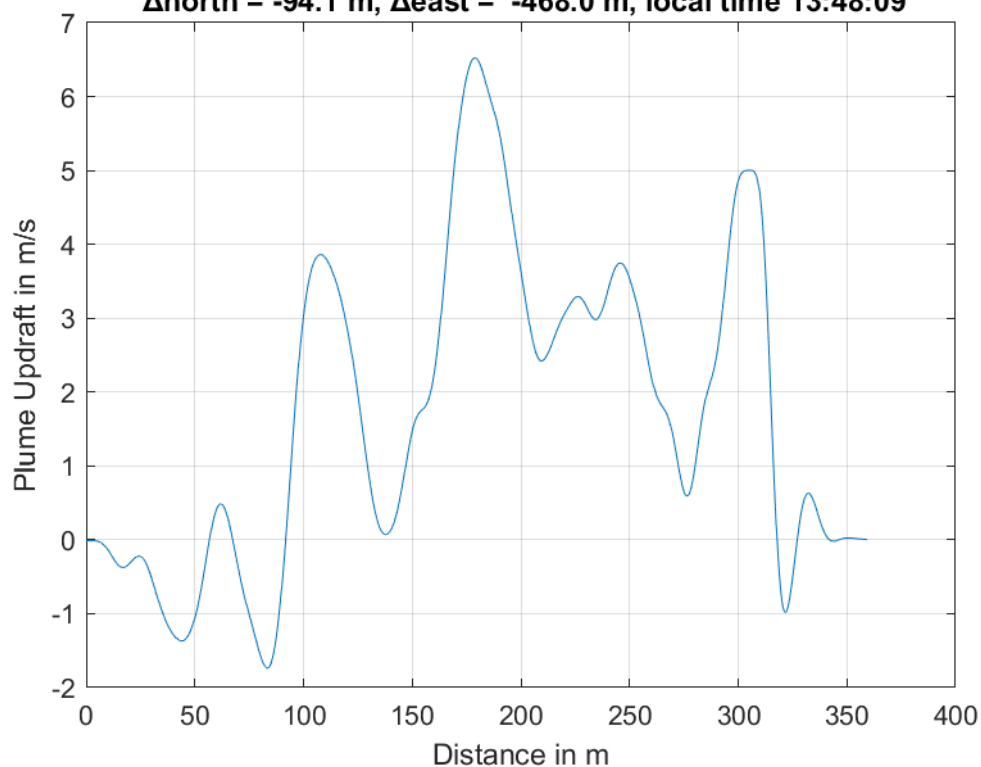
**Plume #26 at 289.2 m MSL, fly-through speed 54.0 m/s,
 Δ north = 25.4 m, Δ east = -381.4 m, local time 13:46:52**



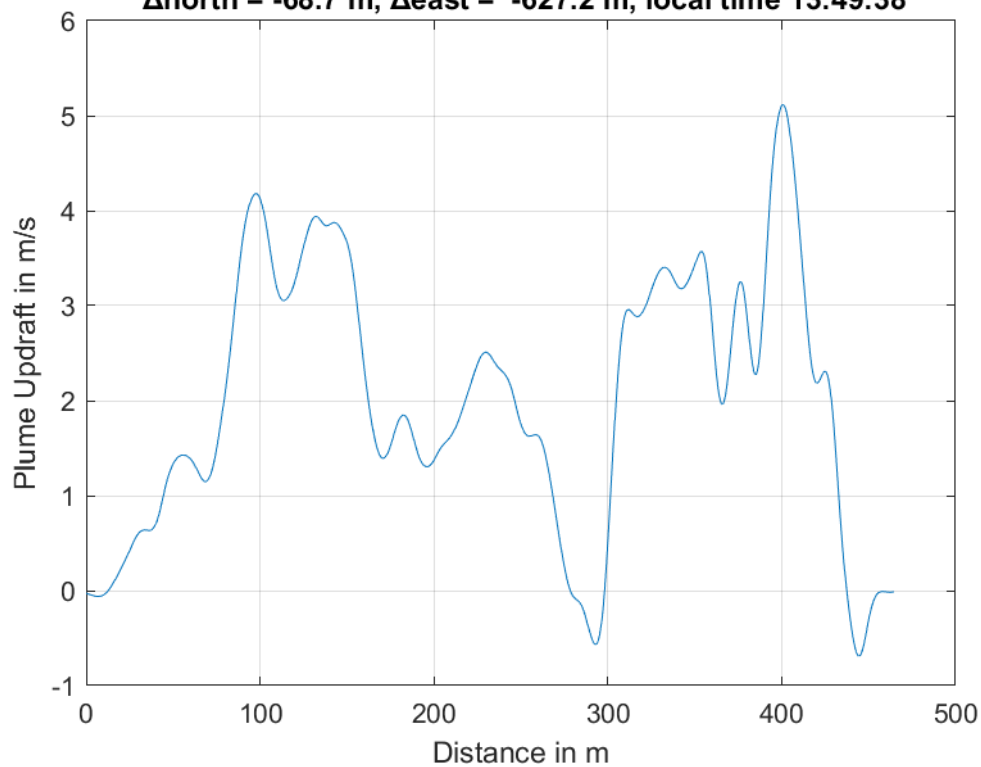
**Plume #27 at 241.6 m MSL, fly-through speed 54.0 m/s,
 Δ north = 28.0 m, Δ east = -188.6 m, local time 13:47:37**



**Plume #28 at 241.1 m MSL, fly-through speed 58.0 m/s,
 $\Delta_{\text{north}} = -94.1$ m, $\Delta_{\text{east}} = -468.0$ m, local time 13:48:09**

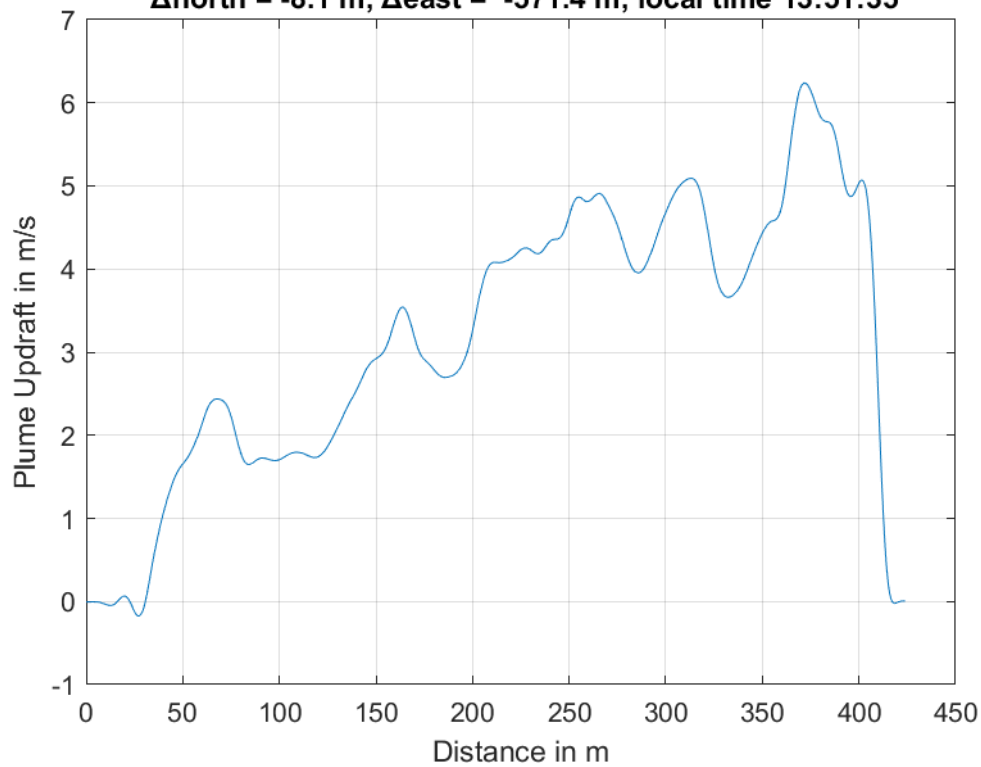


**Plume #29 at 254.0 m MSL, fly-through speed 56.0 m/s,
 $\Delta_{\text{north}} = -68.7$ m, $\Delta_{\text{east}} = -627.2$ m, local time 13:49:38**

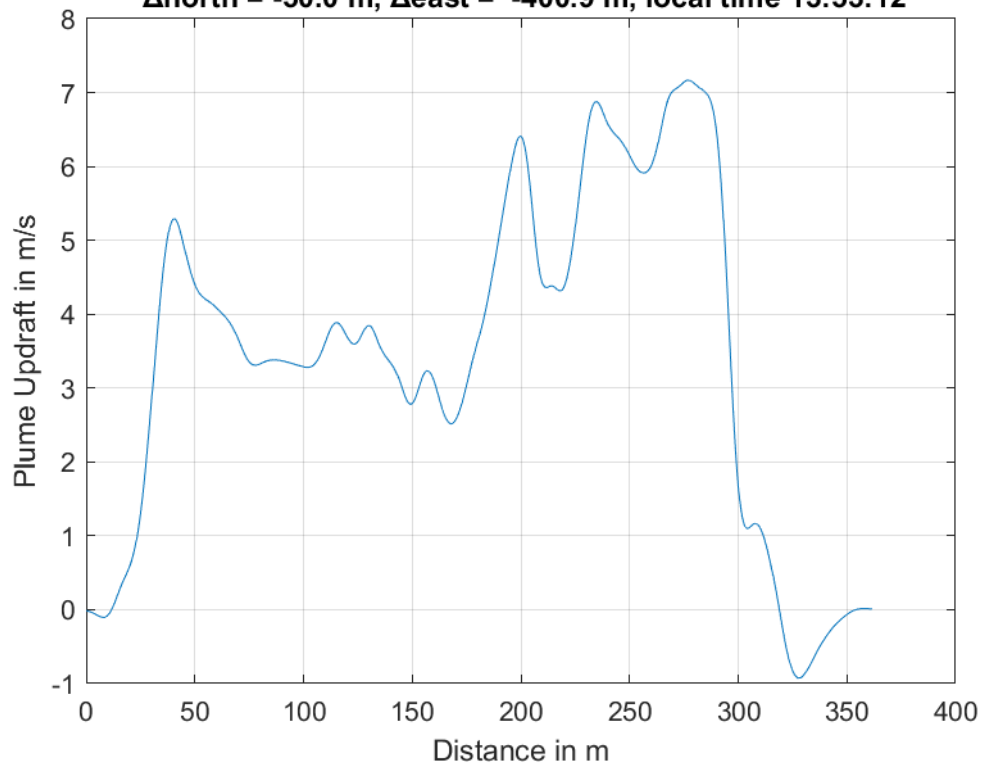




**Plume #30 at 250.2 m MSL, fly-through speed 53.0 m/s,
 $\Delta_{\text{north}} = -8.1$ m, $\Delta_{\text{east}} = -571.4$ m, local time 13:51:35**

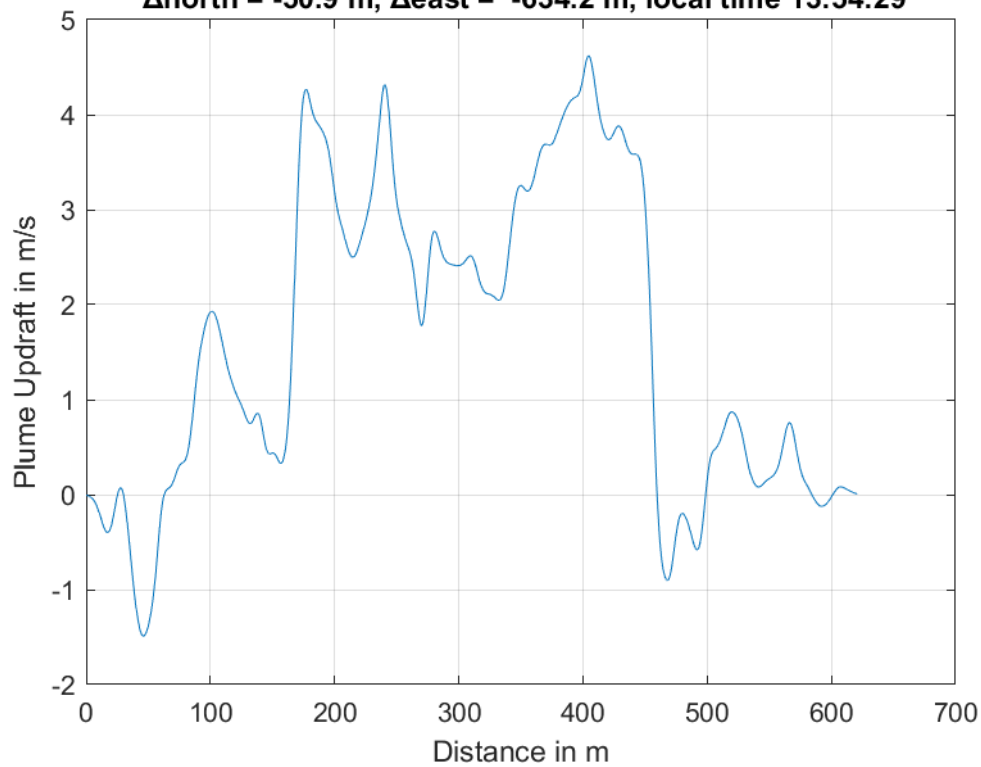


**Plume #31 at 223.0 m MSL, fly-through speed 54.0 m/s,
 $\Delta_{\text{north}} = -50.0$ m, $\Delta_{\text{east}} = -400.9$ m, local time 13:53:12**

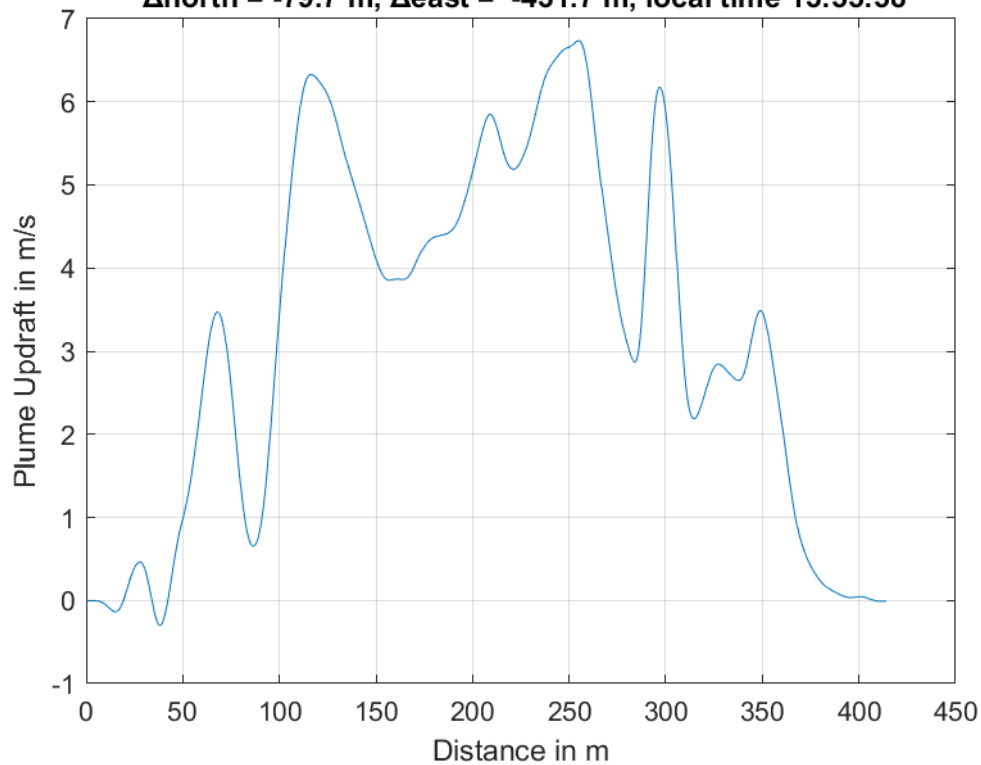




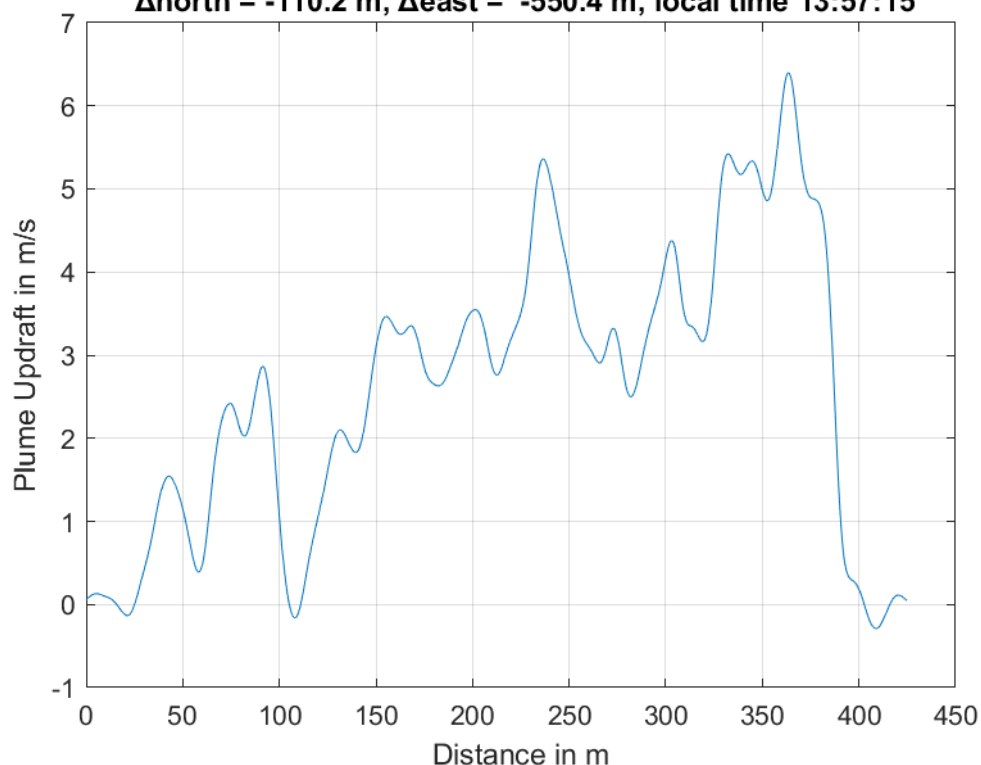
**Plume #32 at 236.3 m MSL, fly-through speed 54.0 m/s,
 $\Delta_{\text{north}} = -50.9$ m, $\Delta_{\text{east}} = -634.2$ m, local time 13:54:29**



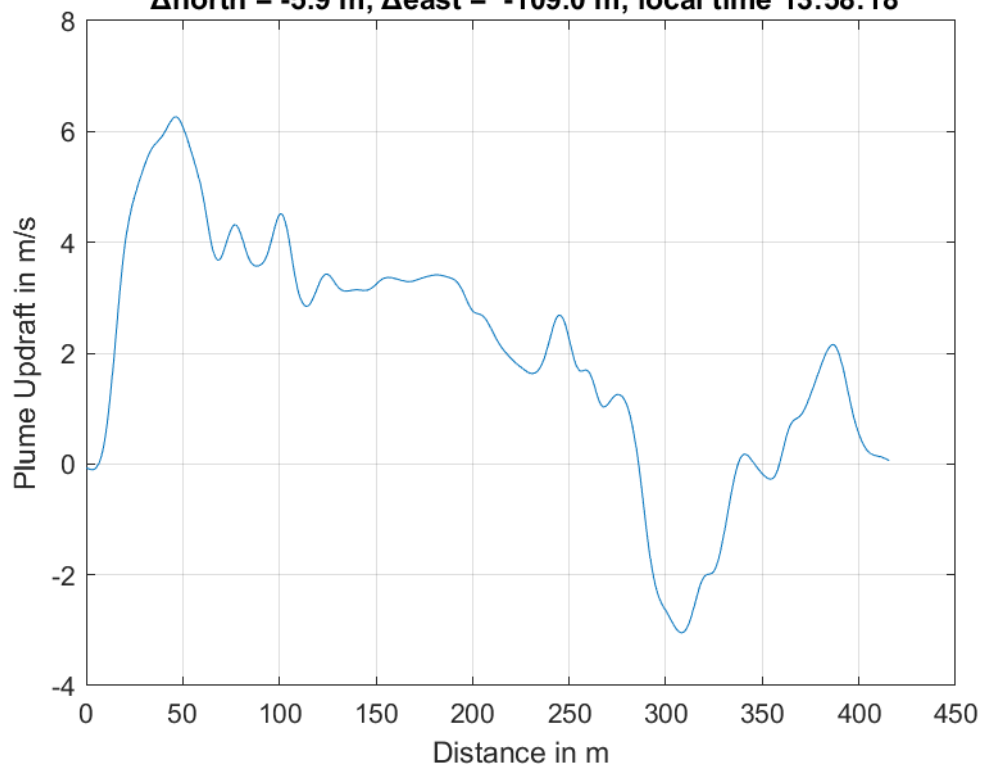
**Plume #33 at 209.5 m MSL, fly-through speed 56.0 m/s,
 $\Delta_{\text{north}} = -79.7$ m, $\Delta_{\text{east}} = -431.7$ m, local time 13:55:58**



**Plume #34 at 225.8 m MSL, fly-through speed 50.0 m/s,
 $\Delta_{\text{north}} = -110.2$ m, $\Delta_{\text{east}} = -550.4$ m, local time 13:57:15**



**Plume #35 at 210.4 m MSL, fly-through speed 54.0 m/s,
 $\Delta_{\text{north}} = -5.9$ m, $\Delta_{\text{east}} = -109.0$ m, local time 13:58:18**



**Plume #36 at 209.9 m MSL, fly-through speed 54.0 m/s,
 $\Delta_{\text{north}} = -33.9$ m, $\Delta_{\text{east}} = -377.2$ m, local time 13:58:53**

